National Library
of Canada

Bibliothèque nationale
du Canada

Canadian Theses Service

Service des thèses canadiennes

Ottawa, Canada
K1A 0N4

NOTICE

The quality of this microform is heavily dependent upon the quality of the original thesis submitted for microfilming. Every effort has been made to ensure the highest quality of reproduction possible.

If pages are missing, contact the university which granted the degree.

Some pages may have indistinct print especially if the original pages were typed with a poor typewriter ribbon or if the university sent us an inferior photocopy.

Reproduction in full or in part of this microform is governed by the Canadian Copyright Act, R.S.C. 1970, c. C-30, and subsequent amendments.

AVIS

La qualité de cette microforme dépend grandement de la qualité de la thèse soumise au microfilmage. Nous avons tout fait pour assurer une qualité supérieure de reproduction.

S'il manque des pages, veuillez communiquer avec l'université qui a conféré le grade.

La qualité d'impression de certaines pages peut laisser à désirer, surtout si les pages originales ont été dactylographiées à l'aide d'un ruban usé ou si l'université nous a fait parvenir une photocopie de qualité inférieure.

La reproduction, même partielle, de cette microforme est soumise à la Loi canadienne sur le droit d'auteur, SRC 1970, c. C-30, et ses amendements subséquents.

NL-339 (r. 88/04) c

Canada

National Library of Canada
Canadian Theses Service
Ottawa, Canada
K1A 0N4

Bibliothèque nationale du Canada
Service des thèses canadiennes

The author has granted an irrevocable non-exclusive licence allowing the National Library of Canada to reproduce, loan, distribute or sell copies of his/her thesis by any means and in any form or format, making this thesis available to interested persons.

The author retains ownership of the copyright in his/her thesis. Neither the thesis nor substantial extracts from it may be printed or otherwise reproduced without his/her permission.

L'auteur a accordé une licence irrévocable et non exclusive permettant à la Bibliothèque nationale du Canada de reproduire, prêter, distribuer ou vendre des copies de sa thèse de quelque manière et sous quelque forme que ce soit pour mettre des exemplaires de cette thèse à la disposition des personnes intéressées.

L'auteur conserve la propriété du droit d'auteur qui protège sa thèse. Ni la thèse ni des extraits substantiels de celle-ci ne doivent être imprimés ou autrement reproduits sans son autorisation.

ISBN 0-315-55408-8

Canada

THE UNIVERSITY OF ALBERTA

FAILURE IN MINE HIGHWALL IN SOFT SEDIMENTARY ROCK

by

C. ANDREW SMALL ©

A THESIS

SUBMITTED TO THE FACULTY OF GRADUATE STUDIES AND RESEARCH

IN PARTIAL FULFILLMENT OF THE REQUIREMENTS FOR THE DEGREE

OF MASTER OF SCIENCE

DEPARTMENT OF CIVIL ENGINEERING

EDMONTON, ALBERTA

FALL, 1989

THE UNIVERSITY OF ALBERTA

RELEASE FORM

NAME OF AUTHOR: C. ANDREW SMALL

TITLE OF THESIS: FAILURE IN MINE HIGHWALL IN SOFT SEDIMENTARY ROCK

DEGREE FOR WHICH THESIS WAS PRESENTED: MASTER OF SCIENCE

YEAR THIS DEGREE GRANTED: FALL, 1989

Permission is hereby granted to the UNIVERSITY OF ALBERTA LIBRARY to reproduce single copies of this thesis and to lend or sell such copies for private, scholarly, or scientific research purposes only.

The author reserves the rights and neither the thesis nor extensive extracts from it may be printed or otherwise reproduced without the author's written permission.

(Signed) C. Andrew Small ....

PERMANENT ADDRESS:

Department of Civil Engineering
University of Alberta, Edmonton
Alberta, Canada T6G 2G7

Dated ....September 30, 1989

UNIVERSITY OF ALBERTA

FACULTY OF GRADUATE STUDIES AND RESEARCH

The undersigned certify that they have read, and recommend to the Faculty of Graduate Studies and Research for acceptance, a thesis entitled FAILURE IN A MINE HIGHWALL IN SOFT SEDIMENTARY ROCK submitted by C. Andrew Small in partial fulfillment of the requirements for the degree of Master of Science.

DR. N.R. MORGENSTERN ....
Supervisor

DR. D.M. CRUDEN ....

DR. K. BARRON K. Barron ....

Date June 30, 1989

ABSTRACT

Highwall failures in open pit mines can be dangerous and costly. Their prediction and prevention by limit equilibrium analyses rely on estimates of pore pressures and strength. Since, both of these factors can be affected by rebound of the highwall upon excavation, proper stability assessment can only be done when the impact of rebound on these parameters is known. Such is the goal of this thesis: to determine how deformations of the highwall influence structure, pore pressures, and strength in the strata behind it.

The study was conducted in Pit 03 at the Highvale Mine, west of Edmonton, Alberta, where the highwall was cut in weak sandstone and mudstone overlying the economic coal deposit. A field program combined inclinometers and surveying to measure movements and piezometers were installed to monitor pore pressures. Laboratory testing on core samples from the field provided estimates of strengths for stability analyses.

Movements of the highwall and rock/soil beyond it were converted to lateral strains which were then used as a measure of how much the material "stretched" due to rebound. It was found that the stretching caused joints to spread slightly, loosening the mass and significantly altering the groundwater flow regime.

A highwall failure in the spring of 1988 was back analysed in detail and concluded that two mechanisms

progressively reduced the strength of the sandstone and mudstone. Firstly, progressive loosening of the sandstone occurred as the joints spread and reduced the shear resistance along them. Secondly, progressive softening developed in the underlying mudstone as it stretched and permitted water to infiltrate. Increased lateral straining accelerated these processes.

Clarification of the mechanism of strength reduction as well as additional observations from this study directly impact highwall design and field monitoring.

ACKNOWLEDGEMENTS

The author is grateful to his supervisor, Dr. N. R. Morgenstern, for providing this challenging and rewarding subject for a thesis. His experience, guidance, and insight were invaluable.

Financial support for this study was provided by the Alberta Office of Coal Research and Technology (#2835-RG-85/22) and the Natural Sciences and Engineering Research Council of Canada.

Art Peterson, professor in Civil Engineering at the University of Alberta, developed the survey plan that turned out to be the key to the deformation monitoring.

Special thanks are extended to the technical staff of the Geotechnical Group, particularly Gerry Cyre, Christine Hereygers, Steve Gambel, and Jay Khajuria. These people provided a great deal of help in the field and in the laboratory. Richard Morley and Ian Wesch deserve recognition for their assistance in collecting field data.

The author is indebted to TransAlta Utilities (TAU), for without their assistance the project would not have been viable. Andrew Hickimbotham and Darryl Mikalson, from the Calgary, and Dennis Nikols, formerly of TAU, provided valuable assistance.

Mark Fenton and John Pawlowicz of the Alberta Research Council, Tim Peterson and Neil Wade of Monenco Engineering, and Po Tsui of the University of Alberta provided important guidance during the planning and field data collection stages of this study.

Bob Coates and Nester Zacharko, of Mobile Augers and Research (1979) Limited, contributed a great deal to the success of the drilling and field instrumentation program at Highvale Mine.

Special thanks go to the TAU and Manalta Coal personnel at the Highvale Mine, especially Bob Kerby, Doug Hessian, Bill Douce, Stan Franklin, Ray Kingdon, Dave Passfield, and Wayne Anderson. Without their enthusiasm and interest in this project, the instrumentation would have been destroyed and a substantial portion of the study ruined.

Recognition goes to Dr. A. J. Valsangkar of the University of New Brunswick for nurturing the author's interest in geotechnical engineering.

The support of the author's friends and family was appreciated with the warmest thanks extended to his wife, Anne. She knew little of what to expect when her husband began this project, but her constant faith and confidence insured its success.

TABLE OF CONTENTS

Chapter PAGE

1 HIGHWALL STABILITY IN OPEN PIT MINING 1

1.1 Thesis Goal and Objectives 1

1.2 Significance of Failure Mechanism 3

1.3 Case Histories 4

1.3.1 Pilot Mine 5

1.3.2 Centralia Mine 7

1.3.3 Vesta Mine 9

1.3.4 Highvale Mine 10

1.4 Current Stability 13

1.5 Distinguishing Features of this Thesis 14

1.6 Thesis Organization 15

2 DESCRIPTION OF STUDY AREA - PIT 03, HIGHVALE MINE 17

2.1 Location 17

2.2 Physiography 17

2.3 Bedrock Geology 18

2.4 Glacial Tectonics 18

2.5 Mining Method 21

2.6 Influence of Coalwall 22

3 FIELD INVESTIGATION PROGRAM 26

3.1 Study Site 26

3.2 Drilling and Sampling Program 27

3.3 Downhole Geophysical Logging 29
3.4 Geological Mapping 30
3.5 Deformation Monitoring 31
    3.5.1 Inclinometers 33
    3.5.2 Maintenance of Inclinometers 35
    3.5.3 Surveying 36
    3.5.4 Alternative Methods to Monitor Highwall
        Deformations 38
3.6 Piezometers 39
4 RESULTS OF FIELD INVESTIGATION PROGRAM 56
4.1 Lithology 56
    4.1.1 Sandstone 56
    4.1.2 Sandstone/Mudstone Contact 57
    4.1.3 Mudstone 58
    4.1.4 Bentonite 59
    4.1.5 Coal Sequence 60
4.2 Deformations 60
    4.2.1 Results of Deformation Monitoring
        Program 60
        Pattern and Magnitude of Movement 61
    4.2.2 Deformation Mechanism 64
    4.2.3 Deformation Field 65
    4.2.4 Movement Trend 67
    4.2.5 Strain Field 69

4.3 Hydrogeology 70
4.3.1 Pore Pressure Response 71
4.3.2 Piezometric Model 71
4.4 Field Investigation Program Conclusions 74
5 GEOTECHNICAL PROPERTIES OF OVERBURDEN 97
5.1 Index Testing 97
5.1.1 Clarification of Terms 100
5.2 Triaxial Testing 101
5.2.1 Unweathered Sandstone 102
5.2.2 Mudstone 103
Softening of Mudstone 104
5.3 Direct Shear Testing 107
5.3.1 Mudstone 107
5.3.2 Bentonite 109
5.4 Conclusions from Laboratory Testing 110
6 ANALYSIS OF FAILURE 122
6.1 Failure Description 122
6.1.1 Slip Surface Geometry 123
6.1.2 Time of Failure 124
6.1.3 Water Pressures 125
6.1.4 Strength Estimates 126
Sandstone 126
Mudstone 127
Bentonite 128

6.2 Failure Back Analysis 129
    6.2.1 Limit Equilibrium Method 129
    6.2.2 Example of Results 130
6.3 Analysis of Toe Failure 133
6.4 Analysis of Rear Failure 134
6.5 Influence of Pore Pressure Assumptions 135
6.6 Combined Results 136
6.7 Effect of Lateral Straining on Strength Reduction 137
    6.7.1 Conceptual Model of Strength Reduction 137
    6.7.2 Estimate of Lateral Strains at Failure 138
    6.7.3 Consider Stable Highwall in Front of S3 ... 140
6.8 Progressive Loosening and Softening 141
    6.8.1 Progressive Loosening 141
    6.8.2 Progressive Softening 142
6.9 Concept of Critical Strain 143
6.10 Failure Mechanism 145
6.11 Comparison with other Stability Investigations at Highvale 146
    6.11.1 Wade and Peterson (1986) 146
    6.11.2 Barron et al (1986) 147
    6.11.3 Tsui (1988) 149
6.12 Conclusions from Failure Analysis 151
7 APPLICATION TO HIGHWALL DESIGN AND REMEDIAL MEASURES ... 152

7.1 Highwall Design 172
        Design Factors 172
        Field Program 173
        Geotechnical Database 174
7.2 Remedial Measures 174
7.3 Deformation Monitoring Program 176
    7.3.1 Objective 176
    7.3.2 Methodology 176
7.4 Pore Pressure Monitoring 178
7.5 Use of Computer Modelling 178
8 CONCLUSIONS 180
8.1 Conclusions 180
8.2 Recommendations for Future Research 181
LIST OF REFERENCES 183
APPENDIX A - BOREHOLE LOGS 186
APPENDIX B - DOWNHOLE GEOPHYSICAL LOGS 216
APPENDIX C - RESULTS OF DEFORMATION MONITORING 222
C.1 Inclinometers 222
C.2 Surveys 223
C.3 Combined Inclinometer and Survey Results 224
APPENDIX D - DISPLACEMENT FIELD 250
APPENDIX E - STRAIN FIELD 259
APPENDIX F - PIEZOMETER RESULTS 268
APPENDIX G - INDEX TESTING RESULTS 276

LIST OF TABLES

Table Page

4.1 Variations in the Semi-log Equation Parameters B and M at Elevation 730 metres 68

5.1 Moisture Contents, Densities, and Limits 99

5.2 Summary of strengths 111

6.1 Estimates of Strength Mobilized at Failure 129

6.2 Example of Stability Analysis for Toe Failure 132

6.3 FOS for Toe Failure Determined at Selected Values of Mudstone Cohesion 133

6.4 Lateral Strains on March 17, 1988 and April 13, 1988 139

6.5 Other Stability Investigations at Highvale Mine 148

LIST OF TABLES IN APPENDICES

Table Page

A.1 Location of Boreholes 186

C.1 Location of Control Points 222

C.2 East end of Pit 03, Highvale Mine
Highwall Position from June, 1987 to May, 1988 225

C.3 Important Dates Related to Deformation Monitoring 226

F.1 Location of Piezometers 268

G.1 Results of Moisture Content Testing 277

G.2 Results of Grain Size Analyses 279

G.3 Results of Atterberg Limits 280

G.4 Liquidity Indices 281

G.5 Activity 282

LIST OF FIGURES

Figure Page

2.1 Location of the (a) Highvale Coal Mine and (b) the study site in Pit 03 23

2.2 Evidence of Glacial Tectonism in Pit 04 at the Highvale Mine (a) location of thrust block and (b) section through thrust block 24

2.3 Schematic of Mining Method at the Highvale Coal Mine 25

3.1 Plan view of study site, June, 1987 42

3.2 Cross section at study site, Station 3835, Line S2-S4-S6, June, 1987 43

3.3 Cross section at study site, Station 3885, Line S1-S3-S5, June, 1987 44

3.4 Gamma, Density, and Caliper geophysical logs for hole S3 45

3.5 Gamma, Density, and Caliper geophysical logs for hole S4 48

3.6 Potential modes of highwall deformation 51

3.7 Instrument status at Station 3835, September to December, 1987 52

3.8 Instrument status at Station 3835, December, 1987 to March, 1988 53

3.9 Instrument status at Station 3835, March to May, 1988 54

3.10 Instrument status at Station 3835, May to September, 1988 55

4.1 Lithology of study site from field investigation program 77

4.2 Location of slickensides observed in core taken from hole S6, June, 1987 78

4.3 Movement of inclinometer S1 79

4.4 Movement of inclinometer S2 80

4.5 Movement of inclinometer S3 81

4.6 Movement of inclinometer S4 82

4.7 Movement of inclinometer S5 83

4.8 Movement of inclinometer S6 84

4.9 Northward movement over time at elevation 730 metres for inclinometer S1. (Day zero was June 23, 1987) 85

4.10 Northward movement over time at elevation 730 metres for inclinometer S2. (Day zero was June 23, 1987) 85

4.11 Northward movement over time at elevation 730 metres for inclinometer S3. (Day zero was June 23, 1987) 86

4.12 Northward movement over time at elevation 730 metres for inclinometer S4. (Day zero was June 23, 1987) 86

4.13 Northward movement over time at elevation 730 metres for inclinometer S5. (Day zero was June 23, 1987) 87

4.14 Northward movement over time at elevation 730 metres for inclinometer S6. (Day zero was June 23, 1987) 87

4.15 Deformations at elevation 730 metres on day 238 (February 15, 1988) 88

4.16 Semi-logarithmic plot of deformations at elevation 730 metres on day 238 (Feb. 15, 1988) 88

4.17 Deformations at elevation 721 metres on day 238 (February 15, 1988) 89

4.18 Variation in B and M at elevation 730 metres after a highwall was cut 89

4.19 Variation in B and M at elevation 730 metres after a coalwall was cut 90

4.20 Range of movements in overburden at elevation 730 metres 90

4.21 Range of strains in overburden at elevation 730 metres 91

4.22 Piezometric head over time for piezometers P12-B and P13-T 92

4.23 Piezometric head distribution 200 m behind the highwall crest.................................... 92
4.24 Piezometric head distribution 150 m behind the highwall crest.................................... 93
4.25 Piezometric head distribution 100 m behind the highwall crest.................................... 93
4.26 Piezometric head distribution 50 m behind the highwall crest.................................... 94
4.27 Piezometric head distribution beneath the highwall crest. One to two weeks after a highwall was cut.. 94
4.28 Piezometric head distribution beneath the highwall crest. Two to three weeks after a highwall was cut.. 95
4.29 Piezometric head distribution beneath the highwall crest. Three to four weeks after a highwall was cut.. 95
4.30 Groundwater flow pattern in the overburden.......... 95
5.1 Grain size distribution of unweathered sandstone. Also shown is distribution of sandstone from failure area, discussed in Chapter 6............... 112
5.2 Grain size distribution of bentonitic mudstone...... 112
5.3 Grain size distribution of siltstone............... 113
5.4 Grain size distribution of bentonite............... 113

5.5 Plasticity chart for bentonitic mudstone and bentonite.......................................114

5.6 Deviator stress during undrained triaxial shearing of unweathered sandstone..........................115

5.7 Deviator stress during drained triaxial shearing of unweathered sandstone..........................115

5.8 Mohr Coulomb plot for peak shear strength of unweathered sandstone..............................116

5.9 Mohr Coulomb plot for residual shear strength of unweathered sandstone..............................116

5.10 Deviator stress during undrained triaxial shearing of bentonitic mudstone..............................117

5.11 Mohr Coulomb plot for peak strength of bentonitic mudstone from CU triaxial testing..................117

5.12 Summary of strengths of mudstone measured by several authors, after Tsui (1988).................118

5.13 Shear stress during initial direct shear of bentonitic mudstone................................118

5.14 Mohr Coulomb plot of peak shear strength for bentonitic mudstone from CU triaxial tests and drained direct shear tests.........................119

5.15 Mohr Coulomb plot of residual strength for bentonitic mudstone from direct shear tests.........119

5.16 Shear stress during initial direct shear of bentonite.......................................120

5.17 Shear stress during direct shear of bentonite to residual 120

5.18 Mohr Coulomb plot of bentonite strength 121

6.1 Plan view of highwall failure in Pit 03 April, 1988 154

6.2 Post Failure Topography at Section A-A' through the west end of the failure, as observed on April 7, 1988 155

6.3 Post failure topography at Section B-B' through the east end of the failure as observed on April 7, 1988 155

6.4 Failure model: Cross section of highwall on March 12, 1988, immediately after cut 21 was made 156

6.5 Failure model at Section A-A': After failure of toe block, one to three weeks after highwall was cut, between Mar. 18 and April 2, 1988 156

6.6 Failure model at Section A-A': After failure of rear block, three to four weeks after highwall was cut, approximately April 4, 1988 157

6.7 Pore Pressure Distribution assumed for failure analyses - one to two weeks after highwall was cut 157

6.8 Pore Pressure Distribution assumed for failure analyses - two to three weeks after highwall was cut 158

6.9 Pore Pressure Distribution assumed for failure analyses - three to four weeks after highwall was cut. Toe had previously failed.................... 158

6.10 Stability analyses for toe failure (a) Geometry, water pressures, and strength parameters, (b) FOS plotted against l. to find FOS that satisfies moment and force equilibrium........................ 159

6.11 Magnitude of mudstone cohesion mobilized at a FOS of unity.. 160

6.12 Assumed slip surfaces for search of critical one at toe failure (i.e. slip surface with lowest FOS).. 160

6.13 Combinations of mudstone and sandstone cohesions mobilized at toe failure........................... 161

6.14 Assumed slip surfaces for search of critical one at rear failure.................................. 161

6.15 Combination of mudstone and sandstone cohesions mobilized at rear failure.......................... 162

6.16 Combined results of toe and rear failures.......... 162

6.17 Conceptual model of reduction in rock mass strength from and undisturbed state beyond the zone of excavation to the highwall face............ 163

6.18 Lateral strain field for March. 17 and April 13, 1988 on line S4-S6................................ 163

6.19 Variation in strain along backscarp of toe failure after a highwall was cut.......................... 164

6.20 Variation in strain along backscarp of rear failure after a highwall was cut.................. 164

6.21 Generalized development of strain along backscarp of toe block after a highwall was cut.............. 165

6.22 Generalized development of strain along backscarp of rear block after a highwall was cut............. 165

6.23 Lateral strains mobilized at elevation 730 metres on March 17, 1988, five days after the highwall was cut.. 166

6.24 Schematic of "Progressive Loosening" concept....... 167

6.25 Schematic of "Progressive Softening" concept....... 168

6.26 Generalized development of strain on line S2-S4-S6 after the coal was excavated. At elevation 730 metres, 15 metres in front of highwall crest....... 169

6.27 Generalized development of strain on line S1-S3-S5 after the highwall and coal were excavated. At elevation 730 metres, 15 metres in front of highwall crest.................................. 169

6.28 Section used by Wade and Peterson (1986) to evaluate stability of highwall in Pit 03........... 170

6.29 Planar Shear Model used by Barron and Stimpson (1986) to analyse failure of highwall in Pit 03 in spring, 1984.................................... 170

6.30 Sections used by Tsui (1988) to analyse two highwall failures which occurred in Pit 03 in July, 1984: (a) Slide 1 and (b) Slide 2.............. 171

LIST OF FIGURES CONTAINED IN APPENDICES

Figure Page

A.1 Borehole Log for hole S1 187

A.2 Borehole Log for hole S2 191

A.3 Borehole Log for hole S3 194

A.4 Borehole Log for hole S4 201

A.5 Borehole Log for hole S5 206

A.6 Borehole Log for hole S6 211

B.1 Gamma, Density, Caliper, and Focussed Electric Resistivity Geophysical Logs for hole S1 217

B.2 Gamma and Focussed Electric Resistivity Geophysical Logs for hole S2 219

B.6 Gamma, Density, Caliper, Neutron Porosity and Focussed Electric Resistivity Geophysical Logs for hole S6 220

C.1 Northward movement of inclinometer S1 relative to its base 228

C.2 Eastward movement of inclinometer S1 relative to its base 229

C.3 Northward movement of inclinometer S2 relative to its base 230

C.4 Eastward movement of inclinometer S2 relative to its base 231

C.5 Northward movement of inclinometer S3 relative to its base 232
C.6 Eastward movement of inclinometer S3 relative to its base 233
C.7 Northward movement of inclinometer S4 relative to its base 234
C.8 Eastward movement of inclinometer S4 relative to its base 235
C.9 Northward movement of inclinometer S5 relative to its base 236
C.10 Eastward movement of inclinometer S5 relative to its base 237
C.11 Northward movement of inclinometer S6 relative to its base 238
C.12 Eastward movement of inclinometer S6 relative to its base 239
C.13 Northward movement over time of the top of inclinometer S6 240
C.14 Eastward movement over time of the top of inclinometer S6 240
C.15 Northward movement over time of base of inclinometer S1 241
C.16 Eastward movement over time of base of inclinometer S1 241

C.17 Northward movement over time of base of inclinometer S2 242

C.18 Eastward movement over time of base of inclinometer S2 242

C.19 Northward movement over time of base of inclinometer S3 243

C.20 Eastward movement over time of base of inclinometer S3 243

C.21 Northward movement over time of base of inclinometer S4 244

C.22 Eastward movement over time of base of inclinometer S4 244

C.23 Northward movement over time of base of inclinometer S5 245

C.24 Eastward movement over time of base of inclinometer S5 245

C.25 Northward movement over time of base of inclinometer S6 246

C.26 Eastward movement over time of base of inclinometer S6 246

C.27 Northward movement over time of base of inclinometer S1. Adjusted for movements that occurred prior to instrument installation 247

C.28 Northward movement over time of base of inclinometer S2. Adjusted for movements that occurred prior to instrument installation 247

C.29 Northward movement over time of base of inclinometer S3. Adjusted for movements that occurred prior to instrument installation 248

C.30 Northward movement over time of base of inclinometer S4. Adjusted for movements that occurred prior to instrument installation 248

C.31 Northward movement over time of base of inclinometer S5. Adjusted for movements that occurred prior to instrument installation 249

C.32 Northward movement over time of base of inclinometer S6. Adjusted for movements that occurred prior to instrument installation 249

D.1 Displacement field at elevation 730 metres on July 3, 1987 (Day 10) 251

D.2 Displacement field at elevation 730 metres on July 29, 1987 Day 36) 251

D.3 Displacement field at elevation 730 metres on August 6, 1987 (Day 44) 252

D.4 Displacement field at elevation 730 metres on August 19, 1987 (Day 57) 252

D.5 Displacement field at elevation 730 metres on September 2, 1987 (Day 71) 253

D.6 Displacement field at elevation 730 metres on September 23, 1987 (Day 92) 253

D.7 Displacement field at elevation 730 metres on October 19, 1987 (Day 118) 254

D.8 Displacement field at elevation 730 metres on November 20, 1987 (Day 150) 254

D.9 Displacement field at elevation 730 metres on November 25, 1987 (Day 155) 255

D.10 Displacement field at elevation 730 metres on December 13, 1987 (Day 173) 255

D.11 Displacement field at elevation 730 metres on January 20, 1988 (Day 211) 256

D.12 Displacement field at elevation 730 metres on February 15, 1988 (Day 238) 256

D.13 Displacement field at elevation 730 metres on March 17, 1988 (Day 268) 257

D.14 Displacement field at elevation 730 metres on April 13, 1988 (Day 295) 257

D.15 Displacement field at elevation 730 metres on April 27, 1988 (Day 309) 258

E.1 Strain field at elevation 730 metres on July 3, 1987 (Day 10) 260

E.2 Strain field at elevation 730 metres on July 29, 1987 (Day 36) 260

E.3 Strain field at elevation 730 metres on August 6, 1987 (Day 44) 261

E.4 Strain field at elevation 730 metres on August 19, 1987 (Day 57) 261

E.5 Strain field at elevation 730 metres on September 2, 1987 (Day 71) 262

E.6 Strain field at elevation 730 metres on September 23, 1987 (Day 92) 262

E.7 Strain field at elevation 730 metres on October 19, 1987 (Day 118) 263

E.8 Strain field at elevation 730 metres on November 20, 1987 (Day 150) 263

E.9 Strain field at elevation 730 metres on November 25, 1987 (Day 155) 264

E.10 Strain field at elevation 730 metres on December 13, 1987 (Day 173) 264

E.11 Strain field at elevation 730 metres on January 20, 1988 (Day 211) 265

E.12 Strain field at elevation 730 metres on February 15, 1988 (Day 238) 265

E.13 Strain field at elevation 730 metres on March 17, 1988 (Day 268) 266

E.14 Strain field at elevation 730 metres on April 13, 1988 (Day 295) 266

E.15 Strain field at elevation 730 metres on April 27, 1988 (Day 309) 267

F.1 Piezometric head over time for pneumatic piezometer P7-T 269

F.2 Piezometric head over time for pneumatic piezometer P7-B 269

F.3 Piezometric head over time for sealed tip standpipe piezometer P8-T 270

F.4 Piezometric head over time for sealed tip standpipe piezometer P9-T 270

F.5 Piezometric head over time for pneumatic piezometer P9-B 271

F.6 Piezometric head over time for pneumatic piezometer P10-T 271

F.7 Piezometric head over time for pneumatic piezometer P710-B 272

F.8 Piezometric head over time for pneumatic piezometer P11-T 272

F.9 Piezometric head over time for pneumatic piezometer P11-B 273

F.10 Piezometric head over time for sealed tip standpipe piezometer P12-T 273

F.11 Piezometric head over time for pneumatic piezometer P12-B 274

V

F.12 Piezometric head over time for pneumatic piezometer P13-T 274

F.13 Piezometric head over time for pneumatic piezometer P13-B 275

1 HIGHWALL STABILITY IN OPEN PIT MINING

Highwall failures can be dangerous and costly. Their prevention and/or prediction requires an understanding of the potential failure mechanism, and more importantly, how it is affected by rebound due to excavation. This author studied a highwall at the Highvale Mine, west of Edmonton, Alberta, to answer this question.

1.1 Thesis Goal and Objectives

The potential failure mechanism has several components including (i) the failure mode, (ii) pore pressures, and (iii) the strength of the rock and soil that make up the highwall. The goal of this thesis was to determine how these components are affected by excavation of a highwall.

To achieve this goal, five objectives were specified:

1. To determine zones of movement that could ultimately become slip planes during a failure;
2. To measure deformations and determine strains in the rock behind the highwall;
3. To measure the porewater pressures from beyond the zone of rebound to beneath the highwall crest;
4. To assess the rock strength before and after it had been disturbed by rebound;
5. To determine the mechanism of highwall failures.

To meet the fourth objective, large scale field test could have been performed, but these are costly and difficult. The best means of determining the in-situ strength was by analysing a failure that occurred. This was the key element of the thesis and not only provided information on the material strength after it had been disturbed by rebound, but also illuminated the failure mechanism. Consequently, the title of this thesis reflects the importance of a failure in the the mine highwall to the success of this study.

The Highvale Coal Mine, west of Edmonton, Alberta, was selected as the research site because of substantial work conducted previously at the mine and its proximity to the University of Alberta. Field work, laboratory testing, and stability analyses were performed to meet the objectives.

It is hoped that in achieving the goal described above, then highwall designers may better attain economical and safe highwalls.

Highwalls are not the only slopes that can benefit from the findings of this thesis. In fact, the goal stated above may be extended to any excavated slope. From a research point of view, two reasons make the highwall an ideal for exploring the effects of excavation:

1. Highwalls are designed with a low factor of safety and a relatively greater probability of failure, in comparison with other excavated slopes, such as

a highway cut. This is acceptable since the highwall is a temporary structure.

2. New highwalls are cut on a routine basis in the same area, thus permitting an investigator to gain a wealth of information on the behaviour of an excavated slope.

1.2 Significance of Failure Mechanism

Open pit mining is often most economical and efficient when the highwall is high and near vertical. However, high, steep highwalls can result in failures that cover the deposit, endanger equipment, threaten workers, disrupt schedules, and cost a great deal to cleanup. Furthermore, considerable expense may be incurred in failure prevention. At the extreme case, failures could destroy mining equipment, such as the multi-million dollar dragline.

Without accurately knowing the failure mechanism and its associated components, planned and economical solutions to improve stability may not be realized. For example, a variety of techniques could be implemented to increase stability, such as reducing the highwall height and angle, improving drainage, breaking up shear zones, anchoring the rock face, or implementing monitoring schemes capable of predicting failures and then limiting the damage. But, only with an understanding of the failure mechanism can the best possible design or prevention measures be selected.

As stated at the outset of this thesis, the failure mechanism consists of several components (failure mode, pore pressures, and strength). Past studies have greatly contributed to understanding the potential modes of failure, but more detailed research is required into the effect of excavation on the pore water pressures and soil or rock strength. Without this, then the accuracy of the entire failure mechanism is cast in doubt.

Inadequate knowledge of the failure mechanism has troubled highwall designers for some time. Examples of these problems are outlined in the case histories below.

1.3 Case Histories

Highwall failures can occur in any open pit mine that extracts coal, oilsand, or other mineral resource but this thesis focuses on a specific class of highwalls, those cut in horizontally bedded soft rock in open pit coal mines in Western North America. Several mines on the Prairies of Western North America fall into this class, including Centralia in Washington State, and Vesta and Highvale in Alberta.

Most open pit coal mines on the Prairies are susceptible to highwall problems because of the soft and deformable bedrock near the surface. In addition, thin seams of highly plastic and very weak bentonite are often found just above or below the ore body and even within it. The result is a highwall that can not only fail, but can deform a great deal before ultimately collapsing.

1.3.1 Pilot Mine for Centralia Mine (Miller and Hilts, 1969)

An open pit coal strip mine was planned near Centralia, Washington that required 75 metre high slopes. The sandstone and siltstone overburden above the coal was highly fractured, jointed, and faulted. Classical approaches to stability indicated that slopes cut in the mine would be stable. To confirm this, an experimental Pilot Mine was created to provide firsthand knowledge of cut slope behaviour.

The Pilot Mine was excavated in the coal field in 1968 and was 70 metres deep and 130 metres long. The first 20 metres was cut at a 45° slope with a 7 metre wide bench at its base. The remainder consisted of two intermediate slopes at 1H:0.5V with a 7 metre bench separating them. In this instance, the entire 70 metre high rock slope above the coal was termed the highwall. Below the highwall, fifteen metres of coal was excavated at a 1H:0.5V slope.

The highwall was instrumented with inclinometers and extensometers to measure movements at and beyond the slope face. Excavation of the overburden resulted in movements of the highwall face from 3 mm to 28 mm. No movements were detected 60 metres behind the wall.

As the coal was removed, a slickensided mudstone was exposed near the base of coal and movements of 30 mm developed along it.

During excavation of the Pilot Mine, six slides and rockfalls occurred in the cut slopes. All six failures occurred after the slickensided mudstone was exposed. Three of them were contained in the highwall while the others slid along the slickensided mudstone.

For the first three, it was believed that movements at the base of the coal stretched the overburden and opened existing cracks and weak planes. This permitted water to penetrate the openings and possibly soften the sandstone and siltstone overburden, reducing the strength. Moreover, cracks opening at the surface allowed ingress of surface water which exerted additional pressures to induce failure.

The Pilot Mine satisfied its purpose of highlighting deficiencies in the stability calculations. The analyses were based on strengths measured in the laboratory and did not take into account the effect of excavation. Based on these findings, Miller and Hilts (1969) attributed the reduction in strength to the presence of faults, joints, and fractures in the rock that opened wider on excavation. From this work, the Centralia Mine was successfully developed in 1970.

1.3.2 Centralia Mine (Lasalata, 1988)

In 1988, the Centralia Mine in Washington State had 80 metres of sand- and siltstones overlying a coal deposit. The average dip of the bedrock was about 6° and considered close to horizontal. After the 80 metres of overburden was removed, 10 metres of coal was mined out before additional stripping of waste rock continued for another 30 metres to access another coal body. The resulting rock slope was 120 metres high and was benched to provide an average slope of less than 2H:1V. The highwall stood at the toe of the slope and was 15 metres high at 45°.

In response to excavation, the highwall moved over 10 metres into the pit, creeping as much as one metre/day, without collapsing. Fortunately, the pit was designed so that these movements were up-dip (consider the consequences if the pit was reversed). Even with these large movements, the stability of the highwall was considered acceptable by mine engineers, that is, relative to the problems encountered prior to 1988.

Before 1988, the highwall experienced several instabilities that were classified as massive multiple block, creep failures. They damaged over a kilometre of the highwall and extended 600 metres back into the native bedrock. The basal shear plane for these immense failures was a 150 mm seam of bentonite, 89 metres below the surface and squeezed between layers of the upper coal deposit, about a metre above its base. It had an undrained shear strength less than 6 kPa and was the same seam encountered at the Pilot Mine that was responsible for the failures in 1968.

To achieve some measure of stability, tension cracks between the blocks were filled with soil to prevent the entry of water but were not effective. An alternative was to predict the onset of failure and sound a warning to minimize damage to equipment and men. Survey prisms attached to the highwall face were monitored daily, but this frequency was still not high enough for effective warnings.

As the failures continued, ongoing field observation and monitoring programs provided additional details on the mechanism. The highwall was then redesigned using stability analyses conducted in terms of total stresses, with $\phi = 0^\circ$ and cohesion equal to the undrained shear strength obtained from laboratory testing, and lower bound strengths.

As a result, the driving forces from the wedges beyond the highwall face were reduced by stripping overburden as far as 600 metres behind the face, and the limited toe block resistance was increased by steepening the highwall. With these measures implemented, the movements were restricted (from 15 to 10 metres), tension cracks were not as frequent, and the frequency of failures reduced.

The stability analyses did not directly consider the of highwall rebound on strength, pore pressures, and so on, but, by using the lower bound strength parameters, the analyses indirectly included this effect as evidenced by the stable highwall.

1.3.3 Vesta Mine (Jenkins, 1988)

The Vesta Mine in eastern Alberta is more than 60 years old and was developed for commercial coal production in the early 1960's. The sandstones and clay shales in certain areas had been damaged, shoved, and sheared by glacial action (Section 2.4), later causing failures of the highwall. These failures began when a portion of the open pit mine intercepted the shear zones and reactivated them. They were limited to small areas where the pit was adversely oriented. The rest of the highwall experienced significant rebound due to excavation without collapse. The basal slip plane throughout the mine was a seam of bentonite found just above the coal which often underwent movements of 30 cm into the pit.

Stability analyses to assess the potential of failure were conducted with effective stress parameters. The laboratory strengths were not reduced to account for excavation and a safe highwall angle was calculated. This was then decreased in accordance with judgement and past experience gathered from the previous performance of the highwalls. In effect, the designers empirically included the influence of excavation on the failure mechanism. No back analyses of failures were conducted to better determine the rock strength at the highwall.

1.3.4 Highvale Mine

The Highvale Coal Mine, in west Central Alberta, has experienced highwall problems since 1983 when failures greatly disrupted mining operations. A number of authors have investigated the geology and failure mechanisms at Highvale, including: Moell et al (1984), Fenton et al (1986), Barron et al (1986), Wade and Peterson (1986), and Tsui (1988).

The upper layers of the bedrock were sandstone and mudstone (the term used for a clay shale by workers at Highvale) with much of it displaced by glacial action. The underlying coal seams were less than 30 metres from the surface.

Overburden stripping created a benched slope with the upper part as high as 15 metres and at an angle of 45°. The lower slope, or highwall, stood 15 to 18 metres above the coal deposit also at a 45° slope. Failures during 1983 and 1984 extended over 100 metres behind the highwall crest (Barron et al, 1986) and severely damaged the bench on which the dragline operated. The failures were slow to develop and gave enough warning for the dragline to operate safely without the need for remedial measures.

In 1985, the frequency of failures tapered off, and those that did occur did not jeopardize the operating bench. In 1987, this author noted remedial measures were necessary as the highwall height had increased to 20 metres and the failures began to pose a risk to the dragline. One method to stabilize the failed area was to construct an "extended bench" or buttress by dumping spoil (waste material) against a potentially dangerous highwall. Then, as the dragline proceeded through the area and continued stripping the overburden, it had to re-excavate the spoil buttress, incurring extra costs due to rehandling.

Field investigations and laboratory testing from 1984 to 1986 (Moell et al 1984, Fenton et al 1986, Barron et al 1986, Wade and Peterson 1986) concluded that the failures were composite block type movements along a horizontal slip surface with a steep backscarp. The horizontal slip surface was either in the upper part of the mudstone above the coal or a seam of bentonite at the base of the mudstone.

Stability analyses performed by Wade and Peterson (1986) used effective stresses and made assumptions about the water pressures. The water pressures at the highwall were extrapolated from piezometers located well behind the highwall crest and did not reflect any changes due to rebound. Furthermore, laboratory strengths were applied in the analyses and did not consider the effects of excavation.

Residual strength parameters were assumed along the basal slip surface.

With the above assumptions, the failures were successfully back analysed, however, later findings by this author found lower pore pressures and rock strengths than those assumed which, in turn, could also adequately explain the failures.

Barron et al (1986) noted numerous tension cracks as a result of the large failures that extended well back from the highwall crest and developed a multiple-block, plane shear mechanism to model them. This model used effective stresses, assumed the bentonite to be the rupture surface, a water table perched on the failure plane, and vertical tension cracks extending to the slip surface.

The effect of excavation was modelled by the development of tension cracks. During the analysis, a tensile strength could be applied over the potential crack and adjusted to simulate field conditions. The multiple block model developed by Barron et al (1986) was used to match the location of tension cracks that opened in the field during a failure. The model was found to be sensitive to variations in the assumed water table and the authors concluded that to improve highwall design the most logical method would be to lower the water table. The amount of reduction required to significantly improve stability was never field tested.

The Highvale Coal Mine was the site for this investigation that began in 1987. The contributions made by the above authors are discussed in greater detail throughout this thesis.

1.4 Current Stability Techniques

Current practice applies two-dimensional, limit equilibrium techniques that utilize effective stresses to assess the stability of a highwall. Coates (1981) and Fredlund (1984) provide a detailed review of these methods. Given the proper failure mechanism, pore pressures, and strengths adjusted for excavation rebound, then these methods are effective. However, limit equilibrium techniques cannot account for the deformation characteristics of the materials.

A superb example of this was at the Centralia Mine (section 1.3.2) where several metres of slip developed along a weak bentonite, yet the slope had not collapsed. Since the slope had not completely failed, then the Factor of Safety would have been greater than unity from limit equilibrium analyses, but these analyses could not predict the amount of deformation. At the Centralia Mine, an adequate Factor of Safety was the only criterion necessary for the operation of the mine. If a deformation criterion was required, i.e. that the movements had to be less than a few metres, then the limit equilibrium method would not be applicable.

More advanced methods of stress analysis, particularly the finite element method (FEM), can satisfy both the stability and deformation criteria. The finite element method can model the actual behaviour of a slope and indicate the stresses and displacements at any point within it. The finite element method is now being employed in a variety of geotechnical problems and is planned to model the highwall at the Highvale Coal Mine.

1.5 Distinguishing Features of this Thesis

The combination of field observation, instrumentation, and laboratory testing has been successfully used by others in assessing highwall performance. Six features distinguish this thesis from other, similar investigations at Highvale and other open pit coal mines:

1. The field instrumentation was designed to detect the first effects of stress relief due to excavation. Most studies implemented monitoring schemes after substantial movement had previously taken place (i.e. surveying the highwall face).
2. The field work was concentrated in a small area so that similar data could be gathered after each cut to improve the quality of information.
3. Instrumentation was maintained until it was immediately at the highwall crest. Previously,

the closest that any instrument had been maintained was 100 metres away from the highwall.

4. Global, or absolute, movements were found. That is, the total displacement of an individual point was measured from its state of rest to when it was excavated out. It is common to measure local displacements relative to a certain point that has previously undergone some displacement.
5. The absolute displacements were converted to a strain field in the rock beyond the highwall face which was then used as a measure of how much the rock/soil stretched. Local displacements found along one or more shear zones do not clearly demonstrate this.
6. A relationship between the strength of the rock mass and strains due to excavation was attempted.

1.6 Thesis Organization

Chapter 2 introduces the Highvale Mine and mining method while the field work is outlined in Chapter 3. The results of the field program are outlined in Chapter 4 where the zones of movement, deformations, and pore pressures are presented. Chapter 5 reviews the laboratory testing program that provided guidelines on the rock strength unaffected by excavation. Chapter 6 describes a failure in the highwall that was analysed to explore the mechanism of strength reduction. Chapter 7 discusses how the findings of this thesis may be applied to future highwall design, monitoring, and remedial measures.

2 DESCRIPTION OF STUDY AREA - PIT 03, HIGHVALE MINE

2.1 Location

The Highvale Mine, shown in Figure 2.1, is located 80 km west of Edmonton, Alberta on the south shore of Wabamun Lake. TransAlta Utilities Corporation (TAU) operates Highvale, one of the largest strip mining operations in Canada, and producing one fifth of Canada's coal (Canadian Mining Handbook, 1987).

Presently, three pits (Pit 02 to 04) are active at Highvale, providing enough coal to generate half of Alberta's power (TransAlta Utilities, 1986) from the nearby Sundance and Keephills power plants.

TAU has kindly permitted the University of Alberta to perform the field investigation program in Pit 03 at the Highvale Mine.

2.2 Physiography

The Highvale Coal Mine is found on the Alberta Plains, a subdivision of the Interior Plains Physiographic Province. Bedrock is typically flatlying with surface elevations about 750 metres. South of the mine, rolling hills rise to elevations over 800 metres.

2.3 Bedrock Geology

Coal is found at depths of 20 to 40 metres, overlain by sand-, silt-, and mudstones of the Paskapoo Formation, Tertiary to Upper Cretaceous in age (Moell et al 1984 and Fenton et al 1986). The rock is cemented to uncemented with traces of montmorillonite found in the sandstone but predominating the silt- and mudstones. A 100 mm seam of bentonite rests just above the coal and is continuous throughout the study area. This thin seam is a major factor affecting the stability of the highwall, often acting as the basal shear plane for potential failures.

The coal is a non-marine, Upper Cretaceous and Paleocene rock, part of the Ardley Coal Zone. Several distinct and continuous seams of coal are separated by silt- and mudstone partings. In general, the dip of the coal and overburden is less than 10 metres per kilometre in a westerly to southwesterly direction.

2.4 Glacial Tectonics

Glaciers advancing over Western Canada and Northern United States exerted tremendous forces on the soft bedrock, shifting, crushing, and shearing it. This damage to the bedrock by glaciers is termed glacial tectonics, ice thrusting, or glaciotectonic deformation. Extreme cases of glacial tectonism occurred when the continental ice sheet pushed against a sloping face. Then, like a bulldozer, it pushed against a sloping face. Then, like a bulldozer, it thrusted the rock ahead of it, fracturing the bedrock and inducing shear zones at the base of the thrust block.

Tsui (1988) and Fenton et al (1986) discuss glaciotectonic deformation and its effect on the bedrock, with particular emphasis on the Highvale Mine, where glacial tectonism is a major factor in highwall stability. The fractures and shear zones created by ice thrusting have impaired the stability of potential slide masses by reducing the strength along the backscarp and creating shear zones that can be reactivated.

Tsui (1988) and Fenton et al (1986) noted thrust blocks displaced 280 to 860 metres from their original position and over 400 metres by 1200 metres in size. During this study, spectacular evidence of glacial tectonism was uncovered by mining in Pit 04, 2.5 kilometres from the study area in Pit 03, Figure 2.2(a). Overburden stripping and subsequent coal mining afforded an excellent opportunity to view the stratigraphy on a large scale.

As shown in Figure 2.2(b), the surface till was underlain by a layer of coal and a siltstone. Beneath this was another layer of glacial till, an unusual occurrence but evidence that the coal and siltstone above had been displaced during glacial times. This was confirmed by a shear plane that was found at the contact between this till and the siltstone above it.

The lower till was underlain by the Paskapoo Formation and Ardley Coal Zone. Further investigation revealed that the coal near the surface was similar to the lower seams of the Ardley Zone, except that it was 40 metres higher. The pre-glacial valley now occupied by Wabamun Lake offered an opportunity for the glaciers to shove a block of bedrock approximately 4 kilometres south.

Much of the thrust block had been mined before this study began, however it was estimated to be over 500 metres long and 200 metres wide. One question remained unanswered: could the exposure in Pit 04 be the bottom of a much larger thrust block with the upper seams of coal and overburden possibly carried further southward? Future coring programs and mining will shed light on this question.

Mining had to be restricted in the vicinity of the thrust block in Pit 04 because failures of the highwall and slope above the bench had so destroyed the area, that it was impassable by the dragline.

Glacial tectonics may explain the intense jointing and pre-sheared zones encountered at Highvale, however, depositional processes, past regional tectonic events, permafrost, and weathering could also be responsible. All of these factors previously contributed to a change in structure, groundwater flows, and strength but this study looks at how these components were further altered by the next process: excavation.

2.5 Mining Method

Figure 2.3 is a schematic of the strip mining procedure used at Highvale. Fifteen to 40 metres of till, sandstone and mudstone overburden, were removed by a dragline sidecast operation in strips 50 metres wide and hundreds of metres long. The dragline took 70 cubic metres of overburden in a single scoop and dumped it on the spoil piles.

Figure 2.3 shows the dragline sitting on a bench that was created during the previous cut. The overburden below the bench and above the coal was removed by "facecutting" that exposed the highwall. Excavation of overburden above the bench is called "chopcutting". At the study site, the highwall was 20 to 23 metres high at an angle of 40° to 50°. The chopcut, or slope above the bench, was 7 to 10 metres high at a 1H:1V slope. Chopcutting had two roles: firstly to create a competent bench for the dragline to walk back on after it completed a strip, and secondly, to control the height of the highwall.

With the overburden removed, electric shovels mined the six horizontally bedded seams of coal. Each seam was from 0.50 to three metres thick, separated by thin partings of silt- and mudstone, resulting in a coal deposit 15 metres thick. The coal was mined so that the exposed face was nearly vertical, referred to in this thesis as a coalwall, and when combined with the highwall, resulted in a rock slope 35 metres high at an average angle of 55° to 60°.

2.6 Influence of Coalwall

The 15 metre high coalwall also experienced instability. However, the failures were small and generally occurred after all the coal had been mined out and did not pose a threat to mining equipment or men nor having little influence on the bench. For these reasons, coalwall stability was not directly investigated, but instead considered integral to highwall stability since significant deformations in the coal reduced the strength of the overburden bedrock.

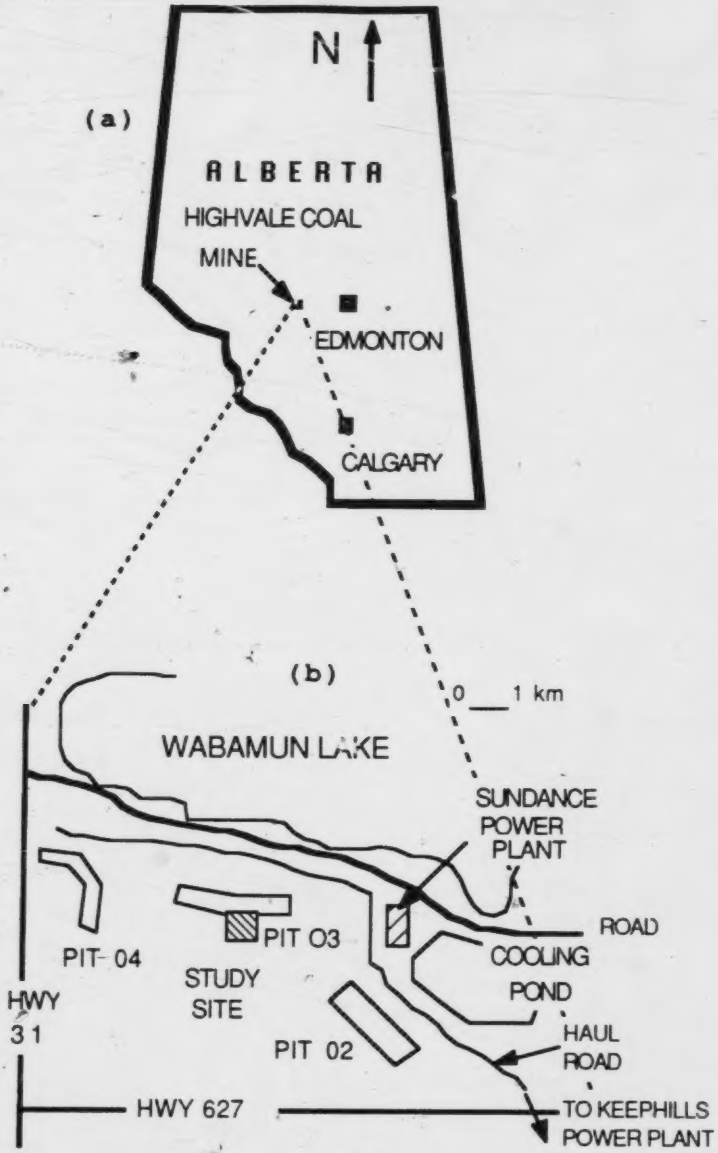
(a)
N
ALBERTA
HIGHVALE COAL MINE
EDMONTON
CALGARY
(b)
0 1 km
WABAMUN LAKE
SUNDANCE POWER PLANT
ROAD
PIT 04
PIT 03
STUDY SITE
COOLING POND
HWY 31
PIT 02
HAUL ROAD
HWY 627
TO KEEPHILLS POWER PLANT

Figure 2.1 Location of the (a) Highvale Coal Mine and (b) the study site in Pit 03.

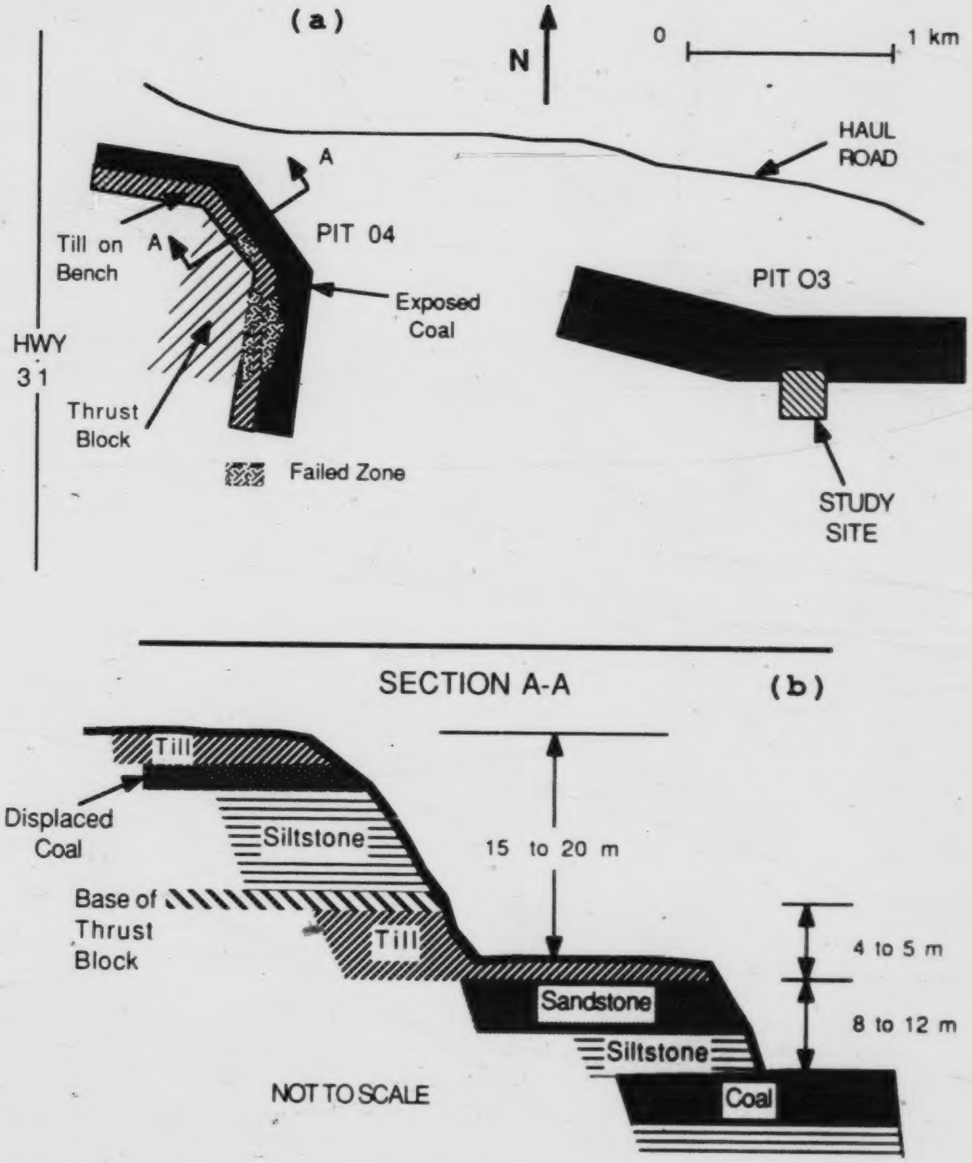
(a)
N
0
1 km
HAUL ROAD
A
A
PIT 04
Till on Bench
Exposed Coal
HWY 31
Thrust Block
Failed Zone
PIT O3
STUDY SITE
SECTION A-A
(b)
Till
Displaced Coal
Siltstone
15 to 20 m
Base of Thrust Block
Till
4 to 5 m
Sandstone
8 to 12 m
Siltstone
NOT TO SCALE
Coal

Figure 2.2 Evidence of Glacial Tectonism in Pit 04 at the Highvale Mine (a) location of thrust block and (b) section through thrust block.

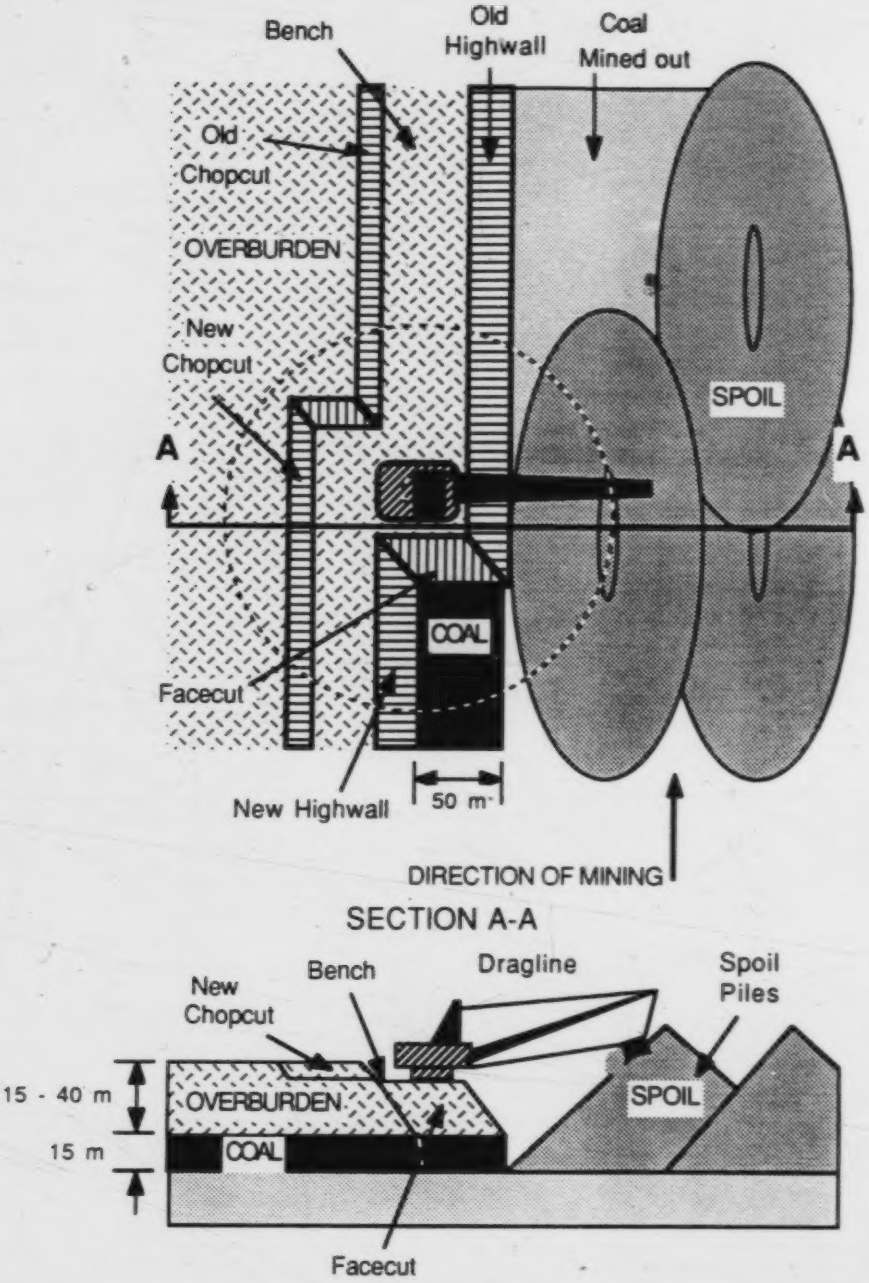
Bench
Old Highwall
Coal Mined out
Old Chopcut
OVERBURDEN
New Chopcut
SPOIL
A
A
COAL
Facecut
New Highwall
50 m
DIRECTION OF MINING
SECTION A-A
New Chopcut
Bench
Dragline
Spoil Piles
15 - 40 m
OVERBURDEN
SPOIL
15 m
COAL
Facecut

Figure 2.3 Schematic of Mining Method at the Highvale Coal Mine.

3 FIELD INVESTIGATION PROGRAM

The field investigation in Pit 03 at the Highvale Mine began in June, 1987. Thirteen boreholes boreholes were drilled, with sampling done in four of them, and five of the holes logged with downhole geophysics. Each hole had instrumentation installed to monitor the response of the overburden to successive excavations.

Chapter 3 describes the study site in Pit 03 and outlines the techniques used in the field investigation program, beginning with the drilling and sampling and concluding with the instrument installation. The results are brought together in Chapter 4.

3.1 Study Site

Figure 3.1 shows a plan view of the study site as it appeared in June, 1987 after six inclinometers, S1 to S6, and fourteen piezometers, P7 to P13, were installed. Figures 3.2 and 3.3 present cross sections through each of the instrument lines. This site in Pit 03 was selected for the following reasons:

1. The highwall in Pit 03 had a history of instability with numerous past studies conducted;
2. These studies showed that glacial tectonics had moderately affected the bedrock in the vicinity of

the study site and that future failures were likely;

3. The geology at the study area was expected to be typical of several other parts of the mine, such that results from this thesis might be extended elsewhere at Highvale;
4. Mining would be active in Pit 03, with three new strips excavated during the study program;
5. The highwall and surface geometry were not complex. That is, the highwall angle would be reasonably constant from one cut to the next, the chopcut was not very high, and the original ground surface was almost flat.
6. Site access was possible year round.

3.2 Drilling and Sampling Program

Mobile Augers and Research Limited performed the drilling and sampling under the author's supervision. A drill rig capable of supporting wet rotary and auger drilling was brought on site for three weeks in June, 1987. The instrumentation scheme called for 13 holes (section 3.6) and since monitoring the overburden behaviour was of prime importance, then the amount of sampling was sacrificed in favour of total length drilled. Only three of the holes, S3, S4, and S6, were continuously sampled from the surface. A fourth, S5, was sampled below a depth of 25 metres. The remaining nine holes were drilled blind with a solid stem auger.

Sampling was performed with four continuous coring systems: wireline CHD 76 Double Tube; conventional NHR Double Tube; conventional HW double tube; and the wireline NQ-3 triple tube. These were chosen to obtain the best quality and largest possible core diameter. The CHD 76 system worked best, providing good quality core at rapid drilling rates.

The Pitcher Sampler was also used, but met with limited success. In theory, the Pitcher Sampler combined the best of sampling techniques by incorporating a shelby tube into a core barrel. It worked well for three samples in the sandstone until the shelby tube became seized inside the core barrel and rotated with the barrel, destroying the sample. This was probably the result of an improper bit and lack of drilling mud in the circulating water. The bit was designed for mudstone and wore too rapidly in the sandstone, creating a "tight" hole that restricted the flow of circulating water carrying cuttings to the surface. The problem was compounded when pure water was used without a polymer additive (drilling mud) to help retain the cuttings in the water. This led to a build up at the bit and the cuttings forcing their way back inside the Pitcher Sampler between the sample tube and core barrel, locking the two together.

The key to the success of the blind drilling program was the "DP Rock Bit" attached to the end of a six inch (150 mm) diameter solid stem auger. In a matter of minutes, the drill rig could be converted from wet rotary to auger drilling and with this bit, 35 metre deep holes were drilled from the surface to three metres into the coal in a few hours. Other auger drilling in the area had failed to reach the top of the mudstone because they were only outfitted with a standard wing bit. The "DP Rock Bit" had replaceable carbide teeth that easily cut through the soft sandstone and mudstone creating holes ideal for the installation of piezometers and inclinometers. Continuous coring of every hole would have resulted in a severe cutback in the total number of holes drilled and the amount of instrumentation installed.

The borehole logs are presented in Appendix A and summarized by the lithology shown in section 4.1.

3.3 Downhole Geophysical Logging

As discussed in section 3.2, not all of the holes could be sampled and therefore to confirm the geology at low cost, downhole geophysical logging was used. Moreover, the geophysics located strata for instrument placement when sampling was omitted. BPB Geophysics provided the following suite of geophysical tools:

- Gamma Ray, Bulk Density, and Borehole Caliper;
- Focussed Electric;
- Multichannel Sonic;
- Neutron Porosity.

The dipmeter was considered, however it's expense did not warrant use. The theory and mechanics of each tool are beyond the scope of this thesis and only the relative trends from the logs were used in the development of the lithology. The set of geophysical logs for hole S3 and S4 is shown in figures 3.4 and 3.5 with the remainder presented in Appendix B. The till, sandstone, shale, and coal seams are clear on these logs.

3.4 Geological Mapping

After each cut was made, the author mapped the highwall face to locate discontinuities, confirm lithology, and detail shear zones. Two vertical traverse lines were established along the highwall face, 50 metres apart, directly in front of the study site. The bentonite and lower part of the mudstone unit could be examined from the top of the exposed coal (top of seam 1). The upper mudstone and lower sandstone were examined by ascending the highwall face in a "cherry picker".

Since Tsui (1988) had extensively mapped discontinuities in the sandstone at a location near the study site, the joint mapping was limited to ensuring that Tsui's findings could also be applied at the study site. Hence, the focus of the geological mapping was on the lithology and identification of shear planes and zones. These results are summarized in section 4.1.

3.5 Deformation Monitoring

The most important factor controlling the layout and depth of the boreholes was the instrumentation to monitor deformations of the highwall. In designing the monitoring scheme, seven points were recognized:

1. In any excavation, the exposed face would move out from a few millimetres to metres without ultimate failure, depending on the material strength and deformation properties and the size of cut. Based on experience from other excavations made in Central Alberta (Vesta Mine, Jenkins 1988), horizontal movements before failure were anticipated to be of the order of centimetres. In addition, vertical movements dependent on the mechanism, were also expected to reach centimetres.
2. Potential modes of movements came from the past studies by Tsui (1988), Barron et al (1986), Fenton et al (1986), and Wade and Peterson (1986), and Moell et al (1984). They indicated that the primary mode would be a translational block or planar shear action, as shown in Figure 3.6, with secondary rotational failures near the highwall crest. In addition, exfoliation from the highwall face was expected to be commonplace.

3. The deformation monitoring program had to detect when movements began and their extent. For a 35 metre high rock slope (the highwall and coalwall combined) movements were estimated to extend approximately two to three times this distance beyond the highwall, or 70 to 100 metres. Therefore, the instruments had to be located at least this far back from the highwall. (In fact, the movements extended 300 metres from the crest.)
4. With successive excavations, then the effect of each cut at different distances from the highwall was tracked by a series of instruments.
5. Although the bedrock was generally flatlying and uniform in the vertical dimension, extreme variations in the geology could be found over a short horizontal distance, possibly as a result of glacial tectonism. Hence, to obtain high quality information, the instrument spacing was not large.
6. Instrument failures were anticipated and therefore redundancy was incorporated into the design.
7. The focus of the study was on highwall stability. As such, the emphasis of the monitoring program was on the overburden above the coal with movements within the coal secondary.

Based on these considerations, six vertical inclinometers (S1 to S6 in Figure 3.1) were installed on two lines, 50 metres apart, perpendicular to the highwall crest, with a pair of inclinometers on each of three strips. Five of the inclinometers penetrated 3 metres into the coal with the sixth 12 metres below the top of coal. The target depth for the sixth inclinometer was originally 6 metres deeper so that it would be 3 metres below the base of the coal but it failed to achieve this depth.

Survey support was implemented from two control reference points well behind the highwall face (BM 1 and BM 2 in Figure 3.1) to provide for redundancy and to track movements of the inclinometers. Additional details of the monitoring program are described by Small and Peterson (1988) and reviewed below.

3.5.1 Inclinometers

Six vertical inclinometers were installed to monitor horizontal displacements in the sandstone, shale, bentonite, and upper coal seams (figure 3.1). S1, S2, S3, S5, and S6 were SINCO (Slope Indicator Company) brand measuring horizontal movements while the sixth (S4) was TRI-VEC manufactured by SOLEXPERTS and measured vertical displacements as well.

The SINCO inclinometers consisted of 70 mm diameter continuous ABS casing with two sets of orthogonal grooves that guided a probe. Two servo-accelerometers in the probe measured its angle from vertical and given the length of the probe, the location of its top with respect to its bottom could be found. Guiding the probe along the casing length yielded the casing shape and any changes in the shape over time were attributed to movements. Further details on the principle of the SINCO inclinometer are provided by Dunnicliff (1988) and Small and Peterson (1988).

The TRI-VEC also utilized a casing that guided a probe containing a servo-accelerometer but similarities with the SINCO end there. Koppel et al (1983) detail the operation of the TRI-VEC system. The casing was 60 mm in diameter without any grooves and came in one metre lengths joined together by sliding couplings. The probe was one metre long and attached to aluminum rods that guided it into the casing and between two couplings. The ends of the probe and insides of the couplings were designed to mate such that the probe could be locked into place between the couplings. This guaranteed that the probe would return to the same location each time a reading was taken. A single servo-accelerometer measured the vertical angle, defining the location of the probe top relative to its bottom (similar to the SINCO system).

The inclinometer casing for both systems was grouted into the boreholes by pumping grout from the bottom of the borehole upward. This attempted to prevent voids from developing between the casing and borehole wall. In one installation, S2, groundwater probably washed away some of the grout after it was placed, allowing the casing to bend within the hole and change its shape. The change in shape was first attributed to movements, however further investigation indicated a flexing of the casing.

3.5.2 Maintenance of Inclinometers

The use of inclinometers was ideal from a logistics point of view when several cuts were made over the course of the study and the instrumentation had to be maintained throughout. New cuts were made in June, 1987, September, 1987, December, 1987, March, 1988, May, 1988, and September, 1988. Figures 3.7 to 3.10 show the locations of the inclinometers along line S2-S4-S6 after each cut was made. The situation was similar along S1-S3-S5.

As the dragline passed by the site on a new strip, some of the inclinometers had to be buried or lowered or both. Before a cut was made in December, 1987, S1, S2, and the accompanying piezometers had to be buried beneath the bench so that they would not be destroyed as the dragline passed by. After the new highwall was created in December, then S1 and S2 (now at the highwall crest) were recovered, brought back to the new bench level, and reactivated. A short time later, S3 and S4 were lowered from the original ground elevation to the new bench level.

In March, 1988 the process was repeated and this time S1 and S2 were destroyed, S3 and S4 were buried and then recovered (Figures 3.9 and 3.10). S5 and S6 were not lowered to the new bench level until May, 1988, just before the dragline made another pass. At that time, the inclinometers were lowered to beneath the expected level of the new bench and buried. After the dragline passed the site, then these were reactivated. S6 was damaged in this procedure and became inoperative. It was the only one of six to be destroyed before the dragline excavated them out.

The inclinometer results are presented in section 4.2 in conjunction with the survey findings. In this manner, the total displacement of a point was obtained.

3.5.3 Surveying

Surveys were performed to find the horizontal coordinates of the tops of the inclinometers as outlined by Small and Peterson (1988). Position accuracies of five millimetres or less were attained by using a one second theodolite, an electronic distance measuring device, numerous redundant readings, and least squares adjustment techniques. Two concrete monuments, BM 1 and BM 2, were installed 200 metres behind the inclinometers (figure 3.1) and located in the TransAlta Utilities (TAU) coordinate system in July, 1987.

Initially, the monuments were assumed fixed throughout the monitoring program. But as a check, a nail on a power pole one kilometre west of the site and 700 metres south of mining activities was set as a reference point. As the monitoring program neared completion and the successive highwalls moved closer to the two monuments, the sights to the nail indicated that the initial assumption was incorrect and that the monuments had in fact moved about 50 mm toward the highwall. This was confirmed in May, 1988 by a second traverse that again tied BM's 1 and 2 into TAU's system, and hence tracked their absolute position.

Since the monuments were located absolutely, then so were any other points referred to them. Therefore, the absolute movement of the tops of the inclinometers could be tracked and one of the primary concerns of the monitoring program was achieved: obtaining the global movements.

Furthermore, given the shape of the casing from the probe readings, any point along the casing length could be tracked similarly. Of particular importance was the displacement of the inclinometer base, since all six experienced large movements at their bottoms. The locations of the zones of movements could not be confirmed but it was suspected that much of it occurred in the mudstone between seams 4 and 5 of the coal.

The survey support provided an additional bonus when an inclinometer was rendered inoperative by excessive movement along a shear plane. When this occurred then the inclinometer casing would be pinched, preventing the probe from passing below this point and therefore losing the base as a reference point. The surveys enabled a continuous record of movements to be maintained by tracking the displacement of a point just above the shear plane.

The results from the surveys are presented in section 4.2 coupled with the inclinometers to provide the global deformation pattern.

3.5.4 Alternative Methods to Monitor Highwall Deformations

Other monitoring techniques were evaluated such as surveying to the highwall face, horizontal extensometers installed in the highwall, and wireline extensometers strung over the slope. But, each method suffered a common drawback: the highwall face acted as the reference point and all movements were relative to the position of the face immediately after excavation. By the time these schemes were implemented, a substantial portion of the total movement may have already developed.

This study found that a point in the bedrock began to feel the effects of excavation approximately 300 metres behind the highwall face and gradually shifted toward the pit with each successive cut. Any monitoring methods that used the highwall as a reference point would not be able to track the extent of movements. Furthermore, such techniques would have to await the excavation of the highwall. By the time the highwall was exposed, this study found that as much as 50% of the total movements had already developed. These would go undected by measurements to the highwall face and 50% of the movements record would be lost. While this may be acceptable in some circumstances, this thesis required that the total deformations be found so that the strains may be determined.

Furthermore, installation and maintenance of the other schemes would be difficult: surveys would have to be conducted from the spoil piles which were unstable reference points; the highwall face was not safe for installing horizontal extensometers; and wires on the ground could be easily destroyed by mine equipment.

On the other hand, vertical inclinometers could be installed far ahead of mining to provide a continuous deformation record. Their maintenance was simple and, when combined with survey support from two safe control points well behind the highwall face, they provided an absolute record of movements.

3.6 Piezometers

Two types of piezometers were used: pneumatic piezometers installed in the low permeability mudstone and sealed open standpipes placed in the sandstone.

The pneumatic piezometer, or pneumatic-pressure transducer, was supplied by Slope Indicator Company (SINCO). The general operation of the pneumatic piezometer is outlined by Dunnicliff (1988).

The sealed tip standpipe was a 50 mm (two inch) PVC pipe with a slotted screen at the bottom. To measure water pressure at a point, the borehole was sealed immediately above and below the screen so that the water level in the pipe represented the total head of water at the slotted screen.

The piezometers were installed in seven boreholes drilled with a solid stem auger adjacent to the inclinometer holes as shown in Figure 3.1. Figures 3.2 and 3.3 show the two piezometers in each hole, one at the bottom and the other at least two metres above it. Four holes had two pneumatics, while the remaining three had one pneumatic at the bottom and a sealed tip standpipe above. The holes were numbered P7 to P13 with the lower piezometer further qualified with a "B" and the upper one with a "T".

At least two piezometers were installed in every zone of interest (i.e. sandstone, mudstone, and coal) to provide redundancy and to act as a backup when one was inoperative. The piezometer holes were drilled near the inclinometer holes in order to monitor pore pressures along potential shear planes detected by the inclinometer.

The piezometers were maintained in conjunction with the inclinometers (Section 3.5.2 and Figures 3.7 tp 3.10) so that they were kept in operation until they were excavated out.

For both types of piezometers, the tips were encased in sand to allow water easy access to the tip. Bentonite seals over one metre long were placed above and below the tips to isolate them from the strata on either side. Sand was also used to separate the two piezometers in a hole and grout was pumped in above the uppermost seal. Care was taken during installation to ensure that the target depth was attained and that the sand, bentonite seal, and grout were properly placed. This arrangement appeared to work well, with only one of the seals around a standpipe showing signs of leaking. After installation was complete, one pneumatic piezometer did not work (P8-B) and a second one failed in October, 1987 when water penetrated the hose and froze, plugging it.

The hydrogeology of the study site as obtained from the piezometers is presented in section 4.3.

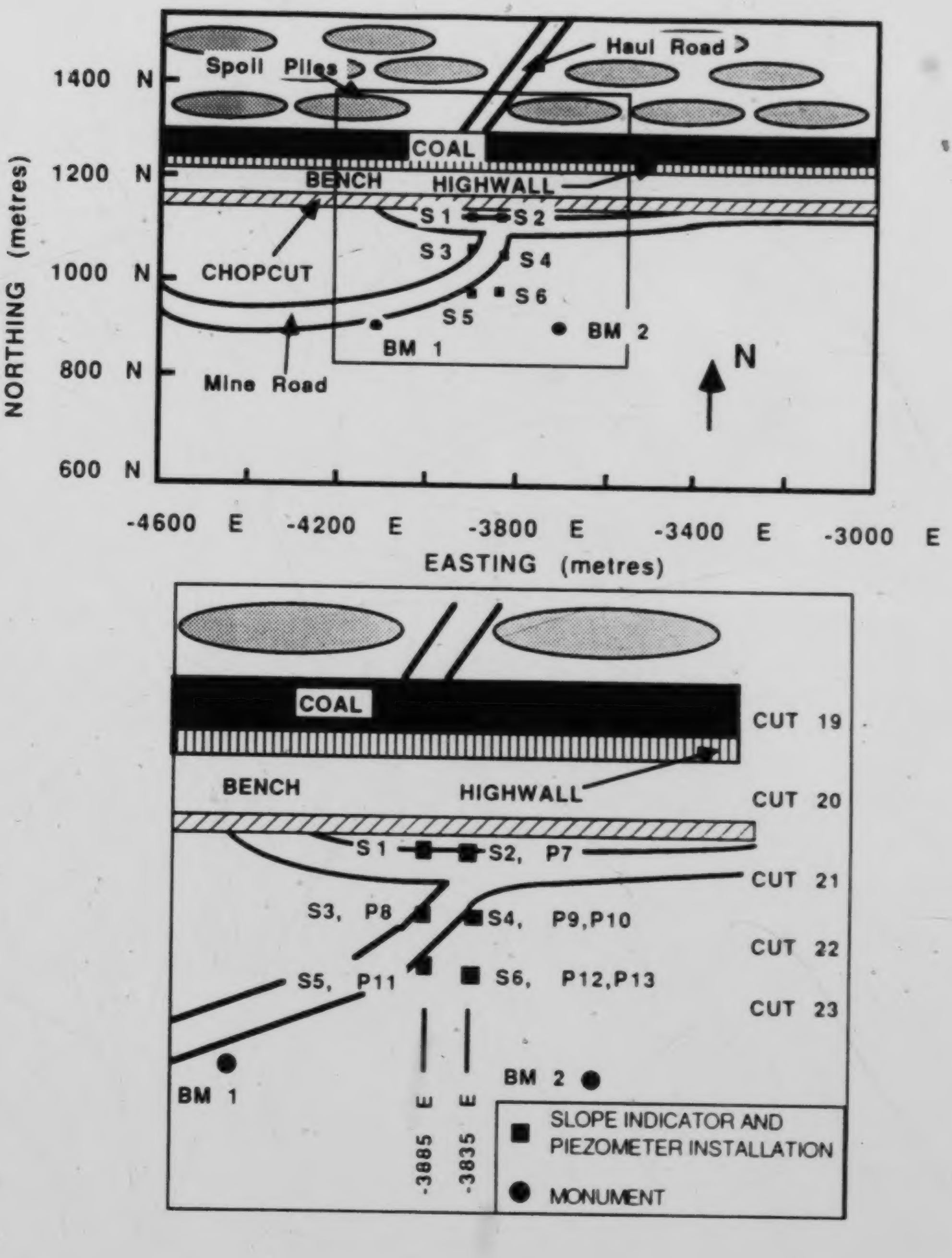
Haul Road
Spoil Piles
1400 N
1200 N
1000 N
800 N
600 N
NORTHING (metres)
COAL
BENCH
HIGHWALL
CHOPCUT
S 1
S 2
S 3
S 4
S 5
S 6
BM 1
BM 2
Mine Road
N
-4600 E
-4200 E
-3800 E
-3400 E
-3000 E
EASTING (metres)
COAL
CUT 19
BENCH
HIGHWALL
CUT 20
S 1
S2, P7
CUT 21
S3, P8
S4, P9,P10
CUT 22
S5, P11
S6, P12,P13
CUT 23
BM 1
BM 2
-3885 E
-3835 E
SLOPE INDICATOR AND PIEZOMETER INSTALLATION
MONUMENT

Figure 3.1 Plan view of study site, June, 1987

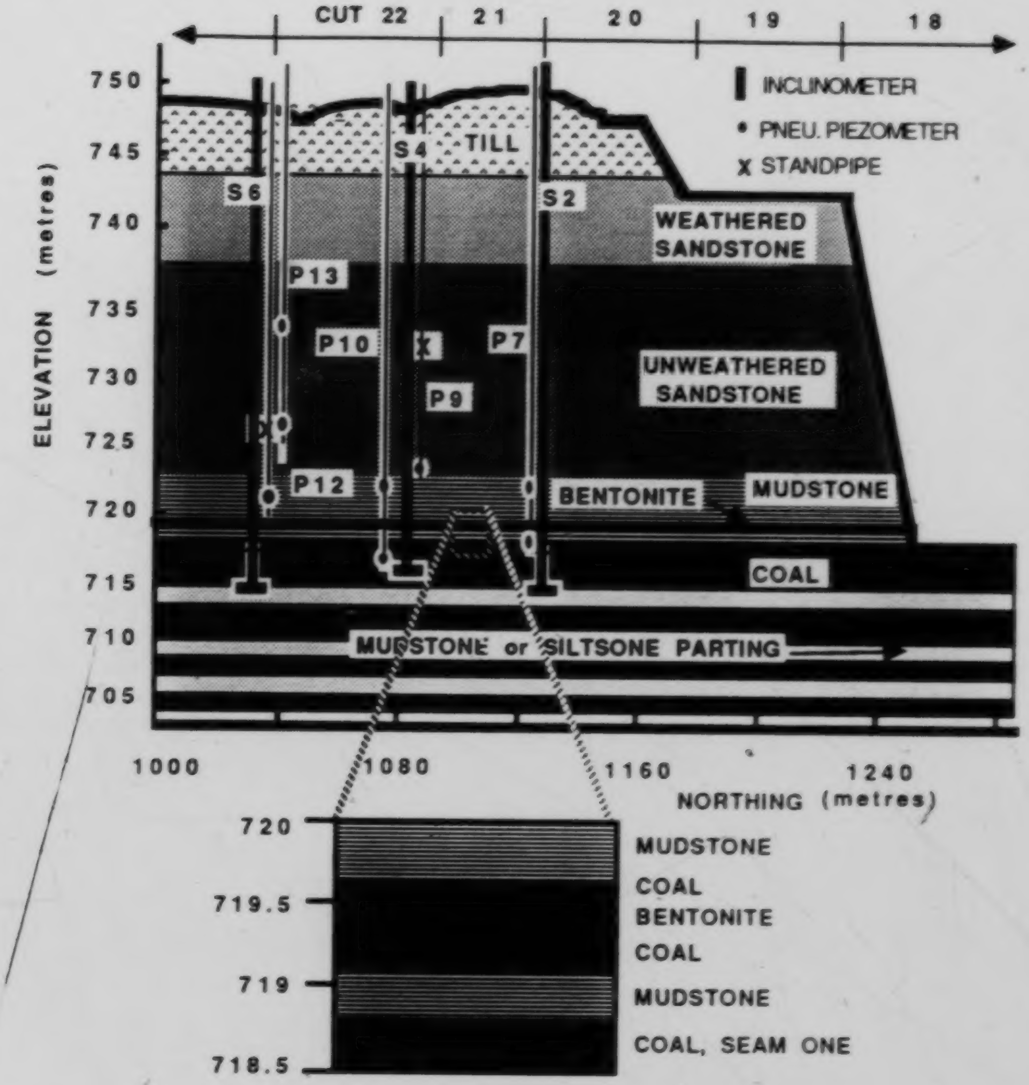
CUT 22
21
20
19
18
INCLINOMETER
PNEU. PIEZOMETER
X STANDPIPE
750
745
740
735
730
725
720
715
710
705
ELEVATION (metres)
TILL
S6
S4
S2
WEATHERED SANDSTONE
P13
P10
P7
P9
UNWEATHERED SANDSTONE
P12
BENTONITE
MUDSTONE
COAL
MUDSTONE or SILTSONE PARTING
1000
1080
1160
1240
NORTHING (metres)
720
719.5
719
718.5
MUDSTONE
COAL
BENTONITE
COAL
MUDSTONE
COAL, SEAM ONE

Figure 3.2 Cross section at study site, Station 3835, Line S2-S4-S6, June, 1987

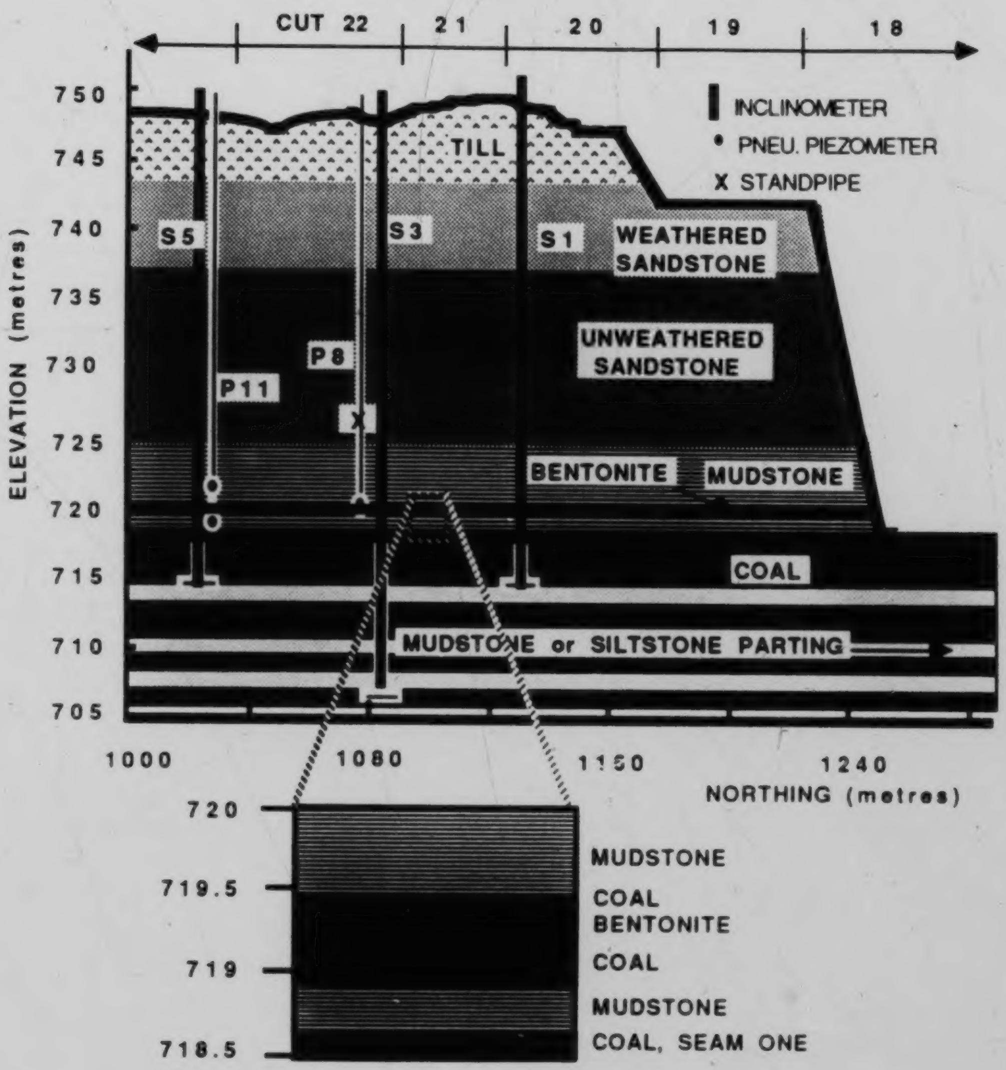
CUT 22
21
20
19
18
INCLINOMETER
PNEU. PIEZOMETER
X STANDPIPE
ELEVATION (metres)
750
745
740
735
730
725
720
715
710
705
TILL
S5
S3
S1
WEATHERED SANDSTONE
UNWEATHERED SANDSTONE
P8
P11
X
BENTONITE
MUDSTONE
COAL
MUDSTONE or SILTSTONE PARTING
1000
1080
1160
1240
NORTHING (metres)
720
719.5
719
718.5
MUDSTONE
COAL
BENTONITE
COAL
MUDSTONE
COAL, SEAM ONE

Figure 3.3 Cross section at study site, Station 3885, Line S1-S3-S5, June, 1987

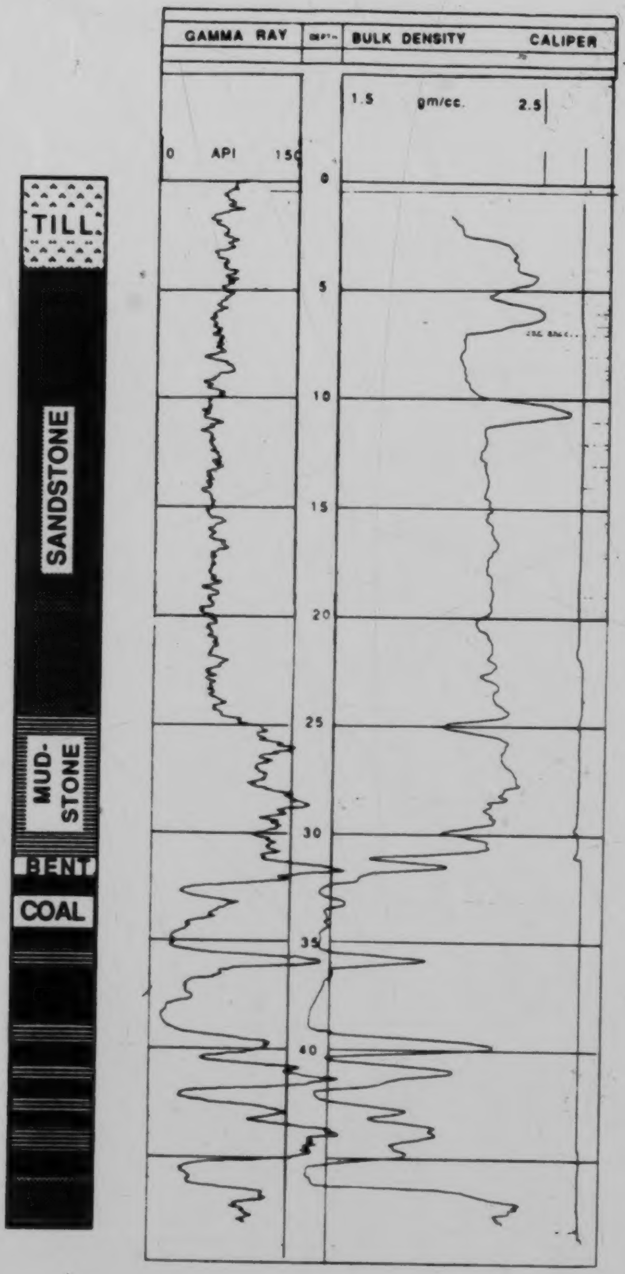

Figure 3.4 Gamma, Density, and Caliper geophysical logs for hole S3

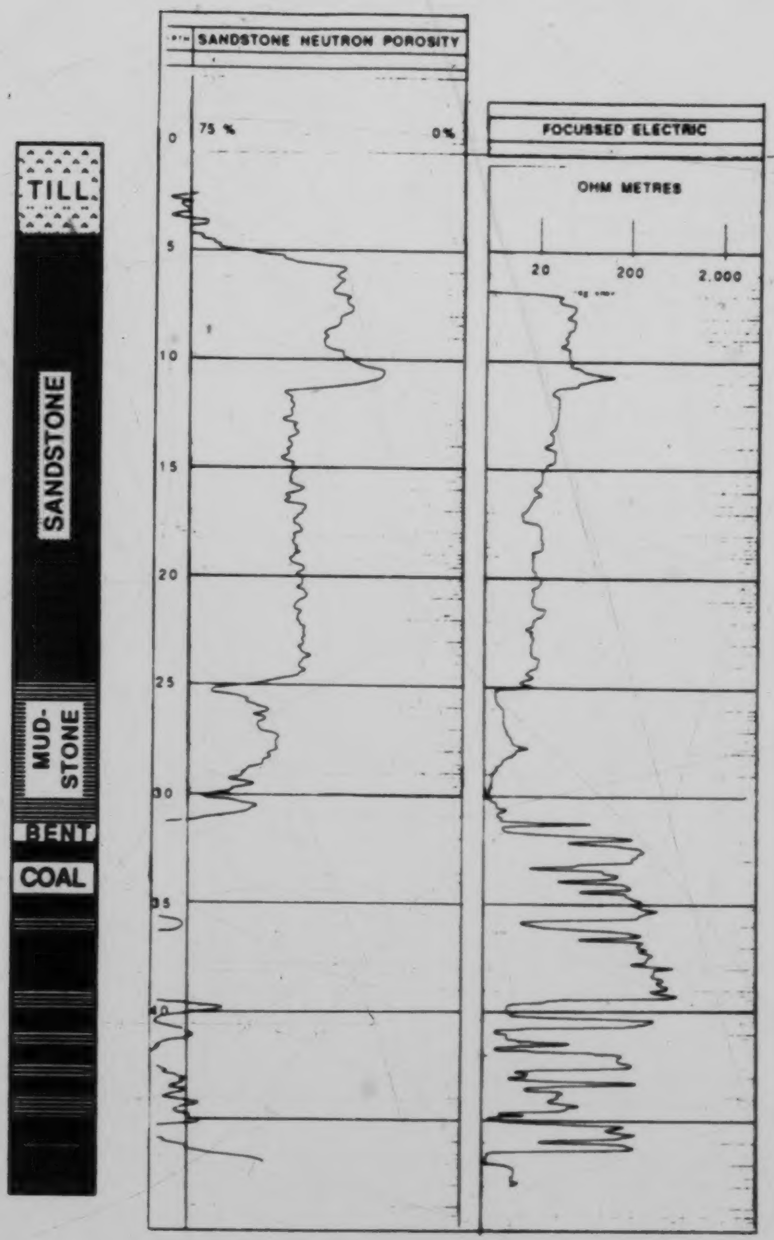

Figure 3.4 (cont'd) Neutron Porosity, and Focussed Electric Resistivity geophysical logs for hole S3

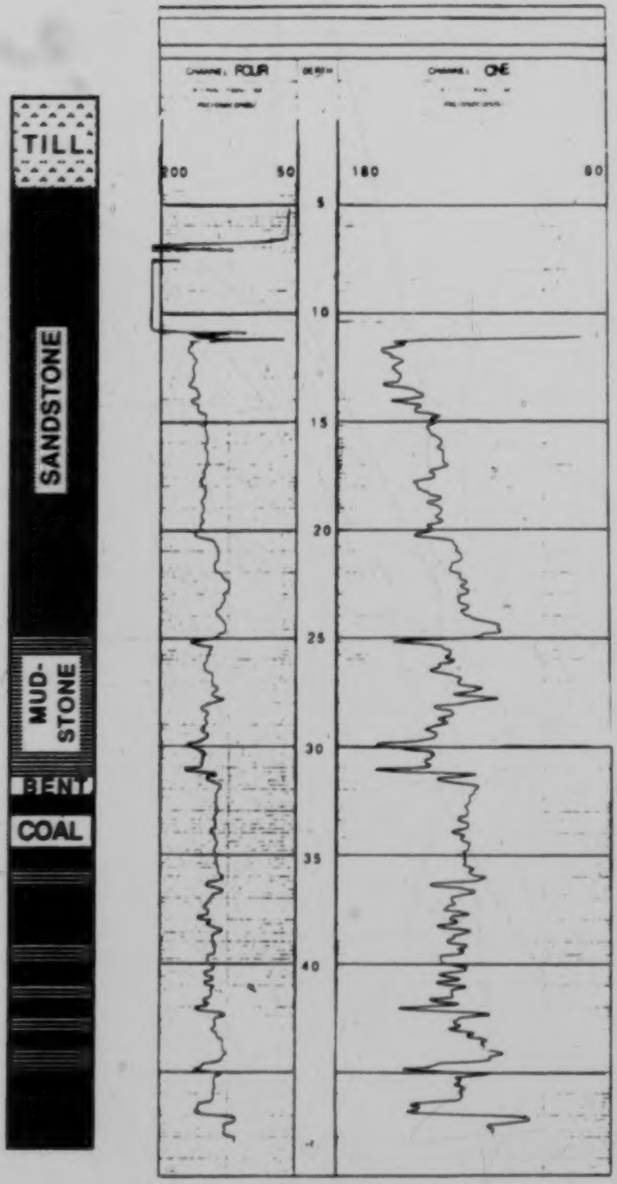

Figure 3.4 (cont'd) Multichannel Sonic geophysical logs for hole S3

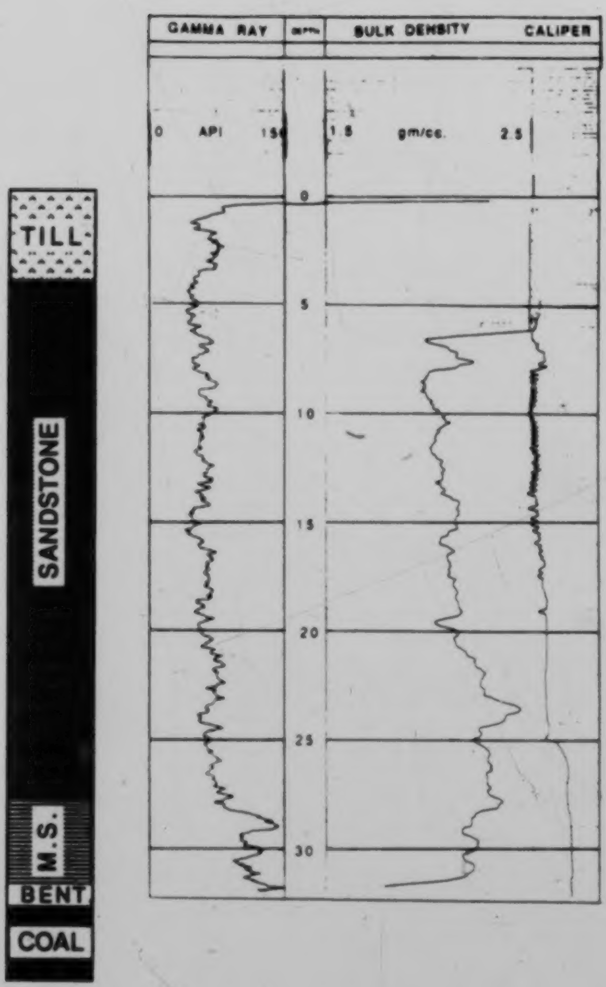

Figure 3.5 Gamma, Density, and Caliper geophysical logs for hole S4

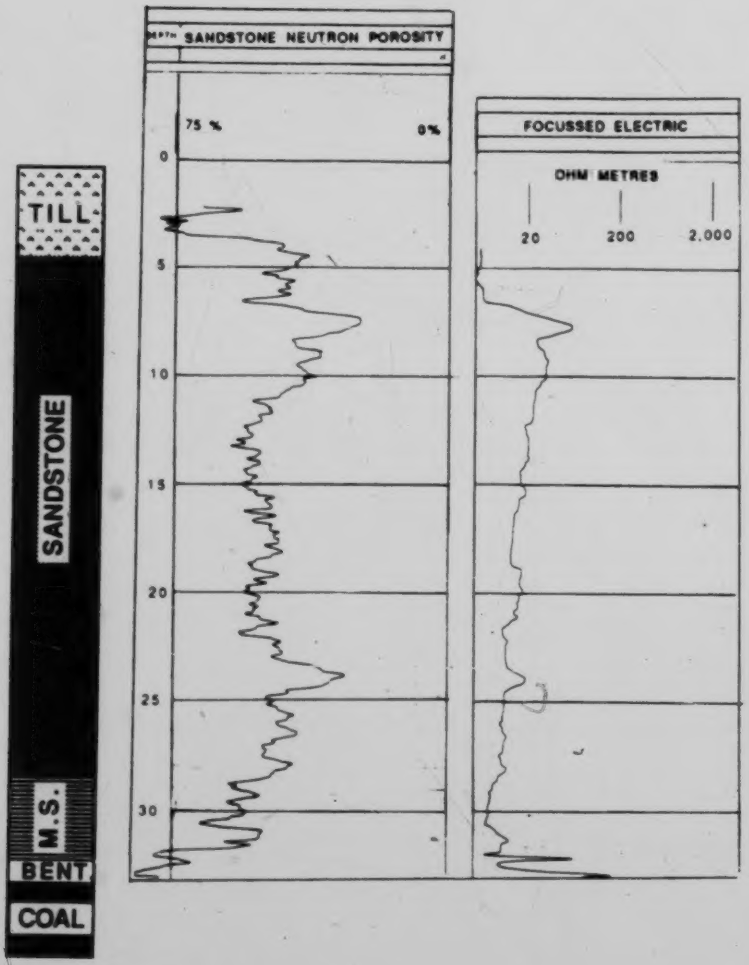

Figure 3.5 (cont'd) Neutron Porosity and Focussed Electric Resistivity geophysical logs for hole S4

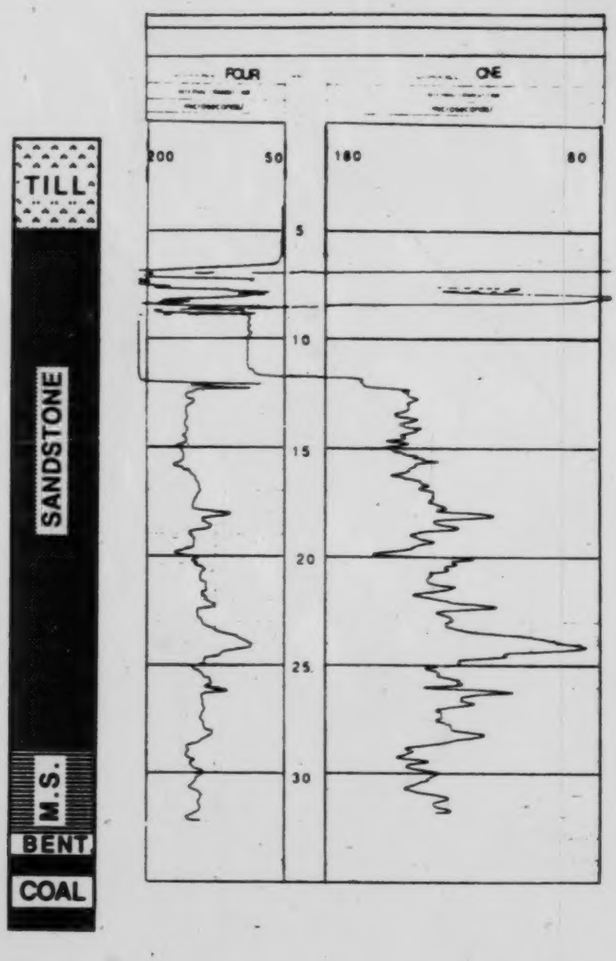

Figure 3.5 (cont'd) Multichannel Sonic geophysical logs for hole S4

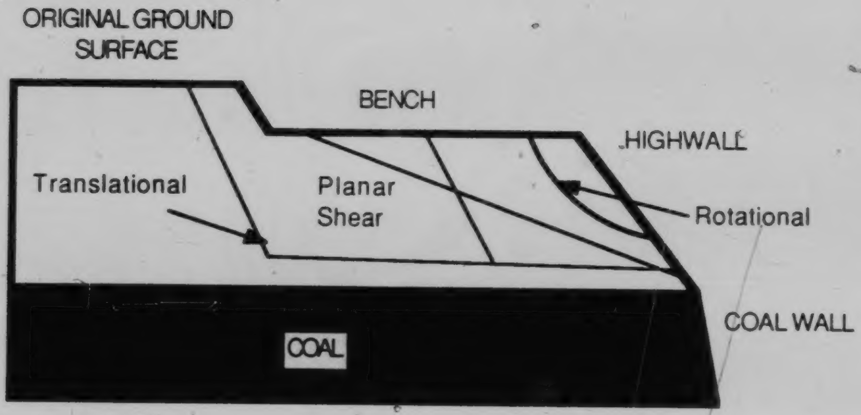
ORIGINAL GROUND SURFACE
BENCH
HIGHWALL
Translational
Planar Shear
Rotational
COAL WALL
COAL

Figure 3.6 Potential modes of highwall deformation

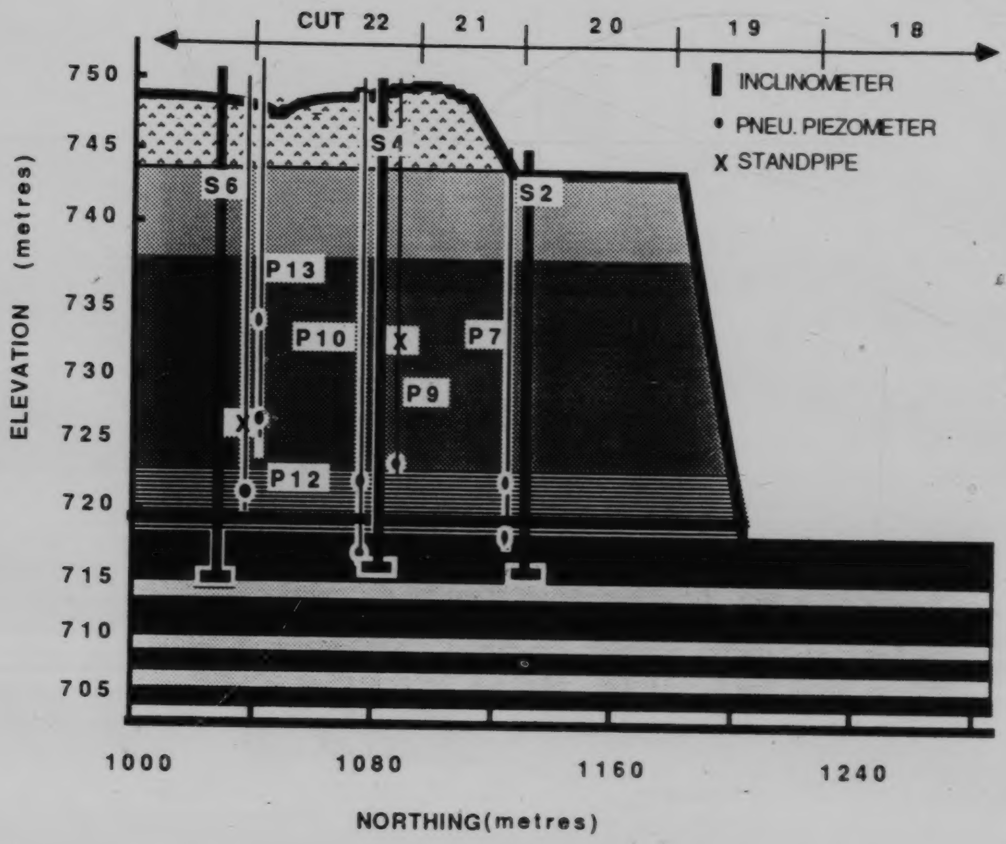
CUT 22
21
20
19
18
INCLINOMETER
PNEU. PIEZOMETER
X STANDPIPE
S6
S4
S2
P13
P10
X
P7
P9
X
P12
750
745
740
735
730
725
720
715
710
705
ELEVATION (metres)
1000
1080
1160
1240
NORTHING(metres)

Figure 3.7 Instrument status at Station 3835, September to December, 1987

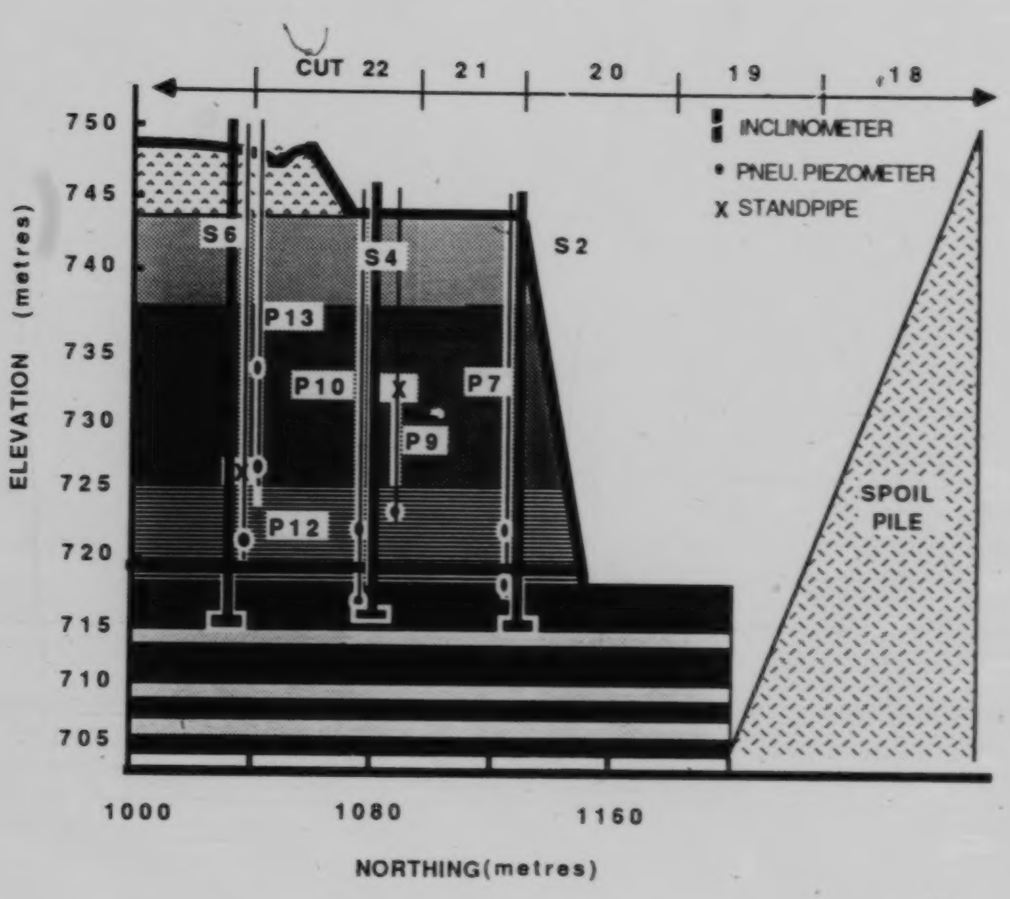
CUT 22
21
20
19
18
INCLINOMETER
PNEU. PIEZOMETER
X STANDPIPE
S6
S4
S2
P13
P10
X
P7
P9
P12
SPOIL PILE
750
745
740
735
730
725
720
715
710
705
ELEVATION (metres)
1000
1080
1160
NORTHING(metres)

Figure 3.8 Instrument status at Station 3835, December, 1987 to March, 1988

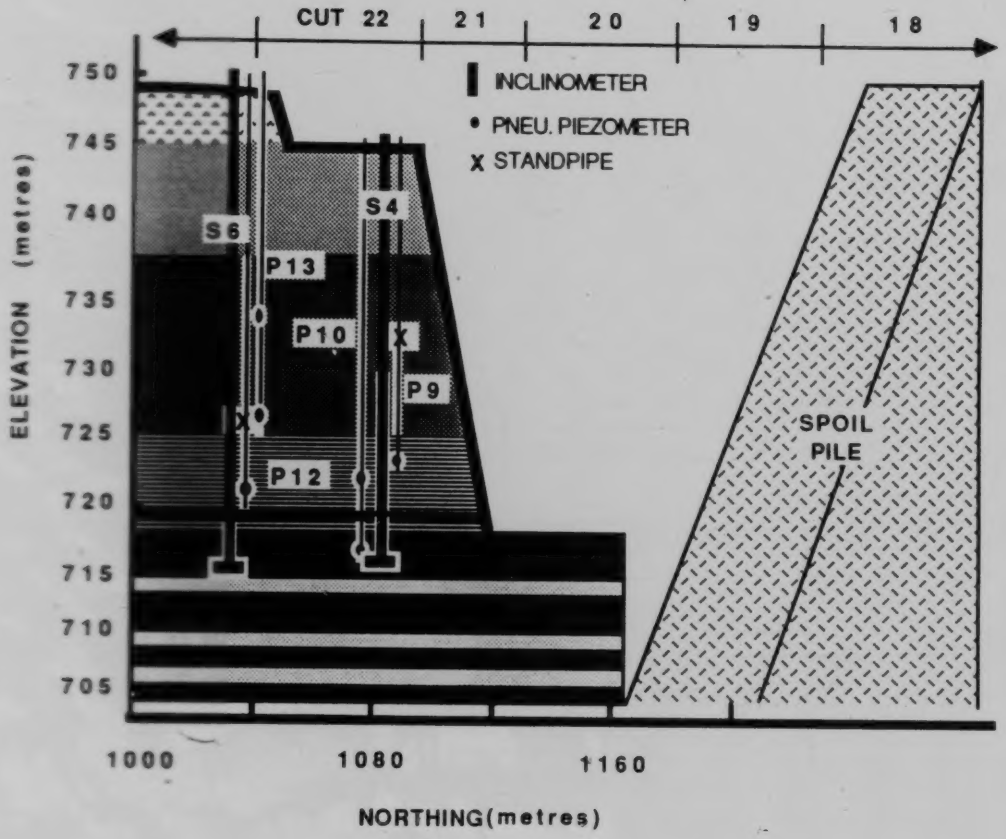
CUT 22
21
20
19
18
INCLINOMETER
PNEU. PIEZOMETER
X STANDPIPE
S6
S4
P13
P10
X
P9
X
P12
SPOIL PILE
750
745
740
735
730
725
720
715
710
705
ELEVATION (metres)
1000
1080
1160
NORTHING(metres)

Figure 3.9 Instrument status at Station 3835, March to May, 1988

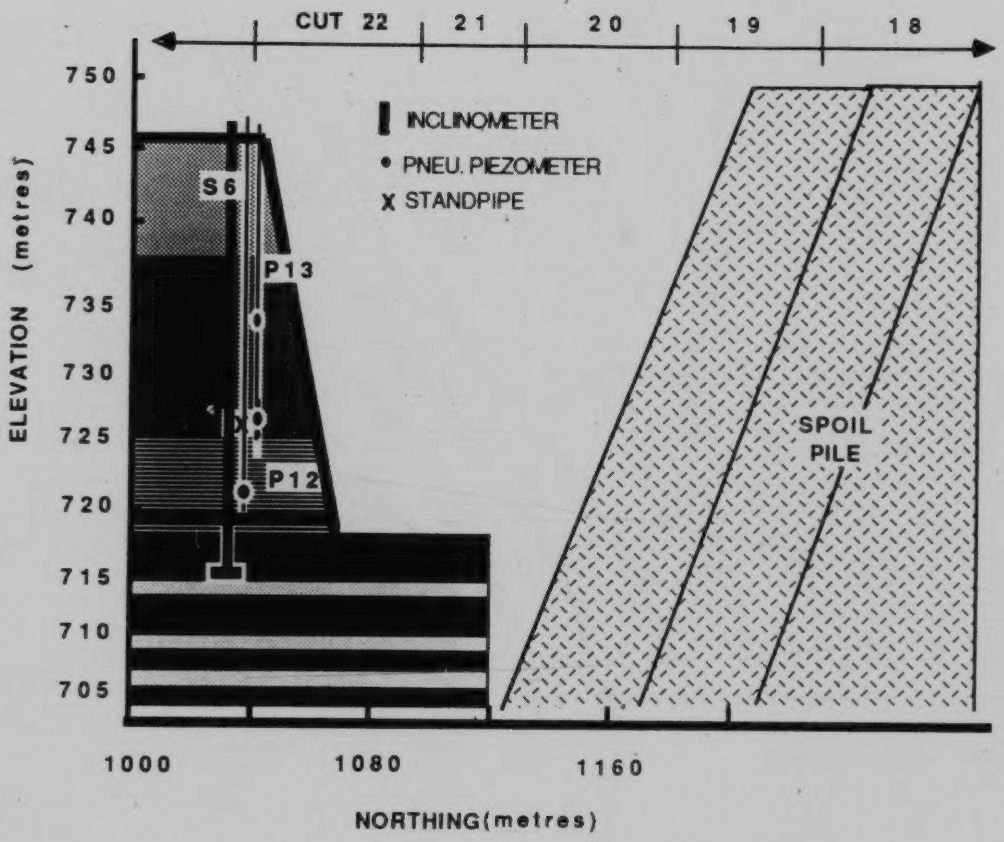
CUT 22
21
20
19
18
INCLINOMETER
PNEU. PIEZOMETER
X STANDPIPE
S6
P13
P12
SPOIL PILE
750
745
740
735
730
725
720
715
710
705
ELEVATION (metres)
1000
1080
1160
NORTHING(metres)

Figure 3.10 Instrument status at Station 3835, May to September, 1988

4 RESULTS OF FIELD INVESTIGATION PROGRAM

The aim of the field investigation program was to determine the lithology at the study site and measure pore pressure and deformation response due to excavation. The results of this program are presented below.

4.1 Lithology

The lithology was determined from geotechnical drilling and sampling, downhole geophysics, and geological mapping of the highwall face. Appendix A contains the borehole logs, and Appendix B the geophysical logs. Figure 4.1 summarizes this information.

The two to five metres of till over the sandstone was expected to have little influence on the stability of the highwall, and therefore was paid little regard.

4.1.1 Sandstone

The sandstone was fine to medium grained with a number of hard cemented layers, the most prominent at elevation 740 metres. Some coal stringers and thin mudstone layers were also recognized. Geophysical logging detected a second layer of high density at elevation 727 metres.

Bedding was near horizontal, and although parts of the sandstone were massive, most were heavily jointed. Three predominant joint sets were noted trending 165°/82° (dip direction/ dip), 65°/80, and 180°/84. Alternatively these joints were described as near vertical, striking East Northeast, North Northwest, and East-West.

Joint spacing was 10 to 30 centimetres for each set and created sandstone blocks. Some were separated with a clay infilling, 5 to 10 mm thick, while wider joints had a sand residue in them. More detailed joint surveys were not attempted since the blocks were small relative to the potential sliding masses. In addition it was difficult to discern which joints were the result of bench blasting and which ones were natural.

4.1.2 Sandstone/Mudstone Contact

The base of the sandstone was a distinct erosional surface cut into mudstone with an irregular shape over 50 metres. This surface is referred herein as the sandstone/ mudstone contact. The location and shape of the contact is shown in Figure 4.1.

On line S1-S3-S5 the contact was at elevation 725.5 metres while along line S2-S4-S6, the contact was at 723 metres. The mud- and siltstone sequence was the same for both lines between elevation 723 metres and the coal, indicating that the upper mudstone found along line S1-S3-S5 may have been eroded along S2-S4-S6 before the sand was laid down.

This difference was found to be associated with variations in the deformation behaviour of the highwall.

Movements were observed along the contact on line S1-S3-S5, however none were measured along the contact on line S2-S4-S6.

Extending back from the highwall face, the mudstone/ sandstone contact along both lines was almost flat, dipping about 0.5°.

After excavation of the highwall, this contact acted as the lower boundary for groundwater discharge from the sandstone.

Evidence of glacial tectonic action was apparent along the contact on line S1-S3-S5 where geophysical logs (Figure 3.4 and Appendix B) showed a marked drop in the density and the sonic logs indicated a crushed zone. This correlated well with the Alberta Research Council Findings (Moell et al, 1984) and it was conjectured that the contact may have been the basal shear plane of the ice thrust block. However, a similar trend was not found in holes S2-S4-S6 and casts this hypothesis in doubt.

4.1.3 Mudstone

Core samples and highwall mapping showed the mudstone had been crushed with jointing in numerous directions. Other terms used to describe the mudstone were shattered, brecciated, and broken (Moell et al, 1984). Short, discontinuous slickensides were detected along many joint contacts. The mudstone had several layers within it, varying in colours from blue-grey to brown with interbeds of carbon, clay clasts, siltstones, and coal. The mudstone was highly bentonitic.

4.1.4 Bentonite

A bentonite layer, 100 mm thick, was located just above the main coal sequence (Figures 3.2, 3.3, and 4.1). The bentonite was squeezed between two minor coal seams, 100 mm thick above and 300 mm thick below. The contact between these seams and the bentonite was wavy with amplitudes of less than one centimetre. Beneath the lower seam, lay 400 mm of mudstone, as shown in Figures 3.2, 3.3, and 4.1. At the highwall face, distinct shear planes were evident within the bentonite and at the contact with the upper coal layer.

A core of the bentonite taken in June, 1987 from hole S6 showed two slickensided surfaces as shown in Figure 4.2. One appeared as an undulating hairline crack within the sample and the other was at the contact with the upper coal layer. If the bentonite was pre-sheared, it would directly affect the stability analysis, controlling whether or not the peak or residual strength parameters could be used.

At the time of sampling, borehole S6 was over 200 metres from the highwall crest. As shown in Section 4.2.1, the monitoring clearly indicated that there was no movement in the bentonite until the highwall crest was 100 metres away. Therefore, any shear planes found in the bentonite were there before excavation began. Hence, it was concluded that the bentonite was presheared and that residual strength parameters should apply.

4.1.5 Coal Sequence

One borehole, S3, was cored to beneath the coal sequence for later installation of a deep inclinometer. The core from the coal seams and partings was not logged in detail, instead the coalwall was examined. The partings separating the economical coal seams typically consisted of siltstone and mudstone. The parting between seams 4 and 5 was of particular concern because it was highly bentonitic. Face mapping detected three shear planes within it, 2 to 5 cm apart, that formed a shear zone.

Siltstone lay beneath the coal sequence.

4.2 Deformations

As described in Section 3.5 six inclinometers were combined with survey support to provide an effective means of monitoring highwall deformations. The surveys enabled absolute movements to be determined, not just movements relative to an arbitrary point, such as the inclinometer base.

4.2.1 Results of Deformation Monitoring Program

The locations of the inclinometers are shown in Figure 3.1 and the complete data and survey results contained in

Appendix C. That Appendix details how the two techniques were combined to yield the global deformation patterns which are summarized in Figures 4.3 to 4.8 for each inclinometer. Movements into the pit were in the in the northward direction and are those reported in Figures 4.3 to 4.8. Eastward movements, parallel to the highwall, were less than 15 millimeters and were small enough to be neglected. A record of important dates related to the deformation monitoring program is provided in Appendix C.

Pattern and Magnitude of Movement

Inclinometers S1 to S5 were tracked until they were destroyed, while S6 was monitored until it was 50 metres from the highwall crest. Of interest is the amount of movement that developed beneath inclinometers S1 to S6. Figures 4.3 to 4.7 indicate that when the inclinometers had reached the highwall crest, their bases had moved 140 to 300 mm into the pit. Movements were likely along shear planes located beneath the inclinometers. As discussed in Section 4.1.5, the majority of movement was likely in a shear zone between coal seams 4 and 5.

Inclinometer S1 was pinched off just above the sandstone/mudstone contact probably due to a shear plane, Figure 4.3. Its new base at elevation 726.2 metres could still be tracked by the survey support.

Inclinometer S2, Figure 4.4, was assumed to have buckled in the borehole because movements into the slope were not likely. It pinched off just below elevation 719.0 metres, coincident with the bentonite seam. Before it was pinched, the inclinometer recorded movements of 50 millimeters within the bentonite.

Inclinometer S3 provided information along its entire length until three weeks after the final highwall was cut. Figure 4.5 shows two shear planes were activated at S3, one at the sandstone/mudstone contact and the second in the bentonite.

Inclinometer S4 was the TRI-VEC system (Section 3.5.1) which used a probe that was 30 cm longer than the SINCO probe and was slightly larger in diameter. As a result, this probe could not pass beyond bends in the inclinometer casing that the SINCO probe could. As a result, S4 became pinched at the bentonite seam when it was still 50 metres from the highwall crest, Figure 4.6. In addition, S4 experienced the largest amount of movements: more than 400 mm of deformation when it was at the highwall crest.

Inclinometer S5 moved as a rigid unit until it was at the highwall crest on May 18, 1988. At that time, slip planes were activated at the sandstone/mudstone contact and within the bentonite seam, Figure 4.7.

Inclinometer S6, Figure 4.8, measured substantial movements in the bentonite when the slope indicator was 50 metres away from the highwall crest.

Figures 4.9 to 4.14 show the movement of the inclinometers over time at elevation 730 metres, within the sandstone. The reader will note that at Day Zero, June 23, 1987, the inclinometers have all been assigned an initial value for movement. This reflects the amount of movement that likely developed before the inclinometers were installed on June 23, 1987. The assumed magnitudes are discussed further in Appendix C and were found to be reasonable.

Figures 4.9 to 4.14 indicate that when the inclinometer was more than 50 metres from the highwall face, then the movements stabilized in a matter of days after a highwall was cut. The same conclusion could be drawn with respect to the excavation of the coalwall, however the data was not as plentiful. Hence, it may be concluded that for points 50 metres and further from the crest, then the movements were instantaneous.

When the inclinometer was within 50 metres of the highwall crest, Figures 4.9 to 4.14 show that movements continued for some time after excavation of the highwall and coalwall. Beneath the highwall crest, the movements tended to creep at rates of 1 to 3.5 mm/day, often until when the next highwall was cut, 50 to 70 days later.

As Figures 4.3 to 4.14 show, the majority of movements were detected by surveying and not by the inclinometers. It became apparent that the inclinometers were best suited for determining the mode of movements (i.e. slip plane development). Hence, it is recommended that the combination of monitoring techniques described above should be applied in all subsequent deformation monitoring schemes at the Highvale Mine.

4.2.2 Deformation Mechanism

Figures 4.3 to 4.8 show that slip developed along discrete planes at the sandstone/mudstone contact and/or within the bentonite seam. Additional movements occurred beneath the inclinometers, possibly also along discrete planes. Figures 4.9 to 4.14 indicated that beyond 50 metres from the highwall crest, the movements were instantaneous and within 50 metres, creep was evident.

As the highwall rebounded into the pit, the overburden and coal experienced a stretching, as can be seen by comparing the inclinometers along line S1-S3-S5 or S2-S4-S6. For example, on February 15, 1988, Inclinometer S1 showed a movement of 360 mm in the sandstone, Figure 4.3, while S3 moved 110 mm at the same elevation, Figure 4.5. Hence, over the 50 metre interval between the two, the sandstone had stretched 250 mm by February 15, 1988.

The stretching could be accounted for by (i) an expansion of the sandstone blocks or (ii) a spreading of the vertical joints between the blocks. The majority of movements were likely taken up by spreading of the joints. Movements associated with expansion of the sandstone blocks would only develop upon stress relief when the sandstone was excavated. As the lower strata were removed, slip planes were activated and induced movement above them. Since there was no additional stress relief in the sandstone, then the movements could only be accounted for by a joint spreading.

The mechanism of joint spreading also occurred in the mudstone, bentonite, coal, and partings within the coal.

Within 50 metres of the highwall crest, creep continued along the slip planes for some time and caused a further widening of the joints.

4.2.3 Deformation Field

The deformation field is defined here as the variation in deformations, or movement, in the bedrock behind the excavated face. Determining the deformation field may be simplified by recognizing that the sand- and mudstone moved in a uniform manner, Figures 4.3 to 4.8, hence a single elevation, 730 metres, may be chosen in the sandstone to represent the deformation field for the entire sandstone unit. Similarly, elevation 721 metres was assumed to represent the deformation field in the mudstone. Since this study focussed on the highwall, the deformation field below the mudstone was not determined.

Figure 4.15 presents the deformation field at elevation 730 metres for the sandstone. It was found by selecting a specific day, say 238, February 15, 1988 and noting the deformations that occurred in each inclinometer at elevation 730 metres on February 15, 1988. These were then plotted against the horizontal distance from the highwall crest to obtain the deformation field, Figure 4.15.

The arithmetic plot in Figure 4.15 was converted to a semi-log graph, Figure 4.16 which showed a striking semi-log relationship. The intercept and slope of the line to satisfy the semi-log equation was found, where:

$$\text{Log } m = \text{Log } B + h\,M \quad \ldots\ldots\ldots\ldots\ldots\ldots (4.1)$$

With:

m = Movement into the pit (northward movement);

B = Intercept of straight line on semi-log plot (movement at the highwall crest);

h = Horizontal distance behind highwall crest;

M = Slope of semi-log line.

On Figure 4.16, a distinction was made between line S1-S3-S5 and line S2-S4-S6 because the deformation modes were not the same in the overburden. Figure 4.17 presents similar results for elevation 721 metres, in the mudstone, on day 238, February 15, 1988. Appendix D contains the complete results at elevations 730 and 721 metres for all 15 dates that a survey was conducted. The semi-log plots showed slight differences from day to day.

4.2.4 Movement Trend

A correlation was sought between the magnitude of movement and the time of excavation of the highwall and coalwall. Considering elevation 730 metres on day 238, and only line S2-S4-S6, the values of B and M at this time were 400 mm and -0.0070 respectively. Day 238 was 70 days after a new highwall was cut. By finding B and M and relating these parameters to when a highwall or coalwall was cut, Table 4.1 and Figures 4.18 and 4.19 were generated.

Aside from one data point, 4 days after the highwall was cut, Figure 4.18 shows B increasing from 175 mm and then stabilizing at 350 to 400 mm. The intercept M shows a similar trend, beginning at -0.0055 and then stabilizing at -0.0070. Figure 4.19 presents the movements measured after the coal was excavated from in front of the site. B increased from 310 to 400 mm immediately after excavation and then levelled off at 400 mm within two weeks. The slope, M stabilized at a value of -0.0064 in less than five days.

Figures 4.18 and 4.19 were used to investigate the creep characteristics of the bedrock. Both B and M stabilized within two to three weeks after either the highwall or coalwall were cut. From this, it was concluded that most

Table 4.1
Variations in the Semi-log Equation

Day Number	Days after H/W cut	B (mm)	M	Days after C/W cut	B (mm)	M
10	8	300	-0.0064			
36				4	310	-0.0064
44				12	350	-0.0064
57				25	400	-0.0064
71				40	400	-0.0064
92	0	175	-0.0055			
118	25	375	-0.0070			
150				8	400	-0.0064
155				13	400	-0.0064
173	4	375	-0.0090			
211	42	350	-0.0070			
238	70	400	-0.0070			
268	10	300	-0.0070			
295	37	350	-0.0070			
309				2	425	-0.0070

B = Intercept of semi-log line = movement at highwall crest.

M = Slope of semi-log line.

movement due to excavation was instantaneous or elastic rebound and that very little creep occurred. However, these figures reflected the general patterns over a distance of 300 metres behind the highwall crest and tended to mask the creep behaviour within 50 metres of the highwall crest, as noted in Figures 4.9 to 4.12.

By combining the results of Figures 4.18 and 4.19 the range of deformations observed at elevation 730 metres were summarized in Figure 4.20. This range of movements was then converted to a range of strains.

4.2.5 Strain Field

Given that the deformation field could be expressed as a function of horizontal distance from the highwall crest (Eqn. 4.1), then converting this field to a strain field was greatly simplified. Instead of discretizing the displacements and finding the average strain over a particular interval, a continuous function can be obtained for the strains by differentiating the deformation field.

The strain field is defined here as the variation in horizontal, or lateral strains, in the bedrock behind the excavated face. Differentiating the deformation field will result in an expression for the lateral strain field:

$$\varepsilon_L = \frac{dm}{dh} \quad \ldots\ldots\ldots\ldots\ldots\ldots\ldots\ldots\ldots\ldots (4.2)$$

where

ε_L = lateral strain, in this case it would be the axial strain experienced by the material in response to unloading and oriented toward the pit;

m = deformation into the pit;

h = horizontal distance beyond the crest of the highwall.

The differential becomes:

$$\varepsilon_L = -\ln 10 \cdot B \cdot M \cdot 10^{M \cdot h} \ldots\ldots \qquad (4.3)$$

The negative sign is included so that the lateral strains may be positive for presentation.

Figure 4.21 presents the range of strains in the sandstone behind the highwall by using equation 4.3 to convert Figure 4.20. All of the deformation field plots presented in Appendix D were likewise converted to strain filed plots.

4.3 Hydrogeology

Figures 3.1 to 3.3 present the locations of the 14 piezometers installed in the overburden and upper coal to measure pore pressures and their response due to excavation. Appendix F reports the variations in total head over time experienced by each piezometer, noting the dates of excavation and distance to the highwall crest. Figure 4.22

presents typical outputs from two of the piezometers located at the back of the study site.

4.3.1 Pore Pressure Response

As shown in Figure 4.22, pneumatic piezometers P13-T and P12-B were installed 200 metres from the highwall crest, and with successive highwall cuts moved 50 metres closer at a time. Pore pressures at P13-T, in the sandstone, appeared to be solely a function of drainage. Piezometer P12-B, in the mudstone, also showed only a drainage response until the highwall was 100 metres away. Then the trends became more interesting. When the highwall was cut 50 metres from the piezometer, pore pressures in the overconsolidated mudstone behaved in a classical fashion: dropping sharply in response to the stress relief and then recovering as steady state seepage was reestablished. A similar trend developed when the highwall was cut right in front of the piezometer.

4.3.2 Piezometric Model

To explore the impact of highwall rebound on the pore pressures, a piezometric model was prepared that summarized the pore pressure conditions throughout the overburden. The ultimate aim of this model was to see if the the groundwater flow regime was altered by the joints in the sandstone and mudstone spreading apart.

Development of the model began by considering the piezometric heads 200 metres from the crest and establishing the flow conditions at that location. For example,Figure 4.22 shows that when P13-T was 200 metres from the crest, the pressure head was 5.9 metres and when P12-B was 200 metres away, the pressure head in the mudstone was 10 metres. These results were plotted on Figure 4,23. In addition, the results from the other piezometers along line S2-S4-S6 when they were 200 metres away from the crest were plotted.

At 200 metres from the crest, the pressure heads in the sandstone satisfied a hydrostatic flow condition, indicating that there was no head loss in the vertical direction. The lower part of the mudstone and upper coal also seemed to fall along a hydrostatic trend, however, the pressures were lower than in the sandstone. It is probable that an impervious layer existed at the top of the mudstone that perched the water in the sandstone and confined the water below it.

Figure 4.24 was prepared in a similar manner for 150 metres from the crest and also shows a perched water table in the sandstone and a confined aquifer in the lower mudstone and upper coal. Comparing Figures 4.23 and 4.24, the pressure heads decreased with proximity to the highwall indicating horizontal flow to the face.

Figure 4.25 shows the pressure head distribution at 100 metres from the highwall and further illustrates the perched findings above. However, in the lower sandstone, a deviation developed from the hydrostatic condition.

At 50 metres from the highwall, the deviation noted in Figure 4.25 becomes extreme as shown in Figure 4.26. In the lower sandstone, flow has apparently changed from horizontal to vertical and the once impervious layer at the upper mudstone has breached.

The trends in Figure 4.26 are reinforced in Figure 4.27 as the predominant flow direction appears to be vertical as water from the sandstone flows through the mudstone into the coal.

Figures 4.27 to 4.29 present the pressure head beneath the highwall crest at different times after the highwall was cut. In Figure 4.27, at one to two weeks after the cut was made, the pore pressures in the sandstone and mudstone were low due to stress relief and vertical flow. As steady state seepage developed over the next two weeks, the pore pressures recovered as shown in Figures 4.28 and 4.29.

The observations in Figures 4.23 to 4.29 led to the development of the piezometric model, Figure 4.30, a schematic of the groundwater flow pattern in the overburden. Between 100 and 50 metres from the highwall crest, the groundwater flow changed from horizontal in the sandstone and mudstone to vertical from the sandstone into the mudstone and coal. The change in flow direction can be attributed to a breaching of an impervious layer at the upper mudstone as this layer stretched upon rebound, causing once tight joints to spread apart and allow water to flow through them.

4.4 Field Investigation Program Conclusions

The following conclusions were drawn from the field investigation program:

1. Bedding in the sandstone was near horizontal with near vertical joints trending Northeast, North North Northwest, and East-West. The joints were moderately spaced and for the most part free of clay infilling.
2. The sandstone/mudstone contact fingered over a distance of 10 metres and was higher along line S1-S3-S5 than line S2-S4-S6.
3. The mudstone was brecciated and highly bentonitic.
4. The 100 mm thick seam of bentonite at the base of the mudstone was presheared.
5. The combination of inclinometers and survey support were an effective means of monitoring absolute deformations in the bedrock.
6. The primary purpose of the inclinometers changed from tracking magnitudes of movement to determining modes of movement. The surveys took on the role of monitoring magnitudes.
7. The deformation pattern and magnitudes were different between lines S1-S3-S5 and S2-S4-S6.

8. As the highwall rebounded into the pit, vertical joints in the sandstone and mudstone spread slightly.
9. The deformation field in the sandstone and mudstone could be represented by the deformations at elevation 730 metres and 721 metres respectively. This was due to the extension of the materials.
10. Beyond a distance of 50 metres from the highwall crest, the movements after a highwall was cut were instantaneous. Within a distance of 50 metres, some creep did occur of the order of a few millimetres per day.
11. The deformation field could be easily converted to a field of lateral strains which was a measure of how much the overburden stretched and joints spread.
12. The hydrogeology at the study site was complex involving at least one water table perched above the mudstone. Beyond 100 metres from the highwall crest, the groundwater tended to flow horizontally toward the highwall face. Within a distance of 100 metres, the mudstone began to leak and allowed water to flow through it and into the coal. As a result the flow direction slowly changed to

vertical until at the highwall it was predominantly vertical into the coal.

13. Apparently, the major impact of highwall rebound is felt between 50 and 100 metres from the highwall. Creep was observed at 50 metres and the groundwater flow was changed between 50 and 100 metres.
14. This monitoring program succeeded in obtaining information, for the first time, in the critical zone within 100 metres of the highwall crest.

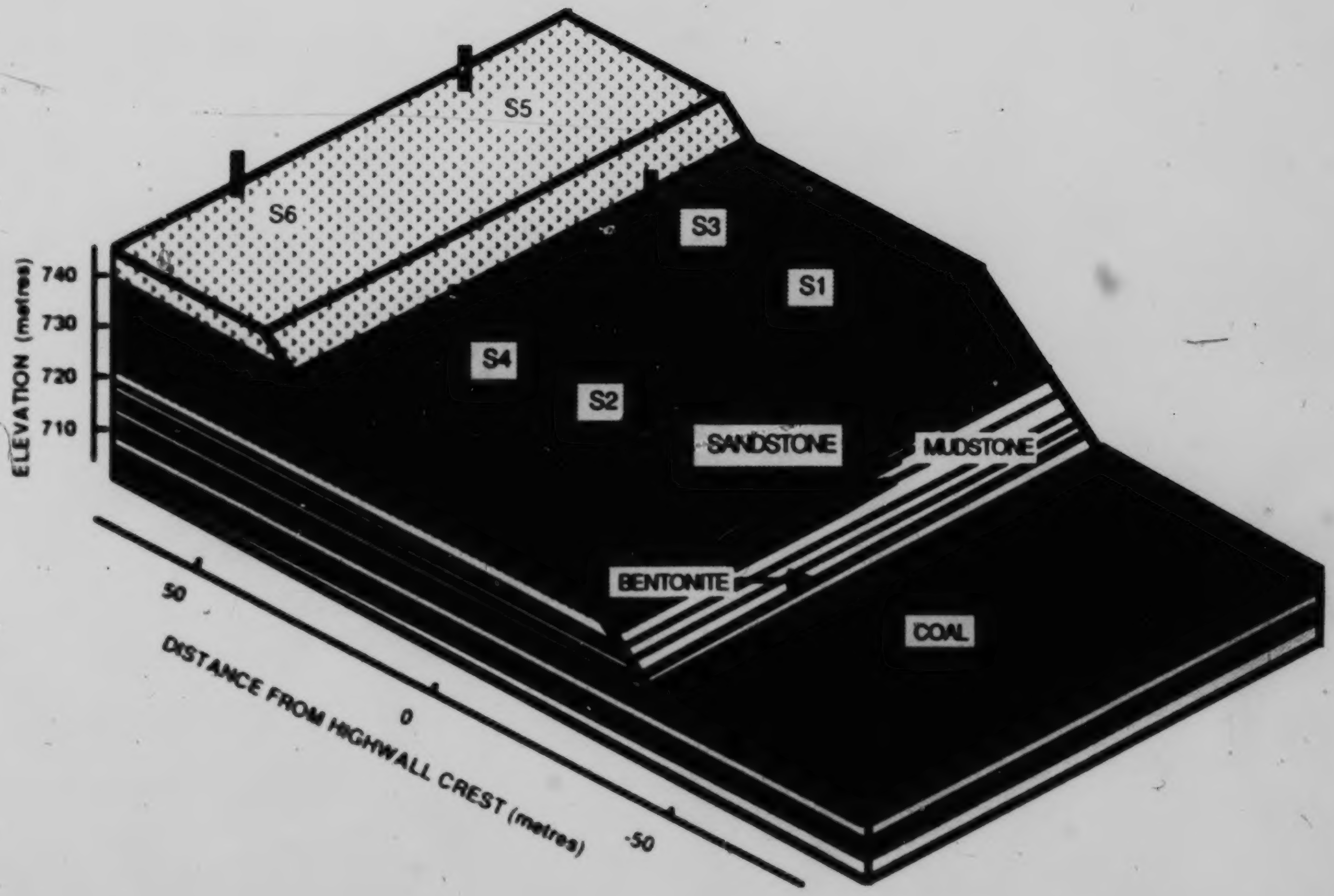

S5
S6
S3
S1
S4
S2
SANDSTONE
MUDSTONE
BENTONITE
COAL
740
730
720
710
ELEVATION (metres)
50
0
-50
DISTANCE FROM HIGHWALL CREST (metres)

Figure 4.1 : Lithology of study site from field investigation program

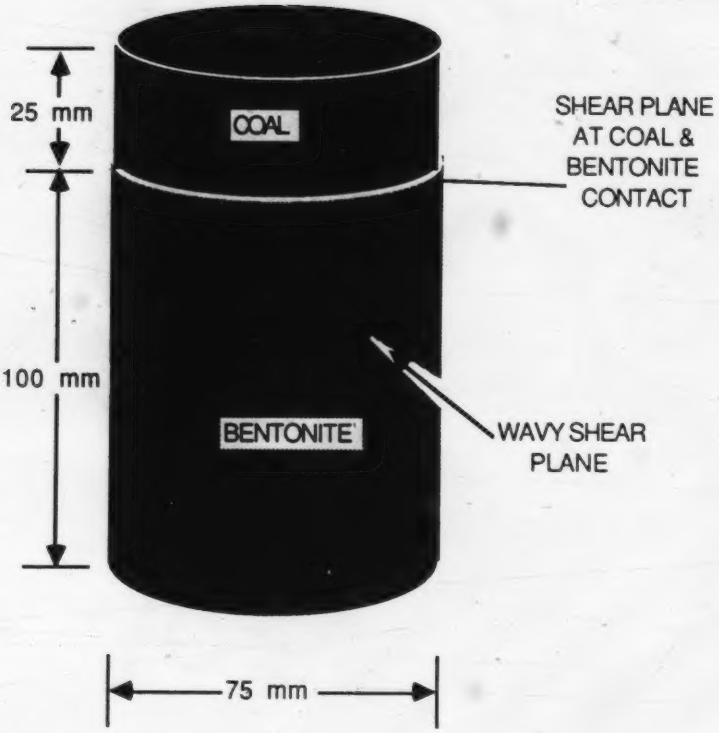
25 mm
COAL
SHEAR PLANE AT COAL & BENTONITE CONTACT
100 mm
BENTONITE
WAVY SHEAR PLANE
75 mm

Figure 4.2 Location of slickensides observed in core taken from hole S6, June, 1987

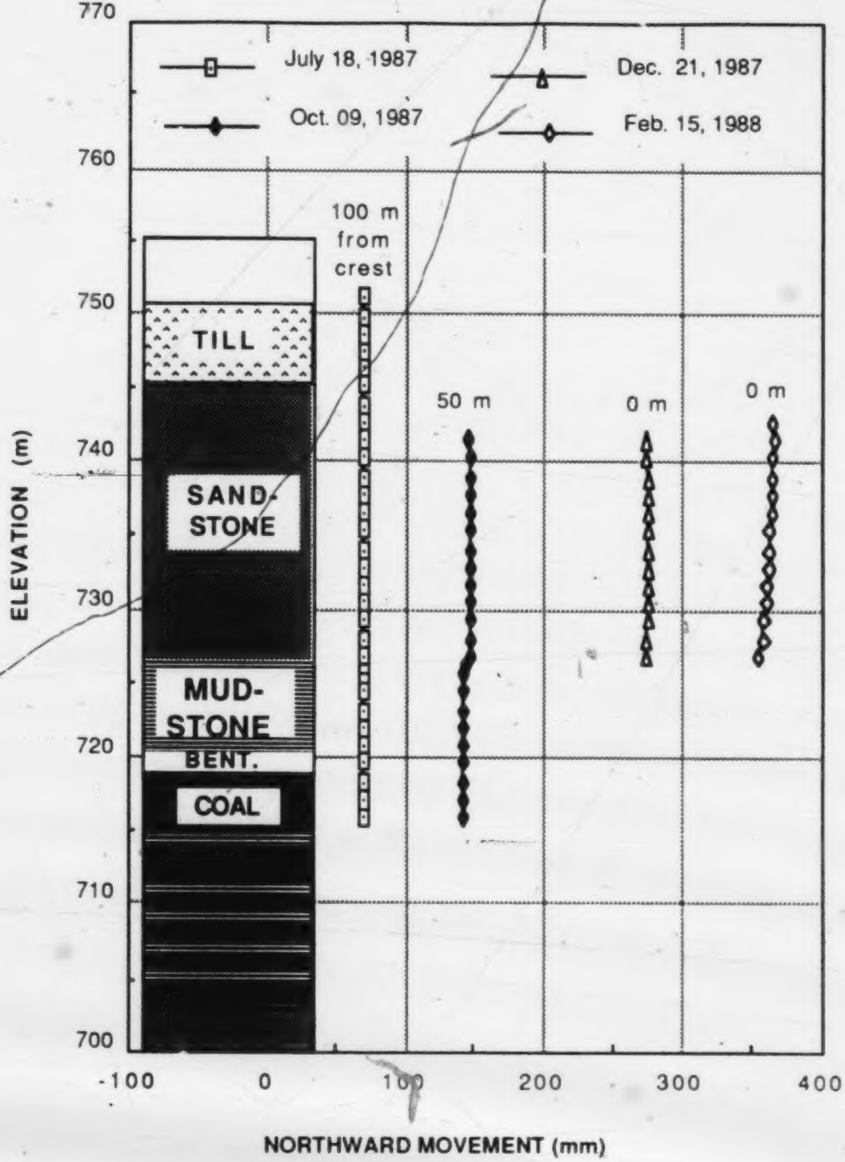

Figure 4.3 Movement of inclinometer S1

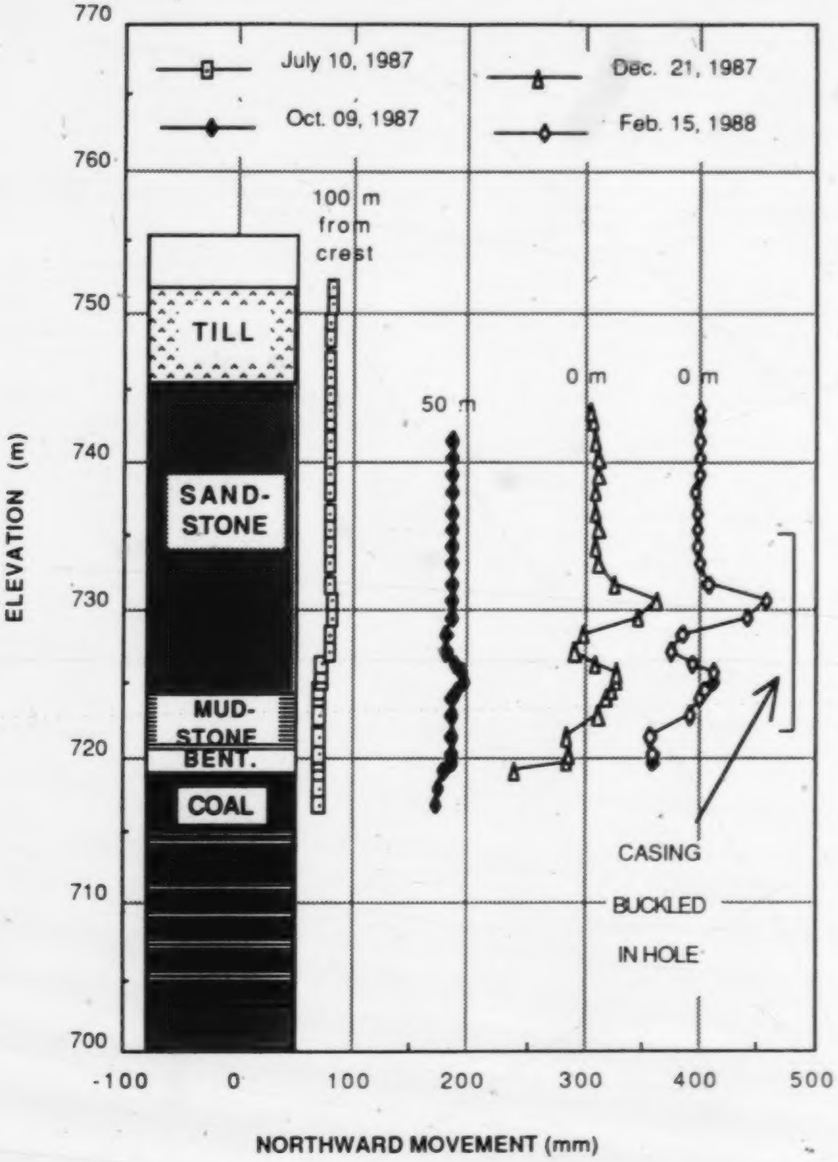

Figure 4.4 Movement of inclinometer S2

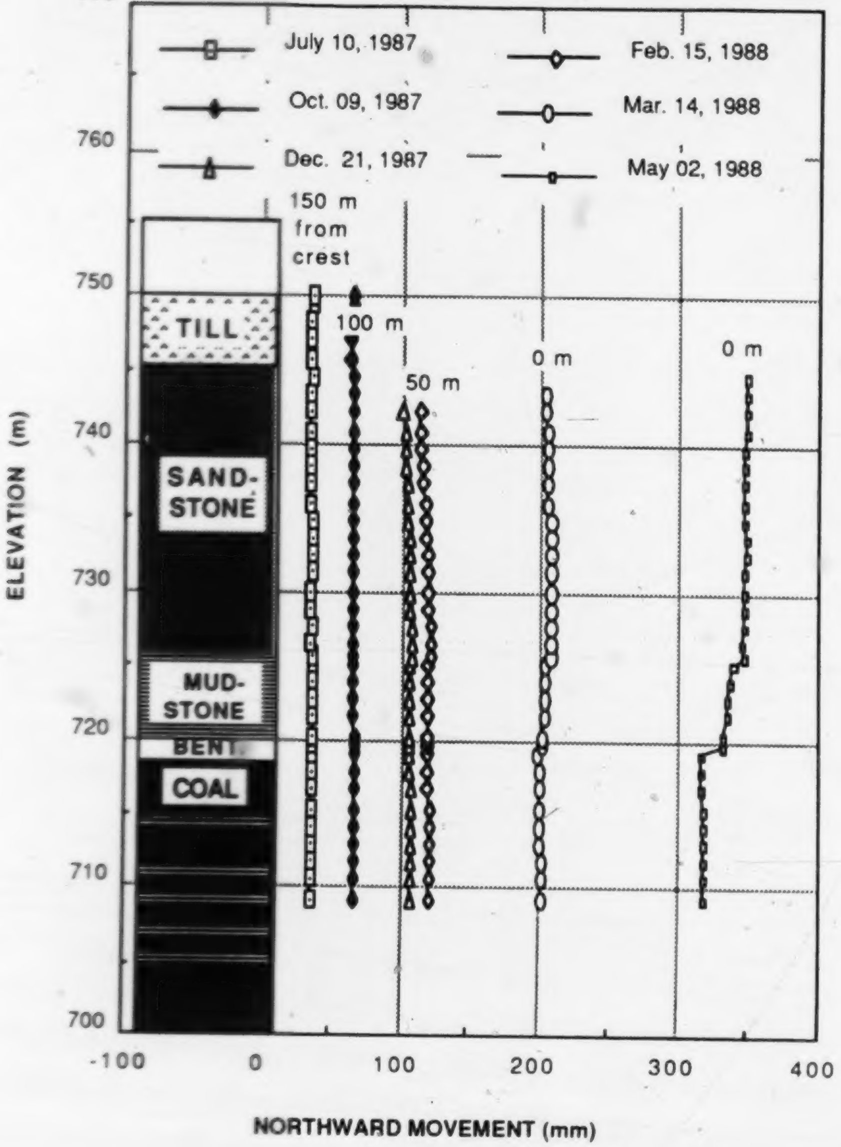

Figure 4.5 Movement of inclinometer S3

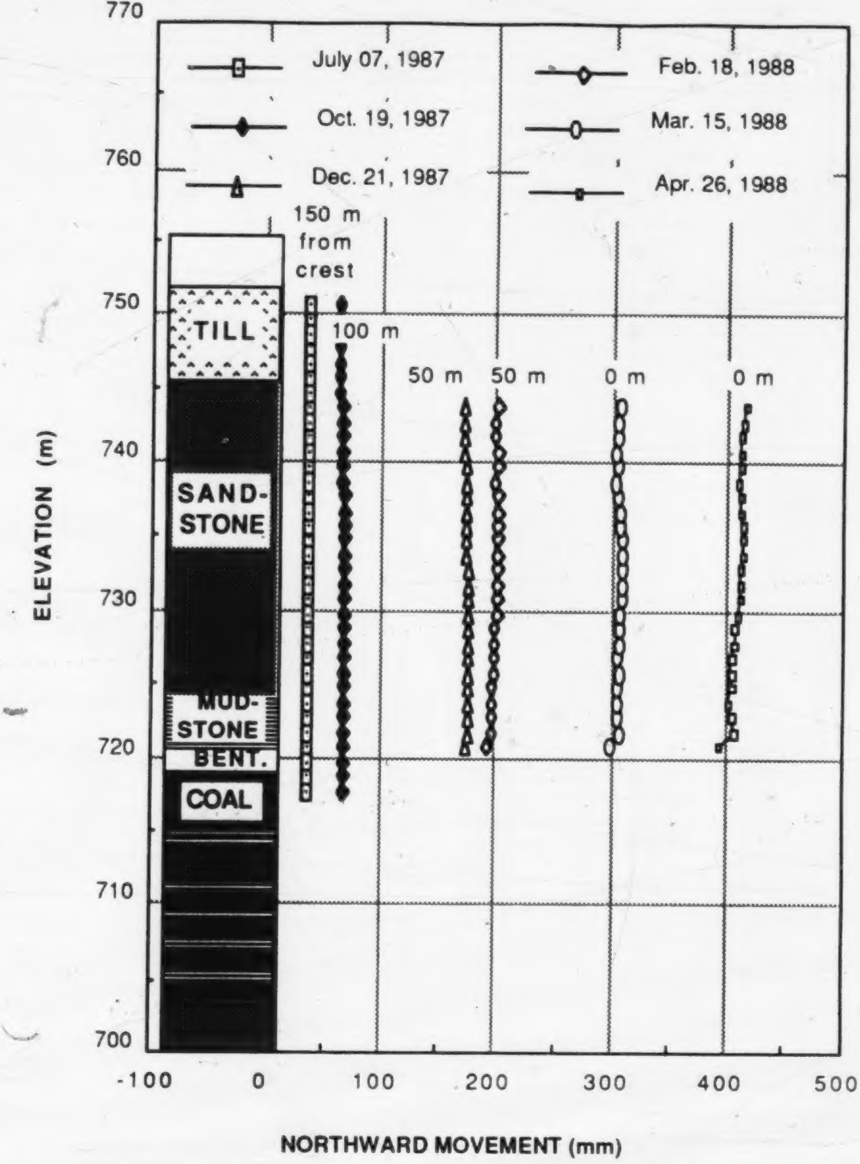

Figure 4.6 Movement of inclinometer S4

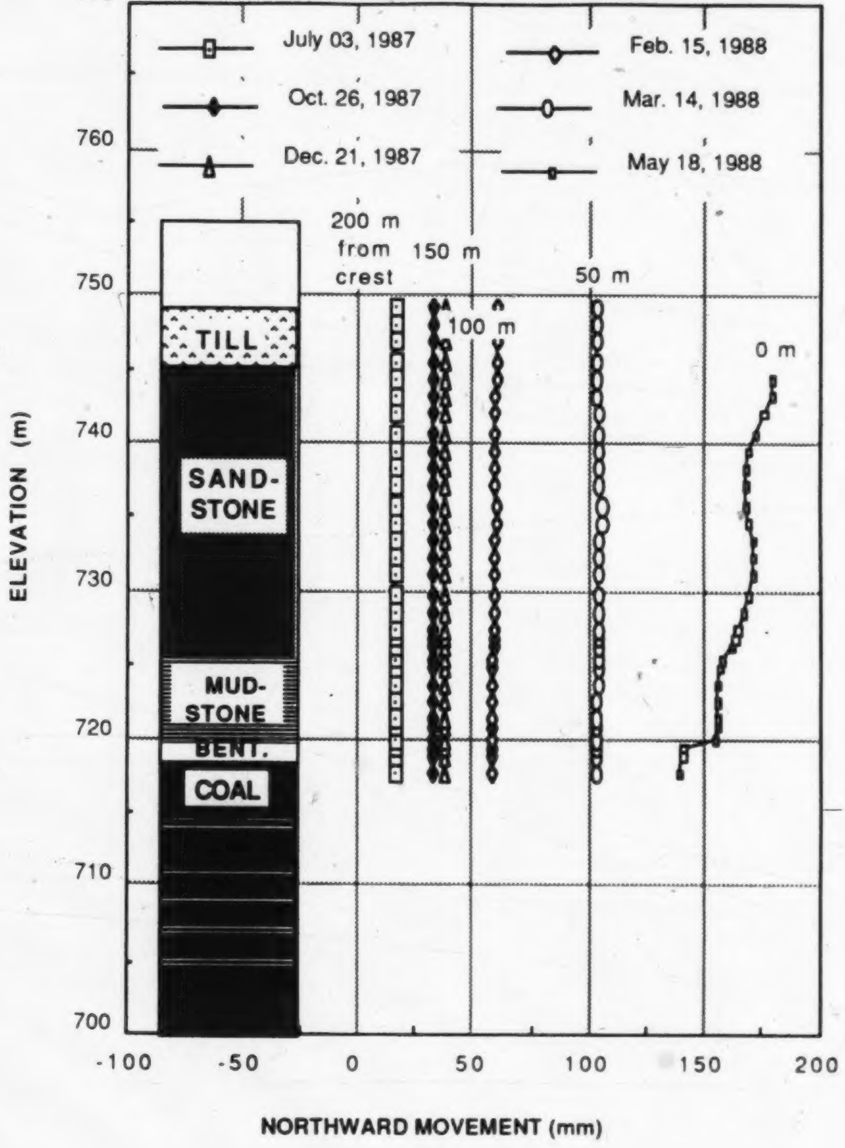

Figure 4.7 Movement of inclinometer S5

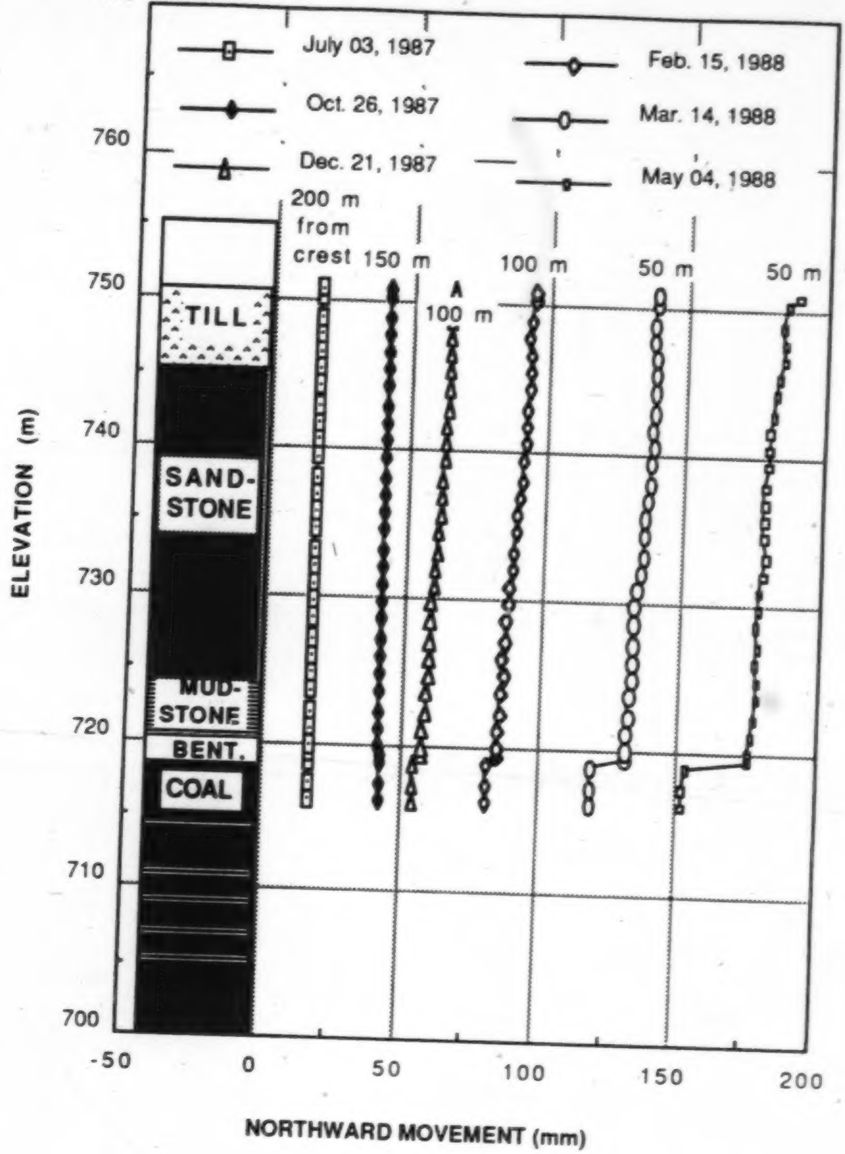

Figure 4.8 Movement of inclinometer S6

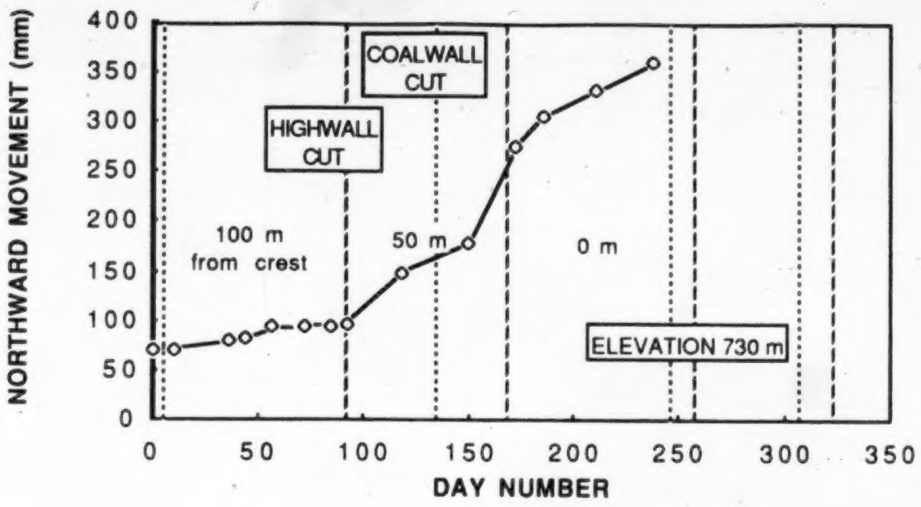

Figure 4.9 Northward movement over time at elevation 730 metres for inclinometer S1. (Day zero was June 23, 1987).

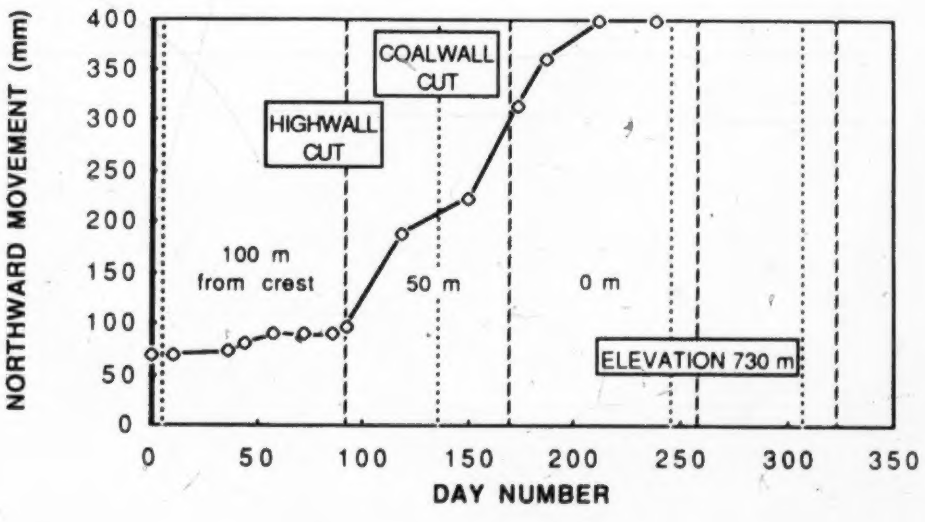

Figure 4.10 Northward movement over time at elevation 730 metres for inclinometer S2. (Day zero was June 23, 1987).

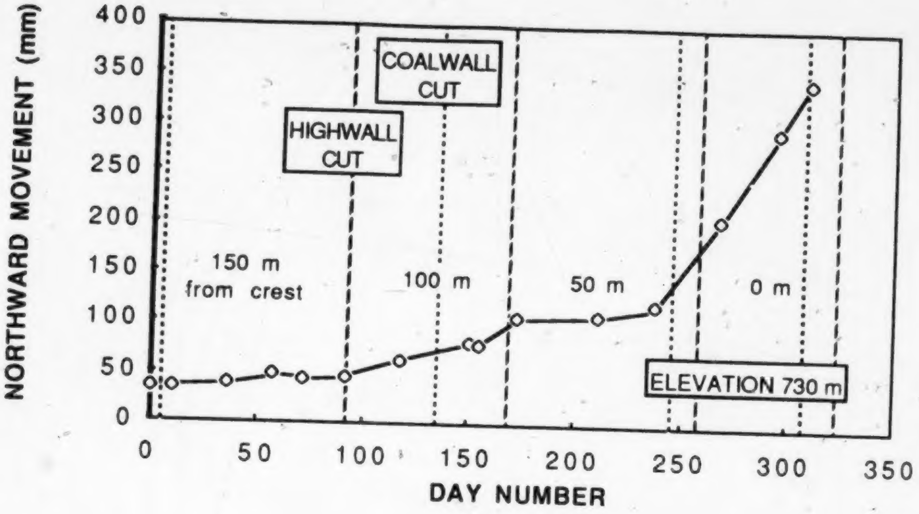

Figure 4.11 Northward movement over time at elevation 730 metres for inclinometer S3. (Day zero was June 23, 1987).

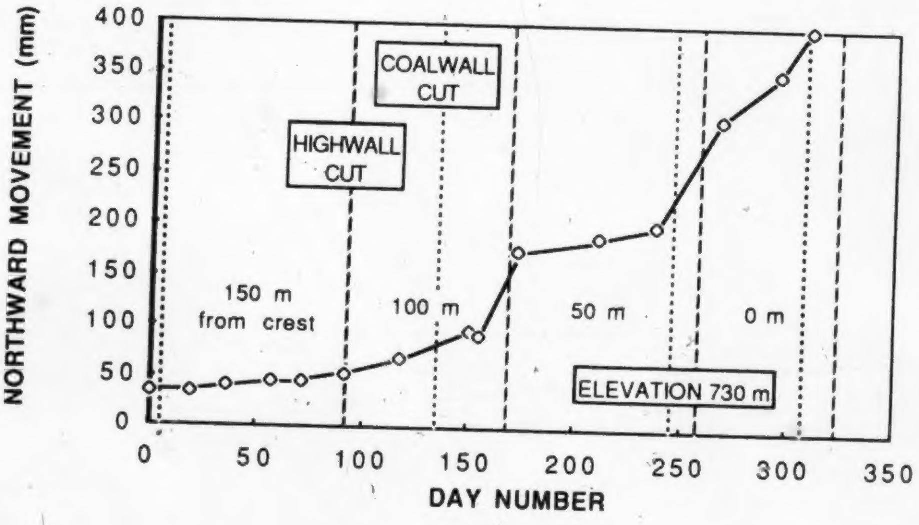

Figure 4.12 Northward movement over time at elevation 730 metres for inclinometer S4. (Day zero was June 23, 1987).

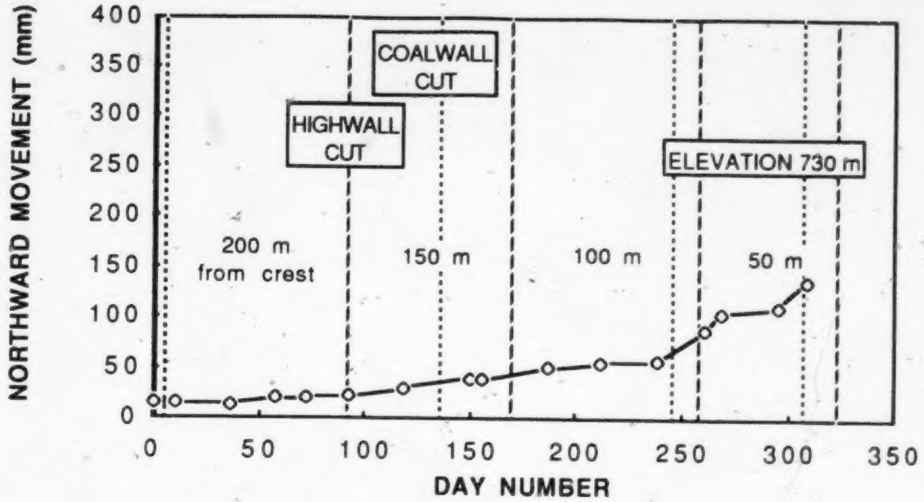

Figure 4.13 Northward movement over time at elevation 730 metres for inclinometer S5. (Day zero was June 23, 1987).

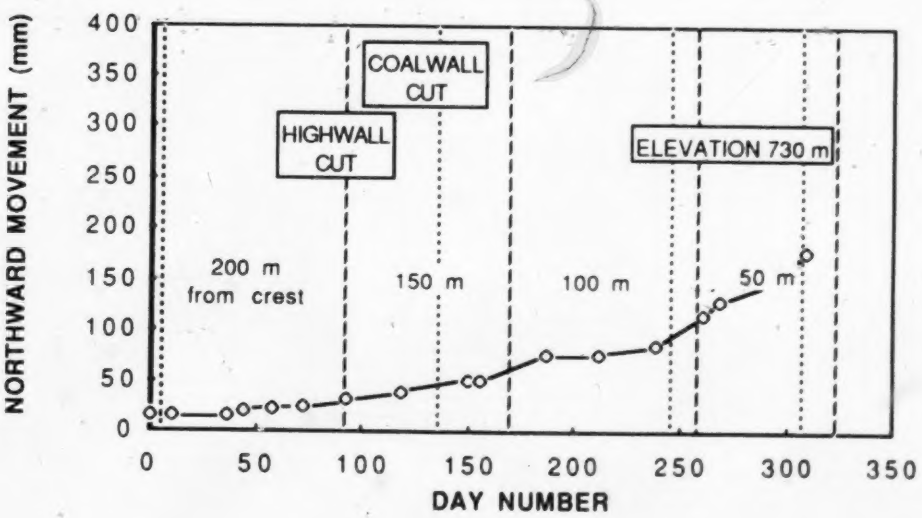

Figure 4.14 Northward movement over time at elevation 730 metres for inclinometer S6. (Day zero was June 23, 1987).

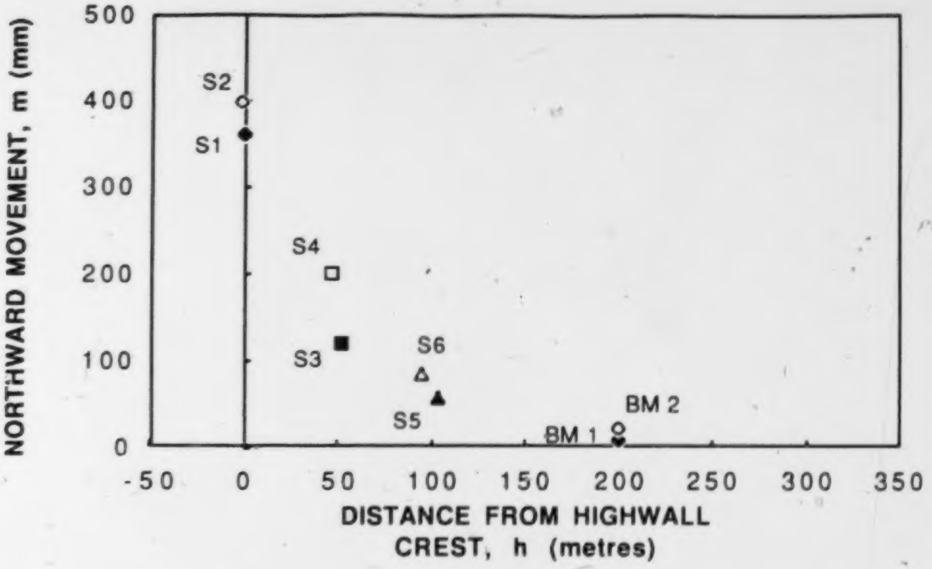

Figure 4.15 Deformations at elevation 730 metres on day 238 (February 15, 1988)

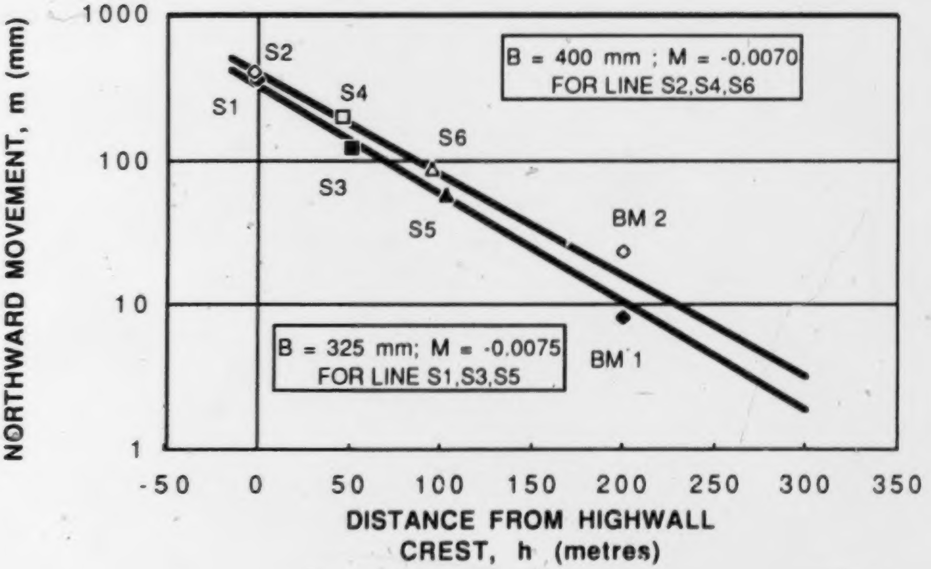

Figure 4.16 Semi-logarithmic plot of deformations at elevation 730 metres on day 238 (Feb. 15, 1988)

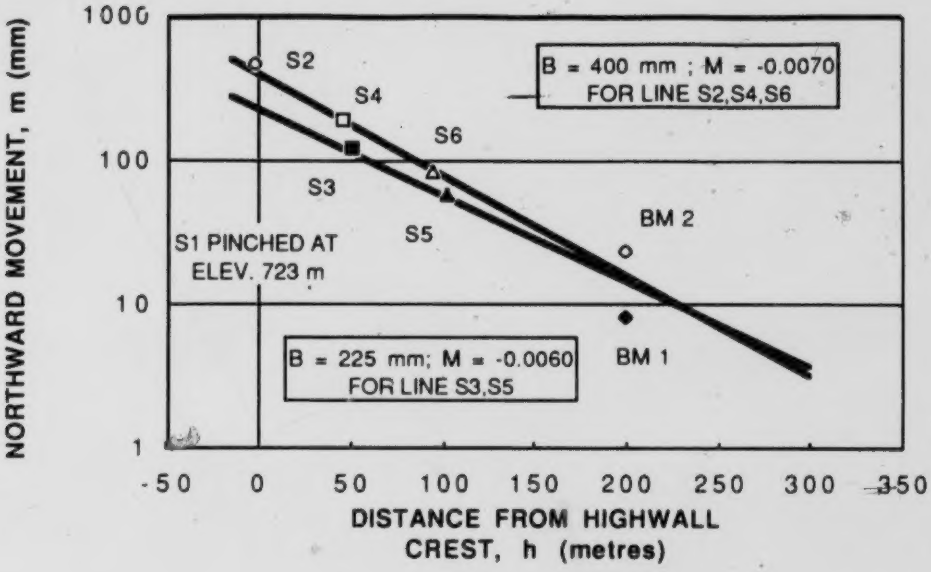

Figure 4.17 Deformations at elevation 721 metres on day 238 (February 15, 1988)

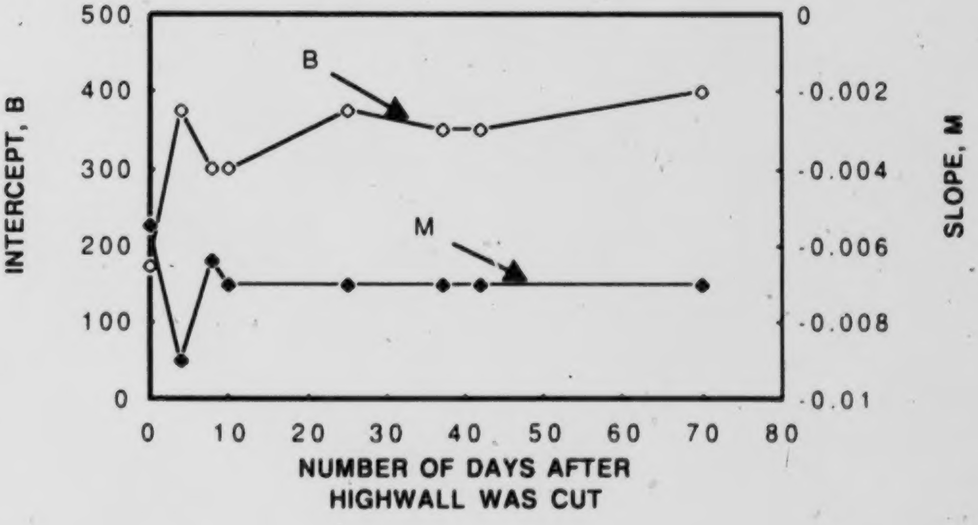

Figure 4.18 Variation in B and M at elevation 730 metres after a highwall was cut

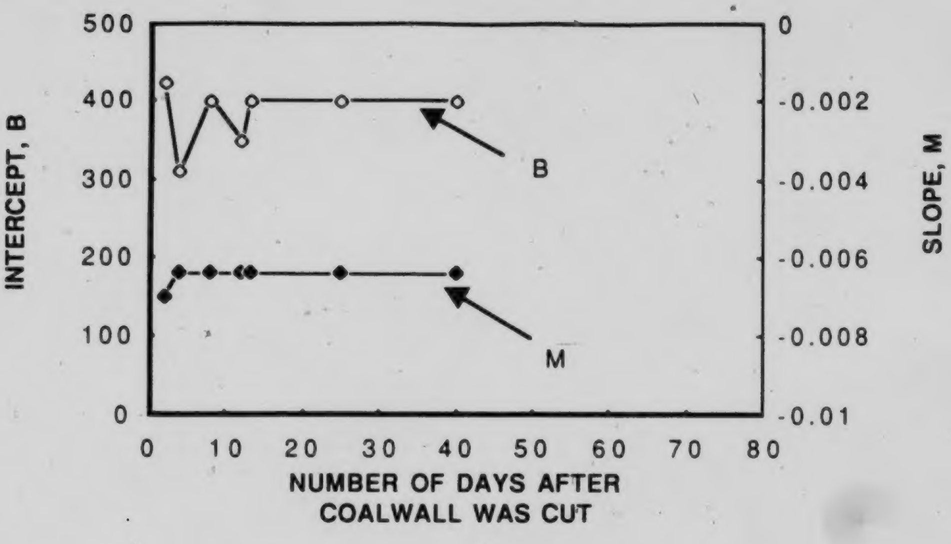

Figure 4.19 Variation in B and M at elevation 730 metres after a coalwall was cut

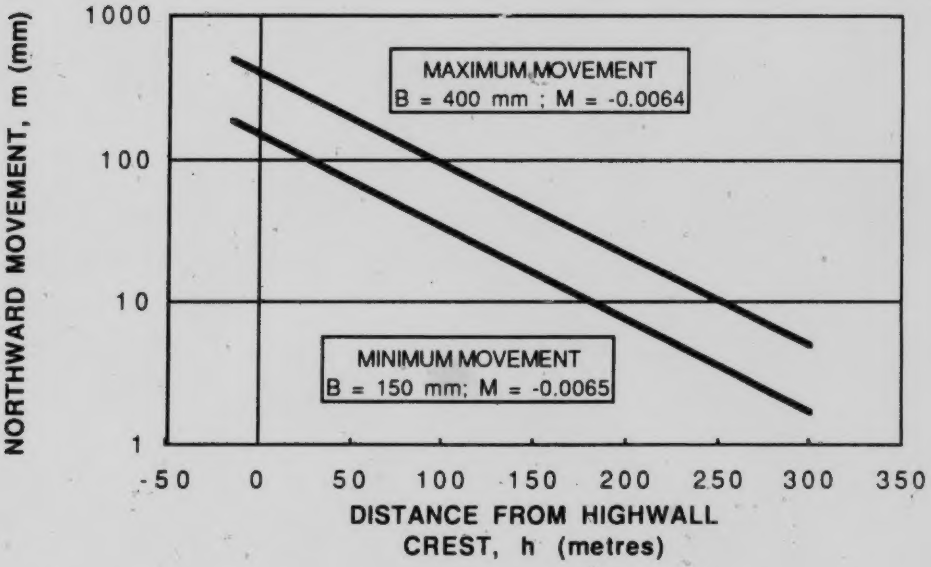

Figure 4.20 Range of movements in overburden at elevation 730 metres

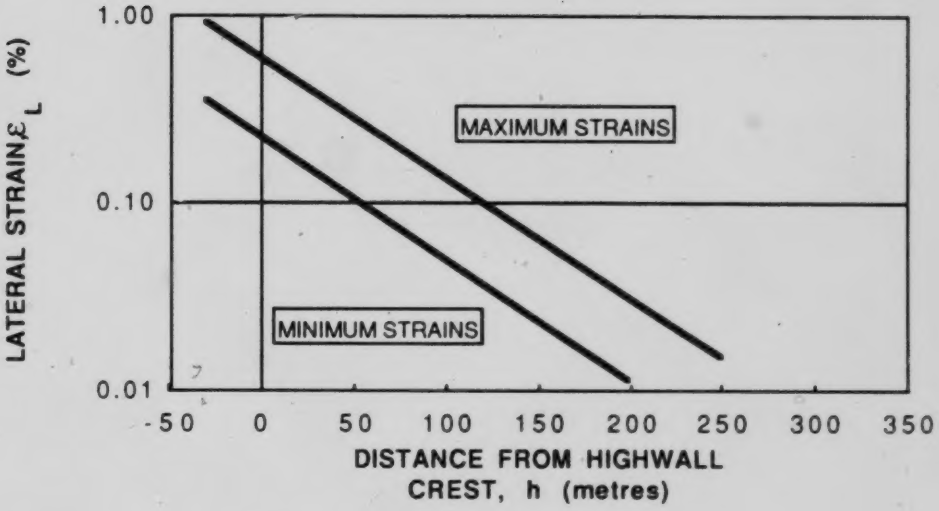

Figure 4.21 Range of strains in overburden at elevation 730 metres

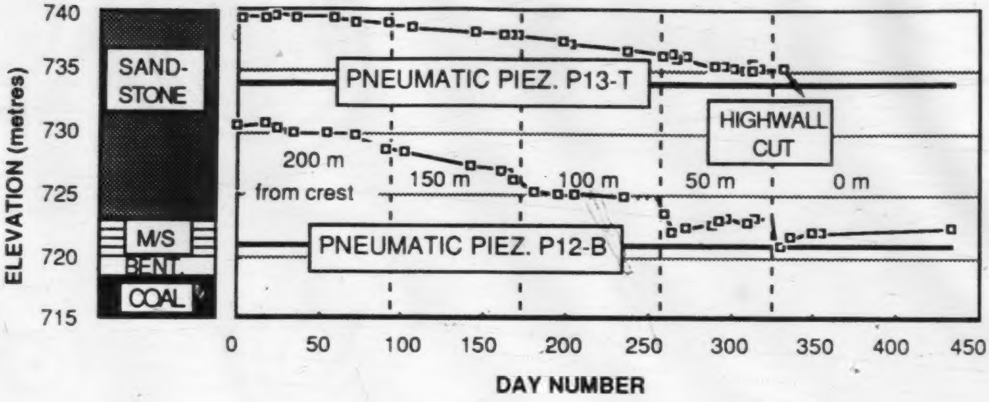

Figure 4.22 Piezometric head over time for piezometers P12-B and P13-T

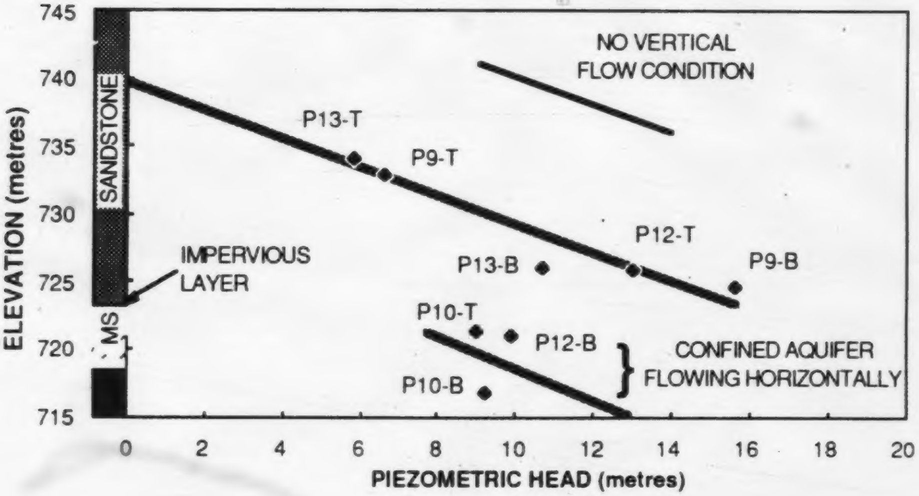

Figure 4.23 Piezometric head distribution 200 m behind the highwall crest.

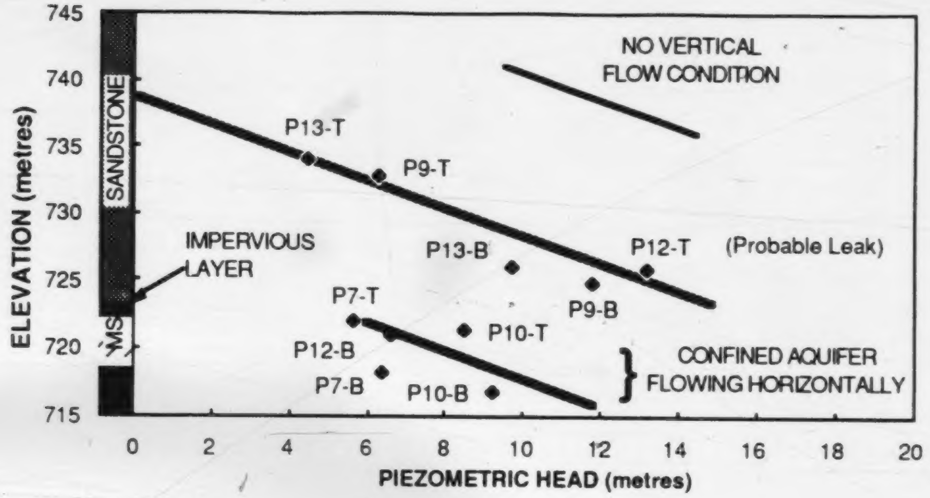

Figure 4.24 Piezometric head distribution 150 m behind the highwall crest.

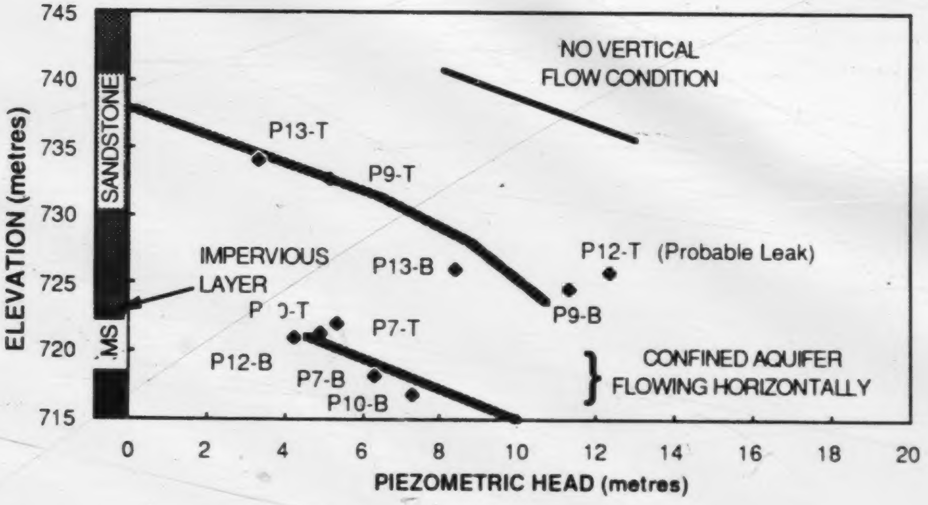

Figure 4.25 Piezometric head distribution 100 m behind the highwall crest.

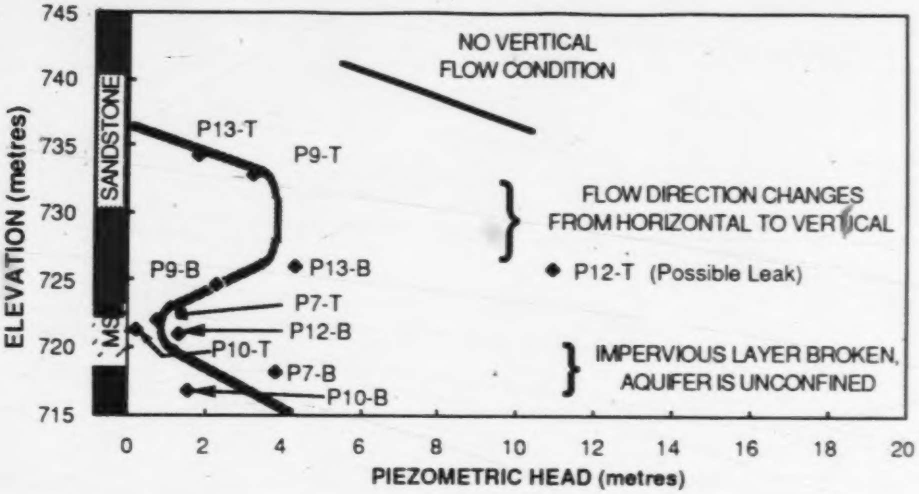

Figure 4.26 Piezometric head distribution 50 m behind the highwall crest.

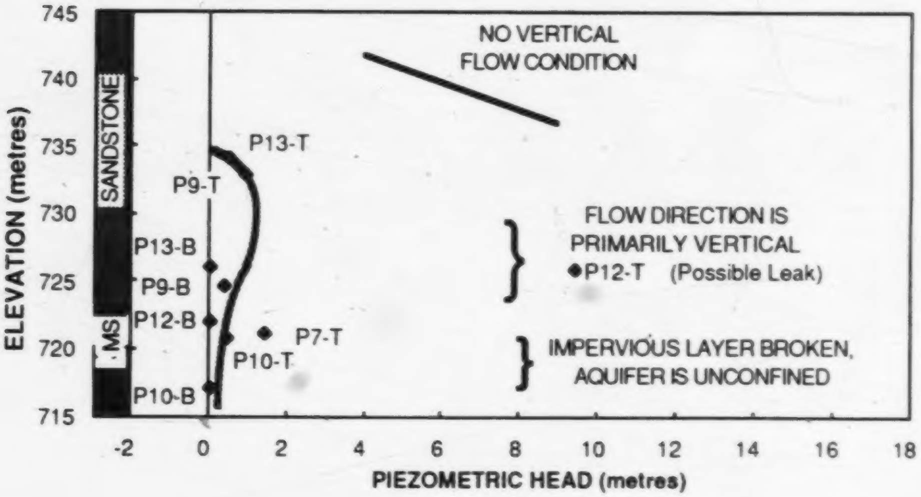

Figure 4.27 Piezometric head distribution beneath the highwall crest. One to two weeks after a highwall was cut.

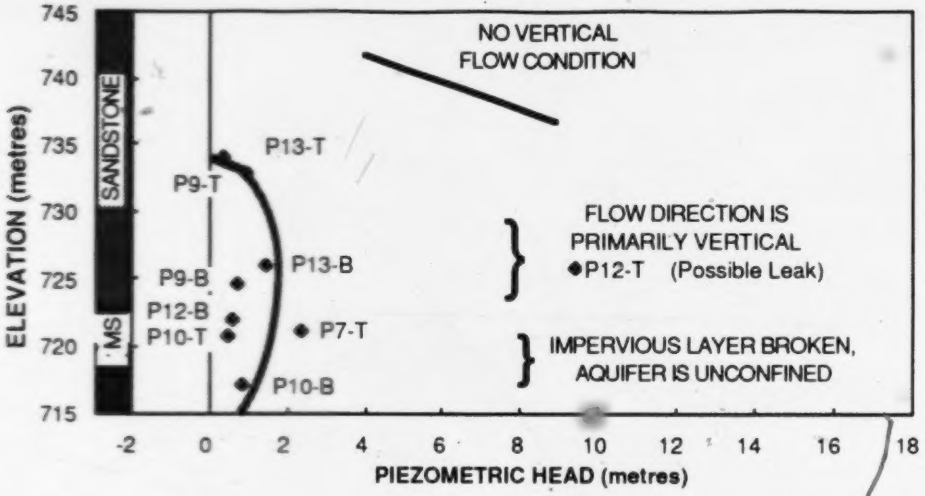

Figure 4.28 Piezometric head distribution beneath the highwall crest. Two to three weeks after a highwall was cut.

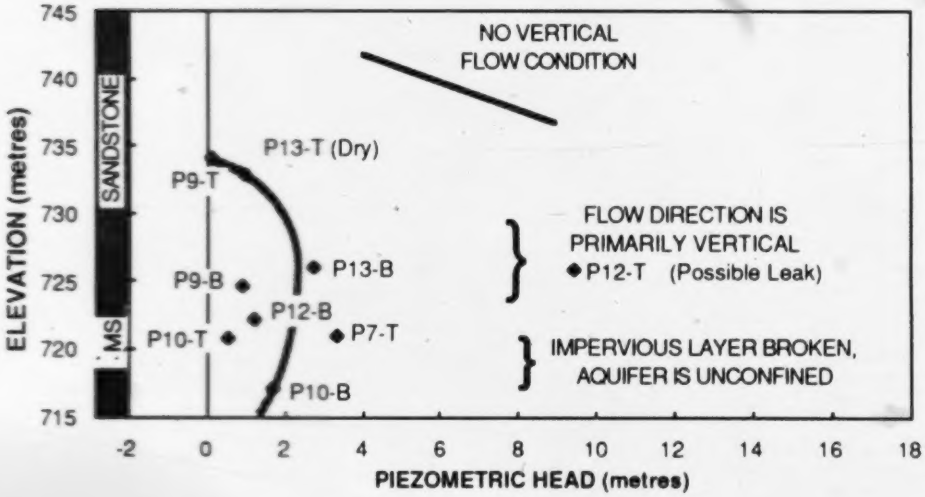

Figure 4.29 Piezometric head distribution beneath the highwall crest. Three to four weeks after a highwall was cut.

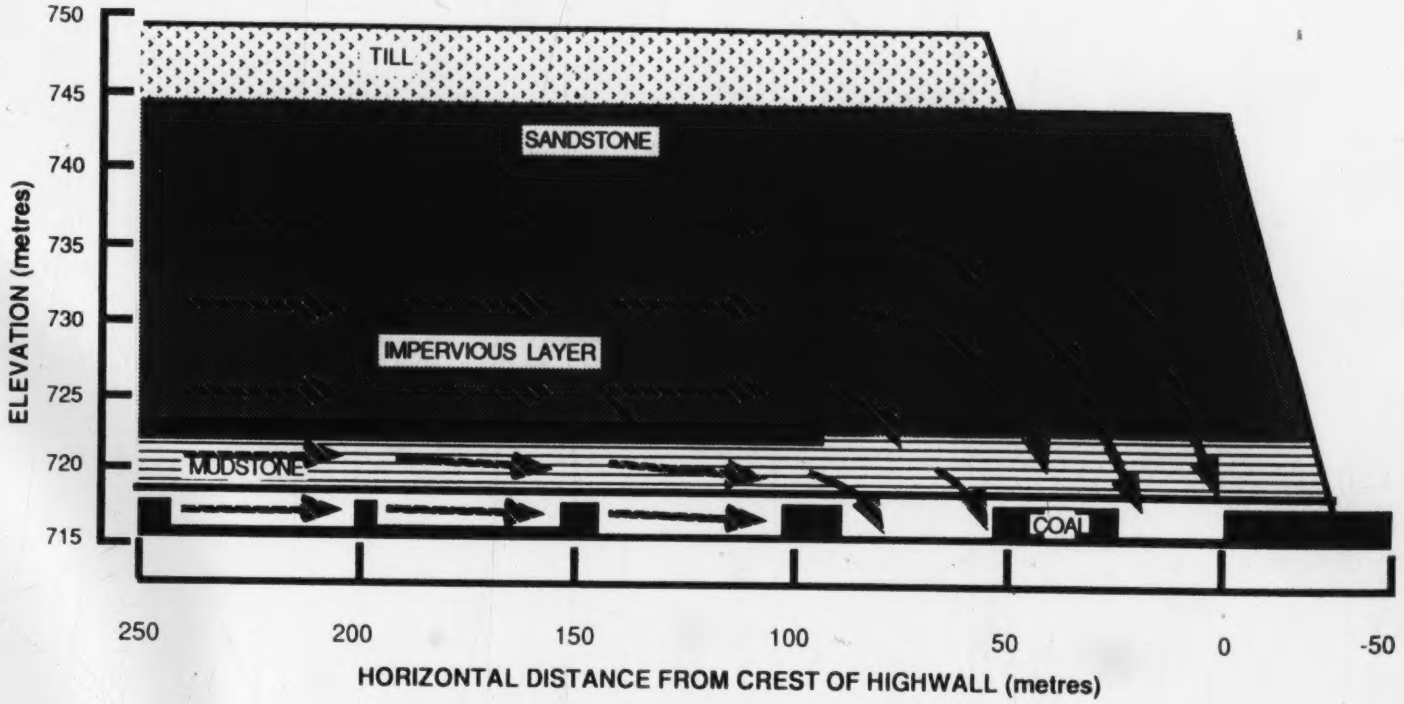

750
745
740
735
730
725
720
715
ELEVATION (metres)
TILL
SANDSTONE
IMPERVIOUS LAYER
MUDSTONE
COAL
250
200
150
100
50
0
-50
HORIZONTAL DISTANCE FROM CREST OF HIGHWALL (metres)

Figure 4.30 : Groundwater Flow Pattern in the Overburden

5 GEOTECHNICAL PROPERTIES OF OVERBURDEN

Samples obtained from the June, 1987 drilling program were tested in the summer of 1988. This chapter presents the results of the laboratory testing that estimated the geotechnical properties of the overburden sandstone, mudstone, and bentonite. These properties were then applied to stability analyses discussed in Chapter 6.

5.1 Index Testing

Index, or classification testing, included 80 moisture contents, 14 grain size analyses, and seven Atterberg Limits. A.S.T.M. procedures (A.S.T.M., 1986) were used throughout the lab testing program. The complete results are contained in Appendix F and summarized in Table 5.1 and Figures 5.1 to 5.5.

Figure 5.1 presents the grain size curves for seven samples of unweathered sandstone, two of which were taken from the highwall face after a failure in April, 1988 (discussed in Chapter 6). The remaining five samples were taken from boreholes S3, S4, and S6 at different depths. Even with the variety of sample locations, the unweathered sandstone had a consistent grain size distribution with 70 to 90 % sand and 10 to 30 % fines. Tsui (1988) stated that the fines are highly bentonitic and may account for the low permeabilities experienced during triaxial testing discussed below.

Figure 5.2 presents the results of five grain size analyses on the bentonitic mudstone. As with the unweathered sandstone, the results for a variety of samples were similar with typically less than 5% sand, 50% silt, and 45% clay. Tsui (1988) noted that most of the silt size particles would probably be clay platelets, even after attempting to break down these particles by 10 minutes of blenderizing. The clay fraction was determined by Tsui (1988) to be of montmorillonite, kaolinite, and illite.

The grain size distribution for a single sample of siltstone is shown in Figure 5.3. This sample had over 30% sand and 40% silt. It was dry, hard, and crumbly upon sampling.

Figure 5.4 presents the grain size for the bentonite and indicates 40% silt and 60% clay. As with the bentonitic mudstone, the silt fraction was probably dominated by clay platelets.

Table 5.1 summarizes the moisture contents, densities, and Atterberg Limits on samples of sandstone, mudstone, siltstone, and bentonite. The weathered sandstone was found to have lower water contents and densities than the unweathered sandstone, in line with the effects of weathering.

The mudstone unit beneath the sandstone consisted of interbedded mudstone and siltstone. From the Unified Soil

Table 5.1

Moisture Contents, Densities, and Limits

Lithology	El.	m.c.		Avg.	Avg.						
	m	rg. %	avg. %	γ_T kn/m^3	γ_d kn/m^3	P_L %	L_L %	I_P %	I_L	CF %	A
Till	745 to 752	20.9 to 27.9	23.9	18.6	15.0						
Weathered Sandstone	738 to 745	9 to 13	11.1	18.9	16.8						
Unweathered Sandstone	723 to 738	12.8 to 25.5	15.5	20.4	17.7						
Mudstone	719 to 725	16.9 to 23.0	19.6	19.8	16.6	21 to 38	58 to 74	34 to 43	-0.42 to -0.03	55 to 65	0.58 to 0.70
Siltstone	721	14.6	14.6	21.7	18.8	17 to 25	47 to 54	29 to 30	-0.36 to -0.08	31 to 47	0.62 to 0.97
Bentonite	719	50.9	50.9	16.8	11.1	51	146	95	0.00	78	1.22

rg.=range avg.=average γ_T=total density γ_d=dry density

L_L=Liquid Limit P_L=Plastic Limit I_P=Plasticity Index

I_L=Liquidity Index CF=Clay Fraction A=Activity

Classification (USC), the siltsone, mudstone, and bentonite were all described as CH: a highly plastic inorganic clay. Figure 5.5 presents the results of the Atterberg Limits that lead to this classification and shows that the different samples of mudstone and siltsone had very similar limits. The results presented here are in agreement with the findings of Tsui (1988) and other workers in the area (Barron et al 1986, Wade and Peterson 1986).

The Liquidity Indices, I_L, for the mud- and siltstone were between -0.4 and zero, indicating that the mudstone unit was overconsolidated. Activities for the unit ranged from 0.58 to 0.97, confirming the presence of montmorillonite. Tsui (1988) found that half of the clay minerals in the mudstone were montmorillonite, a third illite, and the remaining sixth kaolinite.

The bentonite layer had a plasticity index of 95 %, I_L of zero, and an activity of over 1.2. These characteristics pointed to an overconsolidated clay rich in montmorillonite.

5.1.1 Clarification of Terms

The terms sandstone and mudstone are used frequently in this thesis. Sandstone is used to describe the cemented sands underlying the till. To be considered a rock, this strata should have an unconfined compressive strength over one megapascal (Coates, 1981). In fact, the actual strength is less than this and this unit should be referred to as cemented sand. However, it does possess several characteristics of rock, for example jointing, and for this thesis is considered to be a very soft rock.

The term mudstone in this thesis collectively applies to the interbedded silty clays, clays, and in some instances coal that make up the unit beneath the sandstone and above the coal. To be precise, the mudstone should have an undrained shear strength greater than 1.8 MPa (c_u=250 psi, Morgenstern,1979). However, Tsui (1988) noted that the undrained shear strength of the materials at Highvale ranged from 65 to 107 kPa, far less than the 1800 kPa boundary. This strata would therefore be properly described as a stiff clay or clay shale (Morgenstern, 1979). Nevertheless, for simplicity and to maintain consistency with the terminology used by other workers in the mine, the term mudstone is used.

5.2 Triaxial Testing

Consolidated Undrained (CU) tests were performed on four samples of unweathered sandstone and three samples of mudstone. Three Consolidated Drained (CD) tests were conducted on the unweathered sandstone. Initially, all of the sandstone samples were to be tested in a CU manner. However, the permeability of this material was so low that the tests had to be run over several days. Moreover, during shear, the pore pressures passed below atmospheric pressure and beyond the capacity of the measurement system.

Consequently, after four CU tests, the testing program was revised to include three CD tests.

The low permeability mudstones were sheared in an undrained manner at a strain rate that required over a week to reach failure.

5.2.1 Unweathered Sandstone

Five of the seven triaxial samples on unweathered sandstone were 37 mm in diameter while the other two were 100 mm. The larger samples were taken by the Pitcher sampler (Section 3.2). Each sample was twice as long as it was wide to satisfy end constraint conditions. Details of the sample preparation were in accordance with the procedures outline by Bishop and Henkel (1962).

The four CU tests on the sandstone were all performed under a confining stress of 200 kPa to compare different samples. The three CD tests were run at stress levels of 100, 200, and 500 kPa. The samples tested at 100 and 500 kPa were the 100 mm diameter Pitcher samples.

Figures 5.6 and 5.7 present the stress-strain curves for the sandstone from the CU and CD tests. Each of the tests showed strain softening. The peak stresses are plotted in a p-q stress space in Figure 5.8, resulting in an angle of internal friction, ϕ,of 44° and a cohesion intercept of 100 kPa. It was anticipated that the results from the 100 mm samples would lie below the failure envelope as a result of a greater number of fractures. The sample under a confining stress of 100 kPa did fall well below the envelope, however the sample at 500 kPa confining stress did not. A conclusion regarding the effect of sample size on shear strength could not be drawn in this instance.

Residual strength values for the seven tests are plotted in Figure 5.9 and indicate ϕ = 40° and c = 0 kPa.

Wade and Peterson (1986) selected values of 45° and 100 kPa for the friction angle and cohesion in their stability analyses while Tsui (1988) used ϕ = 40° and c = 0 kPa in his work.

5.2.2 Mudstone

Three CU tests were conducted on the mudstone at stress levels of 200, 300, and 450 kPa with the results presented in Figures 5.10 and 5.11. A peak friction angle of 28° and cohesion of zero was obtained from these tests.

The undrained triaxial shearing did not show strain softening characteristics, leading to coincidental peak and residual strength parameters.

Monenco (1983) used ϕ = 25° and c = 0 kPa for stability calculations. Tsui (1988) found ϕ = 22.5° and c = 0 kPa at peak from CU testing. Tsui (1988) plotted test results on the bentonitic mudstone from a number of different sources. This plot is summarized in Figure 5.12. The test results showed a maximum peak friction angle of 37.5° and a maximum cohesion of 135 kPa.

Figure 5.12 also presents the range of residual strength values measured by several workers at the Highvale Mine and shows a band of residual friction angles from 6.5° to 22.5°. A mean value of 11.5° was determined.

Softening of Mudstone

CU tests conducted on the bentonitic mudstone in this study may have subjected the sample to premature softening. This is evidenced by a peak cohesion intercept of zero for an obviously overconsolidated soil or soft rock.

In general, the softening process requires the presence of micro-fractures and joints to permit free water to enter the material. When water comes into contact with surfaces that had previously not been soaked, then the strength along these surfaces is reduced and, so is the strength of the material. The process is accelerated if the confining stresses are reduced and the fractures are allowed to spread apart, exposing new surfaces to the water.

In a triaxial test, the sample should first be subjected to a confining stress that returns the sample to its original in-situ stress state in order to return the fractures and joints to their original closure. Then, when water is introduced to the sample, as during back pressure saturation, it will come into contact with those surfaces that had previously been softened and no further reduction in strength will take place. However, if the confining stress in the laboratory is less than the in-situ stress state, then additional softening can develop.

In this study, during the consolidation stage of the CU tests, the samples were subjected to effective confining stresses of 15 to 100 kPa, approximately 300 kPa less than the original vertical in-situ stress (the horizontal in-situ stresses may have been even larger). This procedure no doubt led to softening of the mudstone before the final confining stresses of 200, 300, and 450 kPa were applied. The small confining stresses were used during back pressure saturation to ensure that the confining stress did not exceed the proposed final stress condition. Consequently, the strength of ϕ = 28°, c = 0 kPa obtained from these tests may be more representative of a softened strength for the mudstone.

Additional CU triaxial tests on this material must recognize the potential for softening. To minimize the effect, the following procedure is recommended:

1. Firstly, select an effective confining stress that is greater than the in-situ stress state and will be applied during back pressure saturation. In this instance, a value of 400 kPa may be chosen. The final effective confining stress just before shear will be greater than this value.

2. Apply the selected stress to the sample, preventing the entry of any water by closing the back pressure lines.
3. Increment the cell pressure by approximately 50 kPa. The sample will now have been subjected to a maximum confining stress of the selected pressure plus 50 kPa (450 kPa in this instance).
4. Perform a B-bar test for this increment.
5. Increment the back pressure 50 kPa and consolidate.
6. Repeat steps 3 to 5 until saturation is achieved.
7. Increase the cell pressure to the final effective confining stress. Ensure that this value is greater than the confining stress exerted on the sample at any time during saturation.
8. Shear the sample.

The potential for softening in the CU test was not recognized in this study until the triaxial testing program was completed. An effort was then made to obtain an "unsoftened strength" in the direct shear test by not adding water to the shear boxes.

5.3 Direct Shear Testing

5.3.1 Mudstone

Two samples were tested under direct shear with the results reported in Figures 5.13 and 5.14. The direct shear boxes were not filled with water in order to restrict the potential for softening. In addition, the boxes were enclosed in cellophane to minimize evaporation. Horizontal displacement rates of 0.0006 mm/min were applied to ensure complete drainage. Normal stresses of 200 and 500 kPa were used and resulted in a Mohr-Coulomb failure envelope with a ϕ of 35° and cohesion of 125 kPa. This is shown in Figure 5.14 and, for comparison, the triaxial test results on the same material are shown. The peak strength for the mudstone approached the upper limit shown in Figure 5.12.

The tests were run with the shear boxes dry in an attempt to minimize the effect of softening, however an alternative problem developed. The initial saturation of these samples was 90% and 95%, and by preventing water from entering the samples, then they remained unsaturated throughout the test. Consequently, the pore water pressures were unknown and the effective stresses could not be determined. Therefore, the failure envelope through the direct shear data points in Figure 5.14 is in terms of total stresses and not effective stresses.

In unsaturated soils, the porewater pressures are typically negative, hence the effective stress envelope for the direct shear results would lie to the right of the total stress envelope. It is not known where the effective stress envelope would be found, however it is interesting to note that the total stress envelope compares favourably with the maximum results from Figure 5.12. For this study, the total stress envelope may represent an upper bound of the shear strength of the mudstone.

After peak was reached in the direct shear test, then the shear box was hand cycled four to six times in an effort to achieve residual conditions. Total displacement at the start of residual shear was about 40 mm. The samples were sheared and the results plotted in Figure 5.15 (for normal stresses of 200 and 500 kPa). Then the samples were unloaded, from 200 to 120 kPa and from 500 to 300 kPa, and allowed to swell. Shearing was repeated and the results also plotted on Figure 5.15. A crude residual envelope may be fit through these points, considering that residual may not have been fully reached during the first stage on the sample at 200 kPa. The total stress residual friction angle of 22° found from the direct shear tests falls within the range stated above.

Examination of the samples after the tests showed flat shiny surfaces believed to be at residual conditions.

5.3.2 Bentonite

Only one sample of bentonite was competent enough for direct shear testing. The sample was tested in an identical fashion as the mudstone direct shear tests, where additional water was not allowed to enter the sample. An initial normal stress of 100 kPa was applied and the sample sheared at a rate of 0.0006 mm/min with the stress-displacement curve shown in Figure 5.17. Difficulties with the data logging system resulted in a gap in the data between a horizontal displacement of 1.8 and 3.8 mm. Some information was obtained to indicate that the trend shown over this gap is reliable.

After the initial shear, the shear box was hand cycled to attain an additional displacement of about 40 mm before shear was restarted. After consolidation, shearing was continued for 4 mm as shown in Figure 5.17. The shear box was then re-aligned, an additional 100 kPa stress applied, consolidation allowed under the 200 kPa, and then shearing restarted. A third stage was also performed under a normal stress of 500 kPa. These results are shown in Figure 5.17 and 5.18. It is possible that residual conditions were not attained during the first stage under 100 kPa because the horizontal displacement of 40 mm may not have been enough to reach residual. Examination of the sample after the third stage of testing showed two flat and shiny surfaces, no doubt at residual.

The direct shear test results for the bentonite suffered the same fate as the results for the mudstone: that the strength envelope in Figure 5.18 is in terms of total stresses and not effective stresses. Interestingly, the lone peak strength value plots closely to the curve obtained by Tsui (1988) while some scatter exists about a residual envelope. Furthermore, the total stress residual friction angle of 12° was in line with Tsui (1988) who found ϕ_r = 11.5°. Tsui also reports that a minimum value of 8.5° is possible for bentonite in the Upper Cretaceous Edmonton Formation.

5.4 Conclusions from Laboratory Testing

Index tests showed that the materials over the study site were uniform in the horizontal dimension. This allows the investigator to compare the findings at one location to another.

Even though the advanced testing program was limited in its scope, and it had some difficulties, the results corresponded well with previous work on similar materials. Furthermore, the requirements of providing strength estimates for the stability analyses in Chapter 6 were met. Table 5.2 summarizes the strengths that were considered for the stability calculations.

Table 5.2

Summary of Strengths

MATERIAL	PEAK STRENGTH		RESIDUAL STRENGTH	
	ϕ	c	ϕ_r	c
Sandstone	44°	100 kPa	40°	0 kPa
Mudstone				
-total stresses	35°	125 kPa	22°	0 kPa
-effective stresses	37.5°	135 kPa	6.5° to 22°	0 kPa
Softened Mudstone	28°	0 kPa		
Bentonite				
-total stresses			12°	0 kPa
-effective stresses	21°	47 kPa	11.5°	0 kPa

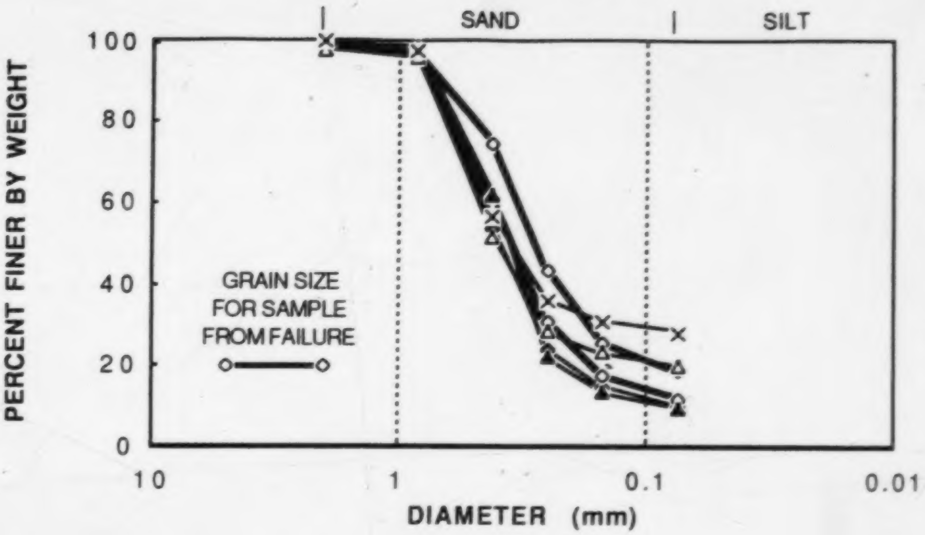

Figure 5.1 Grain size distribution of unweathered sandstone. Also shown is distribution of sandstone from failure area, discussed in Chapter 6.

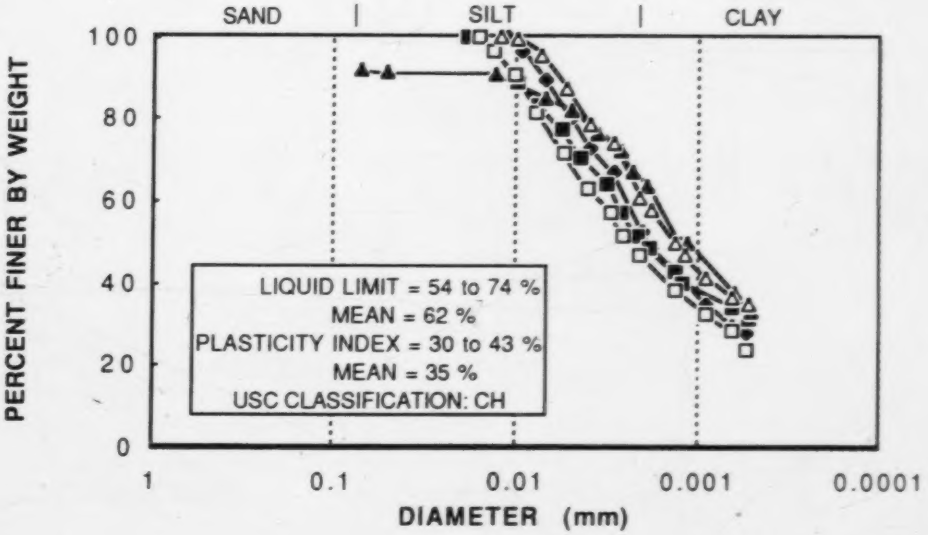

Figure 5.2 Grain size distribution of bentonitic mudstone.

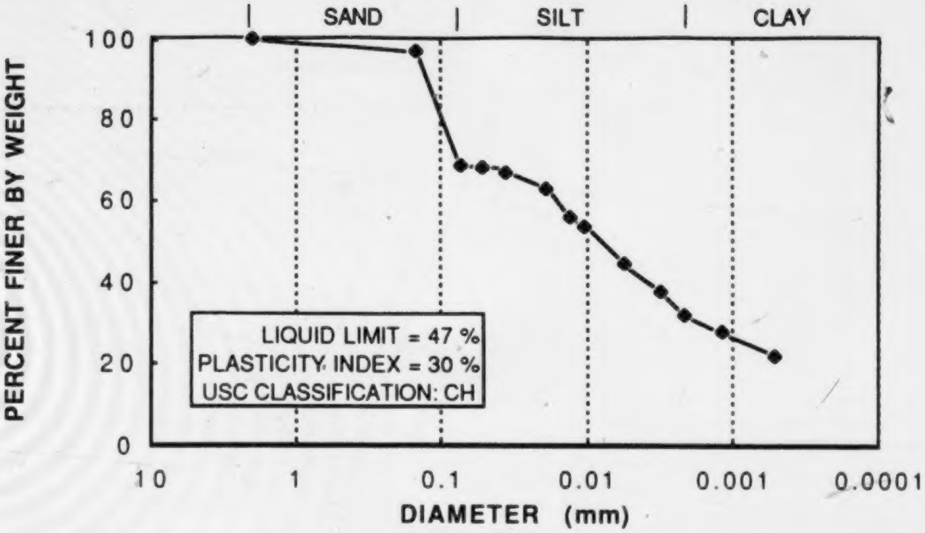

Figure 5.3 Grain size distribution of siltstone

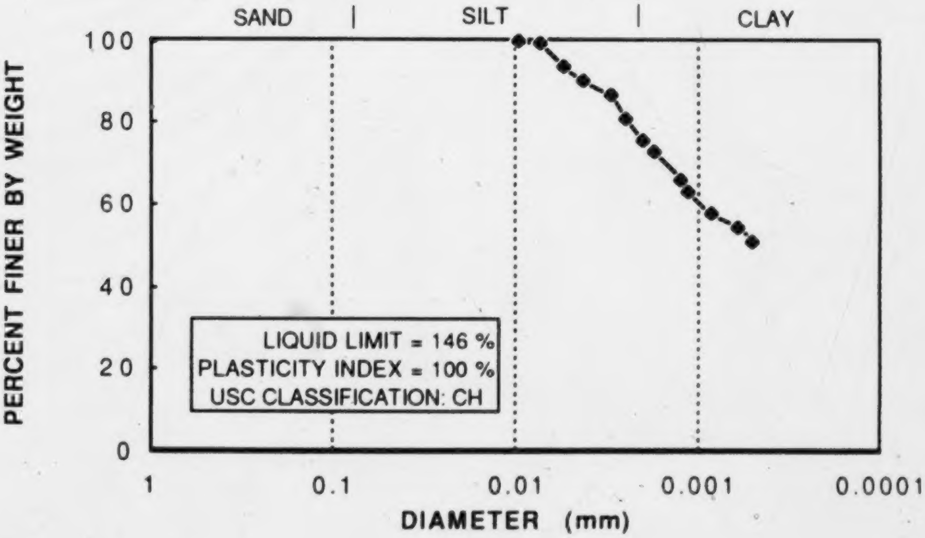

Figure 5.4 Grain size distribution of bentonite

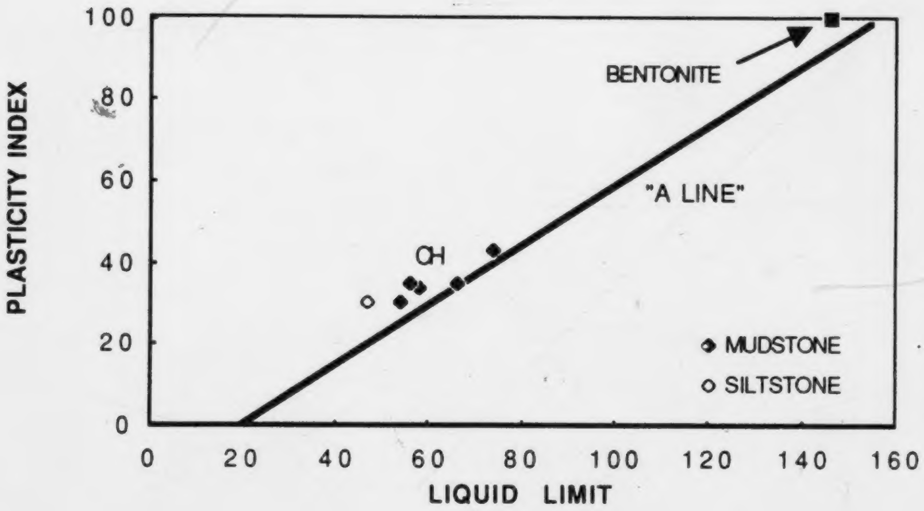

Figure 5.5 Plasticity chart for bentonitic mudstone and bentonite

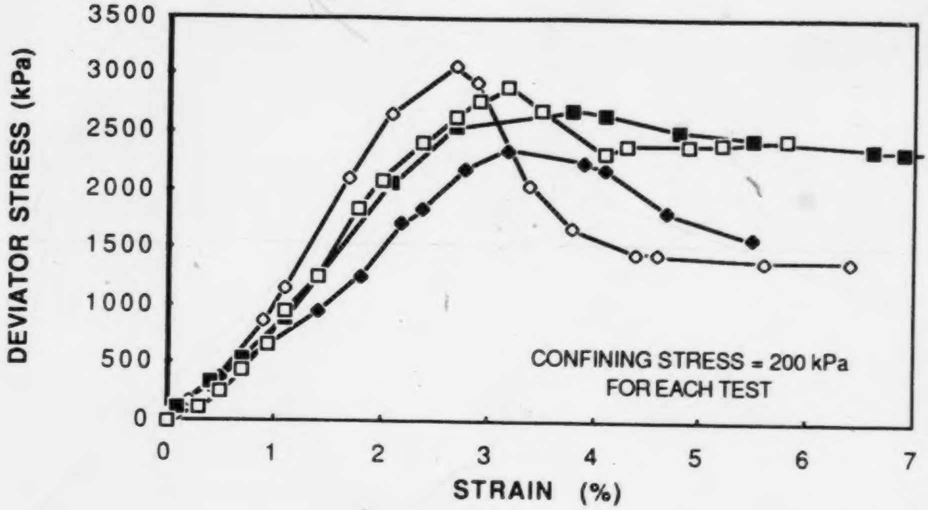

Figure 5.6 Deviator stress during undrained triaxial shearing of unweathered sandstone

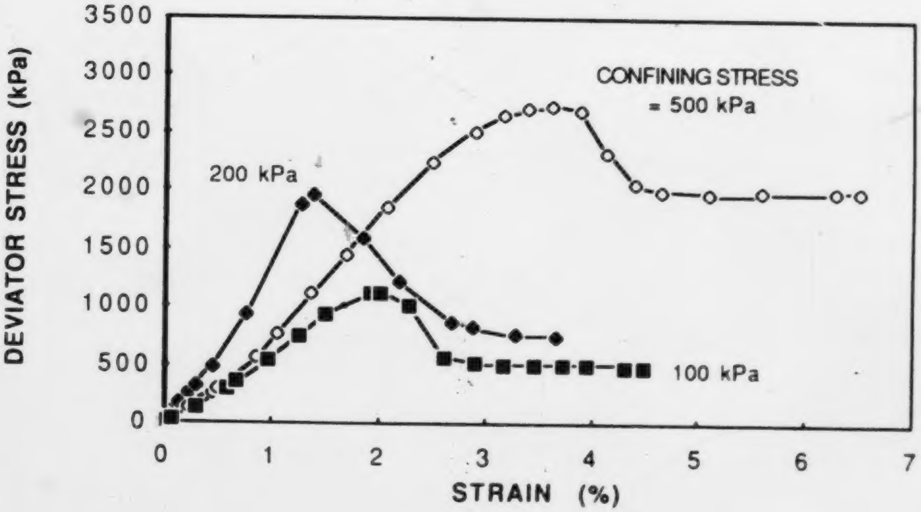

Figure 5.7 Deviator stress during drained triaxial shearing of unweathered sandstone

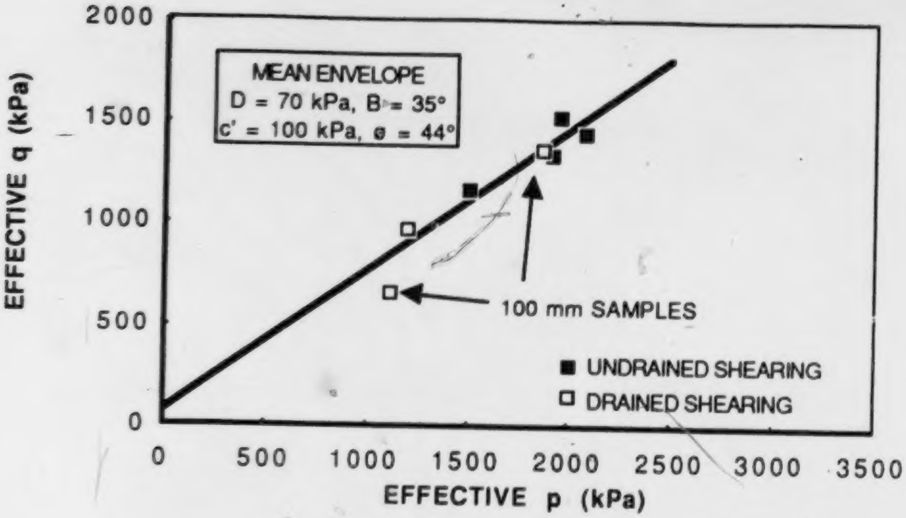

Figure 5.8 Mohr Coulomb plot for peak shear strength of unweathered sandstone

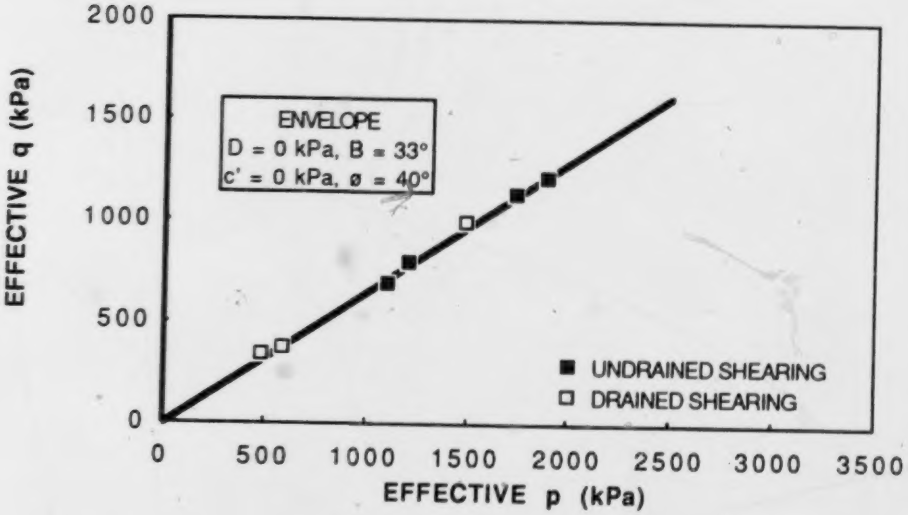

Figure 5.9 Mohr Coulomb plot for residual shear strength of unweathered sandstone

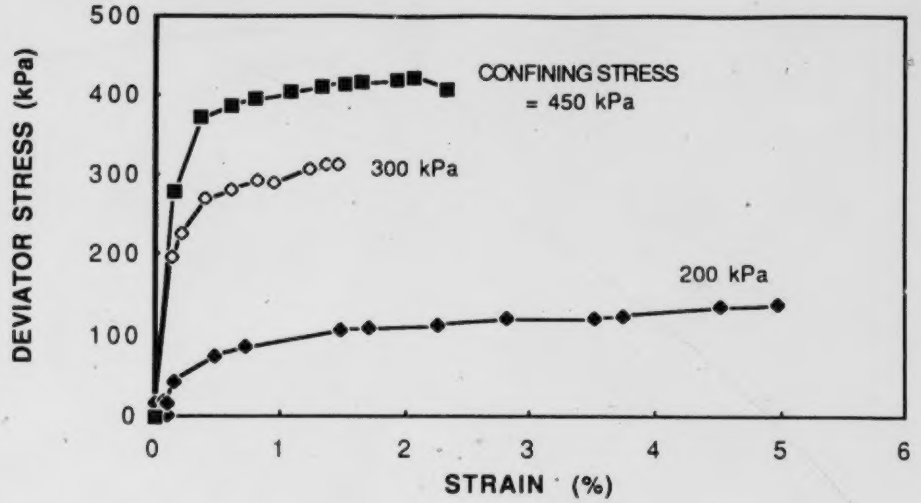

Figure 5.10 Deviator stress during undrained triaxial shearing of bentonitic mudstone

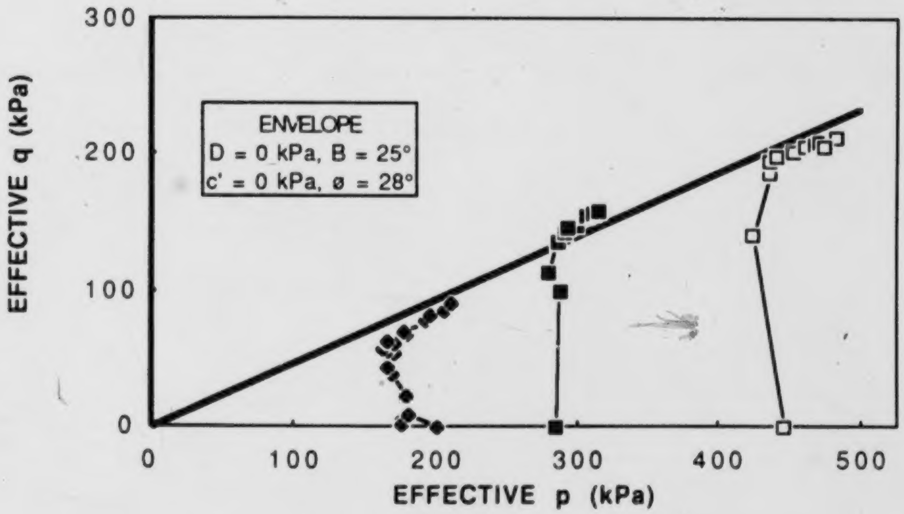

Figure 5.11 Mohr Coulomb plot for peak strength of bentonitic mudstone from CU triaxial testing

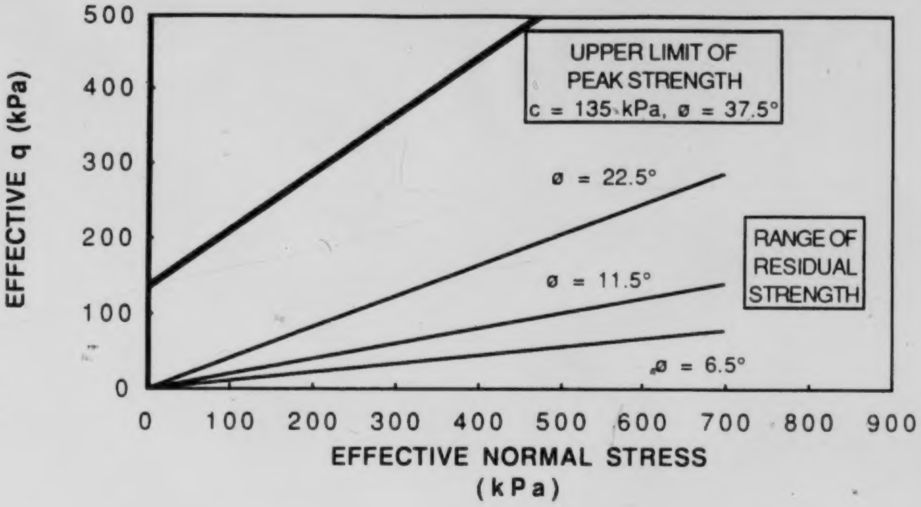

Figure 5.12 Summary of strengths of mudstone measured by several authors, after Tsui (adapted 1988)

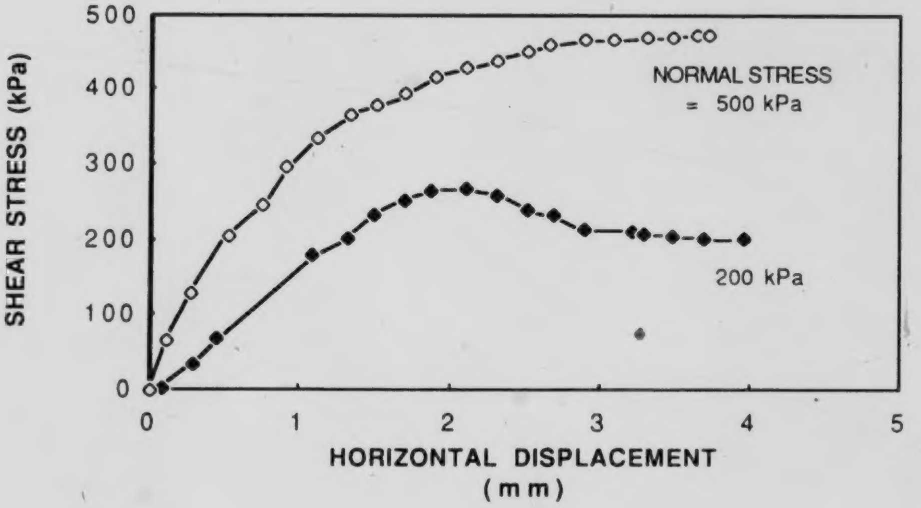

Figure 5.13 Shear stress during initial direct shear of bentonitic mudstone

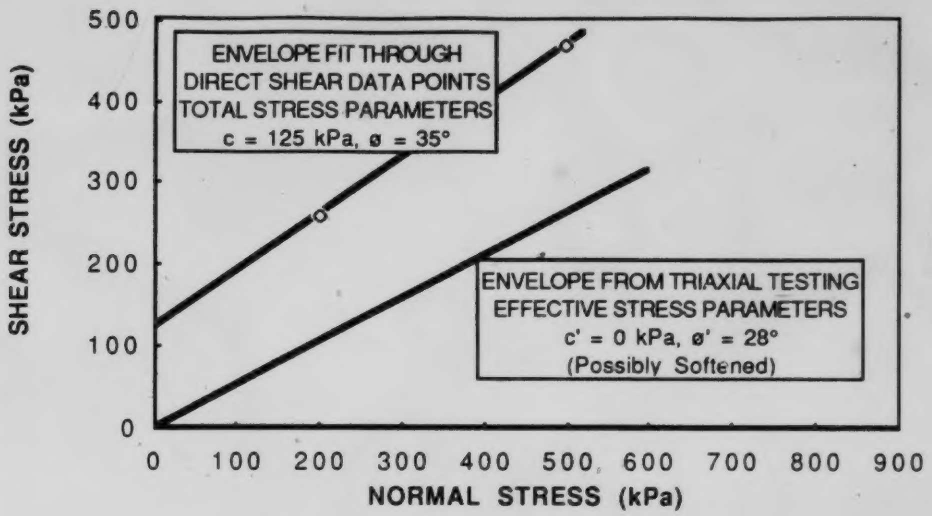

Figure 5.14 Mohr Coulomb plot of peak shear strength for bentonitic mudstone from CU triaxial tests and drained direct shear tests

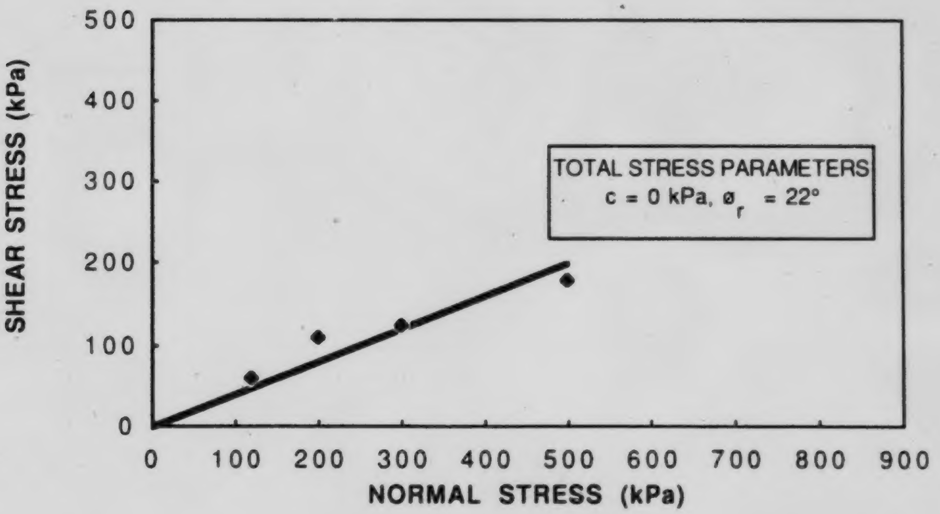

Figure 5.15 Mohr Coulomb plot of residual strength for bentonitic mudstone from direct shear tests

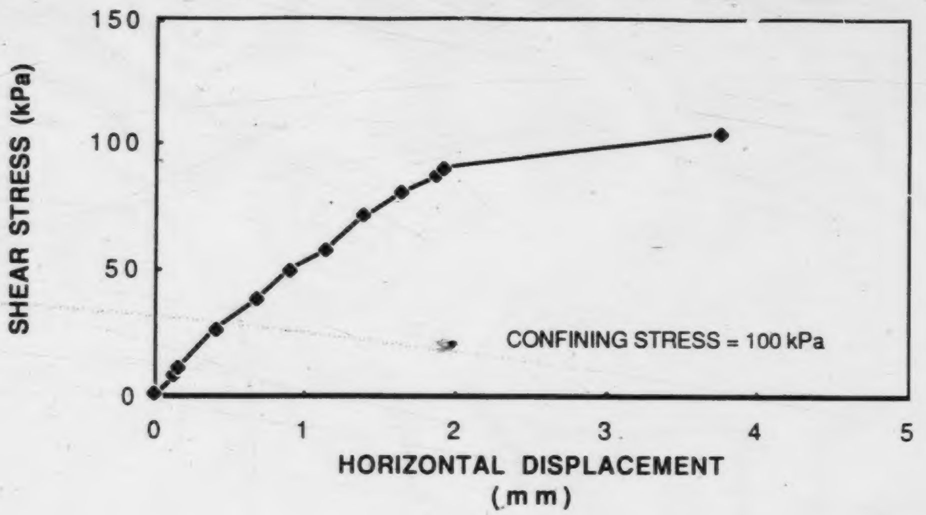

Figure 5.16 Shear stress during initial direct shear of bentonite

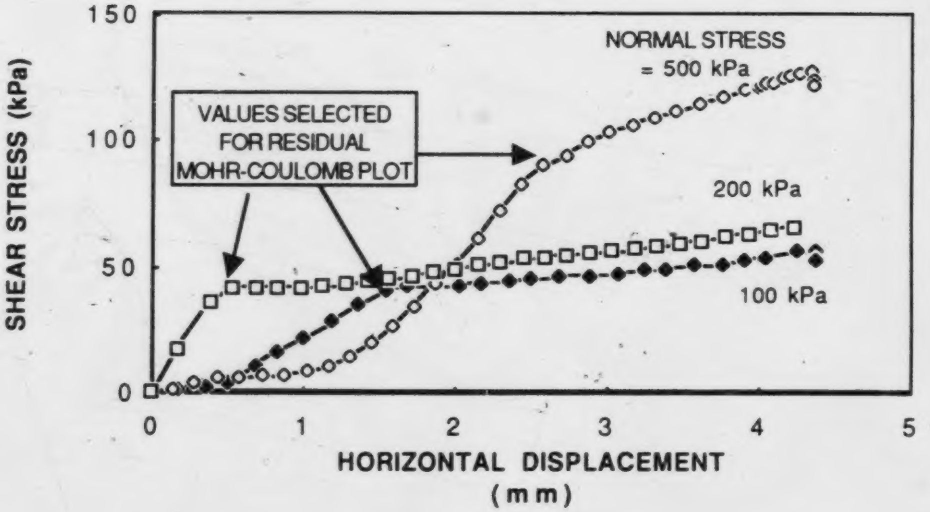

Figure 5.17 Shear stress during direct shear of bentonite to residual

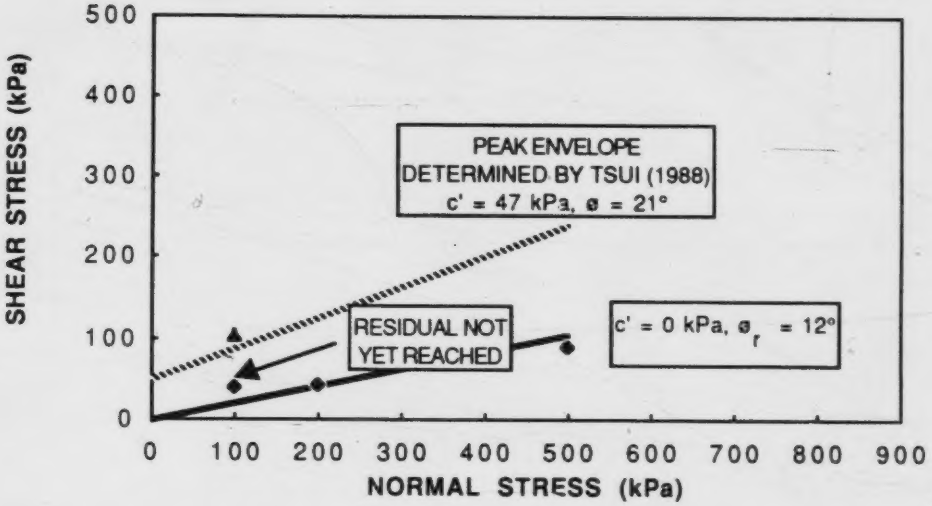

Figure 5.18 Mohr Coulomb plot of bentonite strength

6 ANALYSIS OF FAILURE

One of the objectives of this thesis was to evaluate how the strength of the sandstone and mudstone were influenced by excavation in soft rock. The best way to meet this objective was by a failure of the highwall. Fortunately,one occurred in the highwall, north of the study site in the spring of 1988 that was large enough to show the strengths mobilized at the highwall, yet small enough not to hamper mining activities.

An additional benefit from such a failure was illuminating the processes that lead to instability. This factor is of importance when considering remedial or monitoring programs.

6.1 Failure Description

The highwall failed in front of inclinometer S4, Figure 6.1, on Cut 21 in late March and early April, 1988. On March 12, 1988, the dragline had completed overburden stripping at this location and the failure occurred one to four weeks after that time. It was contained in the highwall and did not extend into the bench.

The failure initiated in front of S4 and progressed over 100 metres eastward along the highwall. Figures 6.2 and 6.3 show cross sections through the failed area and indicate the geometry and stratigraphy before failure and the post failure topography.

At the western end of the failure, two grabens had developed indicating two distinct slips had occurred. On the eastern half, no grabens were present and it was inferred that a single failure took place there.

6.1.1 Slip Surface Geometry

It was likely that the base of the failures was in the 100 mm thick bentonite seam located just above the coal sequence. Significant movements had been measured in this seam before failure (Section 4.2) and its location satisfied the post failure geometry.

The backscarp for the failures, Figures 6.2 and 6.3, were visible in the sandstone inclined 80° to 85° to the horizontal. With the basal slip plane and a portion of the backscarp known, then the likely location of the complete slip surface was estimated as shown in Figures 6.2 and 6.3.

Based on the above observations, the failure was best described as an "earth block slide" in accordance with the classification put forth by Varnes (1978). Other workers at the Highvale Mine have termed this to be a composite failure combining a steep rotational slip plane at the backscarp with a near horizontal basal plane (Wade and Peterson 1986, Fenton et al 1986, and Tsui 1988).

Section A-A' in Figure 6.2, was considered for back analyses of the failure, since two distinct slides had developed at that location. The failure closest to the toe was referred to as the "toe failure" with the second one called the "rear failure".

6.1.2 Time of Failure

The timing of the failures was not precisely known, however, the highwall was intact on March 18, 1988 with the failure first observed by this author on April 7, 1988, 32 days after the highwall was cut in front of S4. At that time, both failures had taken place at Section A-A' and the rear failure had progressed beyond Section B-B'. In the week after April 7, 1988, the rear failure continued eastward for approximately another 20 metres before the highwall finally stabilized.

To establish the timing of the failures, the surface features were examined and the following observations noted:

1. On April 7, 1988, much debris had collected on the graben of the toe failure, Figure 6.2, while the graben for the rear failure was not littered to the same extent. The rear graben still possessed the surface features of the slope face.
2. The backscarp of the rear graben was damp and had not yet dried like the toe block.

It was concluded from these observations that the rear failure probably occurred shortly before April 7, 1988 and that the toe failure preceded this by two to three weeks. Hence, for the back analyses, it was assumed that the toe failure took place one to three weeks after the highwall was cut (between March 18 and April 2, 1988) and the rear failure occurred three to four weeks after the cut (on approximately April 4, 1988).

Figures 6.4 to 6.6 illustrate how the failure probably progressed over time at Section A-A'. Figure 6.4 represents the highwall immediately after it was cut on March 12, 1988 and before the failure commenced. Between March 18 and April 2, 1988, the first slip took place at the toe, as shown in Figure 6.5. On about April 4, 1988 the rear slide developed at Section A-A' as shown in Figure 6.6. It is likely that the slide at Section B-B' followed the failure at A-A'.

6.1.3 Water Pressures

It was fortunate that the failure occurred in front of the most instrumented section of the study site. The hydrogeological results presented in Section 4.3 (Figures 4.22 to 4.30) could then be utilized in the failure back analyses. The pore pressure trends presented in that section were extrapolated to the rear and toe failures by assuming a parabolic decrease in pressure head toward the toe. Recall that the groundwater flow near the highwall face changed from horizontal to vertical from the sandstone through the mudstone and bentonite. The piezometric records indicated that negative pore pressures were unlikely on the slip plane in the mudstone.

Figures 6.7 and 6.8 show the assumed water pressure distributions one to two weeks and two to three weeks after the highwall was cut. These were used in the analyses for the toe failure. Figure 6.9 presents the piezometric head three to four weeks after the cut was made, applicable to the rear failure.

6.1.4 Strength Estimates

In the back analysis of the failures, meaningful estimates of the sandstone, mudstone, and bentonite strengths were necessary. The laboratory strengths reported in Table 5.2 provided guidelines for these estimates, but, it was recognized that the effect of discontinuities in the rock mass and rebound due to excavation would prevent these laboratory values from adequately explaining the failure. It was expected that cohesion in the sandstone and mudstone would have a dominant role in the analysis, and therefore, estimates of the friction angle were made and the cohesion left unassigned. The magnitude of cohesion mobilized at failure was then determined through back analysis.

Sandstone

Failure in the sandstone was assumed to be partly controlled by the near vertical joint set that trended East-West, parallel to the highwall crest (Section 1.1.1). Exposures of the near vertical slip planes at the backscarp, Figures 6.2 and 6.3, were free of any clay and it was therefore assumed that the upper part of the slip plane travelled along a clean joint. Beneath the visible portion of the slip surface, it was assumed that failure took place along other joints and through blocks of intact sandstone.

For the analyses, the part of the slip surface exposed after the failure was assigned residual strength parameters to model the presence of a joint, $\phi = 40°$, $c = 0$ kPa. The remainder of the slip surface in the sandstone was expected to have a friction angle ranging from the residual value of 40° to a peak of 44°. The cohesion along the lower part of the slip surface in the sandstone was found by back analysis.

Mudstone

For the mudstone, the scale of the failures was large compared to the small joint spacing. Consequently, it was assumed that the mudstone would behave in a homogeneous fashion. The peak friction angle of 37.5° obtained from intact samples in the laboratory was initially considered as an upper bound for the frictional strength at failure. However, it was believed that the fissured nature of the mudstone would discount this value and, furthermore, water was available to generate softening.

Alternatively, if the slip planes had been along pre-existing discontinuities in the mudstone, then the residual strength of the material, $\phi_r = 6.5°$ to $22°$, would have been a minimum for the strength at failure.

It was assumed that the slip plane through the mudstone was a combination of shear along joints and through intact lumps, both of which probably experienced a degree of softening. Therefore, for the analyses, an intermediate friction angle of 22° was selected to reflect the combined effects. This was close to the value used by Tsui (1988), and in addition, it was recognized that the mudstone unit was not thick enough for variations in the friction angle to make a large difference. The cohesion mobilized in conjunction with this friction angle was found by back analyses.

Bentonite

In Section 4.1, it was concluded that the bentonite was presheared and residual strength parameters should be applied in stability analyses. A residual angle of 12° was measured in the laboratory on samples near the presheared plane, however, experience with this material has found that the in-situ slip plane may have a lower strength. As a result, an angle of 10° was chosen as a lower bound of the strength along the basal slip plane. Since the bentonite was presheared, then the cohesion was set to zero throughout the analyses.

Table 6.1 summarizes the estimates of material strengths that were used in the failure analyses.

Table 6.1
Estimates of Strength Mobilized at Failure

MATERIAL	FAILURE STRENGTH	
	ϕ	c
Upper Part of Sandstone (joint)	40°	0
Lower Part of Sandstone	40° to 44°	BA
Peak Strength of Mudstone	37.5°	?
Intermediate value for Mudstone	22°	BA
Lower bound for Mudstone	6.5°	0
Bentonite	10°	0 kPa
	8°	0 kPa

BA - To be determined by back analysis

6.2 Failure Back Analysis

6.2.1 Limit Equilibrium Method

Two dimensional, limit equilibrium methods of stability analysis were used to determine the strength parameters mobilized at failure. The slip planes, water pressures, and frictional strengths described in Section 6.1 were input and the sandstone and mudstone cohesions varied until a Factor of Safety of unity was achieved.

Computations were performed with the aid of a personal computer and the slope stability program PC-SLOPE (Fredlund, 1985). PC-SLOPE determined a Factor of Safety (FOS) based on General Limit Equilibrium; calculating a FOS that satisfied moment and force equilibrium. The distribution of interslice shear forces could be selected and, by varying their magnitude, then a single Factor of Safety was obtained that simultaneously satisfied all equilibrium. The results of the computer program were extensively checked by hand calculations using the Janbu Simplified Method of slope stability which satisfied only force equilibrium.

Drained conditions were assumed throughout the analyses. This was expected because of the fissured nature of the materials to adequately dissipate excess pore pressures.

The interslice shear force distribution used for these analyses was based on a finite element formulation (Fredlund, 1984) and the magnitude of the interslice shear forces was apportioned by the variable, λ. For further information on the details of limit equilibrium methods of stability analysis, the reader is referred to (Fredlund, 1984).

6.2.2 Example of Results

For each analysis, the problem geometry, water pressures, and friction angle of the sandstone, mudstone, and bentonite were held constant. A value of cohesion was assigned to the sandstone (i.e. 0, 5, 10, 15 kPa, etc) and a value for mudstone cohesion assumed. PC-SLOPE was then used to determine the FOS that satisfied force and moment equilibrium over a range of λ's.

As an example, the stability of a potential slip surface at the toe, Figure 6.10(a), was considered with the parameters shown in Table 6.2. Note in Figure 6.10(a) that the upper part of the slip surface was assigned zero cohesion to model the presence of a joint. The results from the analysis are presented in Table 6.2 while Figure 6.10(b) plots the force and moment equilibrium FOS against λ to determine the value of FOS that satisfied all equilibrium. In this instance the FOS at all equilibrium was found to be 1.06.

A second value of mudstone cohesion, 20 kPa, was then assumed and a FOS of 0.84 calculated. Table 6.3 and Figure 6.11 present the results from three trials that varied the mudstone cohesion and bracketed a FOS of unity. This procedure then determined that a mudstone cohesion of 35 kPa would have been mobilized at failure, assuming that the other assumptions were correct.

The analysis was continued by assigning additional values of sandstone cohesion and determining the corresponding mudstone cohesion at failure. These results are discussed below.

Table 6.2

Example of Stability Analysis for Toe Failure

Input Parameters:

- Geometry in Figure 6.11(a)
- Water Pressures at one-two weeks after highwall was cut.
- Bentonite ϕ = 10°
- Sandstone ϕ = 40°
- Sandstone c = 10 kPa, below joint
- Mudstone ϕ = 22°
- Mudstone c = 40 kPa

Results of Stability Analysis:

	Factor of Safety	
λ	Force	Moment
0	0.97	1.12
0.2	0.99	1.10
0.4	1.01	1.09
0.6	1.03	1.08
0.8	1.05	1.07
1.0	1.06	1.06

Factor of Safety at all Equilibrium from Figure 6.11(b) is 1.06

Table 6.3

FOS for Toe Failure Determined at Selected Values of Mudstone Cohesion

Input Parameters:

- Geometry in Figure 6.11(a)
- Water Pressures at one-two weeks after highwall was cut.
- Bentonite $\phi = 10°$
- Sandstone $\phi = 40°$
- Sandstone c = 10 kPa, below joint
- Mudstone $\phi = 22°$

Mudstone Cohesion (kPa)	FOS at all Equilibrium
40	1.06
30	0.95
20	0.84

From Figure 6.11, Mudstone Cohesion = 35 kPa at FOS = 1.

6.3 Analysis of Toe Failure

The above example assumed the location of the slip surface and determined the FOS along it. Since the actual location of the slip surface was unknown below the visible exposure of the backscarp, then it was necessary to assume several slip surfaces and determine the most critical one. The geometries assumed for this search are shown in Figure 6.12. Utilizing the same water pressures and strength parameters as in Table 6.2, the FOS for each slip surface was determined and reported in Figure 6.12. The slip surface with the lowest FOS was assumed to be most representative of the actual slip surface.

With the likely actual slip surface geometry established, then the stability analyses were continued by assuming a new value for the cohesion in the sandstone and determining a corresponding cohesion mobilized in the mudstone at failure. The results of this work are presented in Figure 6.13.

During the analyses, when a sandstone cohesion greater than 20 kPa was used, then the force and moment equilibrium FOS would not converge and a solution was not possible. Hence, extrapolations beyond this level of sandstone cohesion are tentative, as shown in Figure 6.13.

6.4 Analysis of Rear Failure

As in the analysis of the toe failure, several slip surface combinations were explored to determine the critical one. Figure 6.14 shows three of the potential slip planes and the calculated FOS. The slip surface with the minimum FOS was then assumed to be the likely location of the actual failure plane.

Values of sandstone cohesion were varied and the corresponding mudstone cohesions at failure back calculated in the same manner as in Section 6.3 with the results shown in Figure 6.15.

6.5 Influence of Pore Pressure Assumptions

The above analysis of the toe failure used the water pressure distribution at one to two weeks after the highwall was cut. Since it was possible that the toe may have failed two to three weeks after the cut was made, then the pore pressure distribution (Figure 6.8) was adjusted to reflect this. The resulting combination of mudstone and sandstone cohesions is shown on Figure 6.14. Although the water pressures were increased twofold, their absolute magnitude was so low to begin with that there was not a significant impact on the results.

At the rear failure, the assumed pore pressure distribution at three to four weeks after the highwall was cut (Figure 6.9) was considered realistic and did not require adjustment.

As shown in Figures 6.7 to 6.8, the pore pressures experienced a recovery from the effects of stress relief to a steady state flow condition. This took approximately four weeks to develop and could partly explain why the failures did not occur immediately after the highwall was excavated.

6.6 Combined Results

Figure 6.16 combines the results from the back analyses of the toe and rear failures and illustrates a dramatic difference between the strengths mobilized at the two failures. The effect of increasing the bentonite friction angle from 10° to 12° is also presented and was found to have a slight impact on the results. Because of the sensitivity of these findings to the bentonite strength, it is recommended that field shear box tests be performed to accurately establish this variable.

Additional parametric analyses were performed that varied the sandstone friction angle from 40° to 44° and the mudstone friction angle from 12° to 37.5°. The findings of these analyses are not reported here since they changed by less than 5%.

Figure 6.16 shows that for any value of sandstone cohesion, then the mudstone cohesion decreased from the rear failure to the toe failure. The same can be said about the sandstone cohesion for any value of mudstone cohesion. It is possible that both the sandstone and mudstone cohesion simultaneously decreased from the rear to the toe. Hence, it can be concluded that the sandstone and mudstone strengths decreased with proximity to the highwall toe.

6.7 Effect of Lateral Straining on Strength Reduction

Several processes were no doubt involved in decreasing the rock strength from the rear to the toe failures, such as local variations in structure and so on. But, the most dominant difference between these two locations was how they were affected by overburden excavation. In Section 4.2.2, it was concluded that rebound due to excavation caused the sandstone and mudstone to undergo significant lateral straining with the magnitude of strain increasing toward the highwall toe. It is conjectured here that the material strength may be inversely related to this lateral straining. That is, with more strain, then less strength might have been available.

6.7.1 Conceptual Model of Strength Reduction

Figure 6.17 illustrates conceptually, how the strength of the sandstone and mudstone might have decreased with proximity to the highwall toe due to lateral straining. Beyond the zone of influence of excavation, where the lateral strains were effectively zero (i.e. beyond a distance of 300 metres from the highwall crest, as found in Section 4.2.2), then it is likely that the material, or rock mass strength was a maximum. At some point within the zone of influence, the lateral strains probably led to a reduction in strength, reaching a minimum at the highwall toe.

The actual extent and rate of strength decrease is unknown, but, the failure at Section A-A' (Figure 6.2) has provided valuable insight into how the strength decreased in the region between the highwall crest and toe.

6.7.2 Estimate of Lateral Strains at Failure

Deformation measurements were taken on March 17, 1988 and April 13, 1988, before and after the failures had developed. The lateral strain field at these dates is shown in Figure 6.18 while Table 6.4 summarizes the strain data at the location of the toe and rear failures. The data in Table 6.4 must be treated with caution, since it was obtained by extending the known strain field beyond the highwall crest to the toe, Figure 6.28, where strain measurements were not possible.

The variation in strain over time at the toe and rear failure locations is shown in Figures 6.19 and 6.20 with the results for March 17 and April 13, 1988 shown as clear symbols. Additional strain data was plotted as dark symbols for similar positions in the highwall after the three previous cuts on June 25, 1987, September 23, 1987, and December 9, 1987. Interestingly, the strains were similar after each cut was made.

Curves fit through the points on Figures 6.19 and 6.20 (ignoring the anomalous strain at December 13, 1987) were

Table 6.4
Lateral Strains on March 17, 1988
and April 13, 1988

Date	Number of Days After Highwall Cut	Location	Lateral Strain (%)
Mar. 17, 1988	5	Toe Failure Rear Failure	0.62 0.54
April 13, 1988	30	Toe Failure Rear Failure	0.70 0.62

transferred to Figures 6.21 and 6.22. These figures were then used to estimate the strains at the time of failure.

When the toe failed, one to three weeks after the highwall was cut, the lateral strains at the time of failure were estimated to be between 0.65% to 0.72%. When the rear failure occurred, the strains were approximately 0.64% to 0.66%. Although the difference in strains was subtle, the increase might have been large enough to trigger a decrease in strength. It is also possible that the extension of the strain field beyond the highwall crest was not accurate and that strains near the toe were greater than estimated.

Because the lateral strains apparently affected the rock mass strength, then it is recommended that a method be developed that would measure the strains immediately at and behind the highwall face.

6.7.3 Consider Stable Highwall in Front of S3

In the previous section, it was tentatively concluded that the higher strains resulted in a lower rock mass strength. The trend was subtle and subject to potential problems with extending the strain data beyond the highwall crest. But, this conclusion received support when the highwall in front of S3 was considered. As shown in Figure 6.1, the highwall remained stable and implied that the rock strength was greater than in front of S4.

Two differences existed between these locations:

1. The sandstone/mudstone contact was two metres higher in front of S3 than in front of S4;
2. The deformation and strain fields were different between the two locations (Section 4.2).

Could the two metres of additional mudstone in front of S3 have been so strong to account for the increase in overall strength? Examination of the borehole and geophysical records did not indicate that the extra two metres of mudstone was remarkably strong and could make an impact on stability. Therefore, the strain field was examined to explain the apparent difference in strengths between line S3-S5 and S4-S6.

Figure 6.23 presents the strain field on March 17, 1988 along lines S4-S6 and S3-S5. It shows that five days after the highwall was cut, the lateral strains along line S4-S6 were greater than along line S3-S5. As listed in Table 6.4, the lateral strains at the toe and rear failure along line S4-S6 were 0.62% and 0.54%, respectively. Along line S3-S5, where the highwall was stable, the lateral strains were found to be 0.20% less.

This observation supported the conclusion that greater lateral strains resulted in lower strengths.

6.8 Progressive Loosening and Softening

The above discussion concluded that as the highwall rebounded into the pit, there was a reduction in strength of the sandstone and mudstone due to lateral straining. Two mechanisms were likely at work: progressive loosening and progressive softening.

6.8.1 Progressive Loosening

In Sections 4.2.2 and 4.3.1, it was determined that the lateral straining caused joints to spread. Figure 6.24 illustrates schematically this phenomenon and is the basis for the mechanism of "Progressive Loosening", where the strength decreased as the material loosened. It is believed that loosening reduced the strength of the sandstone and mudstone in two ways:

1. As the joints opened wider, then the normal stresses and dilatancy reduced. This caused a decrease in shearing resistance along the joints.
2. The intact blocks of sandstone and mudstone likely slid over one another and reduced the contact area between them. The contact stress between the blocks would have increased and might have led to local shearing through the blocks themselves.

Loosening is termed progressive since it was a function of lateral straining. It is probable that progressive loosening damaged the sandstone more than the mudstone because of the former's block-like and brittle nature.

6.8.2 Progressive Softening

Although progressive loosening might have developed in the mudstone, it was more likely that "Progressive Softening" was at work as the opened joints permitted water to infiltrate the mudstone and soften it. As shown in Figure 4.28, the lateral straining caused the ground water flow regime to alter direction and allow water to seep from the sandstone through the mudstone into the coal below. Not only were fresh surfaces exposed by joint widening, but the amount of water to contact these surfaces also increased. The result would have been an acceleration of the softening process in response to lateral strain, i.e. progressive softening. Figure 6.25 presents a schematic of the progressive softening mechanism that may have developed with increasing water content.

Clay shales (mudstone at Highvale Mine) are renowned for their susceptibility to softening. In fact, a failure in Cretaceous clay shale near Devon, Alberta, 60 km east of the Highvale Mine, was adequately explained by assuming softened parameters for the clay shale (Eigenbrod and Morgenstern, 1972).

Progressive softening may have also developed in the sandstone because it contained a significant amount of montmorillonite.

Together, the progressive loosening and softening mechanisms satisfactorily explained the overall progressive reduction in strength.

6.9 Concept of Critical Strain

In Section 6.4.3, it was stated that the toe failed when the lateral strains reached 0.65% to 0.72% and that the rear failure occurred at lateral strains of 0.64% to 0.66%. The reader may have concluded that when the lateral strains exceeded approximately 0.65%, then failure was imminent. This was not necessarily the case and the statement of a "critical strain of 0.65%" could be misleading.

Over the duration of the monitoring program, several sections of the highwall experienced lateral strains greater than 0.65% and did not fail. Figures 6.19 to 6.22 showed how the strains developed after four different highwalls were cut. All four had lateral strains above 0.65% but only one of them failed.

More evidence is available to caution use of the concept of a critical strain. Figure 6.26 presents the strains along line S2-S4-S6 after the coalwall was cut. These strains were found at a distance of 15 metres beyond the highwall crest, coincident with the location of the toe failure on Cut 21. Figure 6.26 shows lateral strains of 0.73% were mobilized after the coalwall was cut, yet three of the four highwalls monitored during this program continued to stand.

Furthermore, the lateral strains along line S1-S3-S5 tended to exceed 0.65% after the coalwall was cut and the highwall remained intact throughout. Figure 6.27 shows the general development of strains 15 metres beyond the crest from the time when the highwall was cut to after the coal had been excavated and indicates that lateral strains developed in excess of 0.65%.

While a variation in pore pressures may partly explain the absence of failures at some locations, there must have been an additional feature that separated the failed section from the others. This feature was probably an unfavourable joint orientation in the sandstone that was not encountered elsewhere. Structure in the mudstone was likely limited because of its brecciated nature.

More strain information is required to develop a database of strains that lead to failure. This study provides a starting point for such a database.

6.10 Failure Mechanism

The above discussion put forth several concepts and ideas that satisfactorily explained the failure on Cut 21 in March and April, 1988. The key features of the failure mechanism were the progressive reduction in strength as a result of lateral straining and the sandstone structure. Secondary contributors to the failure were the presheared bentonite and recovery of water pressures after excavation. Succinctly, the failure mechanism may be described as follows:

> Excavation rebound resulted in a progressive loosening and softening of the sandstone and mudstone. This decreased their strengths to unstable levels and, when combined with unfavourable jointing in the sandstone, resulted in a failure of the highwall.

It is speculated that if the toe block had not failed, then the rear block might have remained stable. This particular aspect is ventured without proof, but is worthy of consideration when designing remedial measures (section 7.2).

6.11 Comparison with other Stability Investigations at Highvale

As discussed in Section 1.2.5, several workers have previously performed stability investigations at Highvale. The stability models prepared by these authors and their estimates of strength are detailed below.

6.11.1 Wade and Peterson (1986)

Wade and Peterson (1986) investigated the stability of the highwall in Pit 03 by assuming a composite slip surface similar to the ones presented in Figures 6.13 and 6.15. The slip surface geometry assumed by these authors is shown in Figure 6.28. A slip indicator installed in 1984 indicated that the base of the slip plane was located at the sandstone/mudstone contact instead of in the bentonite.

The strength parameters used by Wade and Peterson are presented in Table 6.5. These values were obtained from back analyses of previous failures. The frictional strengths in Table 6.5 compared favourably with the values used in this study. The cohesions were based on the degree of disturbance from glacial tectonism (Section 2.4).

An important difference between the analysis by this author and those by Wade and Peterson (1986) was in the assumption of pore water pressures. As indicated in Section 6.1.3, the vertical flow of water resulted in low pore pressures acting on the potential sliding mass. Wade and

Peterson (1986) assumed horizontal flow to the highwall face, and consequently used hydrostatic pore pressures below a groundwater elevation. Such an assumption could lead to an overestimation of the pore pressures by an order of magnitude. As a result, back analyses of failures would result in higher mobilized cohesions and stability analyses of future cuts would require higher cohesions to provide stability.

6.11.2 Barron et al (1986)

Barron et al (1986) assumed a plane shear mechanism, as shown in Figure 6.29, to model a failure in Pit 03 in the spring of 1984. Several tension cracks were located in the failure area and were assumed to penetrate to the basal slip plane, assumed to be the bentonite seam above the coal. The strength parameters for the bentonite used by these authors are shown in Table 6.5. The sandstone and mudstone strength above the bentonite were assumed to be zero because of a tension crack. Water pressures were obtained from 20 piezometers in the area and it was concluded that a phreatic surface was located 7 to 8 metres above the failure plane. The planar shear model developed by Barron et al (1986) accurately simulated the development of the tension cracks.

Two important findings from this study affected the model prepared by Barron et al (1986): (i) the bentonite was presheared and (ii) the water pressures were not hydrostatic

Table 6.5
Other Stability Investigations
at Highvale Mine

	Wade and Peterson (1986)	Barron et al (1986)	Tsui (1988) Slide 1	Tsui (1988) Slide 2
Failure Mode	Composite Rotational	Planar Shear	Composite Rotational	Planar Shear
Base of Slip Plane	SS/MS Contact	Bentonite	SS/MS Contact	SS/MS Contact
Sandstone ϕ = Sandstone c =	45° 100 kPa	In Tension	40° 0 kPa	In Tension
Mudstone ϕ = Mudstone c =	25° (Note 1) 10 kPa	In Tension	11.5° 0	23.6° 0
Bentonite Bentonite c =	- -	24.6° 9.3 kPa	- -	- -
Water Pressure	Hydrostatic	Hydrostatic in Tension Crack	Hydrostatic in Sandstone Zero in Mudstone	Hydrostatic in Tension Crack, Zero in Mudstone

Note 1: The mudstone was assumed to be displaced by glacial thrusting.

below a phreatic surface. This author believes that the strength estimate and water pressures were over estimated by Barron et al (1986). Since these two factors counter one another, it is possible, that if the findings from this study were applied to the planar shear model, then the development of the tension cracks may still be successfully simulated.

6.11.3 Tsui (1988)

Two slides had occurred in Pit 03 in July, 1984 and were analysed by Tsui (1988). Tension cracks were observed just before the slides started and were assumed to mark the top of a steep back scarp that followed vertical joints, as shown in Figure 6.30(a) and (b). The base of slips was assumed to be located at the sandstone/mudstone contact, which was a shear zone created by ice thrusting (Section 2.4).

As with the studies discussed above, a groundwater table was assumed in the sandstone with hydrostatic pore pressures below this level. The water table was assumed to be perched in the sandstone and underlain by an unsaturated zone in the upper portion of the mudstone. These assumptions were based on piezometers installed in the sandstone and coal sequences. None had been placed in the mudstone and, consequently, no information was available on the potential for vertical flow through the mudstone.

Slide 1 was treated as a composite rotational failure and assumed zero cohesion for the sandstone. Tsui adequately explained the failure by assigning c = 0 kPa, ϕ = 11.5° to the mudstone. Slide 2 was analyzed as a plane failure with a vertical tension crack extending to the sandstone/mudstone contact. A mudstone strength of zero cohesion and a friction angle of 23.6° was back calculated. The difference between mudstone strengths was attributed to the presence of coal chips in the latter slide.

The sandstone and mudstone strengths obtained by Tsui (1988) were lower than those found by this study. This may partly be explained by the differing water pressure distributions, but, by applying hydrostatic pore pressures on the backscarp and no pore pressures on the basal slip plane, the net effect may be similar to utilizing the pressure distributions described in this report.

Considering the state of the highwall in 1984, the fact that Tsui found lower strengths than this author is not unexpected. The highwall in 1984 had been extensively disrupted by glacial tectonism (Section 2.4) which, in turn, would have reduced the deformation modulus of the sandstone and mudstone. Excavation would have resulted in substantial movements and instabilities, as evidenced by the number of tension cracks observed by the above authors. It is probable that if deformation monitoring had been performed at that time, it would have found lateral strains far greater than those measured at the study site described in this report. Hence, the findings by Tsui (1988) support the hypothesis offered by this author that greater lateral straining caused a reduction in strength.

6.12 Conclusions from Failure Analysis

The objective of determining the strength after excavation was met by the findings from the highwall failure described above. Several conclusions were drawn from back analyses of this failure:

1. Highwall failures did not occur immediately after excavation and required one to four weeks to develop. Time was required for the pore pressures to recover and progressive loosening and softening to develop.
2. The failure mode was a retrogressive composite rotational failure, described as an earth block slide by Varnes (1978)
3. Water pressures at the time of failure were low due to the vertical flow through the overburden.
4. The basal slip plane was a presheared surface within the bentonite seam, just above the top of the coal.
5. Variations in the friction angle of the bentonite had an impact on stability
6. Variations in the friction angle of the sandstone and mudstone had a minor influence on the stability.

7. Highwall stability was very sensitive to cohesions in the sandstone and mudstone.
8. The role of lab testing was relegated to providing an estimate of the range of friction angles for the analyses. The cohesions obtained in the lab could not be used to satisfactorily explain the condition of stability in the field.
9. The strength of the sandstone and mudstone decreased closer to the highwall toe.
10 Rock mass strength was inversely related to lateral strains caused by rebound.
11. Lateral straining resulted in a progressive loosening and softening of the sandstone and mudstone.
12. Failure occurred when the lateral strains exceeded 0.65%, however this value of strain cannot be viewed as a boundary number above which failure always occurred. Lateral strains as high as 0.73% were measured without any instabilities.

    Lateral strains of approximately 0.65% may be considered as necessary to lead to failure, but additional factors, such as unfavourably oriented joints, also play a role.
13. Other stability investigations conducted at Highvale in the past might benefit from the

findings described above. In most cases, the water pressures were over estimated and resulted in an over estimation of the strengths of sandstone, mudstone, and bentonite.

14. The work by Tsui (1988) tentatively supports the inverse relation between strength and lateral strains found by this author.

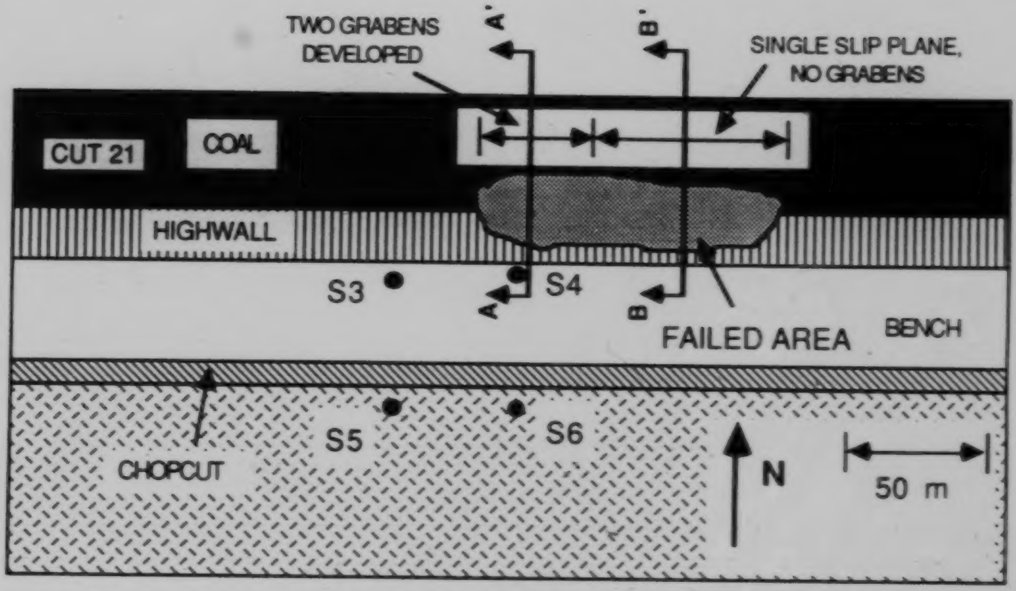
TWO GRABENS DEVELOPED
A'
B'
SINGLE SLIP PLANE, NO GRABENS
CUT 21
COAL
HIGHWALL
S3
S4
A
B
FAILED AREA
BENCH
S5
S6
CHOPCUT
N
50 m

Figure 6.1 Plan view of highwall failure in Pit
03 April, 1988

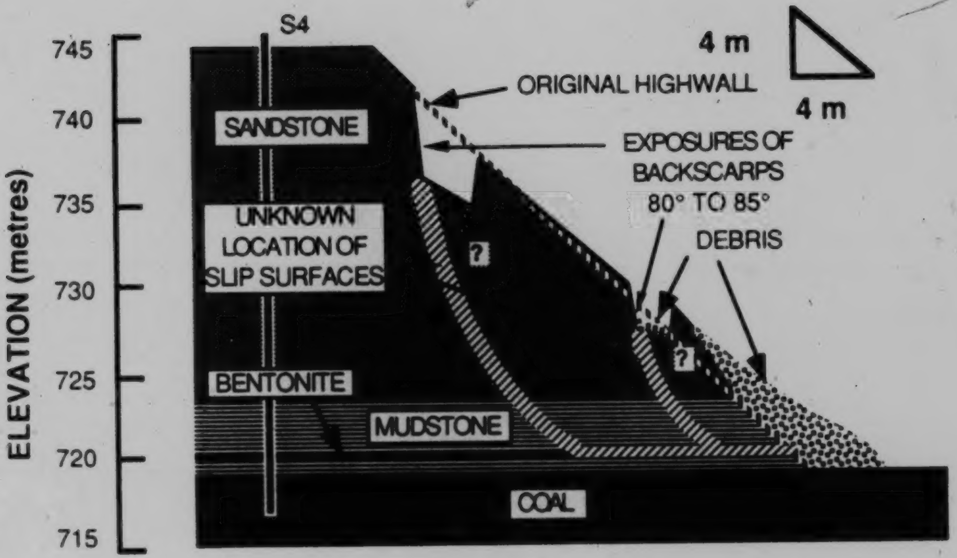

S4
745
740
735
730
725
720
715
ELEVATION (metres)
4 m
4 m
ORIGINAL HIGHWALL
EXPOSURES OF BACKSCARPS 80° TO 85°
DEBRIS
SANDSTONE
UNKNOWN LOCATION OF SLIP SURFACES
?
?
BENTONITE
MUDSTONE
COAL

Figure 6.2 Post Failure Topography at Section A-A' through the west end of the failure, as observed on April 7, 1988.

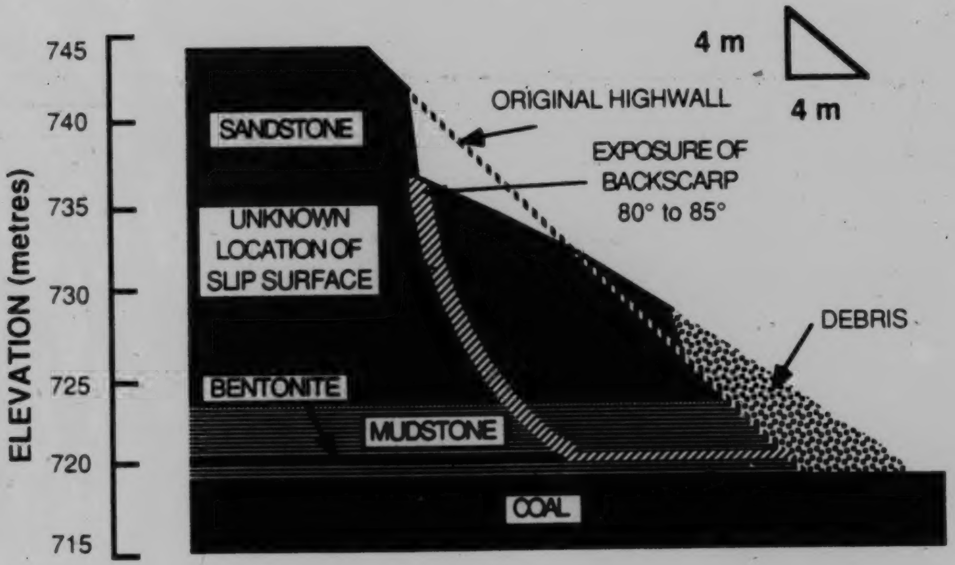

745
740
735
730
725
720
715
ELEVATION (metres)
4 m
4 m
ORIGINAL HIGHWALL
EXPOSURE OF BACKSCARP 80° to 85°
DEBRIS
SANDSTONE
UNKNOWN LOCATION OF SLIP SURFACE
BENTONITE
MUDSTONE
COAL

Figure 6.3 Post failure topography at Section B-B' through the east end of the failure as observed on April 7, 1988.

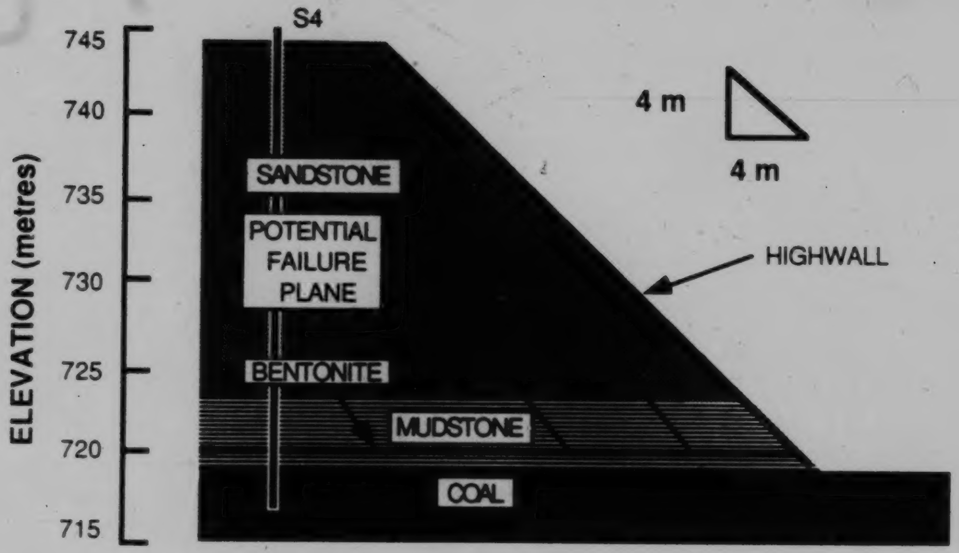
S4
745
740
735
730
725
720
715
ELEVATION (metres)
SANDSTONE
POTENTIAL FAILURE PLANE
BENTONITE
MUDSTONE
COAL
4 m
4 m
HIGHWALL

Figure 6.4 Failure model: Cross section of highwall on March 12, 1988, immediately after cut 21 was made.

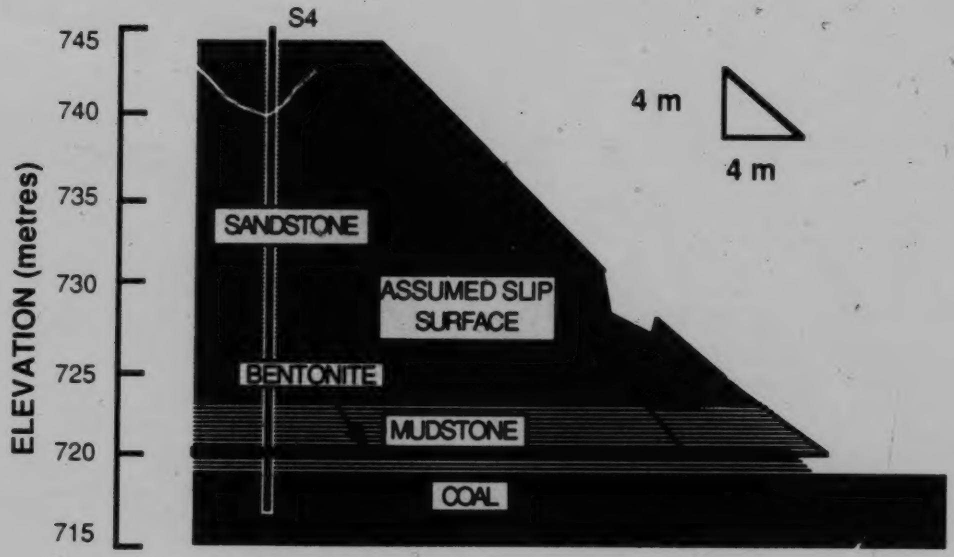
S4
745
740
735
730
725
720
715
ELEVATION (metres)
SANDSTONE
ASSUMED SLIP SURFACE
BENTONITE
MUDSTONE
COAL
4 m
4 m

Figure 6.5 Failure model at Section A-A': After failure of toe block, one to three weeks after highwall was cut, between Mar. 18 and April 2, 1988.

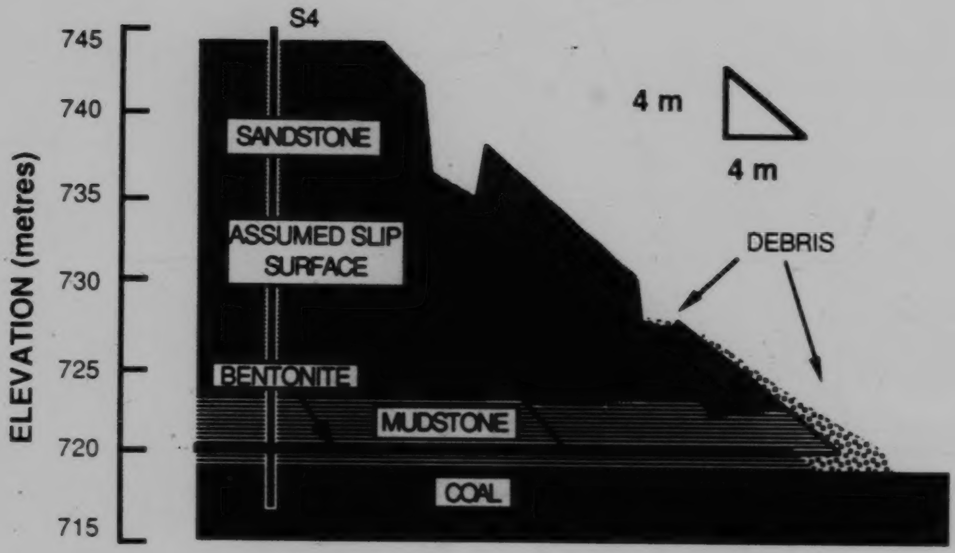
S4
745
740
735
730
725
720
715
ELEVATION (metres)
SANDSTONE
ASSUMED SLIP SURFACE
BENTONITE
MUDSTONE
COAL
4 m
4 m
DEBRIS

Figure 6.6 Failure model at Section A-A': After failure of rear block, three to four weeks after highwall was cut, approximately April 4, 1988.

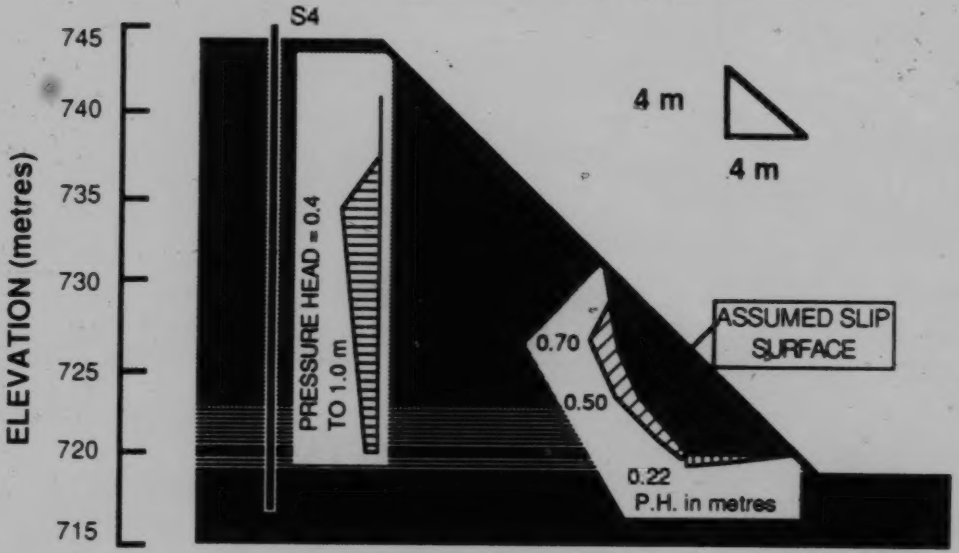
S4
745
740
735
730
725
720
715
ELEVATION (metres)
PRESSURE HEAD = 0.4 TO 1.0 m
4 m
4 m
ASSUMED SLIP SURFACE
0.70
0.50
0.22
P.H. in metres

Figure 6.7 Pore Pressure Distribution assumed for failure analyses - one to two weeks after highwall was cut.

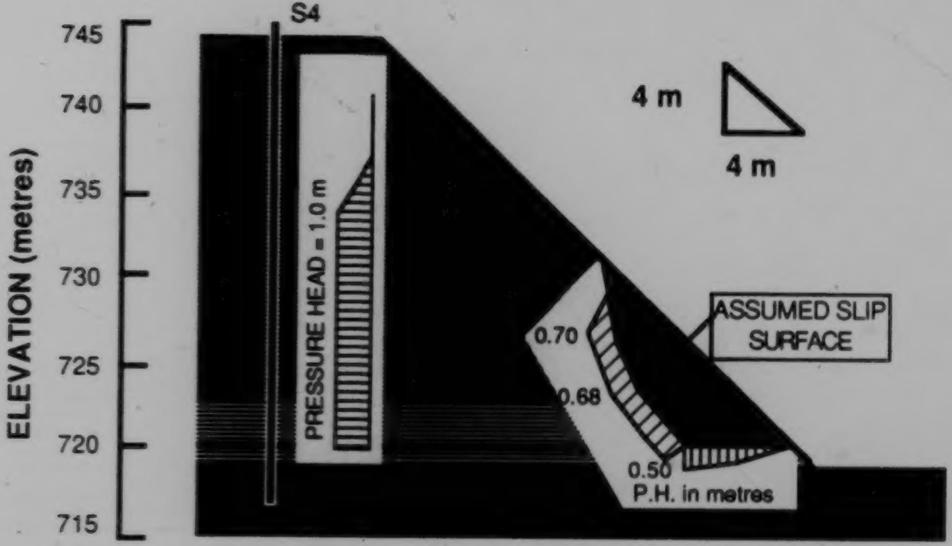
S4
745
740
735
730
725
720
715
ELEVATION (metres)
PRESSURE HEAD = 1.0 m
4 m
4 m
ASSUMED SLIP SURFACE
0.70
0.68
0.50
P.H. in metres

Figure 6.8 Pore Pressure Distribution assumed for failure analyses - two to three weeks after highwall was cut.

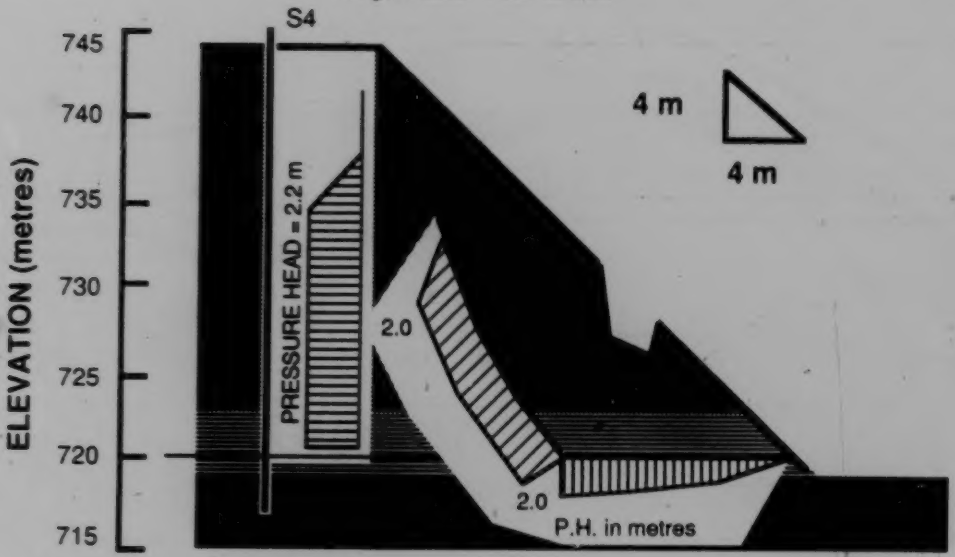
S4
745
740
735
730
725
720
715
ELEVATION (metres)
PRESSURE HEAD = 2.2 m
4 m
4 m
2.0
2.0
P.H. in metres

Figure 6.9 Pore Pressure Distribution assumed for failure analyses - three to four weeks after highwall was cut. Toe had previously failed.

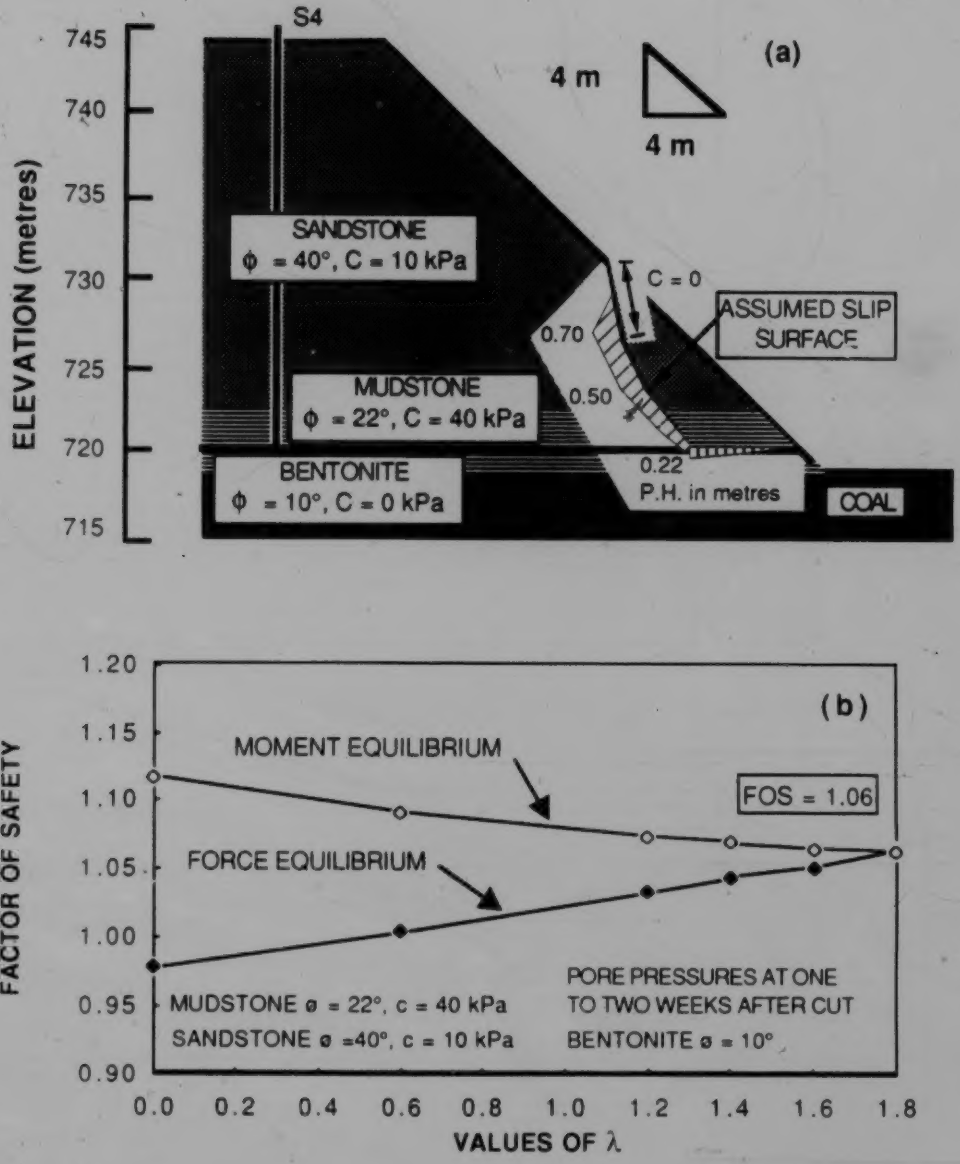

Figure 6.10 Stability analyses for toe failure (a) Geometry, water pressures, and strength parameters, (b) FOS plotted against λ. to find FOS that satisfies moment and force equilibrium.

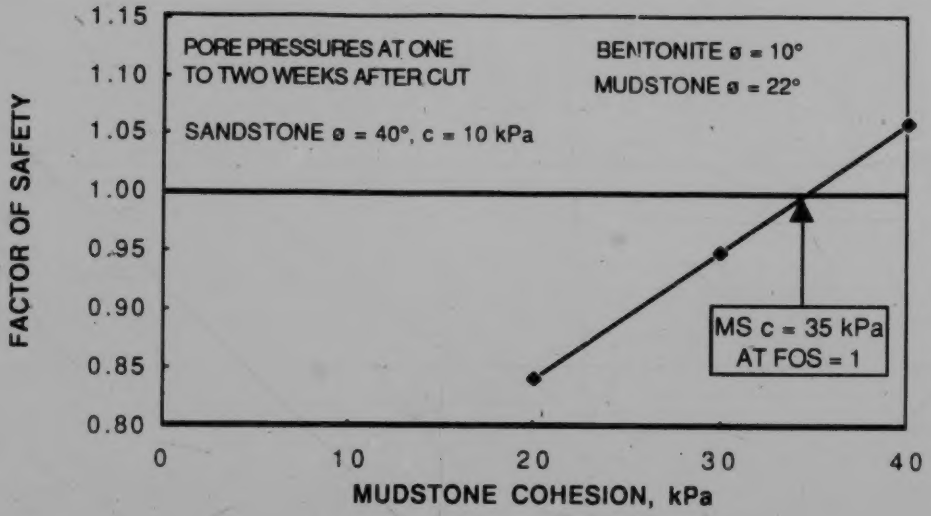

Figure 6.11 Magnitude of mudstone cohesion mobilized at a FOS of unity.

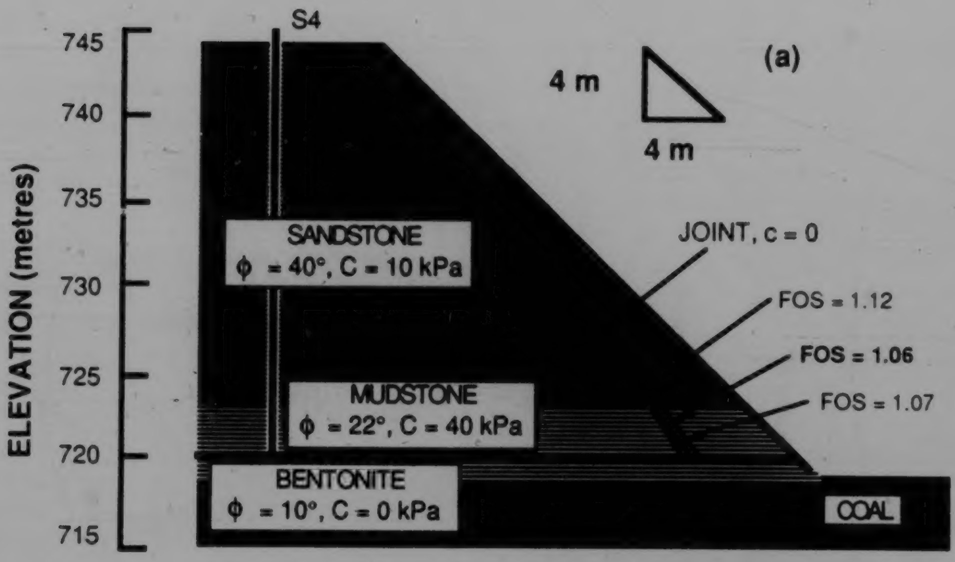

S4
(a)
4 m
4 m
ELEVATION (metres)
745
740
735
730
725
720
715
SANDSTONE
ϕ = 40°, C = 10 kPa
JOINT, c = 0
FOS = 1.12
FOS = 1.06
FOS = 1.07
MUDSTONE
ϕ = 22°, C = 40 kPa
BENTONITE
ϕ = 10°, C = 0 kPa
COAL

Figure 6.12 Assumed slip surfaces for search of critical one at toe failure (i.e. slip surface with lowest FOS).

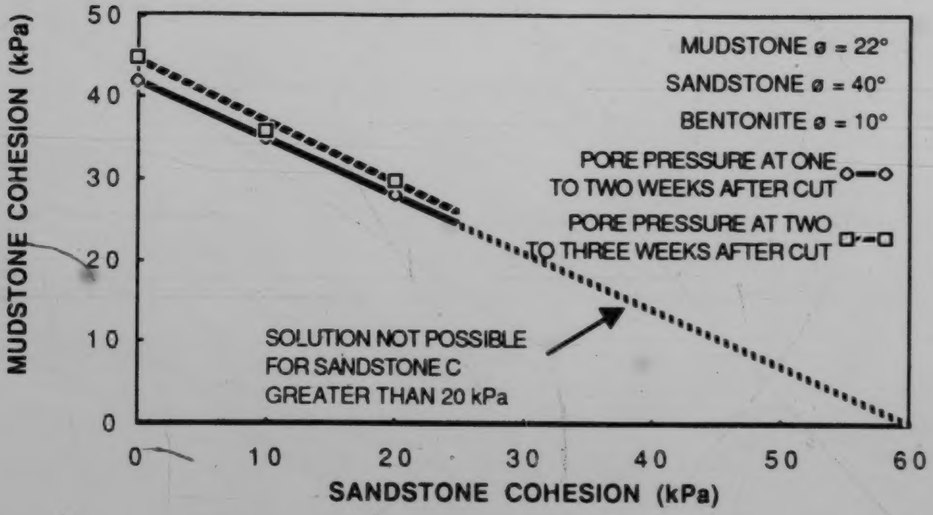

Figure 6.13 Combinations of mudstone and sandstone cohesions mobilized at toe failure.

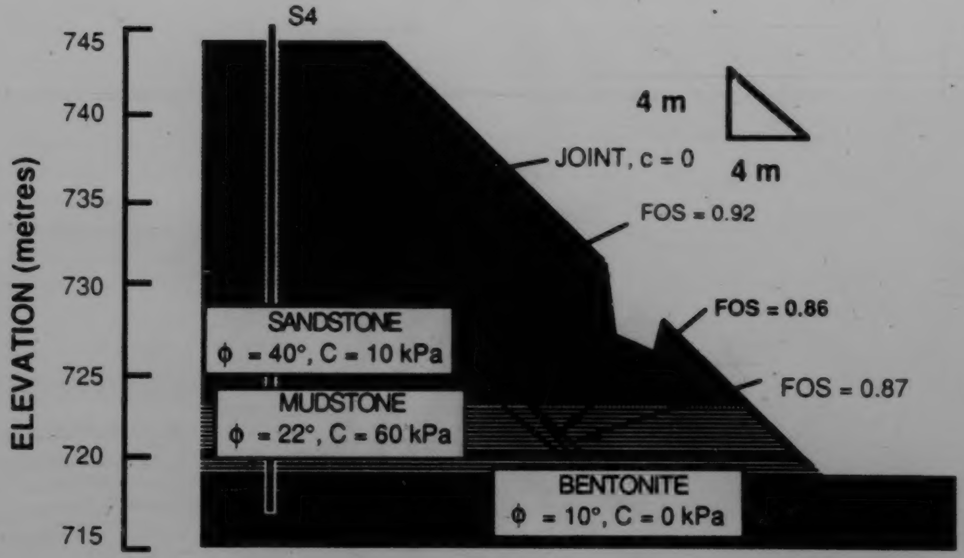
S4
ELEVATION (metres)
745
740
735
730
725
720
715
4 m
4 m
JOINT, c = 0
FOS = 0.92
FOS = 0.86
FOS = 0.87
SANDSTONE
ϕ = 40°, C = 10 kPa
MUDSTONE
ϕ = 22°, C = 60 kPa
BENTONITE
ϕ = 10°, C = 0 kPa

Figure 6.14 Assumed slip surfaces for search of critical one at rear failure.

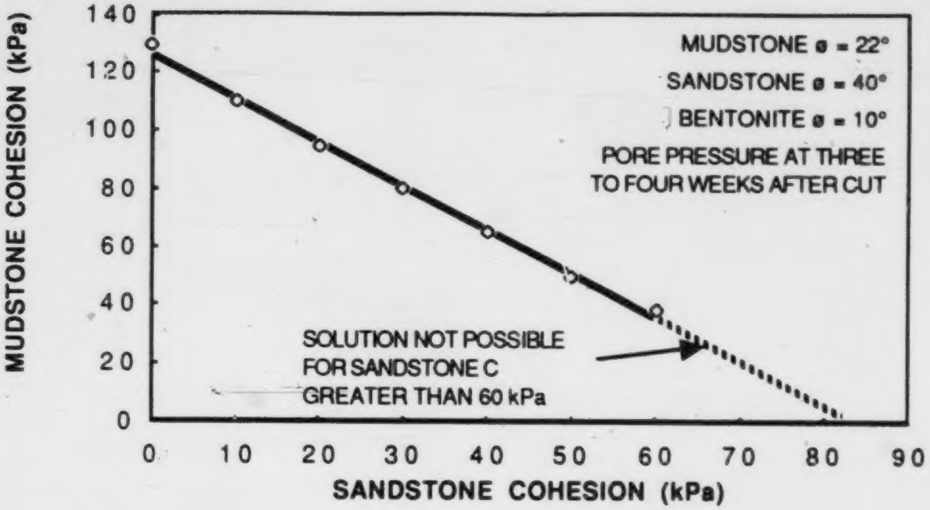

Figure 6.15 Combination of mudstone and sandstone cohesions mobilized at rear failure.

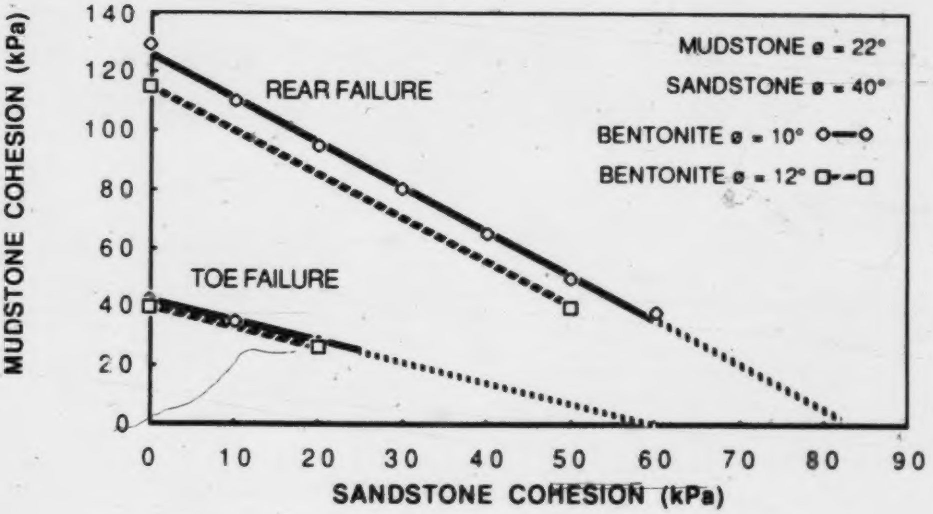

Figure 6.16 Combined results of toe and rear failures.

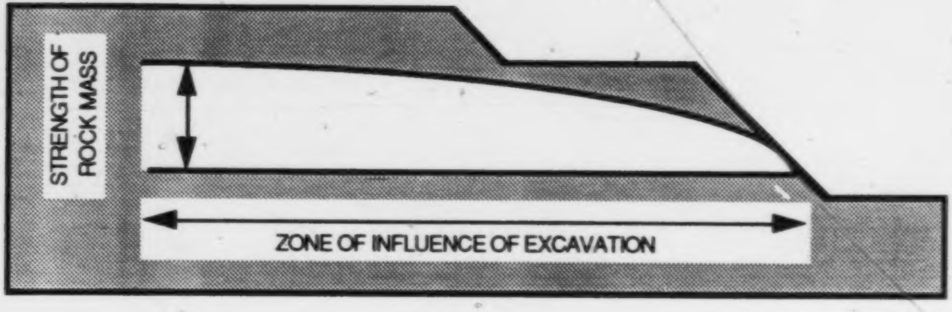
STRENGTH OF ROCK MASS
ZONE OF INFLUENCE OF EXCAVATION

Figure 6.17 Conceptual model of reduction in rock mass strength from and undisturbed state beyond the zone of excavation to the highwall face.

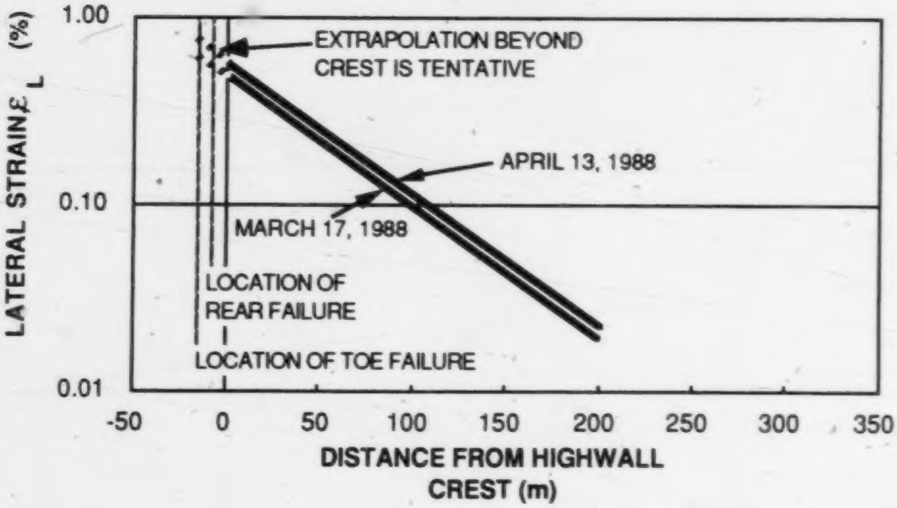

Figure 6.18 Lateral strain field for March. 17 and April 13, 1988 on line S4-S6.

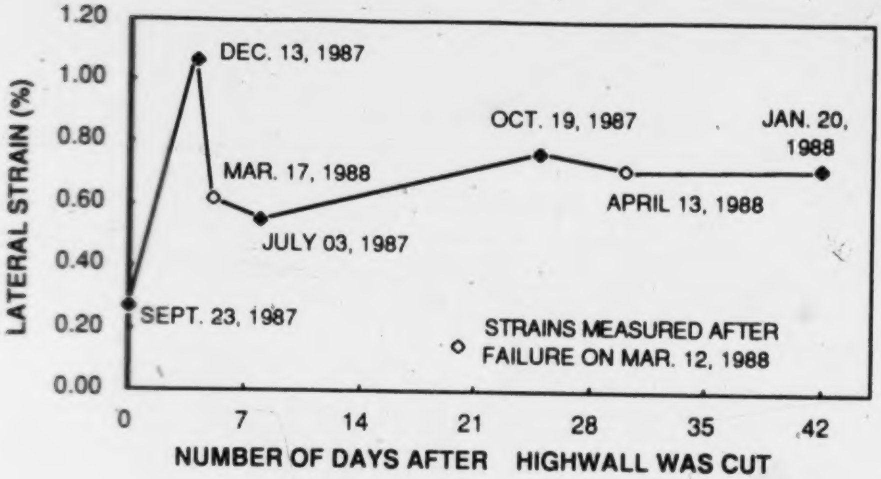

Figure 6.19 Variation in strain along backscarp of toe failure after a highwall was cut.

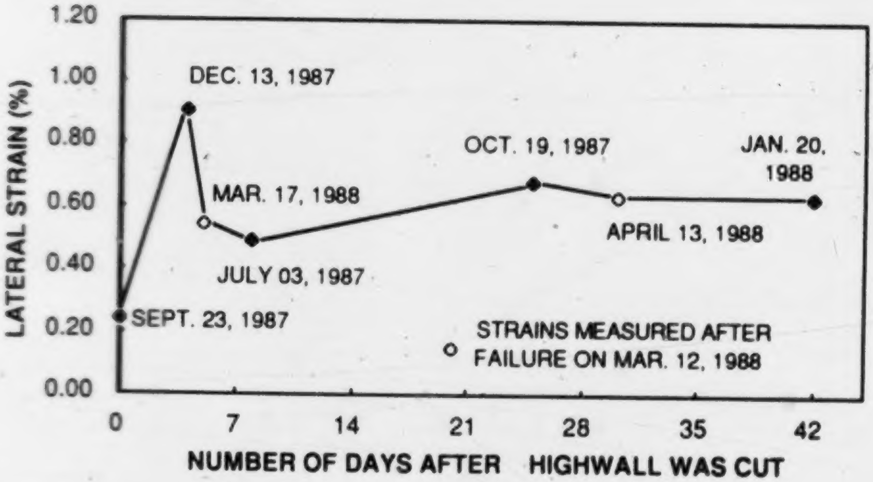

Figure 6.20 Variation in strain along backscarp of rear failure after a highwall was cut.

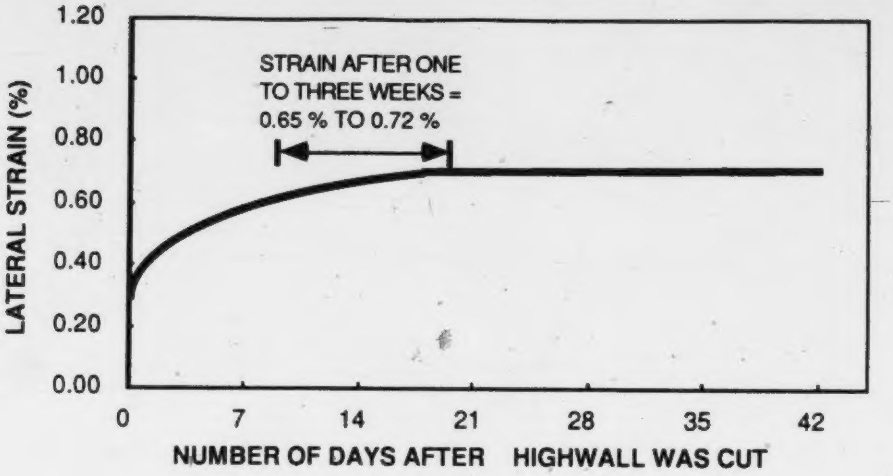

Figure 6.21 Generalized development of strain along backscarp of toe block after a highwall was cut.

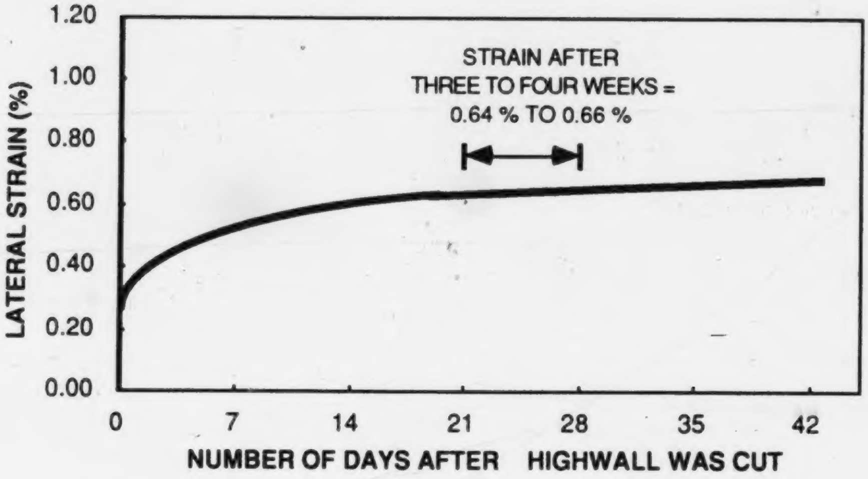

Figure 6.22 Generalized development of strain along backscarp of rear block after a highwall was cut.

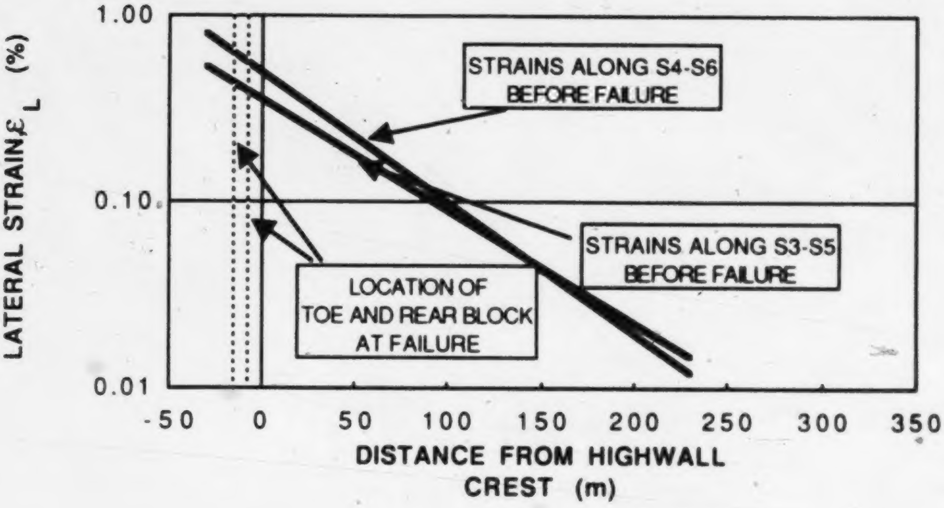

Figure 6.23 Lateral strains mobilized at elevation 730 metres on March 17, 1988, five days after the highwall was cut.

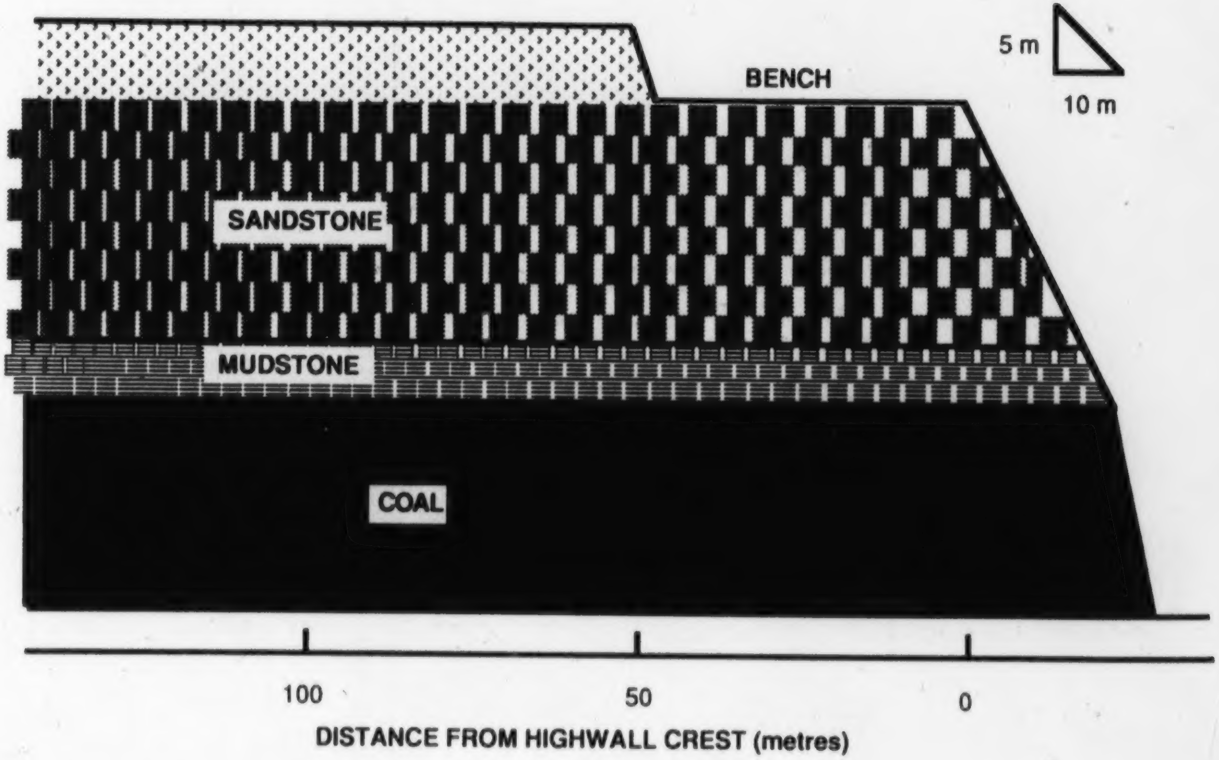
5 m
10 m
BENCH
SANDSTONE
MUDSTONE
COAL
100
50
0
DISTANCE FROM HIGHWALL CREST (metres)

Figure 6.24 : Schematic of "Progressive Loosening" concept

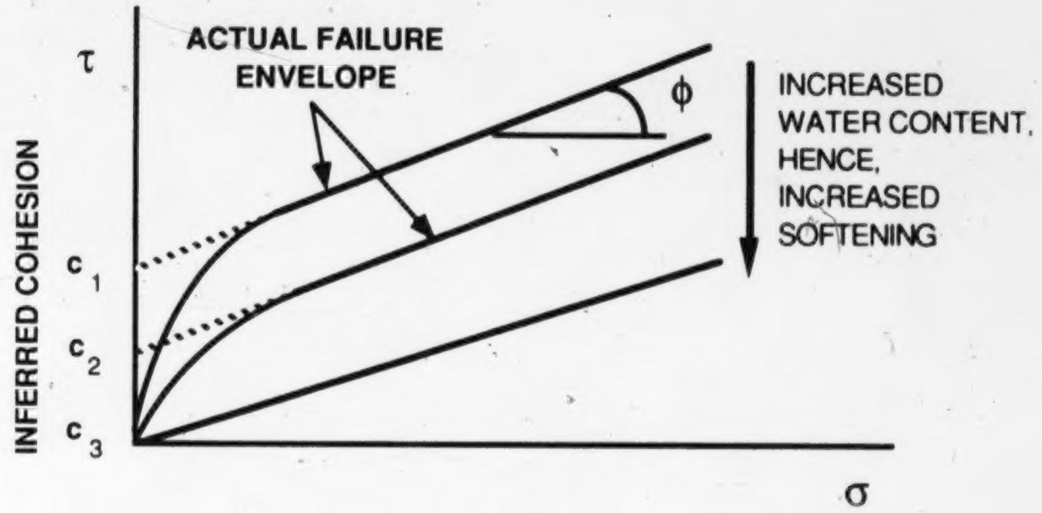
τ
ACTUAL FAILURE ENVELOPE
ϕ
INCREASED WATER CONTENT, HENCE, INCREASED SOFTENING
INFERRED COHESION
c_1
c_2
c_3
σ

Figure 6.25 Schematic of "Progressive Softening" concept.

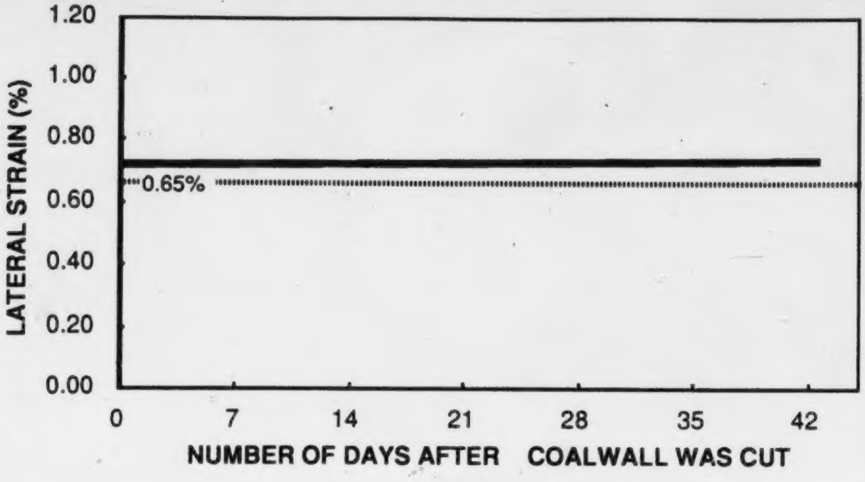

Figure 6.26 Generalized development of strain on line S2-S4-S6 after the coal was excavated. At elevation 730 metres, 15 metres in front of highwall crest.

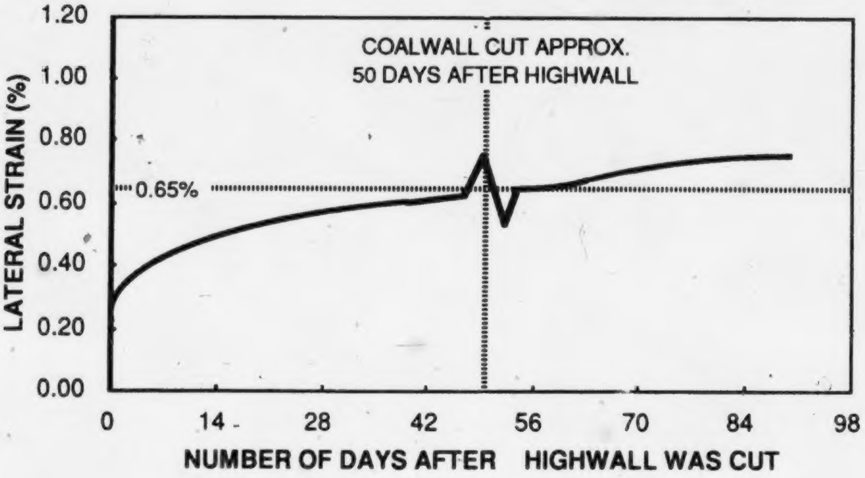

Figure 6.27 Generalized development of strain on line S1-S3-S5 after the highwall and coal were excavated. At elevation 730 metres, 15 metres in front of highwall crest.

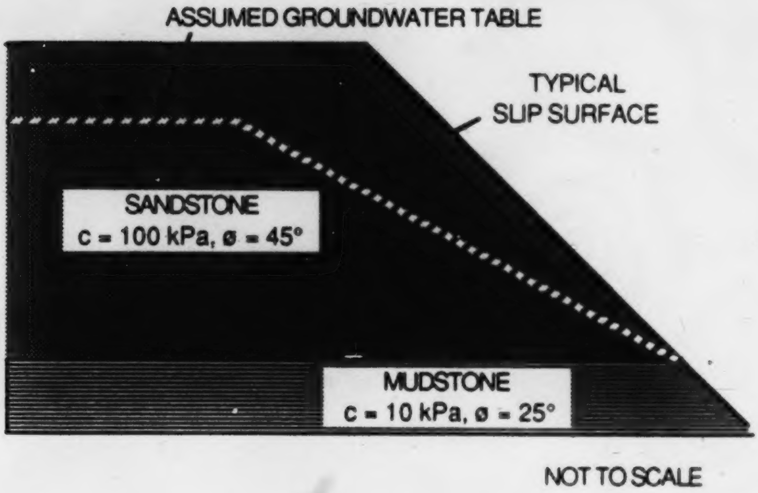
ASSUMED GROUNDWATER TABLE
TYPICAL SLIP SURFACE
SANDSTONE
c = 100 kPa, ø = 45°
MUDSTONE
c = 10 kPa, ø = 25°
NOT TO SCALE

Figure 6.28 Section used by Wade and Peterson (adapted 1986) to evaluate stability of highwall in Pit 03.

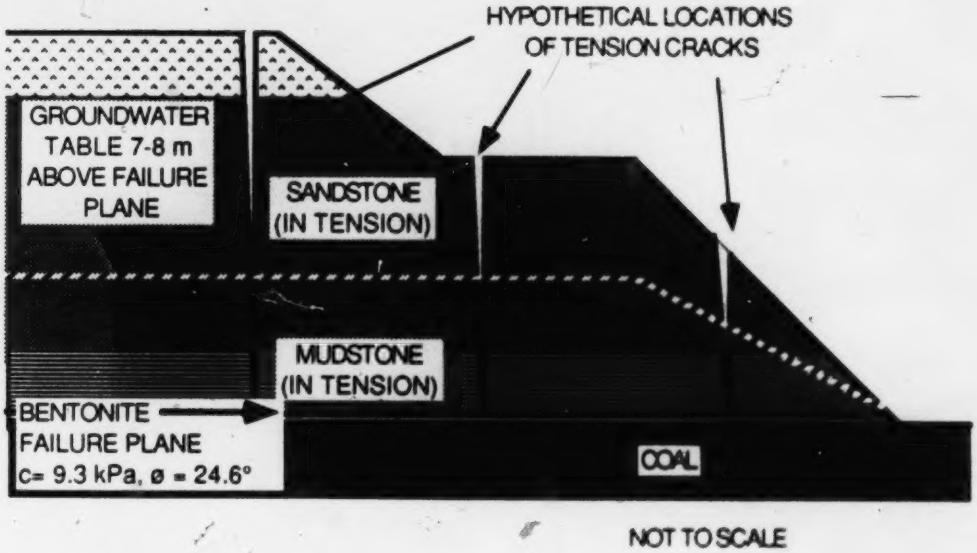
HYPOTHETICAL LOCATIONS OF TENSION CRACKS
GROUNDWATER TABLE 7-8 m ABOVE FAILURE PLANE
SANDSTONE (IN TENSION)
MUDSTONE (IN TENSION)
BENTONITE FAILURE PLANE
c= 9.3 kPa, ø = 24.6°
COAL
NOT TO SCALE

Figure 6.29 Planar Shear Model used by Barron and Stimpson (adapted 1986) to analyse failure of highwall in Pit 03 in spring, 1984.

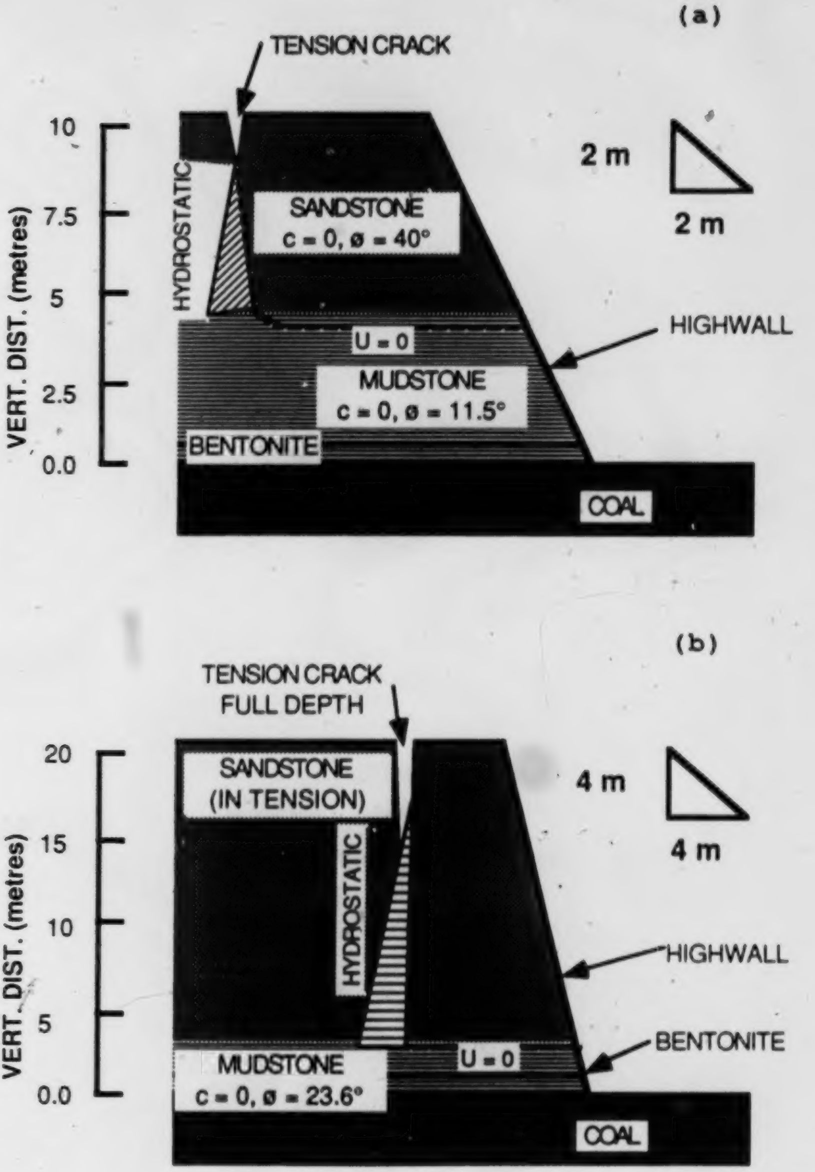
(a)
TENSION CRACK
10
7.5
5
2.5
0.0
VERT. DIST. (metres)
HYDROSTATIC
SANDSTONE
c = 0, ø = 40°
U = 0
MUDSTONE
c = 0, ø = 11.5°
BENTONITE
COAL
2 m
2 m
HIGHWALL
(b)
TENSION CRACK
FULL DEPTH
20
15
10
5
0.0
VERT. DIST. (metres)
SANDSTONE
(IN TENSION)
HYDROSTATIC
MUDSTONE
c = 0, ø = 23.6°
U = 0
COAL
4 m
4 m
HIGHWALL
BENTONITE

Figure 6.30 Sections used by Tsui (adapted 1988) to analyse two highwall failures which occurred in Pit 03 in July, 1984: (a) Slide 1 and (b) Slide 2.

7 APPLICATION TO HIGHWALL DESIGN AND REMEDIAL MEASURES

Chapters 4 to 6 presented several aspects of highwall stability that directly impact highwall design and, if necessary, remedial measures.

7.1 Highwall Design

Design Factors

The conclusions drawn from the failure analysis in Chapter 6 need to be considered when designing a highwall at the Highvale Mine. Six factors have important bearing on stability analyses:

1. The presheared bentonite may be the basal slip plane.
2. The water pressures are low near the highwall face.
3. Refinement of the values of friction angles for the sandstone and mudstone is not warranted.
4. Cohesions in the sandstone and mudstone are low.
5. Sandstone structure may determine whether the highwall stands or falls.
6. Strength of overburden progressively reduced with degree of rebound.

Field Program

To assess stability, a field investigation program should be undertaken to accurately determine three parameters:

1. Friction angle of the presheared surface in the bentonite. This may be done by field shear box testing or careful sampling of the shear zone for laboratory tests.
2. Pore pressures at the highwall crest and close to the highwall toe. A bank of inclined piezometers could be installed from the highwall crest and located at several locations in the sandstone, mudstone, and coal.
3. Orientation and characteristics of the joint sets in the sandstone.

The main feature of these parameters is that they are obtainable for minimal cost and effort. Such a field program would be modest and could provide valuable information. This author recommends that the program be implemented in areas that have experienced substantial instability in the past or are predicted to do so from analyses.

A fourth parameter should be included in a field program: determining lateral strains, however this requires substantial cost and commitment.

Geotechnical Database

A database of geotechnical parameters should be maintained of observed pore pressures, lateral strains, and measured laboratory and field strengths. In addition, it would also include key parameters from geophysical logging and the results of field joint surveys.

The value of such a database would be improved by back analysing selected failures and incorporating their results. Even small failures can provide valuable information about mobilized strength parameters and pore pressures.

With a database, then correlations may be established, for example, between strains and certain geophysical parameters that may allow the designer to predict the strains at future locations. It may also be possible to improve the tentative correlation between lateral strains and rock strength. With this information, then the rock mass strength may be estimated and the stability analyses improved.

7.2 **Remedial Measures**

When highwall designers are confronted with stability problems, two techniques are typically implemented to mitigate the hazard:

1. Reduce the pore pressures at the unstable section by installing wells or drains;
2. Buttress the slope.

The finding that the groundwater in the overburden tends to flow vertically into the coal must be considered for a depressurization scheme to be effective.

The worst time that the highwall could fail is when the dragline is stripping overburden and creating the new highwall. As the dragline makes the new cut, it sits above the old highwall that has been exposed for one to three months. The coal has been excavated below the old highwall and the lateral strains have reached a maximum. Progressive loosening and softening has reduced the strength of the overburden to a minimum. The highwall's Factor of Safety is at its lowest when the dragline revisists the area.

It is at this time that buttressing would be effective by increasing the resisting forces at the toe. However, buttressing, or building an extended bench, severely affects the economics of mining. Improved design techniques may assist in determining a viable buttress design. In the failure described in Chapter 6, it is possible that the failure of the toe block triggered the much larger collapse of the highwall. If this can be proven, then the extent of the buttress may be significantly reduced to just supporting the lower portion of the highwall.

Other schemes may be attempted such as rock anchors but the rock strength is too low. Even if anchors were installed to control the strains, they could not be installed in time to significantly impact the strain development.

Remedial programs are often costly and are reactive instead of proactive. In a mining environment, this approach is not always economical. Monitoring programs that provide warning of failures have been found to be successful at other strip mining operations (Fair and Lord, 1984). Deformation monitoring schemes should be considered an integral part of highwall engineering.

7.3 Deformation Monitoring Program

A deformation monitoring program will permit better understanding of the behaviour of the rock behind the highwall. If necessary, such a program could be developed to provide warning of an imminent failure.

7.3.1 Objective

A deformation monitoring program should satisfy two main objectives: first, to establish the potential failure mode and, second, to determine the lateral strains. To achieve these goals, instruments must be located on a line perpendicular to the highwall crest.

7.3.2 Methodology

Numerous methods exist to monitor highwall deformations, but this study proved the effectiveness and reliability of the survey/inclinometer combination. This technique was ideally suited for the strip mining environment at Highvale. Surveying from fixed control points well behind active mining provided surface deformations and, by tying the inclinometers into the survey network, a reasonably complete picture of the deformation field was obtained.

Ideally, in future programs, the survey control points would be located 500 metres from the highwall to ensure that they do not move. However, this distance may be too large for accurate measurements and secondary control points could be established closer to the study site. These points would then be referenced to the primary ones.

Inclinometers provide valuable information on the modes of deformation and potential failure. By positioning them at projected future crest locations, they stand a good chance of remaining in operation during successive cuts.

Inclinometers are ideal survey targets since they can be tracked from their position on the original ground surface to when they are brought down onto the bench.

An important consideration when designing a monitoring program is the reliability of the reference points. For example, one could establish a point on the highwall face immediately after excavation and then track its movement by regular surveys. In this instance, the highwall becomes the reference point and the measured deformations will be relative to its location at the time the point was established. In Chapter 4, it was found that by the time any such point could be affixed to the highwall, the highwall has already moved 50% of its total movement. In other words, measurements relative to the highwall will miss 50% of the movement and extending this information to strains becomes impossible.

7.4 Pore Pressure Monitoring

This study found that the pore pressures changed significantly within 100 metres from the crest and extrapolating pore pressures from piezometers beyond this limit is dangerous. In addition, the possibility of vertical flow must be evaluated throughout the mine. Hence, a network of piezometers should be installed in the sandstone, mudstone, and coal at strategic locations that might ensure their longevity. If piezometers are destroyed before nearing the highwall, then additional ones should be installed near the highwall crest. The difficulty with doing this on a regular basis is that the piezometers need time to stabilize and the global groundwater flow pattern will not be determined.

7.5 Use of Computer Modelling

Computer models, utilizing the Finite Element Technique, can simulate the natural geology and effect of excavations. Given the appropriate stress-strain and failure properties of the materials as well as the correct deformation modes, then the model can accurately estimate the stresses and strains that will develop after a highwall is excavated.

The major contribution of the Finite Element Method is to assist in understanding the effect of excavation on the rock mass. This is achieved by matching the behaviour of the model to the observed field performance; often referred to as historical matching. By gaining more insight into the processes and mechanisms of highwall deformations at one location, the design approaches can be improved.

With limited modifications to the model, it may be extrapolated to nearby or similar parts of the mine and, while the results must be treated with caution, they may be used to support limit equilibrium stability analyses. It may be possible to estimate the lateral strains at a future location and via the correlations established from the database described in section 7.1, the rock mass strength may be empirically estimated. The stresses at each element may then be compared to these strengths to see if the element is stable or has failed. In this manner, the stability of the highwall can be determined.

8 CONCLUSIONS

This study of highwall stability at the Highvale Mine has provided valuable insight into how deformations of the highwall impact pore water pressures, material strengths, and the failure mechanism.

8.1 Conclusions

Detailed conclusions were drawn in Chapters 4 to 6, with the most important ones listed below:

1. Deformations of the highwall were effectively monitored with slope indicators and surveying.
2. Excavation rebound induced lateral strains at the highwall of 0.60% to 0.73%.
3. Lateral straining caused once impervious layers to open and permit groundwater flow through them. This significantly alterred the flow regime and, in turn, the pore water pressures.
4. Lateral straining led to a reduction in rock mass strength.
5. Mechanisms of strength reduction involved a progressive loosening and softening of the rock mass.
6. Highwall failures were controlled by the amount of strength reduction and the orientation of weak planes in the sandstone.

Incorporating these findings into current stability evaluations will improve their accuracy and applicability.

8.2 Recommendations for Future Research

In Section 7.1, recommendations were made to highwall designers to implement a field investigation program and develop a database of geotechnical information. On a broader scale, the following areas require additional research:

1. Evaluation of the progressive loosening mechanism.
2. Computer modelling with the Finite Element Method.

The loosening mechanism could be further explored by making more detailed measurements of strains. This would be done with instruments that would compliment the surveys and inclinometers, such as surface strain guages and possibly extensometers. Ideally, these instruments would detect the blocks of sandstone spreading apart, or loosening.

An alternative method to investigate the presence of loosening is the use of geophysics. Surface geophysics could be performed along test lines parallel to the highwall crest at 25 to 50 metres intervals. Crosshole geophysics could also be run between inclinometers. The loosening mechanism would be evident by a variation in the material's shear modulus obtained from these methods.

At the time of writing, the University of Alberta geotechnical group was developing a computer model to simulate highwall behaviour. Historical deformation data for that work is provided in this thesis.

LIST OF REFERENCES

AMERICAN SOCIETY FOR TESTING MATERIALS. 1986. Soil and Rock; Building Stones. Volume 04.08.

BISHOP, A. W. AND HENKEL, D. J. 1962. The Measurement of Soil Properties in the Triaxial Test. Spottiswoode Ballantyne Ltd. pp 106 to 131.

BARRON, K., STIMPSON, B., AND KOSAR, K. 1986. A regressive mode of highwall failure in coal strip mines. Canadian Institute of Mining Bulletin. 79 (892), pp 73 to 78.

Canadian Mining Handbook, 1987.

COATES, D. F. 1981. Rock Mechanics Principles. Monograph 874, Canadian Centre for Mineral and Energy Technology. Canadian Government Publishing Centre. pp 6-31 to 6-32.

DUNNICLIFF, J., 1988. Geotechnical Instrumentation for Monitoring Field Performance. (John Wiley and Sons). pp 250 to 268 and 118 to 127.

EIGENBROD, K. D. AND MORGENSTERN, N. R. 1972. A Slide in Cretaceous Bedrock, Devon, Alberta. Geotechnical Practice for Stability in Open Pit Mining. Ed. C. O. Brawner and V. Milligan. American Institute of Ming Engineering. pp 223 to 238.

FAIR, A. E. AND LORD, E. R. F. 1984. Methods used to Control Block Slides in Oilsands at Syncrude's Dragline Operation in Northern Alberta, Canada. Proceedings 37th Canadian Geotechnical Conference, 1984, Toronto.

FENTON, M.M., TRUDELL, M.R., PAWLOWICZ, J.G., JONES, C.E., MORAN, S.R., AND NIKOLS, D.J. 1986. Glaciotectonic Deformation and Geotechnical Stability in Open Pit Coal Mining. International Symposium on Geotechnical Stability in Surface Mining, Calgary, Alberta. pp 225 to 233.

FREDLUND, D. G. 1984. Analytical Methods for Slope Stability Analysis. Fourth International Society of Soil Mechanics and Foundation Engineering Conference. Landslide Symposium, Toronto.

FREDLUND, D. G. 1985. PC-SLOPE Slope Stability Analysis, User's Manual S-30. Geo-Slope Programming Ltd., Calgary, Alberta.

HOEK, E. AND BROWN, E.T. 1981. Empirical Strength Criterion for Rock Masses. American Society of Civil Engineers, Geotechnical Engineering Division. Vol. 106, No. GT9, pp 1013 to 1035.

JENKINS, G. Personal Communication on January 14, 1989

KOPPEL, J., AMSTAD, CH.,AND KOVARI, K., 1983. The Measurement of Displacement Vectors with the 'Trivec' Borehole Probe. Proceedings of the International Symposium on Field Measurements in Geomechanics, Zurich. Ed: K. Kovari. Vol. 1, pp 209 to 218.

LASALATA, F. Personal Communication on December 16, 1988.

MILLER,R. P. AND HILTS, D. E. 1969. Experimental Open-Pit Mine Slope Stability Study. Rock Mechanics Theory and Practice: Proceedings of the Eleventh Symposium on Rock Mechanics, Berkley, California.(Society of Mining Engineers, AIMMPE). pp 147 to 167.

MOELL,C. E., PAWLOWICZ, J.G., TRUDELL, M.R., FENTON, M.M., LANGENBERG, C.W., STERENBERG, G. J., AND JONES, C.E.,. 1984. Highwall Stability Project, Highvale Mine, Report of 1984 Activities. Alberta Research Council Report to TransAlta Utilities Corporation.

MONENCO LIMITED. 1983. Laboratory Testing on Geotechnical Samples from the 1983 Summer Drilling Program at the Highvale Mine. Report to TransAlta Utilities.

MORGENSTERN, N. R., 1979. Geotechnical Behaviour of Clay Shales - An Overview. International Symposium on Soil Mechanics, Mexico. (International Society for Soil Mechanics and Foundation Engineering).

SMALL, C. A. AND PETERSON, A. E. 1988. Monitoring Highwall Deformations. Proceedings Canadian Society for Civil Engineering Annual Conference, Calgary. pp 15 to 34.

TRANSALTA UTILITIES CORPORATION. 1986. Some Facts 1986. Public Affairs Department, TransAlta Utilities Corporation, Calgary, Alberta.

TSUI, P. C. 1988. Geotechnical Investigations of Glaciotectonic Deformation in Central and Southern Alberta. Ph. D thesis, University of Alberta, Edmonton, Alberta, Canada.

VARNES, D. J. 1978. Slope Movement and Types and Processes. From Landslides: Analysis and Control.

Transportation Research Board, National Agency of Sciences, Washington, D.C. Special Report 176, Chapter 2.

WADE, N.H. AND PETERSON, T.W.P. 1986 Highwall monitoring, instrumentation, and stability analysis at the Highvale coal mine, Alberta. International Symposium on Geotechnical Stability in Surface Mining, Calgary, Alberta. pp 373-384.

APPENDIX A - BOREHOLE LOGS

Figures A.1 to A.6 present the borehole logs for holes S1 to S6 from the field investigation program. Table A.1 presents the hole locations and the corresponding TAU hole numbers.

Table A.1

Location of Boreholes

U of A HOLE NUMBER	T.A.U. HOLE NUMBER	NORTHING (metres)	EASTING (metres)	GROUND ELEVATION (metres)
S1	HV87-411	1131.2	-3885.3	750.47
S2	HV87-412	1133.2	-3833.9	751.15
S3	HV87-413	1080.4	-3887.3	749.89
S4	HV87-414	1085.4	-3837.2	751.37
S5	HV87-415	1028.5	-3884.6	748.77
S6	HV87-416	1036.1	-3836.2	750.51

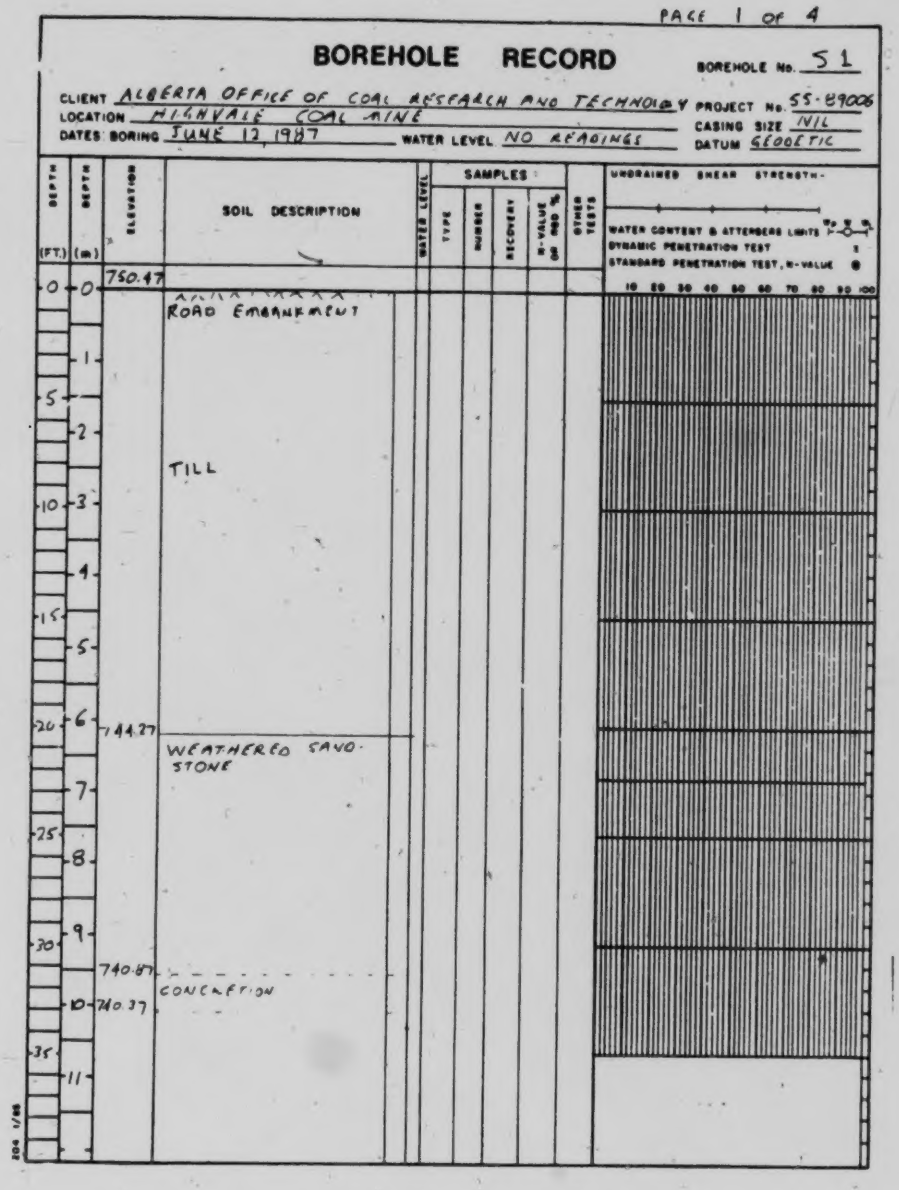

PAGE 1 OF 4

BOREHOLE RECORD

BOREHOLE No. S1

CLIENT ALBERTA OFFICE OF COAL RESEARCH AND TECHNOLOGY
PROJECT No. 55-89006
LOCATION HIGHVALE COAL MINE
CASING SIZE NIL
DATES: BORING JUNE 12, 1987
WATER LEVEL NO READINGS
DATUM GEODETIC

DEPTH (FT.)	DEPTH (m)	ELEVATION	SOIL DESCRIPTION	WATER LEVEL	SAMPLES: TYPE	NUMBER	RECOVERY	N-VALUE OR RQD %	OTHER TESTS
0	0	750.47	ROAD EMBANKMENT						
			TILL						
20	6	744.27	WEATHERED SANDSTONE						
		740.87	CONCRETION						
	10	740.37							

UNDRAINED SHEAR STRENGTH -
WATER CONTENT & ATTERBERG LIMITS Wp W WL
DYNAMIC PENETRATION TEST
STANDARD PENETRATION TEST, N-VALUE ●
10 20 30 40 50 60 70 80 90 100
0
5
10
15
20
25
30
35
0
1
2
3
4
5
6
7
8
9
10
11
204 1/85

Figure A.1 Borehole Log for hole S1

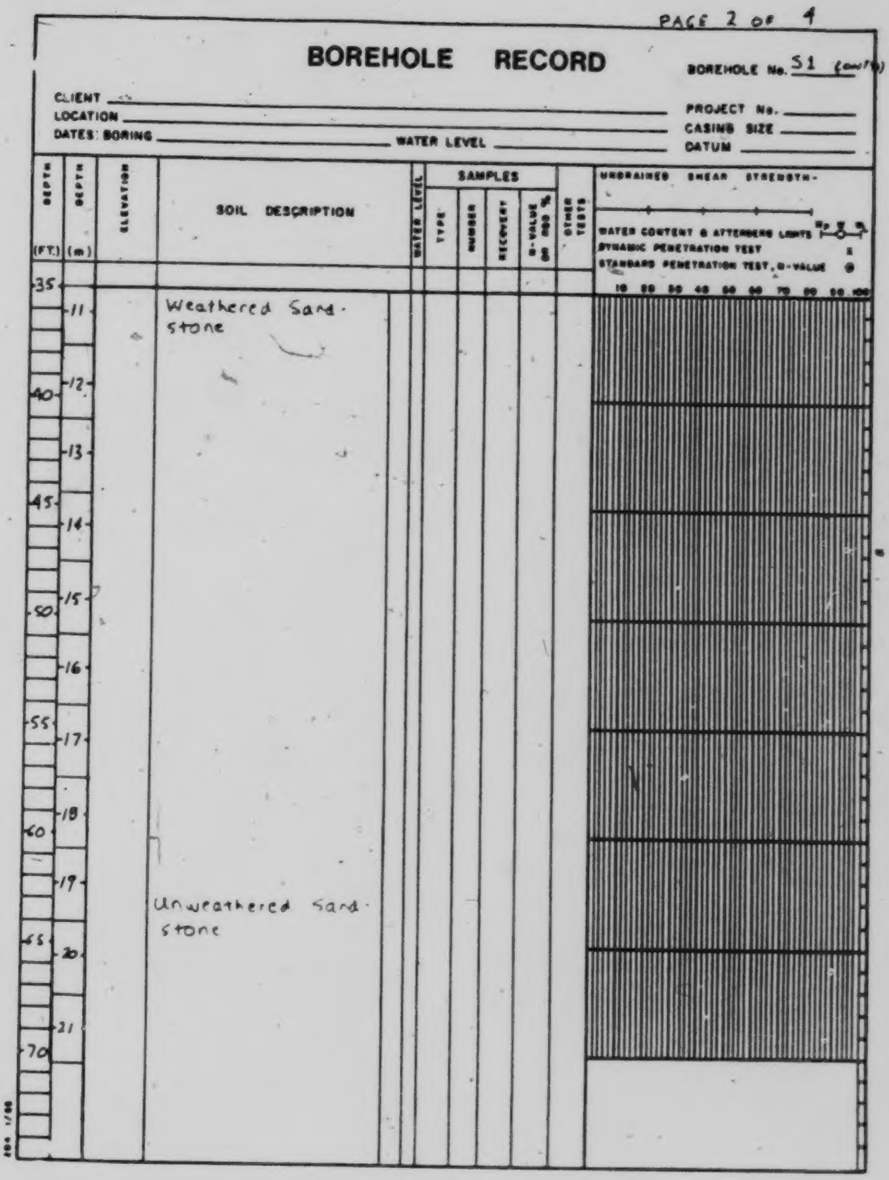

PAGE 2 OF 4

BOREHOLE RECORD

BOREHOLE No. S1 (cont'd)

CLIENT
LOCATION
DATES: BORING
WATER LEVEL
PROJECT No.
CASING SIZE
DATUM

DEPTH (FT.)	DEPTH (m)	ELEVATION	SOIL DESCRIPTION	WATER LEVEL	SAMPLES TYPE	SAMPLES NUMBER	SAMPLES RECOVERY	SAMPLES N-VALUE OR RQD %	OTHER TESTS
35									
	11		Weathered Sandstone						
	12								
40									
	13								
45									
	14								
	15								
50									
	16								
55									
	17								
	18								
60									
	19								
			Unweathered Sandstone						
65									
	20								
	21								
70									

UNDRAINED SHEAR STRENGTH-
WATER CONTENT & ATTERBERG LIMITS
DYNAMIC PENETRATION TEST
STANDARD PENETRATION TEST, N-VALUE
10 20 30 40 50 60 70 80 90 100

Figure A.1 (cont'd) Borehole Log for hole S1

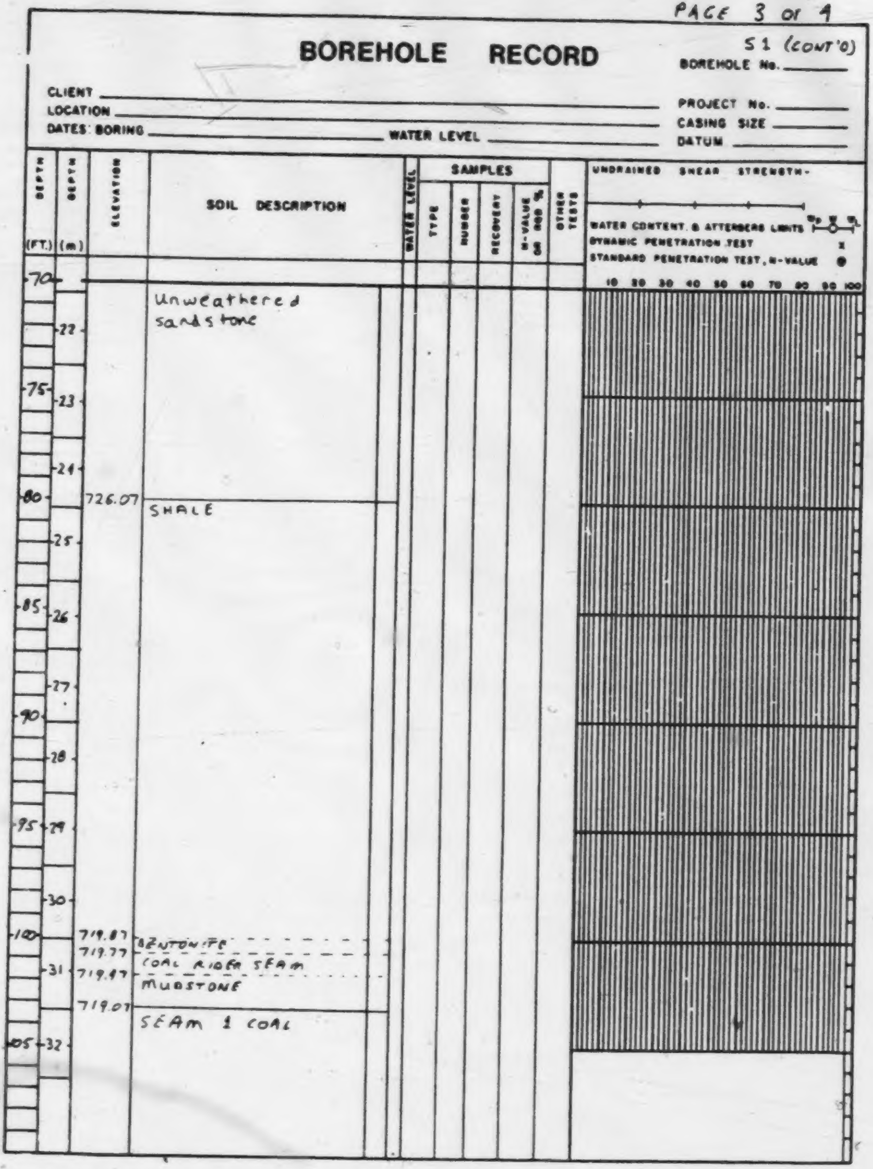

PAGE 3 OF 4

BOREHOLE RECORD

BOREHOLE No. S1 (CONT'D)

CLIENT ______

LOCATION ______

DATES: BORING ______ WATER LEVEL ______

PROJECT No. ______

CASING SIZE ______

DATUM ______

DEPTH (FT.)	DEPTH (m)	ELEVATION	SOIL DESCRIPTION	WATER LEVEL	SAMPLES TYPE	SAMPLES NUMBER	SAMPLES RECOVERY	SAMPLES N-VALUE OR RQD %	OTHER TESTS
70			Unweathered sandstone						
	22								
75	23								
	24								
80		726.07	SHALE						
	25								
85	26								
	27								
90									
	28								
95	29								
	30								
100		719.87	BENTONITE						
		719.77	COAL RIDER SEAM						
	31	719.47	MUDSTONE						
		719.07	SEAM 1 COAL						
105	32								

UNDRAINED SHEAR STRENGTH -

WATER CONTENT & ATTERBERG LIMITS w_P w w_L

DYNAMIC PENETRATION TEST x

STANDARD PENETRATION TEST, N-VALUE ●

10 20 30 40 50 60 70 80 90 100

204 1/88

Figure A.1 (cont'd) Borehole Log for hole S1

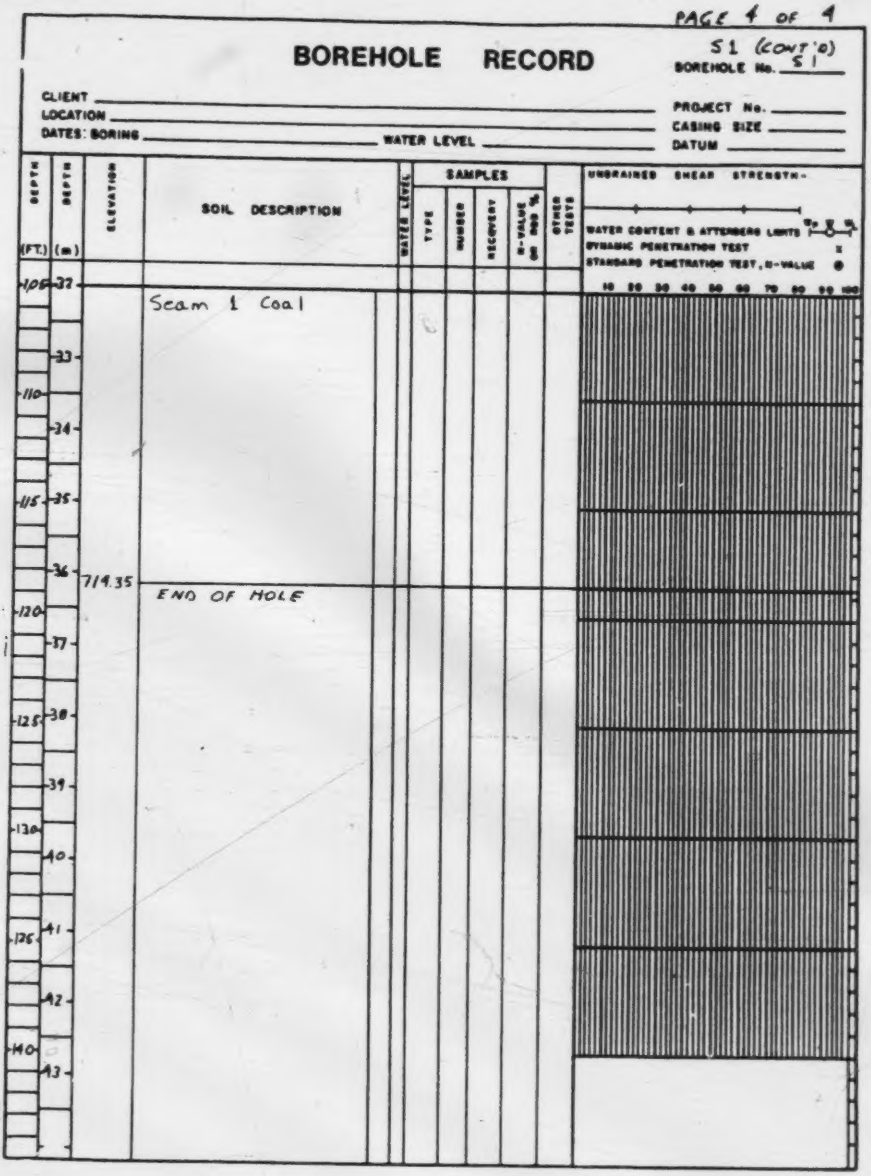

PAGE 4 OF 4

BOREHOLE RECORD

S1 (CONT'D)
BOREHOLE No. S1

CLIENT
LOCATION
DATES: BORING
WATER LEVEL
PROJECT No.
CASING SIZE
DATUM

DEPTH (FT.)	DEPTH (m)	ELEVATION	SOIL DESCRIPTION	WATER LEVEL	SAMPLES TYPE	SAMPLES NUMBER	SAMPLES RECOVERY	SAMPLES N-VALUE OR RQD %	OTHER TESTS
105	32		Seam 1 Coal						
	36	719.35	END OF HOLE						

UNDRAINED SHEAR STRENGTH-
WATER CONTENT & ATTERBERG LIMITS
DYNAMIC PENETRATION TEST
STANDARD PENETRATION TEST, N-VALUE ●

Wp
W
WL
x
10 20 30 40 50 60 70 80 90 100
105
110
115
120
125
130
135
140
32
33
34
35
36
37
38
39
40
41
42
43

Figure A.1 (cont'd) Borehole Log for hole S1

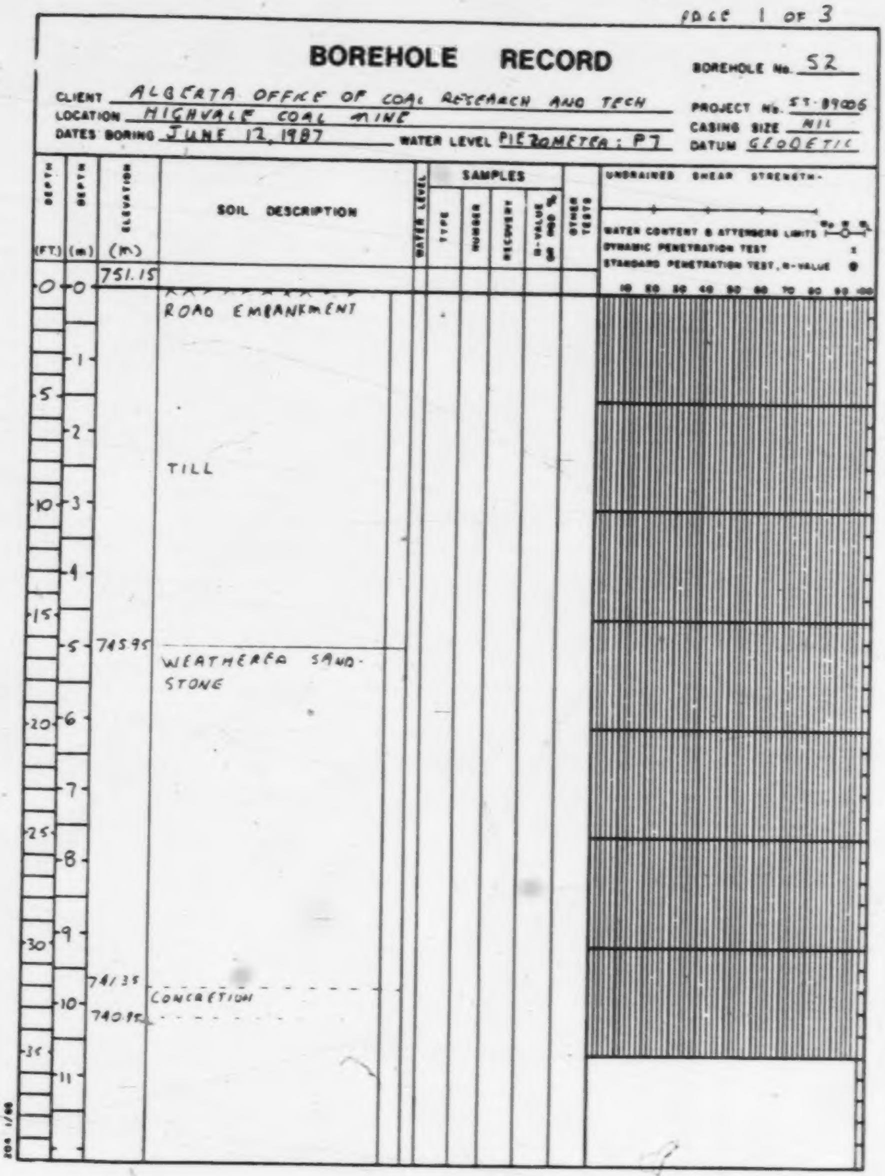

PAGE 1 OF 3

BOREHOLE RECORD

BOREHOLE No. S2

CLIENT ALBERTA OFFICE OF COAL RESEARCH AND TECH
LOCATION HIGHVALE COAL MINE
DATES BORING JUNE 12, 1987
WATER LEVEL PIEZOMETER : P7
PROJECT No. ST-89006
CASING SIZE NIL
DATUM GEODETIC

DEPTH (FT.)	DEPTH (m)	ELEVATION (m)	SOIL DESCRIPTION
0	0	751.15	ROAD EMBANKMENT
			TILL
	5	745.95	WEATHERED SANDSTONE
		741.35	CONCRETION
		740.95	

WATER LEVEL
SAMPLES
TYPE
NUMBER
RECOVERY
N-VALUE OR RQD %
OTHER TESTS
UNDRAINED SHEAR STRENGTH -
WATER CONTENT & ATTERBERG LIMITS
DYNAMIC PENETRATION TEST
STANDARD PENETRATION TEST, N-VALUE
10 20 30 40 50 60 70 80 90 100
0 5 10 15 20 25 30 35
0 1 2 3 4 5 6 7 8 9 10 11

Figure A.2 Borehole Log for hole S2

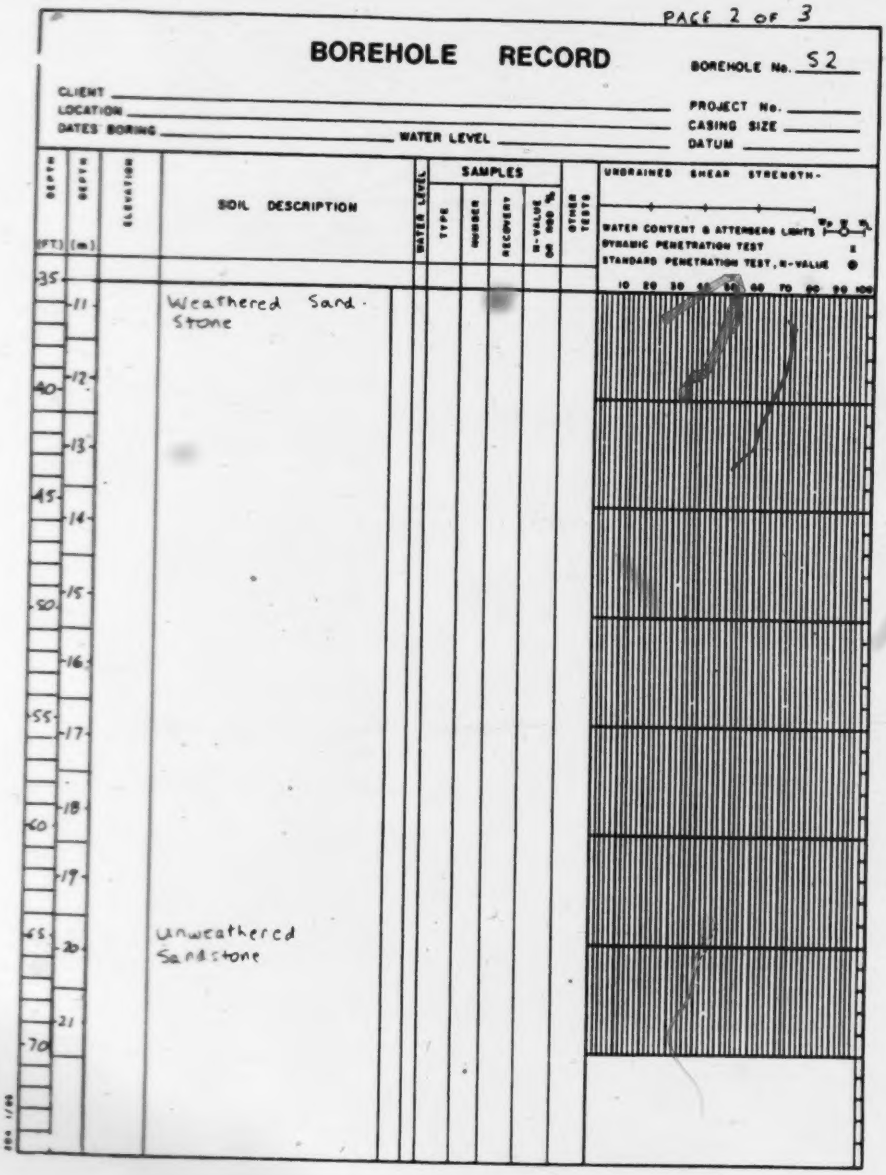

PAGE 2 OF 3

BOREHOLE RECORD

BOREHOLE No. S2

CLIENT
LOCATION
DATES BORING
WATER LEVEL
PROJECT No.
CASING SIZE
DATUM

DEPTH (FT)	DEPTH (m)	ELEVATION	SOIL DESCRIPTION	WATER LEVEL	SAMPLES TYPE	SAMPLES NUMBER	SAMPLES RECOVERY	SAMPLES N-VALUE OR RQD %	OTHER TESTS
35	11		Weathered Sand-Stone						
40	12								
	13								
45	14								
50	15								
	16								
55	17								
60	18								
	19								
65	20		Unweathered Sandstone						
70	21								

UNDRAINED SHEAR STRENGTH -
WATER CONTENT & ATTERBERG LIMITS W_P W W_L
DYNAMIC PENETRATION TEST
STANDARD PENETRATION TEST, N-VALUE ●
10 20 30 40 50 60 70 80 90 100

Figure A.2 (cont'd) Borehole Log for hole S2

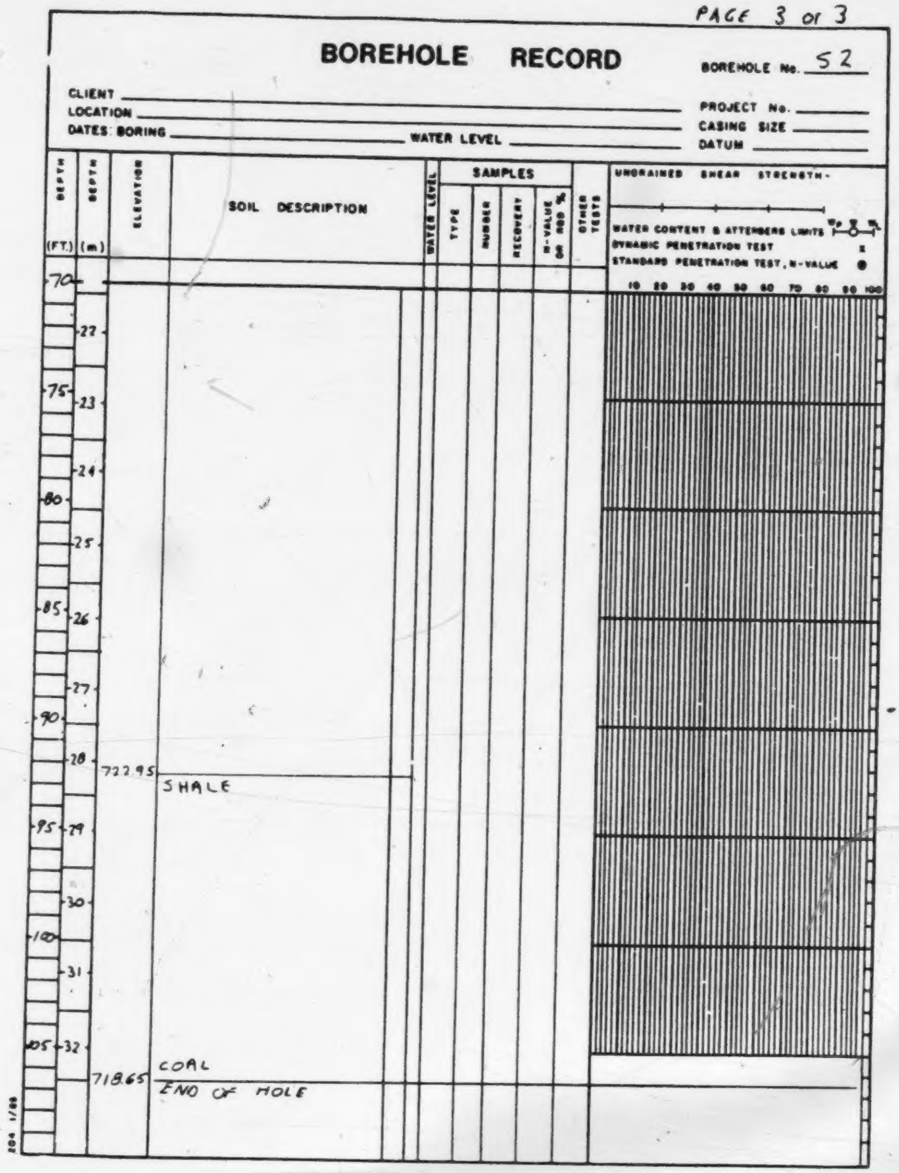

PAGE 3 of 3

BOREHOLE RECORD

BOREHOLE No. S2

CLIENT
LOCATION
DATES: BORING
WATER LEVEL
PROJECT No.
CASING SIZE
DATUM

DEPTH (FT.)	DEPTH (m)	ELEVATION	SOIL DESCRIPTION
	28	722.95	SHALE
		718.65	COAL
			END OF HOLE

WATER LEVEL
SAMPLES
TYPE
NUMBER
RECOVERY
N-VALUE OR RQD %
OTHER TESTS
UNDRAINED SHEAR STRENGTH -
WATER CONTENT & ATTERBERG LIMITS
W_P W W_L
DYNAMIC PENETRATION TEST
STANDARD PENETRATION TEST, N-VALUE
10 20 30 40 50 60 70 80 90 100
70
75
80
85
90
95
100
105
27
23
24
25
26
27
28
29
30
31
32
204 1/88

Figure A.2 (cont'd) Borehole Log for hole S2

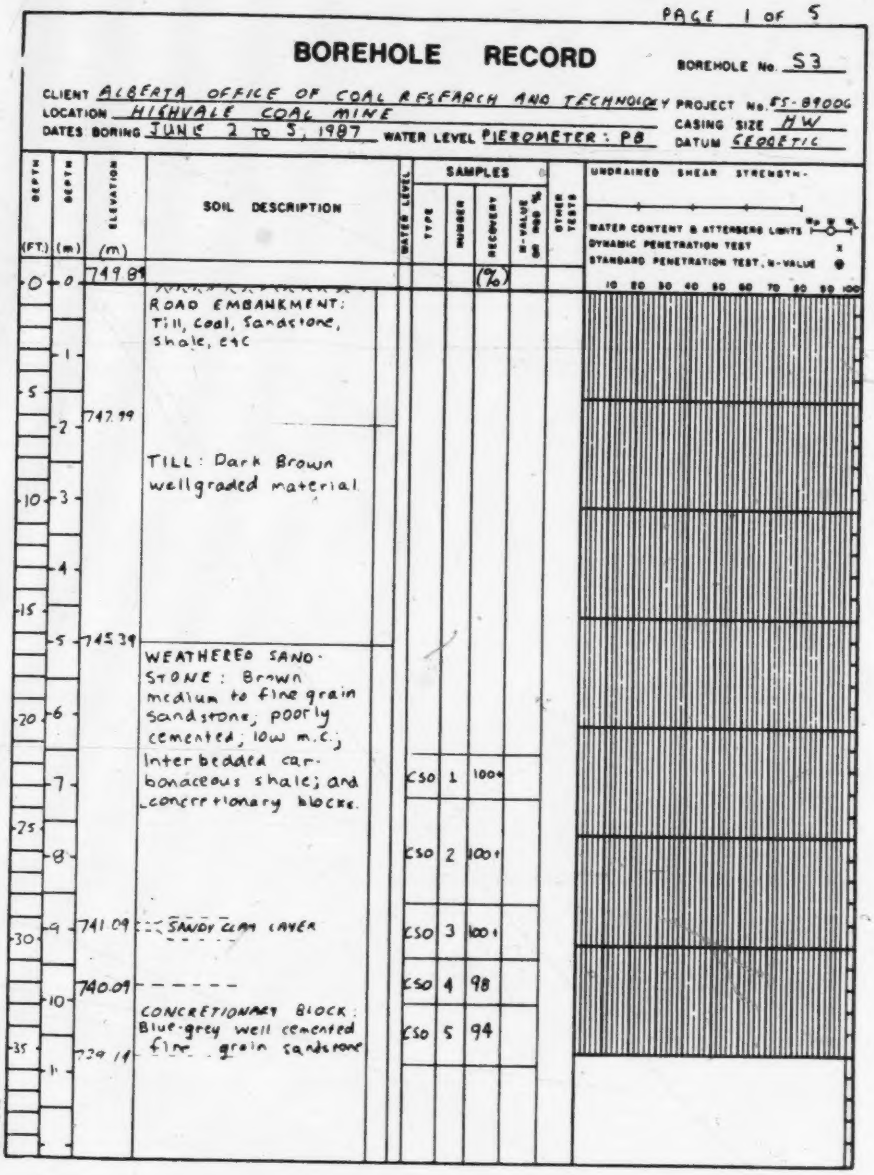

PAGE 1 OF 5

BOREHOLE RECORD

BOREHOLE No. S3

CLIENT ALBERTA OFFICE OF COAL RESEARCH AND TECHNOLOGY

PROJECT No. ES-8900G

LOCATION HIGHVALE COAL MINE

CASING SIZE HW

DATES BORING JUNE 2 TO 5, 1987

WATER LEVEL PIEZOMETER: P8

DATUM GEODETIC

DEPTH (FT.)	DEPTH (m)	ELEVATION (m)	SOIL DESCRIPTION	WATER LEVEL	SAMPLES TYPE	SAMPLES NUMBER	SAMPLES RECOVERY (%)	SAMPLES N-VALUE OR RQD %	OTHER TESTS
0	0	749.89	ROAD EMBANKMENT: Till, Coal, Sandstone, Shale, etc						
	2	747.99	TILL: Dark Brown wellgraded material						
	5	745.39	WEATHERED SANDSTONE: Brown medium to fine grain sandstone; poorly cemented; low m.c.; Interbedded carbonaceous shale; and concretionary blocks.						
	7				CSO	1	100+		
	8				CSO	2	100+		
	9	741.09	SANDY CLAY LAYER		CSO	3	100+		
		740.09			CSO	4	98		
	10		CONCRETIONARY BLOCK: Blue-grey well cemented fine grain sandstone		CSO	5	94		
		739.14							

0
5
10
15
20
25
30
35
1
2
3
4
5
6
7
8
9
10
11
UNDRAINED SHEAR STRENGTH-
WATER CONTENT & ATTERBERG LIMITS Wp W WL
DYNAMIC PENETRATION TEST x
STANDARD PENETRATION TEST, N-VALUE ●
10 20 30 40 50 60 70 80 90 100
204 1/88

Figure A.3 Borehole Log for hole S3

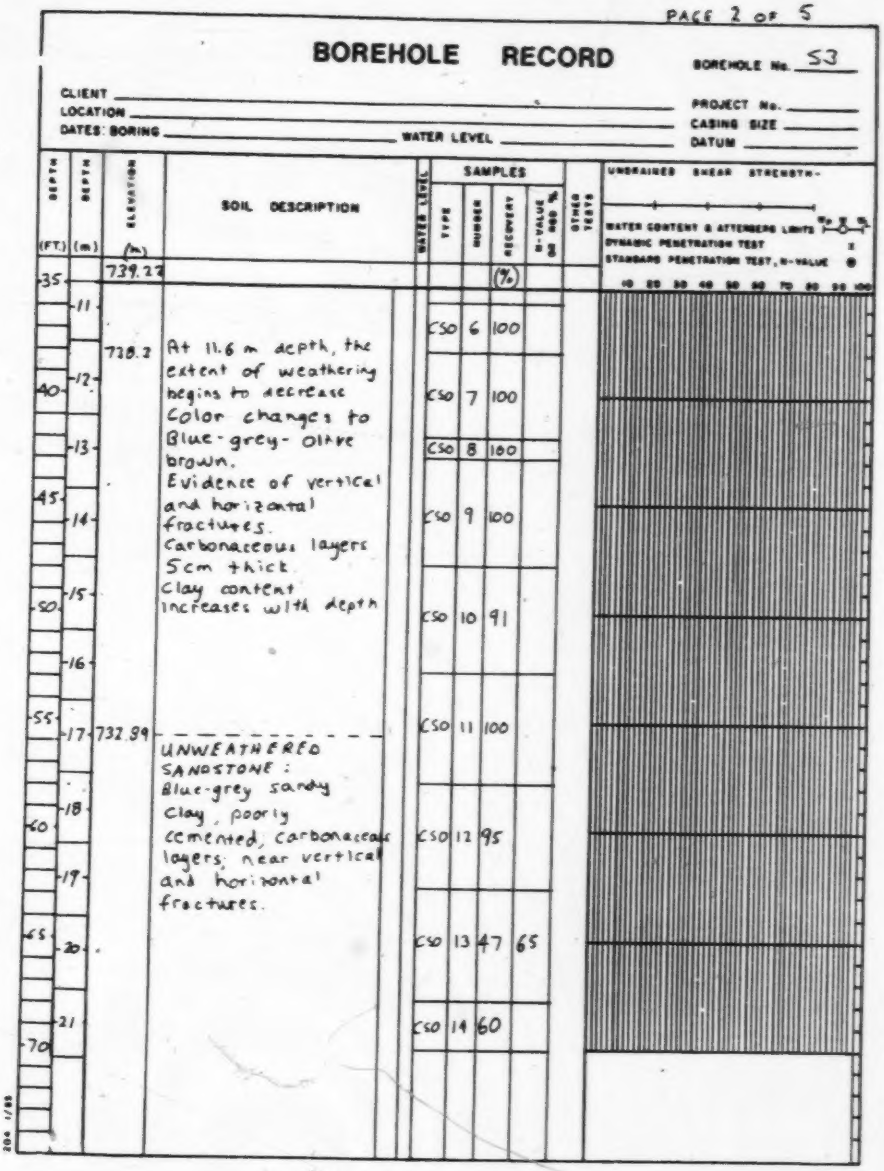

PAGE 2 OF 5

BOREHOLE RECORD

BOREHOLE No. S3

CLIENT
LOCATION
DATES: BORING
WATER LEVEL
PROJECT No.
CASING SIZE
DATUM

DEPTH (FT.)	DEPTH (m)	ELEVATION (m)	SOIL DESCRIPTION	WATER LEVEL	SAMPLES TYPE	SAMPLES NUMBER	SAMPLES RECOVERY	SAMPLES N-VALUE OR RQD %	OTHER TESTS	UNDRAINED SHEAR STRENGTH- / WATER CONTENT & ATTERBERG LIMITS W_p W W_L / DYNAMIC PENETRATION TEST X / STANDARD PENETRATION TEST, N-VALUE ● / 10 20 30 40 50 60 70 80 90 100
35		739.27					(%)			
	11				CSO	6	100			
		738.2	At 11.6 m depth, the extent of weathering begins to decrease Color changes to Blue-grey- olive brown. Evidence of vertical and horizontal fractures. Carbonaceous layers 5cm thick. Clay content increases with depth							
40	12				CSO	7	100			
	13				CSO	8	100			
45	14				CSO	9	100			
50	15				CSO	10	91			
	16									
55					CSO	11	100			
	17	732.89	UNWEATHERED SANDSTONE: Blue-grey sandy Clay, poorly cemented, carbonaceous layers; near vertical and horizontal fractures.							
	18									
60					CSO	12	95			
	19									
65	20				CSO	13	47	65		
	21				CSO	14	60			
70										

204 1/88

Figure A.3 (cont'd) Borehole Log for hole S3

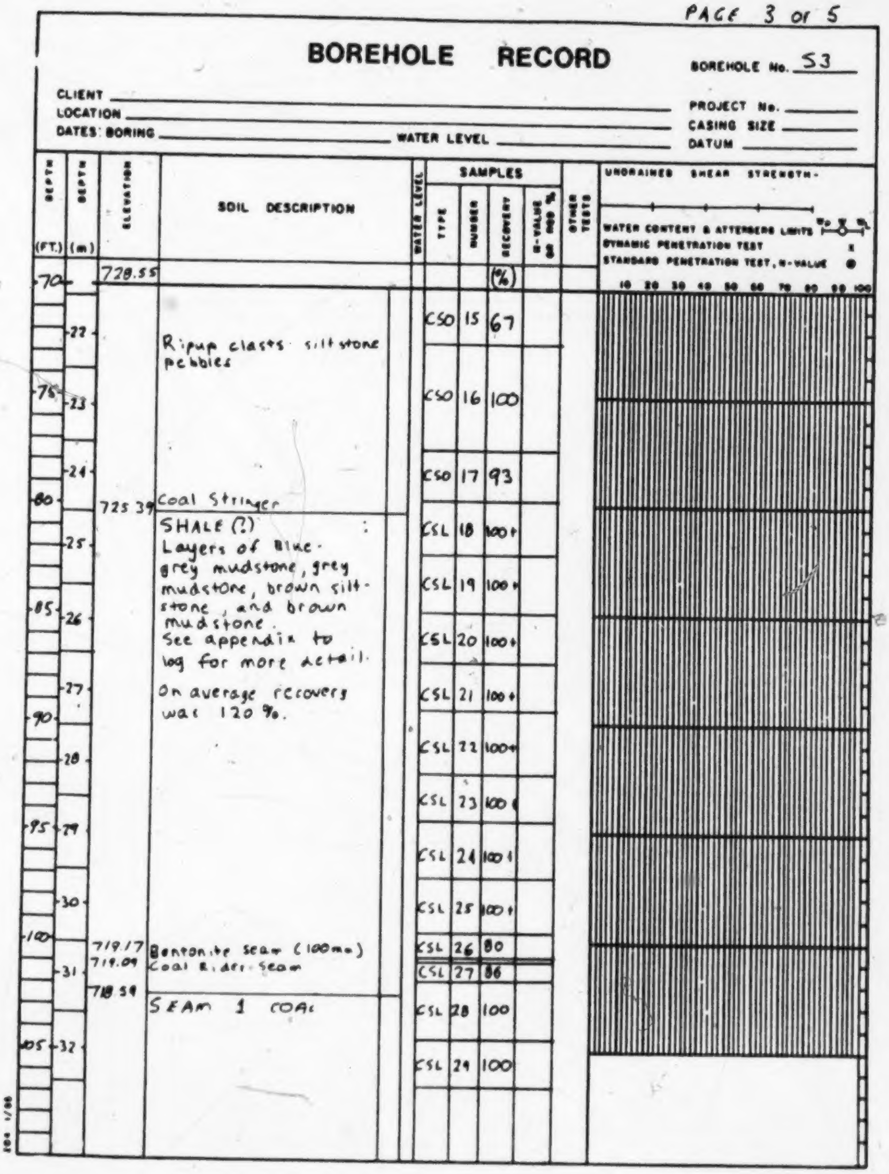

PAGE 3 of 5

BOREHOLE RECORD

BOREHOLE No. S3

CLIENT
LOCATION
DATES: BORING
WATER LEVEL
PROJECT No.
CASING SIZE
DATUM

DEPTH (FT.)	DEPTH (m)	ELEVATION	SOIL DESCRIPTION	WATER LEVEL	SAMPLES TYPE	SAMPLES NUMBER	SAMPLES RECOVERY	SAMPLES N-VALUE OR RQD %	OTHER TESTS
70		728.55					(%)		
					CSO	15	67		
	22		Ripup clasts siltstone pebbles						
75	23				CSO	16	100		
	24				CSO	17	93		
80		725.39	Coal Stringer						
			SHALE (?) : Layers of blue-grey mudstone, grey mudstone, brown siltstone, and brown mudstone. See appendix to log for more detail. On average recovery was 120 %.		CSL	18	100+		
	25				CSL	19	100+		
85	26				CSL	20	100+		
	27				CSL	21	100+		
90					CSL	22	100+		
	28				CSL	23	100+		
95	29				CSL	24	100+		
	30				CSL	25	100+		
100		719.17	Bentonite seam (100mm)		CSL	26	80		
	31	719.09	Coal Rider Seam		CSL	27	86		
		718.59	SEAM 1 COAL		CSL	28	100		
105	32				CSL	29	100		

UNDRAINED SHEAR STRENGTH -
WATER CONTENT & ATTERBERG LIMITS
DYNAMIC PENETRATION TEST
STANDARD PENETRATION TEST, N-VALUE
10 20 30 40 50 60 70 80 90 100
204 1/88

Figure A.3 (cont'd) Borehole Log for hole S3

PAGE 4 OF 5

BOREHOLE RECORD

BOREHOLE No. S3

CLIENT
LOCATION
DATES: BORING WATER LEVEL
PROJECT No.
CASING SIZE
DATUM

DEPTH (FT.)	DEPTH (m)	ELEVATION	SOIL DESCRIPTION	WATER LEVEL	SAMPLES TYPE	SAMPLES NUMBER	SAMPLES RECOVERY	N-VALUE OR RQD %	OTHER TESTS
105	32	717.89							
			Seam 1 Coal						
	33				CSL	30	100		
110									
	34								
115	35	714.79	PARTING						
		714.39	SEAM 2 COAL						
	36								
120									
	37								
125	38								
	39	710.89	PARTING						
130		710.29	SEAM 3 COAL						
	40	709.59	PARTING						
		708.99	SEAM 4 COAL						
135	41								
	42	707.59	PARTING						
140		707.19	SEAM 5 COAL						
	43								

THE ALBERTA RESEARCH COUNCIL TOOK OVER SUPERVISION OF THE SAMPLING FROM SAMPLE 30 TO THE END OF THE HOLE.

UNDRAINED SHEAR STRENGTH-

WATER CONTENT & ATTERBERG LIMITS W_p W W_L
DYNAMIC PENETRATION TEST x
STANDARD PENETRATION TEST, N-VALUE ●

10 20 30 40 50 60 70 80 90 100

204 1/88

Figure A.3 (cont'd) Borehole Log for hole S3

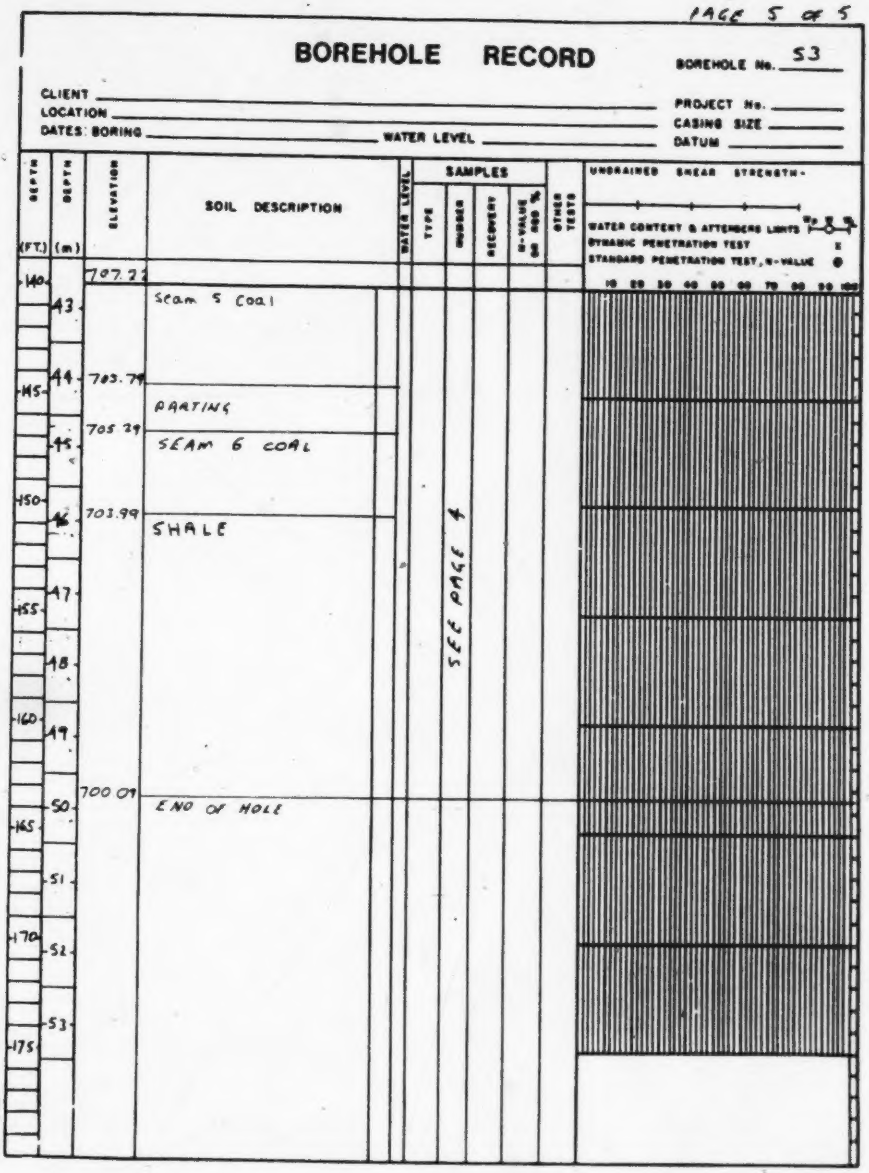

PAGE 5 OF 5

BOREHOLE RECORD

BOREHOLE No. S3

CLIENT

LOCATION

DATES: BORING

WATER LEVEL

PROJECT No.

CASING SIZE

DATUM

DEPTH (FT.)	DEPTH (m)	ELEVATION	SOIL DESCRIPTION	WATER LEVEL	SAMPLES TYPE	SAMPLES NUMBER	SAMPLES RECOVERY	SAMPLES N-VALUE OR RQD %	OTHER TESTS
140	43	707.22	Seam 5 Coal			SEE PAGE 4			
145	44	703.79	PARTING						
	45	705.29	SEAM 6 COAL						
150	46	703.99	SHALE						
155	47								
	48								
160	49								
165	50	700.09	END OF HOLE						
	51								
170	52								
175	53								

UNDRAINED SHEAR STRENGTH -
WATER CONTENT & ATTERBERG LIMITS
DYNAMIC PENETRATION TEST
STANDARD PENETRATION TEST, N-VALUE
10 20 30 40 50 60 70 80 90 100

Figure A.3 (cont'd) Borehole Log for hole S3

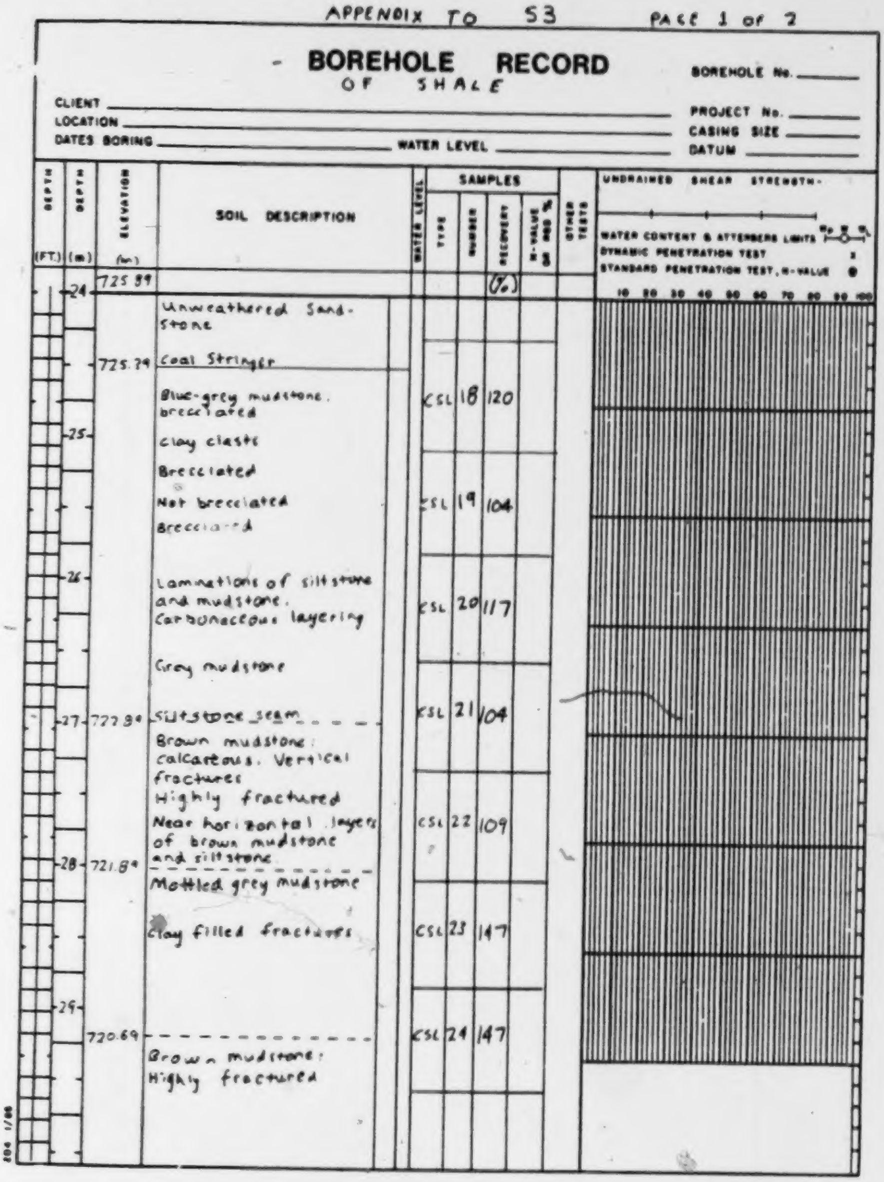

APPENDIX TO S3 PAGE 1 of 2

- BOREHOLE RECORD
OF SHALE

BOREHOLE No. ______
CLIENT ______
LOCATION ______
DATES BORING ______ WATER LEVEL ______
PROJECT No. ______
CASING SIZE ______
DATUM ______

DEPTH (FT.)	DEPTH (m)	ELEVATION (m)	SOIL DESCRIPTION	WATER LEVEL	SAMPLES TYPE	SAMPLES NUMBER	SAMPLES RECOVERY	SAMPLES N-VALUE or RQD %	OTHER TESTS
	24	725.89					(%)		
			Unweathered Sandstone						
		725.79	Coal Stringer						
			Blue-grey mudstone, brecciated		CSL	18	120		
	25		clay clasts						
			Brecciated						
			Not brecciated		CSL	19	104		
			Brecciated						
	26		Laminations of siltstone and mudstone. Carbonaceous layering		CSL	20	117		
			Grey mudstone						
	27	722.89	Siltstone seam		CSL	21	104		
			Brown mudstone: calcareous. Vertical fractures						
			Highly fractured						
			Near horizontal layers of brown mudstone and siltstone		CSL	22	109		
	28	721.89	Mottled grey mudstone						
			Clay filled fractures		CSL	23	147		
	29								
		720.69			CSL	24	147		
			Brown mudstone: Highly fractured						

UNDRAINED SHEAR STRENGTH -
WATER CONTENT & ATTERBERG LIMITS Wp W WL
DYNAMIC PENETRATION TEST ×
STANDARD PENETRATION TEST, N-VALUE ●
10 20 30 40 50 60 70 80 90 100

204 1/86

Figure A.3 (cont'd) Borehole Log for hole S3

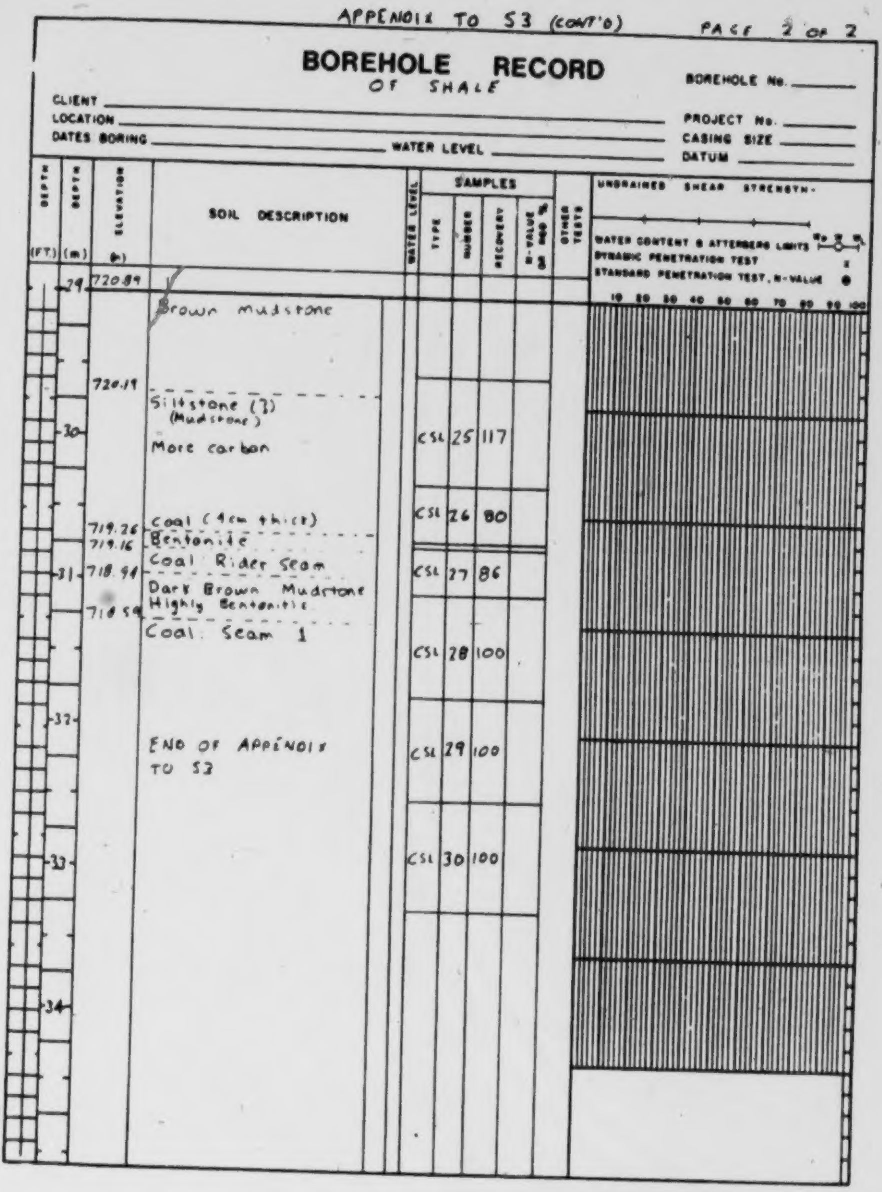

APPENDIX TO S3 (CONT'D) PAGE 2 OF 2

BOREHOLE RECORD
OF SHALE

CLIENT
LOCATION
DATES BORING
WATER LEVEL
BOREHOLE No.
PROJECT No.
CASING SIZE
DATUM

DEPTH (m)	ELEVATION (m)	SOIL DESCRIPTION	TYPE	NUMBER	RECOVERY
29	720.89				
		Brown mudstone			
	720.19	Siltstone (?) (Mudstone)			
30		More carbon	CSL	25	117
	719.26	Coal (4cm thick)	CSL	26	80
	719.16	Bentonite			
		Coal Rider Seam	CSL	27	86
31	718.94	Dark Brown Mudstone Highly Bentonitic			
	718.59	Coal Seam 1	CSL	28	100
32		END OF APPENDIX TO S3	CSL	29	100
33			CSL	30	100
34					

DEPTH (FT.)
WATER LEVEL
SAMPLES
N-VALUE OR RQD %
OTHER TESTS
UNDRAINED SHEAR STRENGTH
WATER CONTENT & ATTERBERG LIMITS
DYNAMIC PENETRATION TEST
STANDARD PENETRATION TEST, N-VALUE
10 20 30 40 50 60 70 80 90 100

Figure A.3 (cont'd) Borehole Log for hole S3

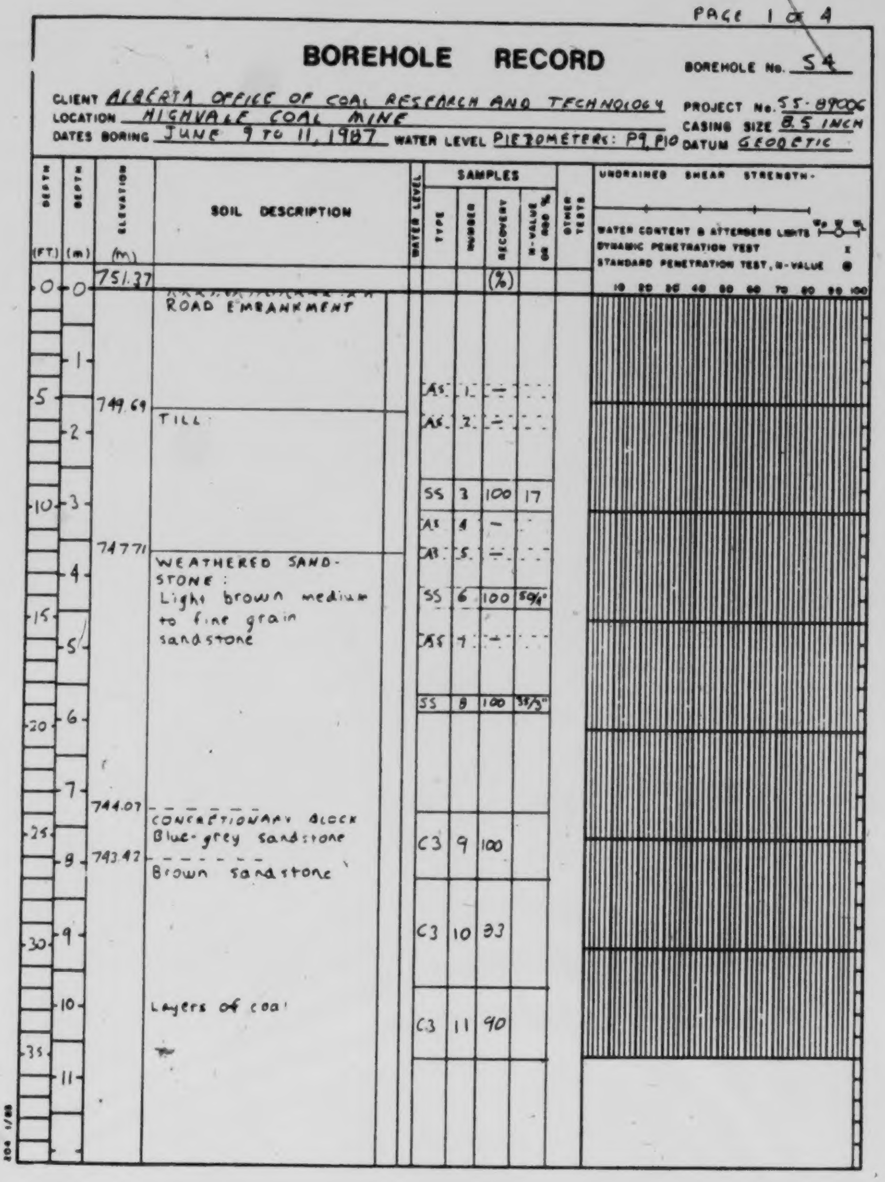

PAGE 1 of 4

BOREHOLE RECORD

BOREHOLE No. S4

CLIENT ALBERTA OFFICE OF COAL RESEARCH AND TECHNOLOGY
LOCATION HIGHVALE COAL MINE
DATES BORING JUNE 9 TO 11, 1987
WATER LEVEL PIEZOMETERS: P9, P10
PROJECT No. 55-89006
CASING SIZE 8.5 INCH
DATUM GEODETIC

ELEVATION (m)	SOIL DESCRIPTION	TYPE	NUMBER	RECOVERY (%)	N-VALUE OR RQD %
751.37	ROAD EMBANKMENT				
		AS	1	-	
749.69	TILL	AS	2	-	
		SS	3	100	17
		AS	4	-	
		AS	5	-	
747.71	WEATHERED SANDSTONE: Light brown medium to fine grain sandstone				
		SS	6	100	50/4"
		AS	7	-	
		SS	8	100	35/3"
744.07	CONCRETIONARY BLOCK Blue-grey sandstone	C3	9	100	
743.42	Brown sandstone	C3	10	33	
	Layers of coal	C3	11	90	

DEPTH (FT)
DEPTH (m)
WATER LEVEL
SAMPLES
OTHER TESTS
UNDRAINED SHEAR STRENGTH -
WATER CONTENT & ATTERBERG LIMITS
DYNAMIC PENETRATION TEST
STANDARD PENETRATION TEST, N-VALUE
10 20 30 40 50 60 70 80 90 100
0 5 10 15 20 25 30 35
0 1 2 3 4 5 6 7 8 9 10 11
204 1/88

Figure A.4 Borehole Log for hole S4

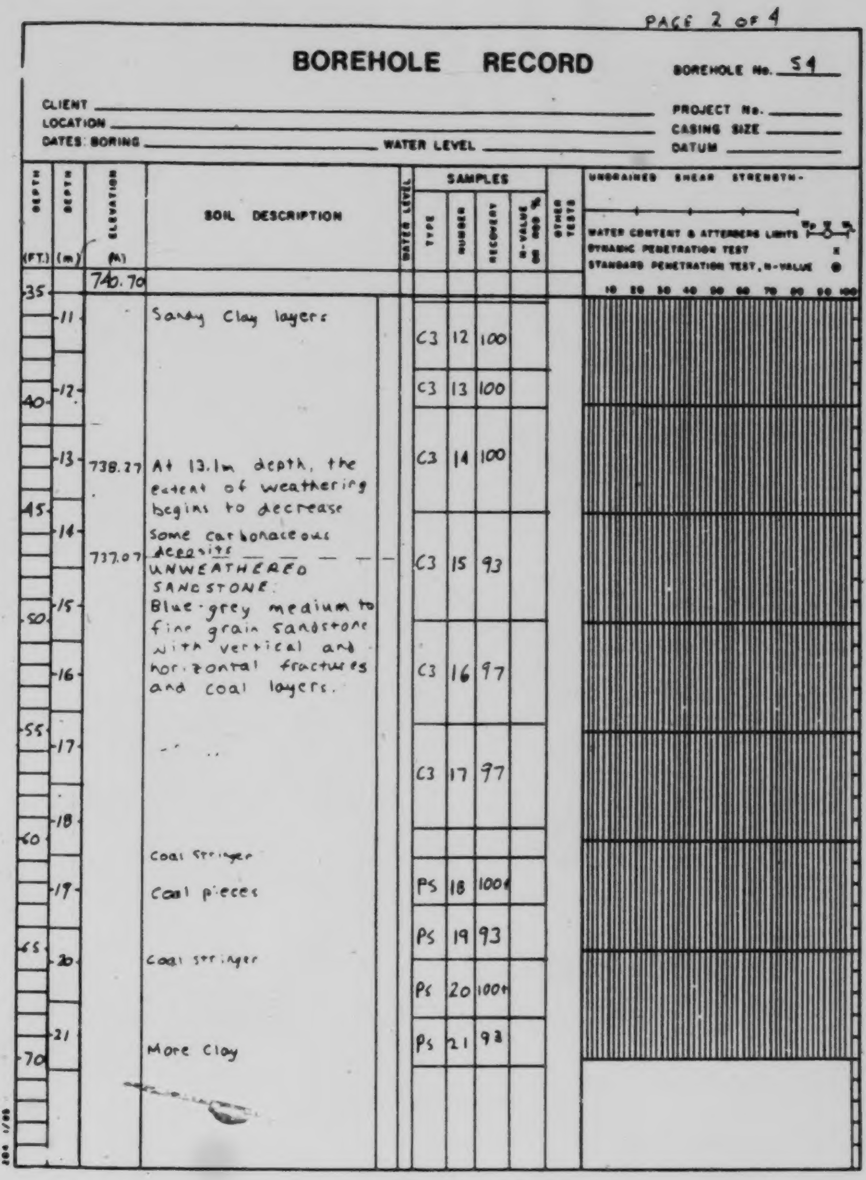

PAGE 2 OF 4

BOREHOLE RECORD

BOREHOLE No. S4

CLIENT

LOCATION

DATES: BORING

WATER LEVEL

PROJECT No.

CASING SIZE

DATUM

DEPTH (FT.)	DEPTH (m)	ELEVATION (M)	SOIL DESCRIPTION	WATER LEVEL	SAMPLES TYPE	SAMPLES NUMBER	SAMPLES RECOVERY	SAMPLES N-VALUE OR RQD %	OTHER TESTS
35		740.70							
	11		Sandy Clay layers		C3	12	100		
40	12				C3	13	100		
	13	738.27	At 13.1m depth, the extent of weathering begins to decrease		C3	14	100		
45	14	737.07	Some carbonaceous deposits UNWEATHERED SANDSTONE. Blue-grey medium to fine grain sandstone with vertical and horizontal fractures and coal layers.		C3	15	93		
50	15								
	16				C3	16	97		
55	17				C3	17	97		
	18								
60			Coal stringer						
	19		Coal pieces		PS	18	100+		
					PS	19	93		
65	20		Coal stringer		Ps	20	100+		
	21				Ps	21	93		
70			More Clay						

UNDRAINED SHEAR STRENGTH -
WATER CONTENT & ATTERBERG LIMITS
DYNAMIC PENETRATION TEST
STANDARD PENETRATION TEST, N-VALUE
10 20 30 40 50 60 70 80 90 100

Figure A.4 (cont'd) Borehole Log for hole S4

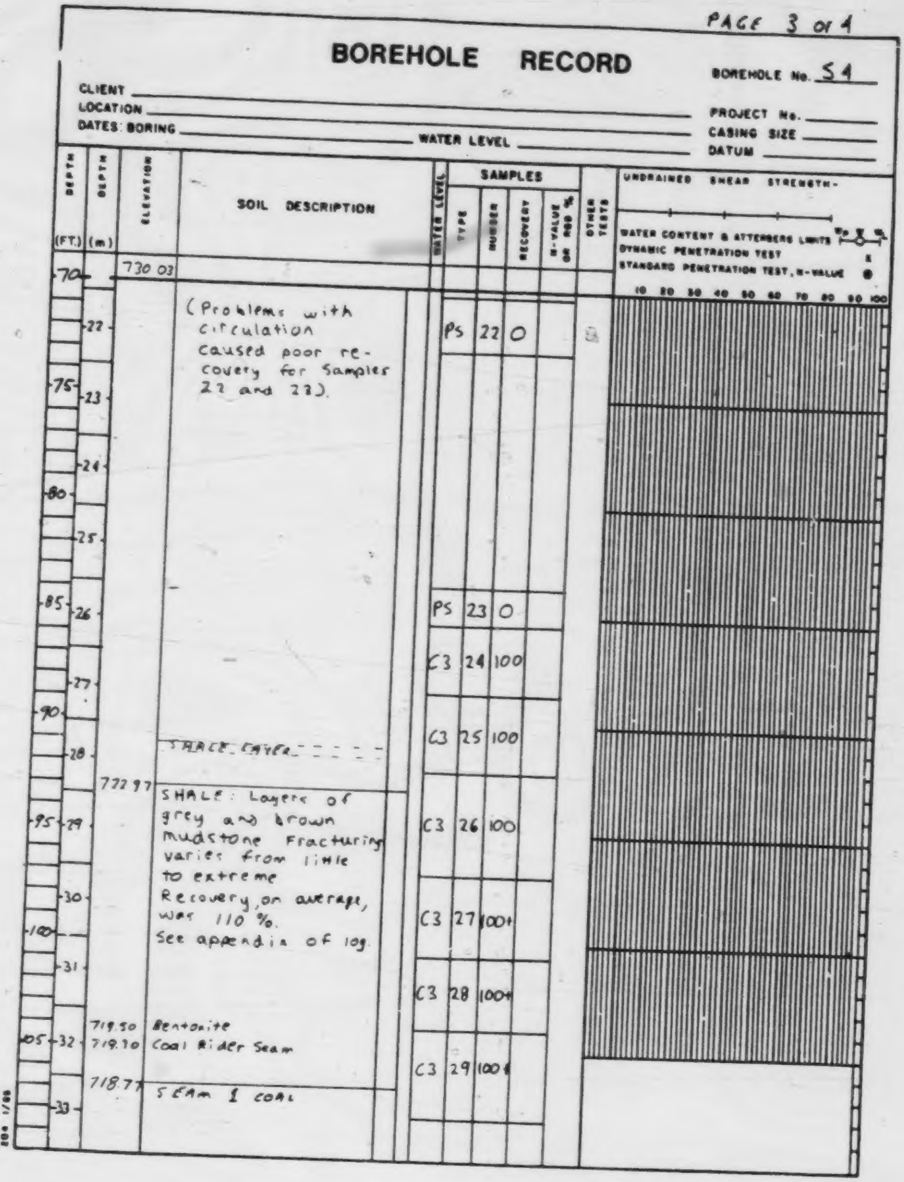

PAGE 3 OF 4

BOREHOLE RECORD

BOREHOLE No. S4

CLIENT

LOCATION

DATES: BORING

WATER LEVEL

PROJECT No.

CASING SIZE

DATUM

DEPTH (FT.)	DEPTH (m)	ELEVATION	SOIL DESCRIPTION	WATER LEVEL	SAMPLES TYPE	SAMPLES NUMBER	SAMPLES RECOVERY	SAMPLES N-VALUE OR RQD %	OTHER TESTS
70		730 03							
	22		(Problems with circulation caused poor re-covery for Samples 22 and 23).		PS	22	0		
75	23								
80	24								
	25								
85	26				PS	23	0		
					C3	24	100		
90	27								
	28		SHALE LAYER		C3	25	100		
95	29	722 97	SHALE: Layers of grey and brown mudstone Fracturing varies from little to extreme Recovery, on average, was 110 %. See appendix of log.		C3	26	100		
100	30				C3	27	100+		
	31				C3	28	100+		
105	32	719.50 719.10	Bentonite Coal Rider Seam		C3	29	100+		
	33	718.77	SEAM 1 COAL						

UNDRAINED SHEAR STRENGTH -
WATER CONTENT & ATTERBERG LIMITS
DYNAMIC PENETRATION TEST
STANDARD PENETRATION TEST, N-VALUE
10 20 30 40 50 60 70 80 90 100
200 1/80

Figure A.4 (cont'd) Borehole Log for hole S4

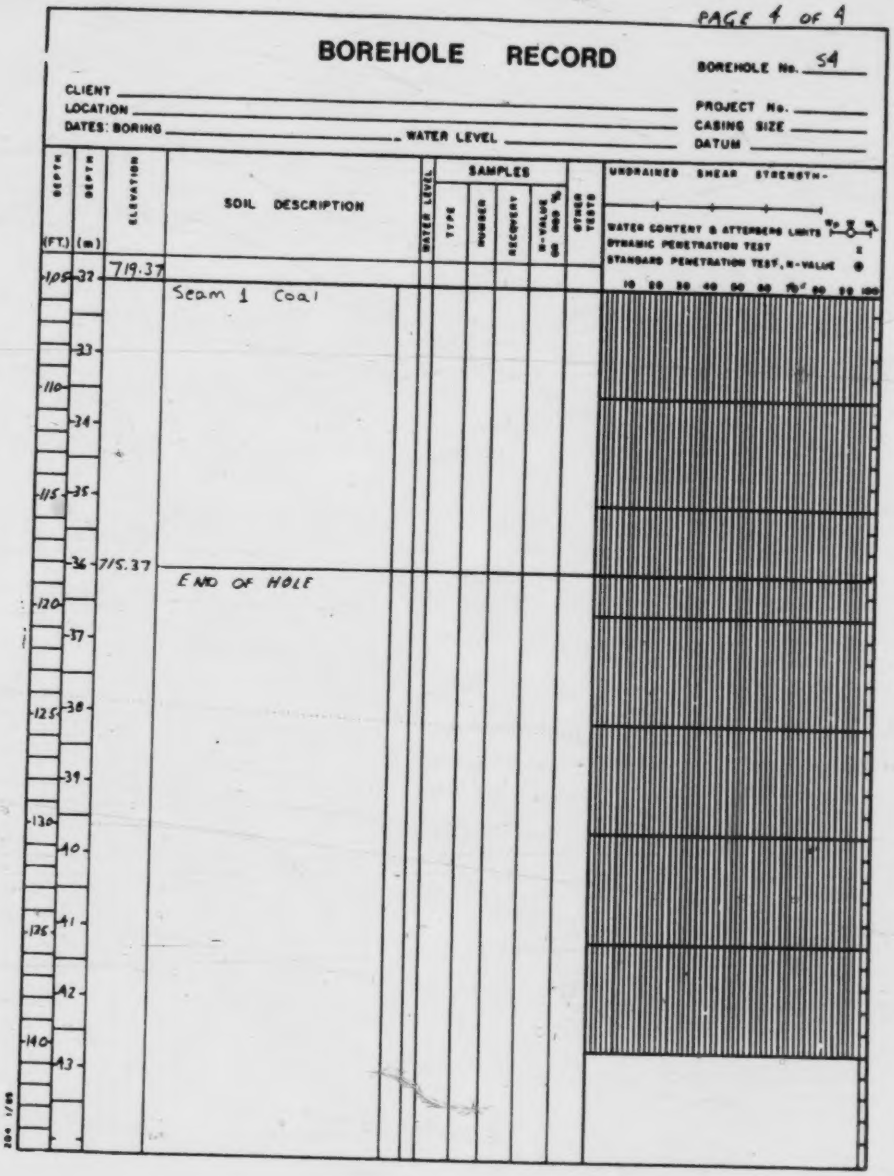

PAGE 4 OF 4

BOREHOLE RECORD

BOREHOLE No. S4

CLIENT

LOCATION

DATES: BORING

WATER LEVEL

PROJECT No.

CASING SIZE

DATUM

DEPTH (FT.)	DEPTH (m)	ELEVATION	SOIL DESCRIPTION	WATER LEVEL	SAMPLES TYPE	SAMPLES NUMBER	SAMPLES RECOVERY	SAMPLES N-VALUE OR RQD %	OTHER TESTS
105	32	719.37	Seam 1 Coal						
	36	715.37	END OF HOLE						

UNDRAINED SHEAR STRENGTH-
WATER CONTENT & ATTERBERG LIMITS Wp W WL
DYNAMIC PENETRATION TEST
STANDARD PENETRATION TEST, N-VALUE ●
10 20 30 40 50 60 70 80 90 100
105 110 115 120 125 130 135 140
32 33 34 35 36 37 38 39 40 41 42 43
204 1/85

Figure A.4 (cont'd) Borehole Log for hole S4

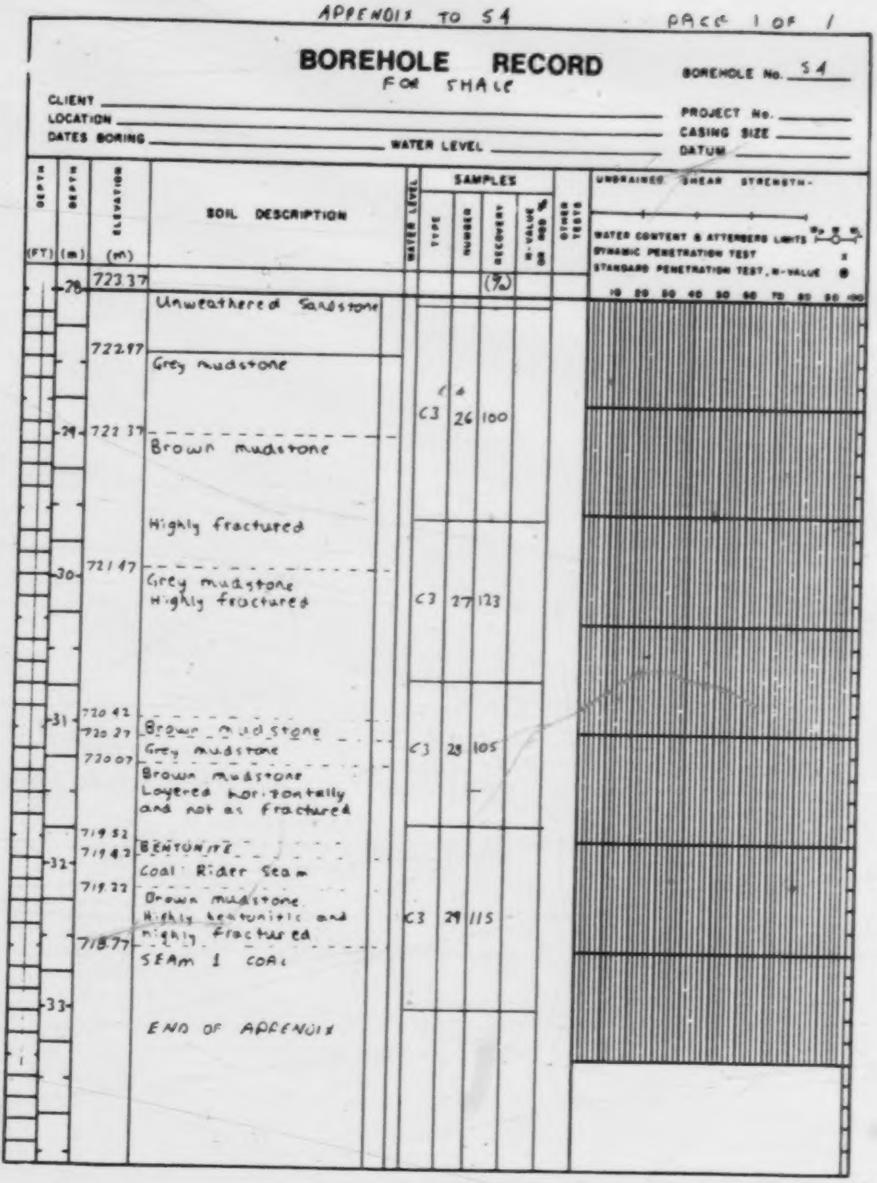

APPENDIX TO S4 PAGE 1 OF 1

BOREHOLE RECORD
FOR SHALE

BOREHOLE No. S4
CLIENT
LOCATION
DATES BORING
WATER LEVEL
PROJECT No.
CASING SIZE
DATUM

DEPTH (FT)	DEPTH (m)	ELEVATION (m)	SOIL DESCRIPTION	WATER LEVEL	SAMPLES TYPE	SAMPLES NUMBER	SAMPLES RECOVERY (%)	SAMPLES N-VALUE OR RQD %	OTHER TESTS
	28	723.37	Unweathered Sandstone						
		722.97	Grey mudstone		C C3	4 26	100		
	29	722 37	Brown mudstone Highly fractured						
	30	721 47	Grey mudstone Highly fractured		C3	27	123		
	31	720 42	Brown mudstone						
		720 27	Grey mudstone		C3	28	105		
		720 07	Brown mudstone Layered horizontally and not as fractured						
		719.52	BENTONITE						
	32	719.42	Coal Rider Seam						
		719.22	Brown mudstone Highly bentonitic and highly fractured		C3	29	115		
		718.77	SEAM 1 COAL						
	33		END OF APPENDIX						

UNDRAINED SHEAR STRENGTH -
WATER CONTENT & ATTERBERG LIMITS
Wp W WL
DYNAMIC PENETRATION TEST
x
STANDARD PENETRATION TEST, N-VALUE
●
10 20 30 40 50 60 70 80 90 100
204 1/85

Figure A.4 (cont'd) Borehole Log for hole S4

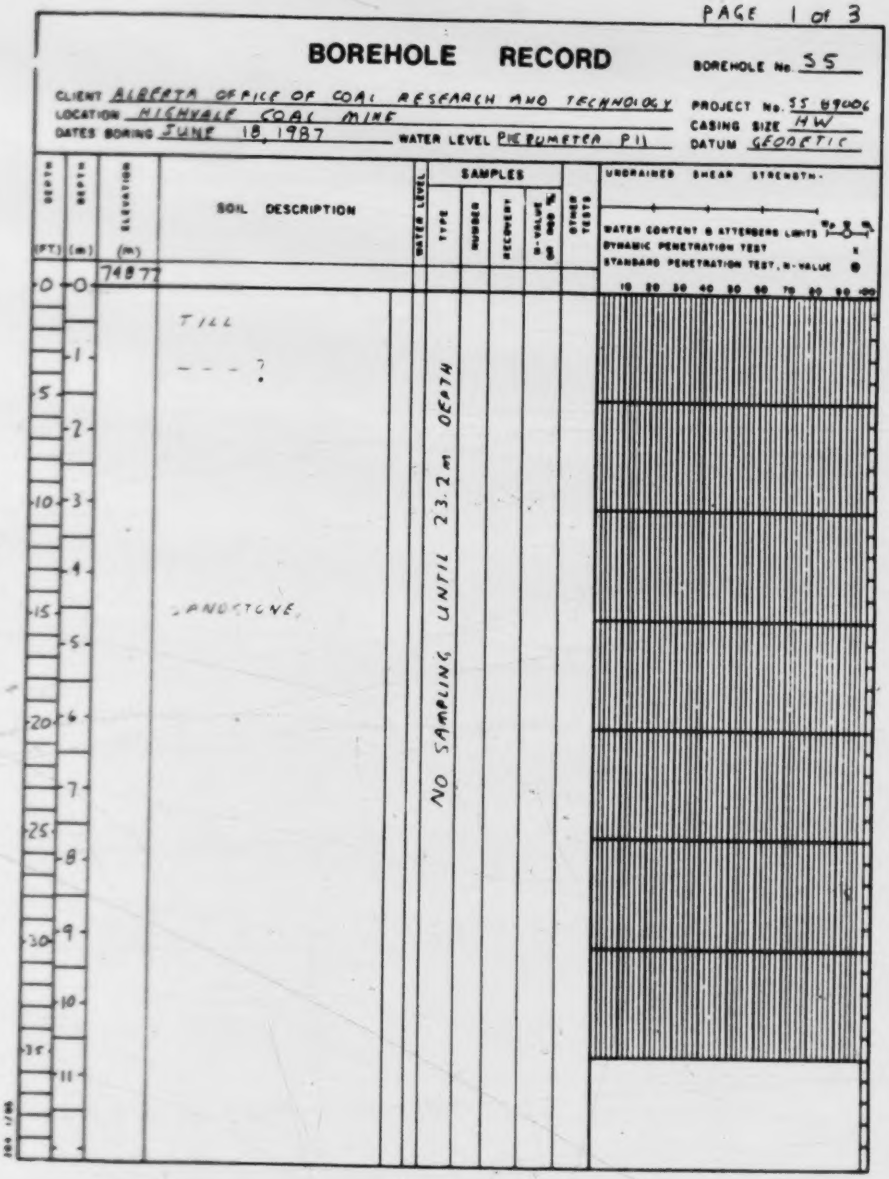

PAGE 1 of 3

BOREHOLE RECORD

BOREHOLE No. S5

CLIENT ALBERTA OFFICE OF COAL RESEARCH AND TECHNOLOGY
LOCATION HIGHVALE COAL MINE
DATES BORING JUNE 18, 1987
WATER LEVEL PIEZOMETER P11
PROJECT No. SS 89006
CASING SIZE HW
DATUM GEODETIC

ELEVATION (m): 74877

TILL

- - - ?

SANDSTONE

NO SAMPLING UNTIL 23.2m DEPTH

DEPTH (FT)
DEPTH (m)
ELEVATION (m)
SOIL DESCRIPTION
WATER LEVEL
SAMPLES
TYPE
NUMBER
RECOVERY
N-VALUE OR RQD %
OTHER TESTS
UNDRAINED SHEAR STRENGTH-
WATER CONTENT & ATTERBERG LIMITS
DYNAMIC PENETRATION TEST
STANDARD PENETRATION TEST, N-VALUE
10 20 30 40 50 60 70 80 90 100
0 5 10 15 20 25 30 35
0 1 2 3 4 5 6 7 8 9 10 11

Figure A.5 Borehole Log for hole S5

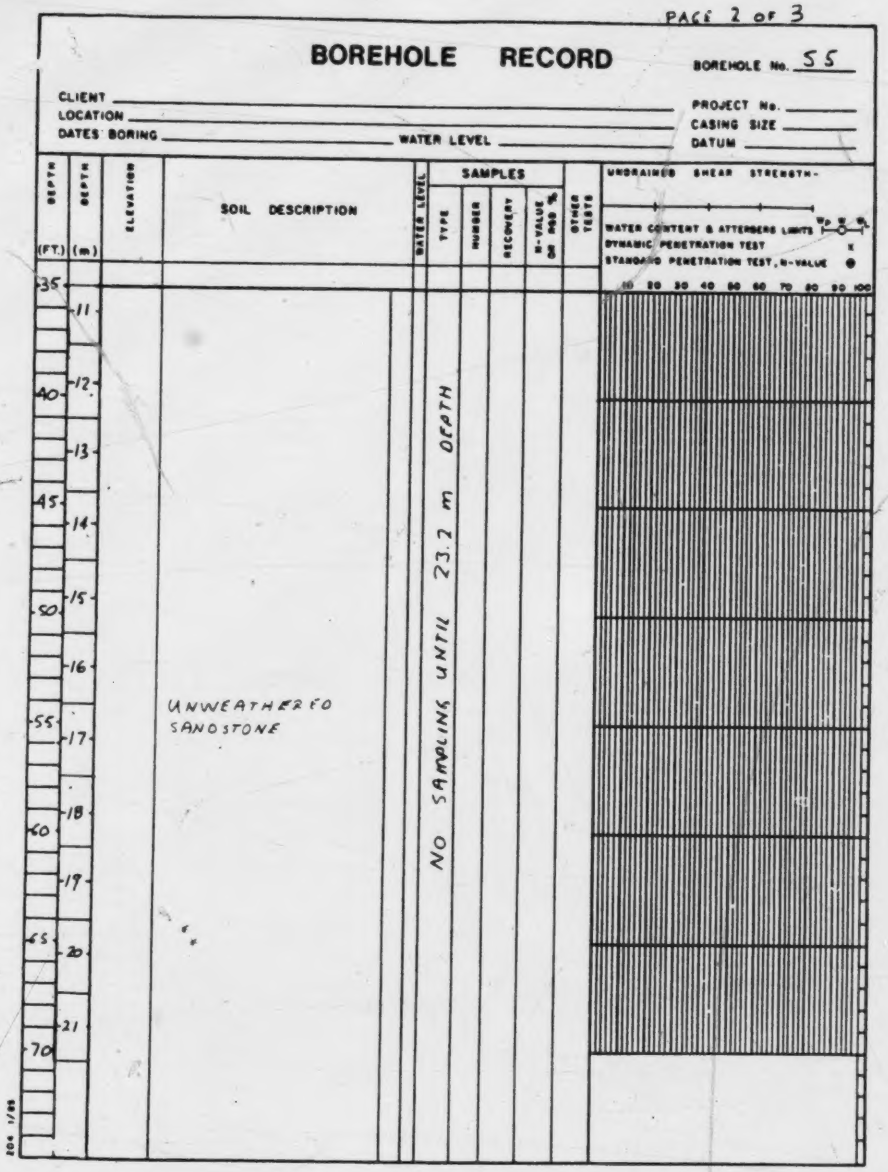

PAGE 2 of 3

BOREHOLE RECORD

BOREHOLE No. S5

CLIENT
LOCATION
DATES BORING
WATER LEVEL
PROJECT No.
CASING SIZE
DATUM

DEPTH (FT.)	DEPTH (m)	ELEVATION	SOIL DESCRIPTION	WATER LEVEL	SAMPLES TYPE	SAMPLES NUMBER	SAMPLES RECOVERY	SAMPLES N-VALUE OR RQD %	OTHER TESTS	UNDRAINED SHEAR STRENGTH-
35 – 70	11 – 21		UNWEATHERED SANDSTONE		NO SAMPLING UNTIL 23.2 m DEPTH					

WATER CONTENT & ATTERBERG LIMITS
W_P W W_L
DYNAMIC PENETRATION TEST x
STANDARD PENETRATION TEST, N-VALUE ●
10 20 30 40 50 60 70 80 90 100
35
40
45
50
55
60
65
70
11
12
13
14
15
16
17
18
19
20
21
204 1/85

Figure A.5 (cont'd) Borehole Log for hole S5

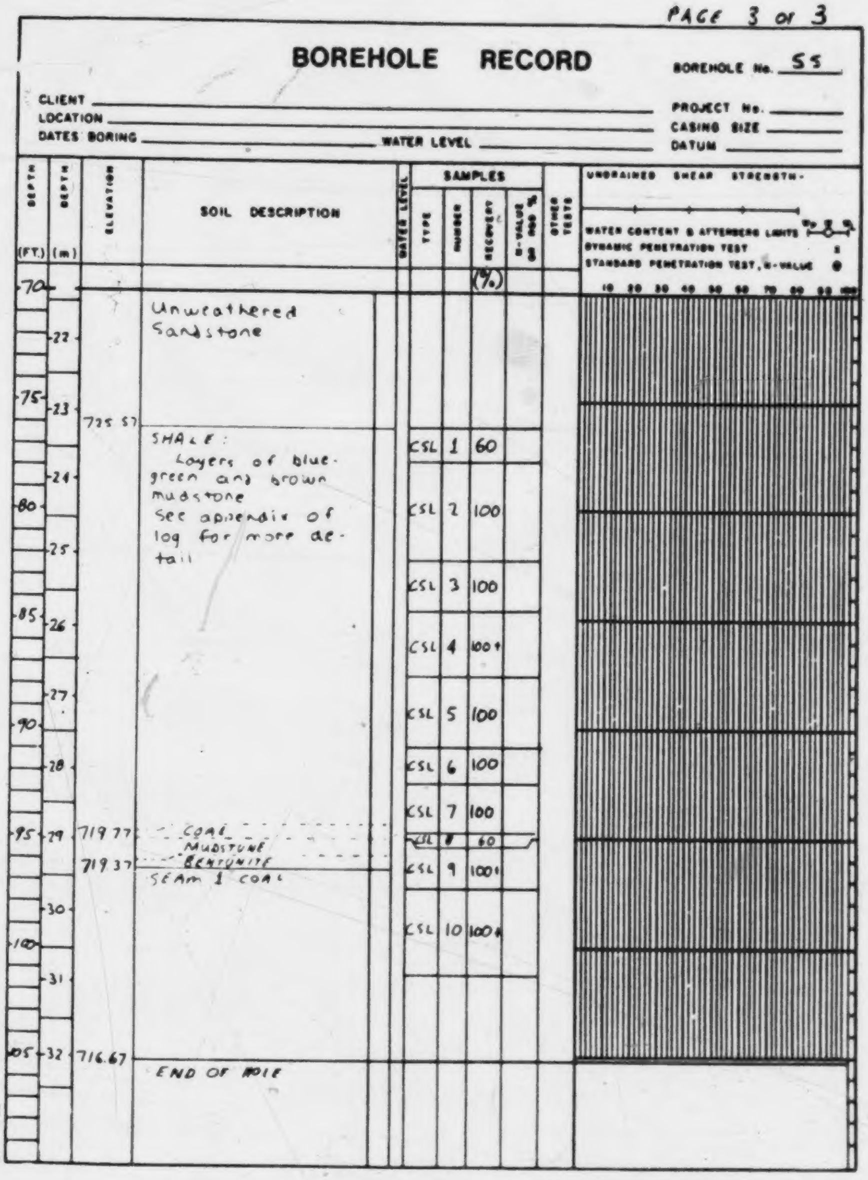

PAGE 3 OF 3

BOREHOLE RECORD

BOREHOLE No. S5

CLIENT
LOCATION
DATES BORING
WATER LEVEL
PROJECT No.
CASING SIZE
DATUM

DEPTH (FT.)	DEPTH (m)	ELEVATION	SOIL DESCRIPTION	WATER LEVEL	SAMPLES TYPE	SAMPLES NUMBER	SAMPLES RECOVERY (%)	SAMPLES N-VALUE OR RQD %	OTHER TESTS
70			Unweathered Sandstone						
	22								
75	23	725.57	SHALE: Layers of blue-green and brown mudstone See appendix of log for more detail		CSL	1	60		
80	24				CSL	2	100		
	25				CSL	3	100		
85	26				CSL	4	100+		
90	27				CSL	5	100		
	28				CSL	6	100		
					CSL	7	100		
95	29	719.77	COAL MUDSTONE BENTONITE		CSL	8	60		
		719.37	SEAM 1 COAL		CSL	9	100+		
100	30				CSL	10	100+		
	31								
105	32	716.67	END OF HOLE						

UNDRAINED SHEAR STRENGTH-
WATER CONTENT & ATTERBERG LIMITS
DYNAMIC PENETRATION TEST
STANDARD PENETRATION TEST, N-VALUE
10 20 30 40 50 60 70 80 90 100
204 1/88

Figure A.5 (cont'd) Borehole Log for hole S5

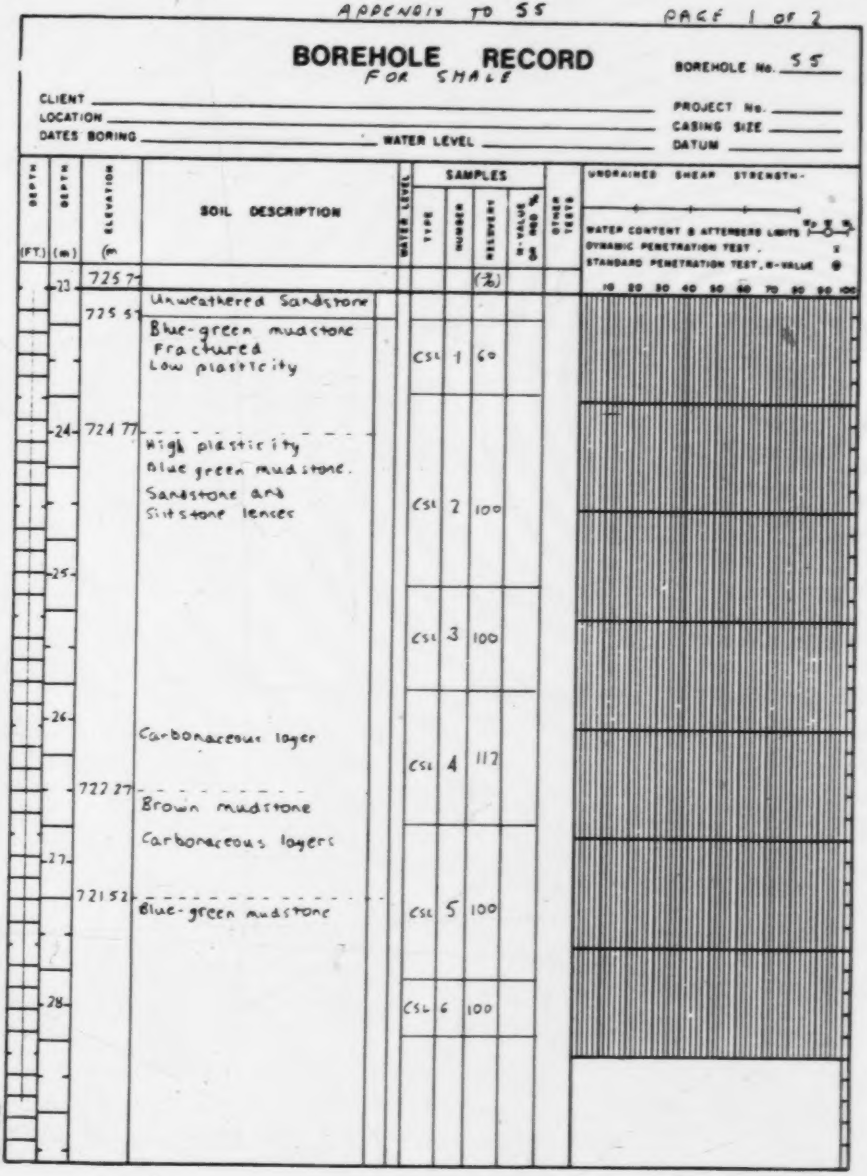

APPENDIX TO S5 PAGE 1 OF 2

BOREHOLE RECORD
FOR SHALE

BOREHOLE No. S5

CLIENT
LOCATION
DATES BORING
WATER LEVEL
PROJECT No.
CASING SIZE
DATUM

DEPTH (FT.)	DEPTH (m)	ELEVATION (m	SOIL DESCRIPTION	WATER LEVEL	SAMPLES TYPE	SAMPLES NUMBER	SAMPLES RECOVERY	SAMPLES N-VALUE or RQD %	OTHER TESTS
	23	725 71					(%)		
		725 51	Unweathered Sandstone						
			Blue-green mudstone Fractured Low plasticity		CSL	1	60		
	24	724 77	High plasticity Blue green mudstone. Sandstone and Siltstone lenses		CSL	2	100		
	25				CSL	3	100		
	26		Carbonaceous layer		CSL	4	112		
		722 27	Brown mudstone Carbonaceous layers						
	27	721 52	Blue-green mudstone		CSL	5	100		
	28				CSL	6	100		

UNDRAINED SHEAR STRENGTH-
WATER CONTENT & ATTERBERG LIMITS
DYNAMIC PENETRATION TEST.
STANDARD PENETRATION TEST, N-VALUE

204 1/88

Figure A.5 (cont'd) Borehole Log for hole S5

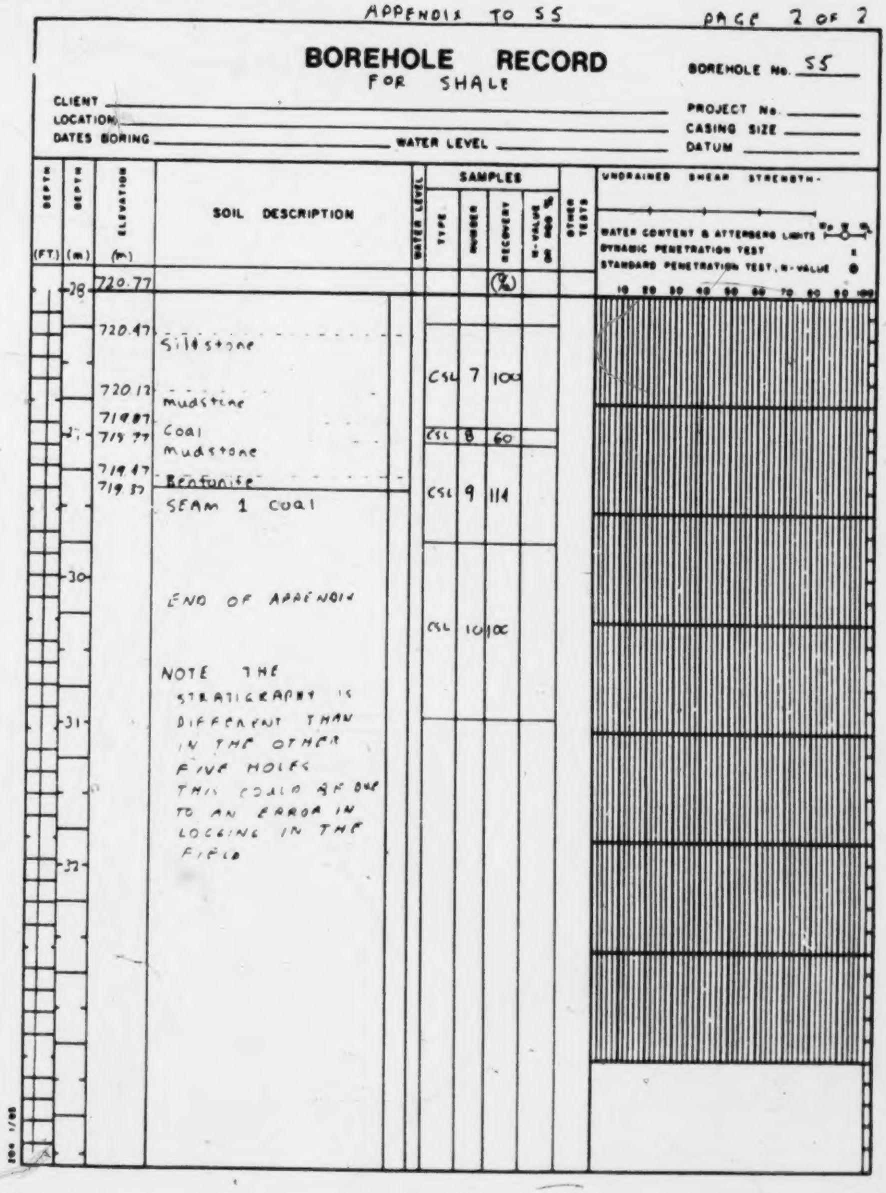

APPENDIX TO S5 PAGE 2 OF 2

BOREHOLE RECORD
FOR SHALE

BOREHOLE No. S5

CLIENT
LOCATION
DATES BORING
WATER LEVEL
PROJECT No.
CASING SIZE
DATUM

DEPTH (FT)	DEPTH (m)	ELEVATION (m)	SOIL DESCRIPTION	WATER LEVEL	SAMPLES TYPE	SAMPLES NUMBER	SAMPLES RECOVERY (%)	SAMPLES N-VALUE OR RQD %	OTHER TESTS
	28	720.77							
		720.47	Siltstone		CSL	7	100		
		720.12	mudstone						
		719.87	Coal		CSL	8	60		
	29	719.77	Mudstone						
		719.47	Bentonite						
		719.37	SEAM 1 Coal		CSL	9	114		
	30		END OF APPENDIX		CSL	10	100		
	31		NOTE THE STRATIGRAPHY IS DIFFERENT THAN IN THE OTHER FIVE HOLES THIS COULD BE DUE TO AN ERROR IN LOGGING IN THE FIELD						
	32								

UNDRAINED SHEAR STRENGTH -
WATER CONTENT & ATTERBERG LIMITS
DYNAMIC PENETRATION TEST
STANDARD PENETRATION TEST, N-VALUE
10 20 30 40 50 60 70 80 90 100

Figure A.5 (cont'd) Borehole Log for hole S5

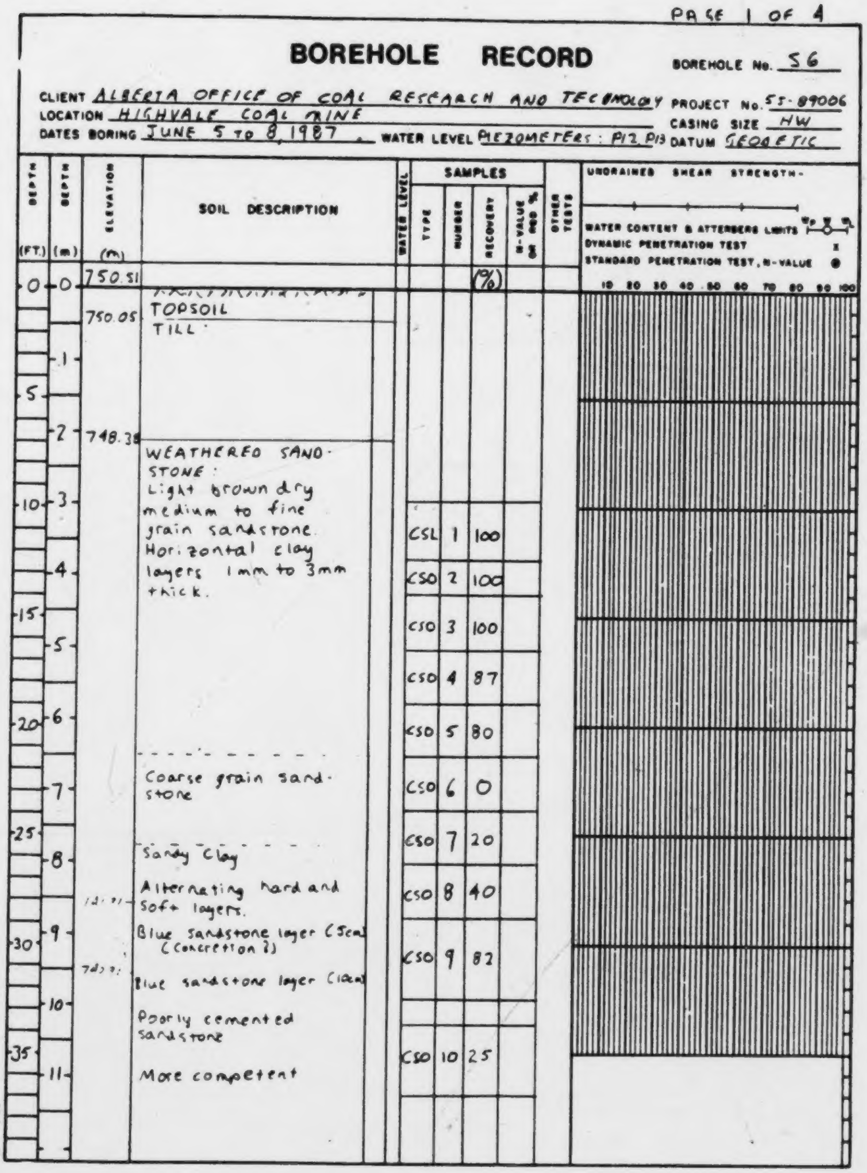

PAGE 1 OF 4

BOREHOLE RECORD

BOREHOLE No. S6

CLIENT ALBERTA OFFICE OF COAL RESEARCH AND TECHNOLOGY
PROJECT No. 55-89006
LOCATION HIGHVALE COAL MINE
CASING SIZE HW
DATES BORING JUNE 5 TO 8, 1987
WATER LEVEL PIEZOMETERS: P12, P13
DATUM GEODETIC

DEPTH (FT.)	DEPTH (m)	ELEVATION (m)	SOIL DESCRIPTION	WATER LEVEL	SAMPLES TYPE	SAMPLES NUMBER	SAMPLES RECOVERY	SAMPLES N-VALUE OR RQD %	OTHER TESTS
0	0	750.51					(%)		
		750.05	TOPSOIL						
			TILL						
	1								
5									
	2	748.38	WEATHERED SANDSTONE: Light brown dry medium to fine grain sandstone. Horizontal clay layers 1mm to 3mm thick.						
10	3				CSL	1	100		
	4				CSO	2	100		
15					CSO	3	100		
	5				CSO	4	87		
20	6				CSO	5	80		
	7		Coarse grain sandstone		CSO	6	0		
25					CSO	7	20		
	8		Sandy Clay						
		[illegible]	Alternating hard and soft layers.		CSO	8	40		
30	9		Blue sandstone layer (5cm (Concretion?)		CSO	9	82		
		[illegible]	Blue sandstone layer (10cm						
	10		Poorly cemented sandstone						
35	11		More competent		CSO	10	25		

UNDRAINED SHEAR STRENGTH -
WATER CONTENT & ATTERBERG LIMITS W_P W W_L
DYNAMIC PENETRATION TEST x
STANDARD PENETRATION TEST, N-VALUE ●
10 20 30 40 50 60 70 80 90 100

204 1/88

Figure A.6 Borehole Log for hole S6

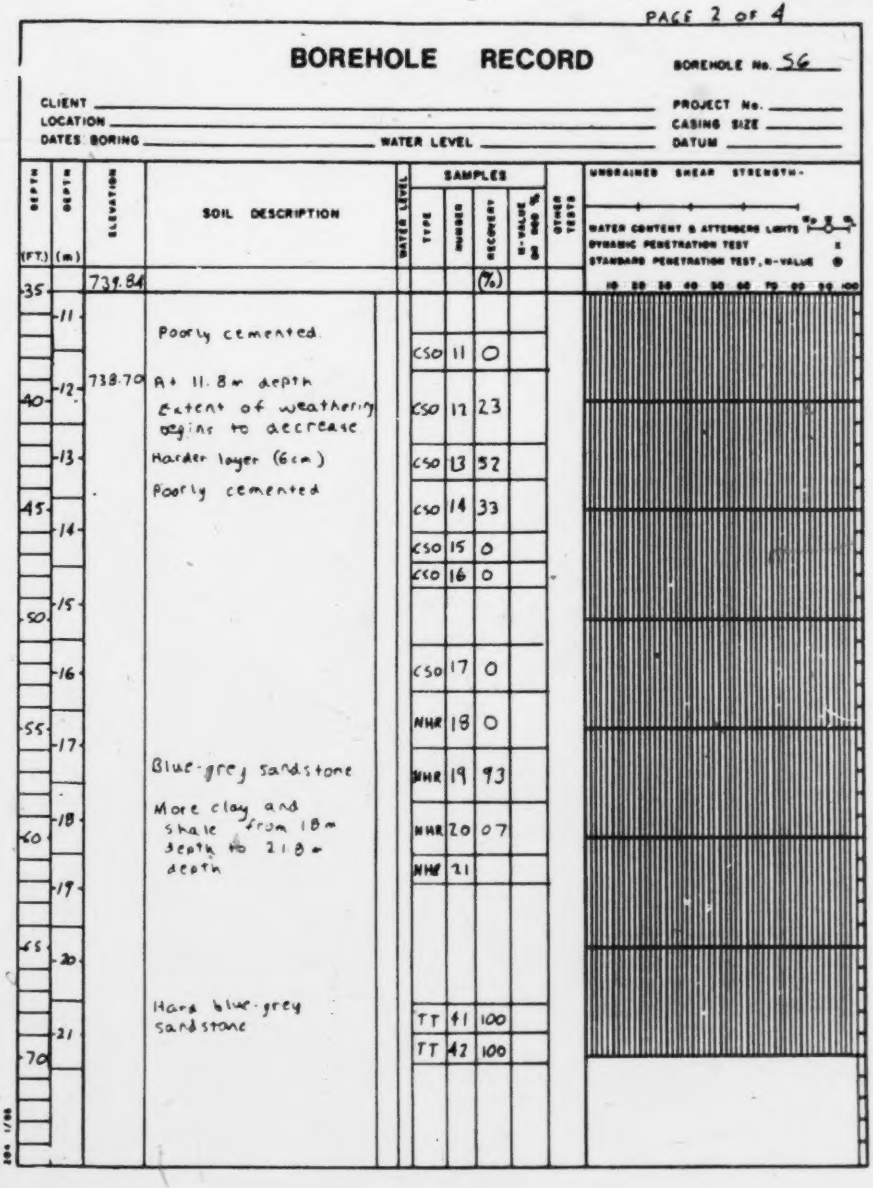

PAGE 2 OF 4

BOREHOLE RECORD

BOREHOLE No. S6

CLIENT ____
LOCATION ____
DATES: BORING ____ WATER LEVEL ____
PROJECT No. ____
CASING SIZE ____
DATUM ____

DEPTH (FT.)	DEPTH (m)	ELEVATION	SOIL DESCRIPTION	WATER LEVEL	SAMPLES TYPE	SAMPLES NUMBER	SAMPLES RECOVERY	SAMPLES N-VALUE OR RQD %	OTHER TESTS
35		739.84					(%)		
	11		Poorly cemented.		CSO	11	0		
40	12	738.70	At 11.8m depth Extent of weathering begins to decrease		CSO	12	23		
	13		Harder layer (6cm)		CSO	13	52		
45			Poorly cemented		CSO	14	33		
	14				CSO	15	0		
					CSO	16	0		
50	15								
	16				CSO	17	0		
55	17				NHR	18	0		
			Blue-grey sandstone		NHR	19	93		
60	18		More clay and shale from 18m depth to 21.8m depth		NHR	20	07		
					NHR	21			
	19								
65	20								
	21		Hard blue-grey sandstone		TT	41	100		
70					TT	42	100		

UNDRAINED SHEAR STRENGTH-
WATER CONTENT & ATTERBERG LIMITS W_p W W_L
DYNAMIC PENETRATION TEST x
STANDARD PENETRATION TEST, N-VALUE ●
10 20 30 40 50 60 70 80 90 100

Figure A.6 (cont'd) Borehole Log for hole S6

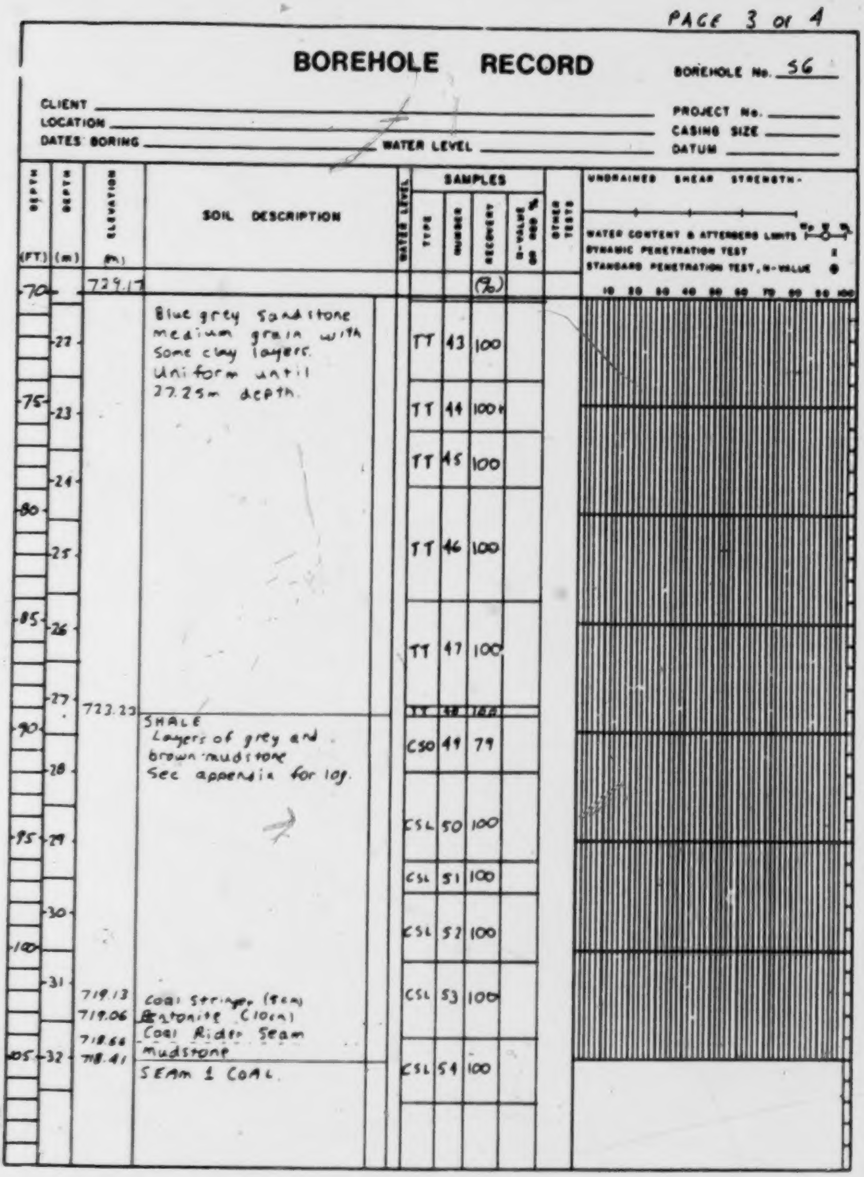

PAGE 3 OF 4

BOREHOLE RECORD

BOREHOLE No. S6

CLIENT
LOCATION
DATES: BORING
WATER LEVEL
PROJECT No.
CASING SIZE
DATUM

DEPTH (FT)	DEPTH (m)	ELEVATION (m)	SOIL DESCRIPTION	WATER LEVEL	SAMPLES TYPE	SAMPLES NUMBER	SAMPLES RECOVERY (%)	SAMPLES N-VALUE OR RQD %	OTHER TESTS	UNDRAINED SHEAR STRENGTH- / WATER CONTENT & ATTERBERG LIMITS / DYNAMIC PENETRATION TEST / STANDARD PENETRATION TEST, N-VALUE ● / 10 20 30 40 50 60 70 80 90 100
70		729.17								
	22		Blue grey sandstone medium grain with some clay layers. Uniform until 27.25m depth.		TT	43	100			
75	23				TT	44	100			
	24				TT	45	100			
80	25				TT	46	100			
85	26				TT	47	100			
	27	723.23			TT	48	100			
90			SHALE Layers of grey and brown mudstone See appendix for log.		CSO	49	79			
	28				CSL	50	100			
95	29				CSL	51	100			
	30				CSL	52	100			
100	31	719.13	Coal Stringer (8cm)		CSL	53	100			
		719.06	Bentonite (10cm)							
		718.66	Coal Rider Seam							
105	32	718.41	mudstone							
			SEAM 1 COAL		CSL	54	100			

Figure A.6 (cont'd) Borehole Log for hole S6

PAGE 4 OF 4

BOREHOLE RECORD

BOREHOLE No. S6

CLIENT
LOCATION
DATES BORING
WATER LEVEL
PROJECT No.
CASING SIZE
DATUM

UNDRAINED SHEAR STRENGTH -
WATER CONTENT & ATTERBERG LIMITS W_p W W_L
DYNAMIC PENETRATION TEST x
STANDARD PENETRATION TEST, N-VALUE ●
10 20 30 40 50 60 70 80 90 100

DEPTH (FT.)	DEPTH (m)	ELEVATION	SOIL DESCRIPTION	WATER LEVEL	SAMPLES				OTHER TESTS
					TYPE	NUMBER	RECOVERY	N-VALUE OR RQD %	
105	32		Seam 1 coal						
	33				CSL	55	84		
110									
	34								
115	35				CSL	56	89		
		714.96	END OF HOLE						
	36								
120									
	37								
125	38								
	39								
130									
	40								
135	41								
	42								
140									
	43								

Figure A.6 (cont'd) Borehole Log for hole S6

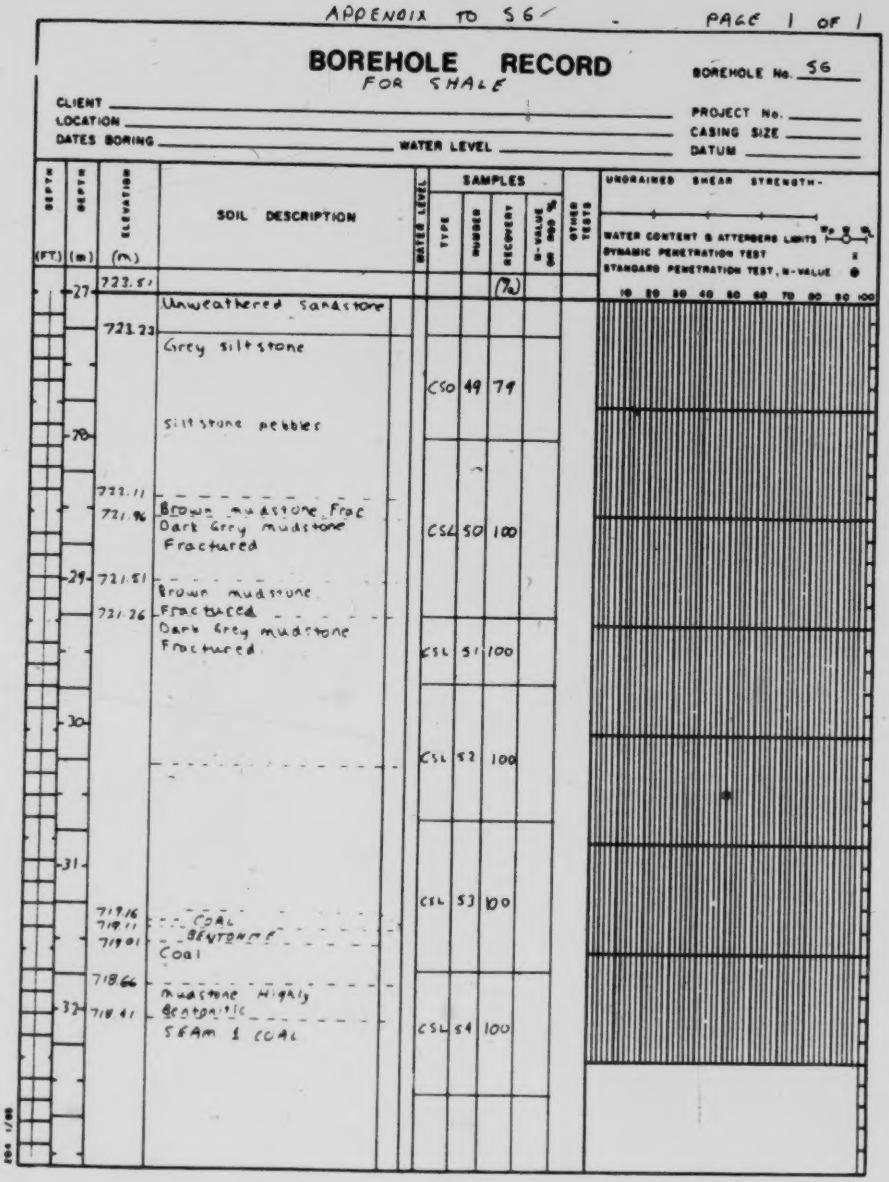

APPENDIX TO S6 - PAGE 1 OF 1

BOREHOLE RECORD
FOR SHALE

BOREHOLE No. S6

CLIENT
LOCATION
DATES BORING WATER LEVEL
PROJECT No.
CASING SIZE
DATUM

DEPTH (FT.)	DEPTH (m)	ELEVATION (m)	SOIL DESCRIPTION	WATER LEVEL	SAMPLES TYPE	SAMPLES NUMBER	SAMPLES RECOVERY	SAMPLES N-VALUE OR RQD %	OTHER TESTS
	27	723.51					(%)		
			Unweathered Sandstone						
		723.23	Grey siltstone		CSO	49	79		
			Siltstone pebbles						
	28								
		722.11	Brown mudstone Frac						
		721.96	Dark Grey mudstone Fractured		CSL	50	100		
	29	721.51	Brown mudstone Fractured						
		721.26	Dark Grey mudstone Fractured		CSL	51	100		
	30				CSL	52	100		
	31				CSL	53	100		
		719.16	COAL						
		719.11	BENTONITE						
		719.01	Coal						
		718.66	Mudstone Highly Bentonitic						
	32	718.41	SEAM 1 COAL		CSL	54	100		

UNDRAINED SHEAR STRENGTH-
WATER CONTENT & ATTERBERG LIMITS W_p W W_L
DYNAMIC PENETRATION TEST x
STANDARD PENETRATION TEST, N-VALUE ●

Figure A.6 (cont'd) Borehole Log for hole S6

APPENDIX B - DOWNHOLE GEOPHYSICAL LOGS

Figures B.1 to B.5 present the geophysical logs for holes S1, S2, and S6. The geophysical logs for S3 and S4 are shown in Figures 3.4 and 3.5. Hole S5 was not logged geophysically.

Hole locations are presented in Table A.1.

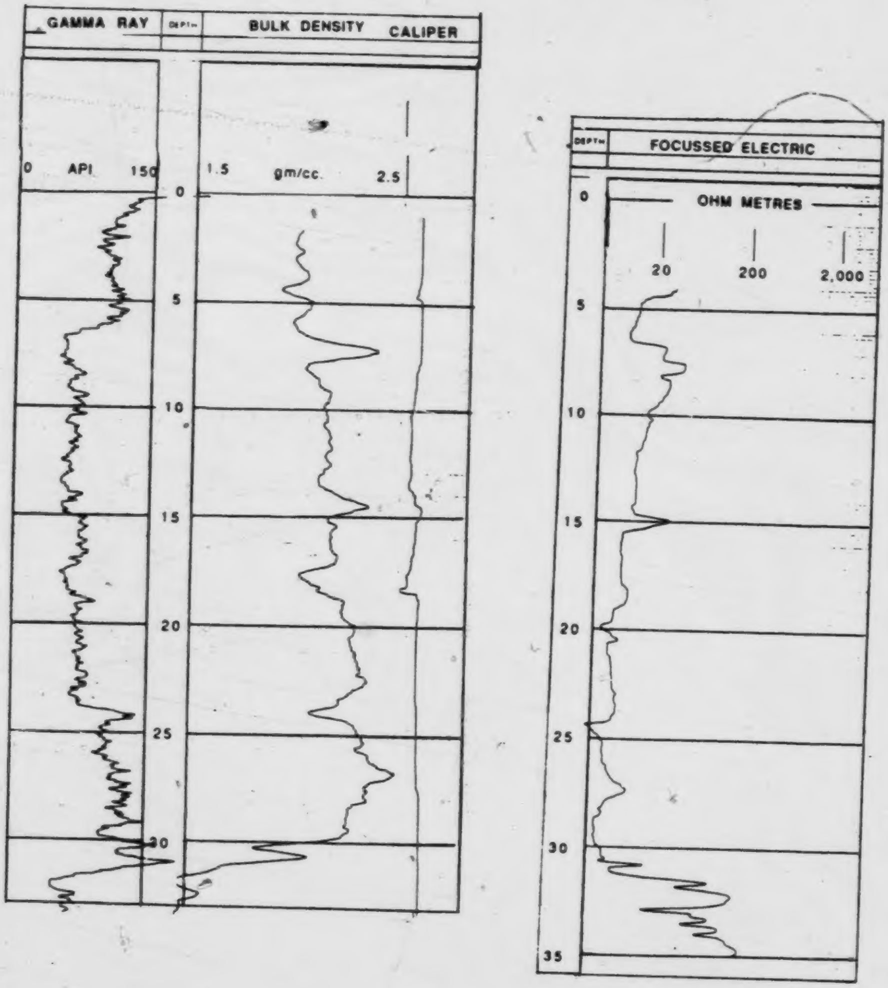

Figure B.1 Gamma, Density, Caliper, and Focussed Electric Resistivity Geophysical Logs for hole S1

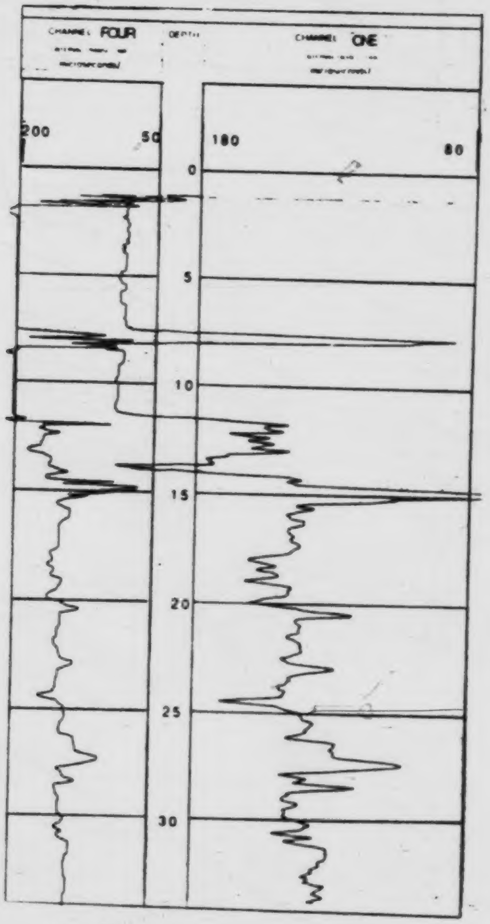

Figure B.1 (cont'd) Multichannel Sonic Geophysical Logs for hole S1

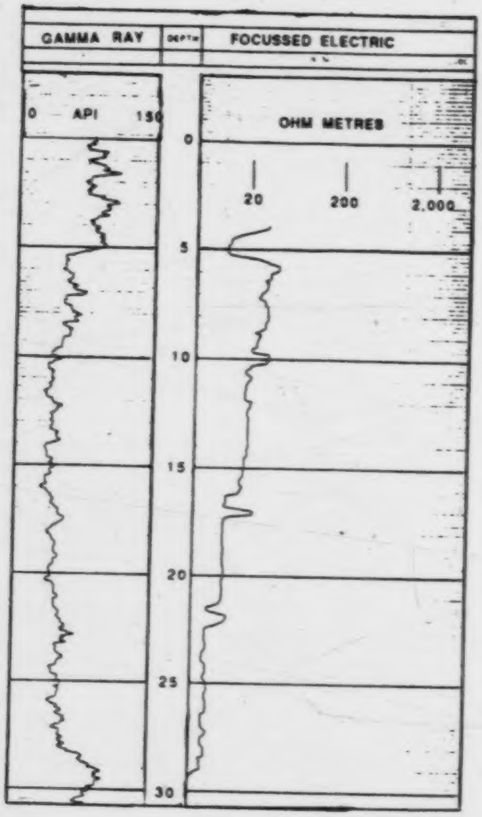

Figure B.2 Gamma and Focussed Electric Resistivity Geophysical Logs for hole S2

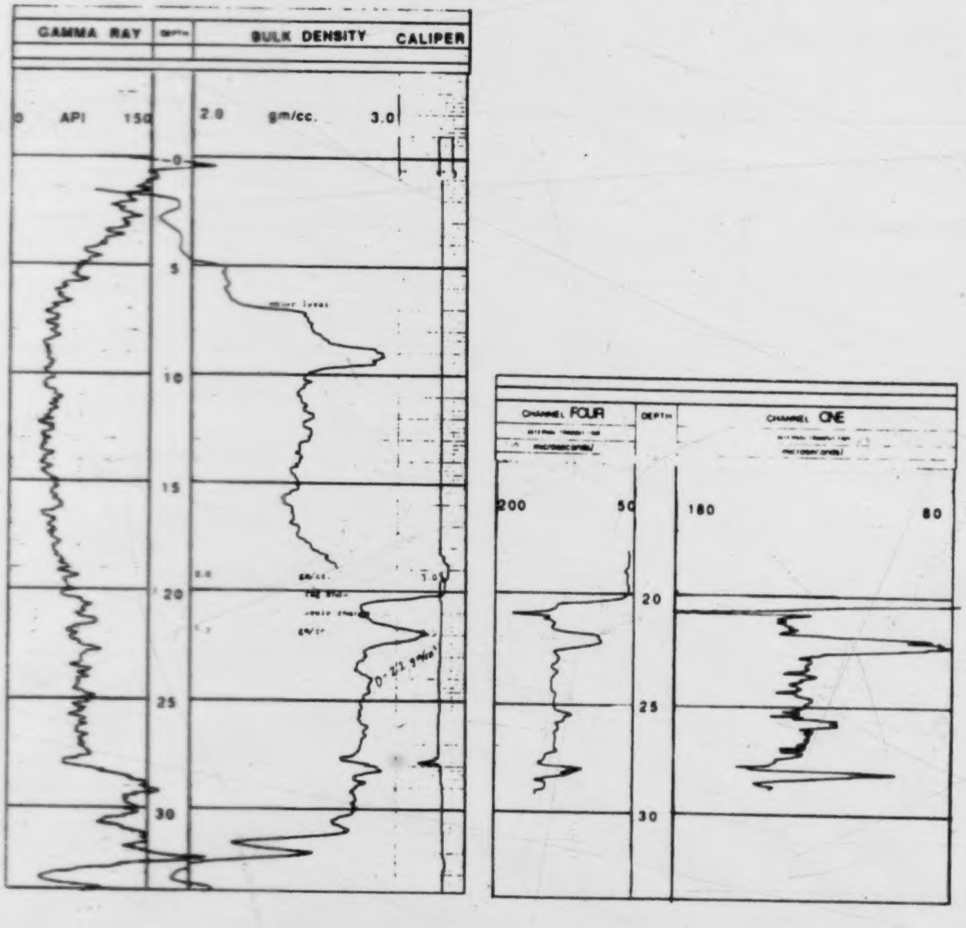

Figure B.6 Gamma, Density, Caliper, Neutron Porosity and Focussed Electric Resistivity Geophysical Logs for hole S6

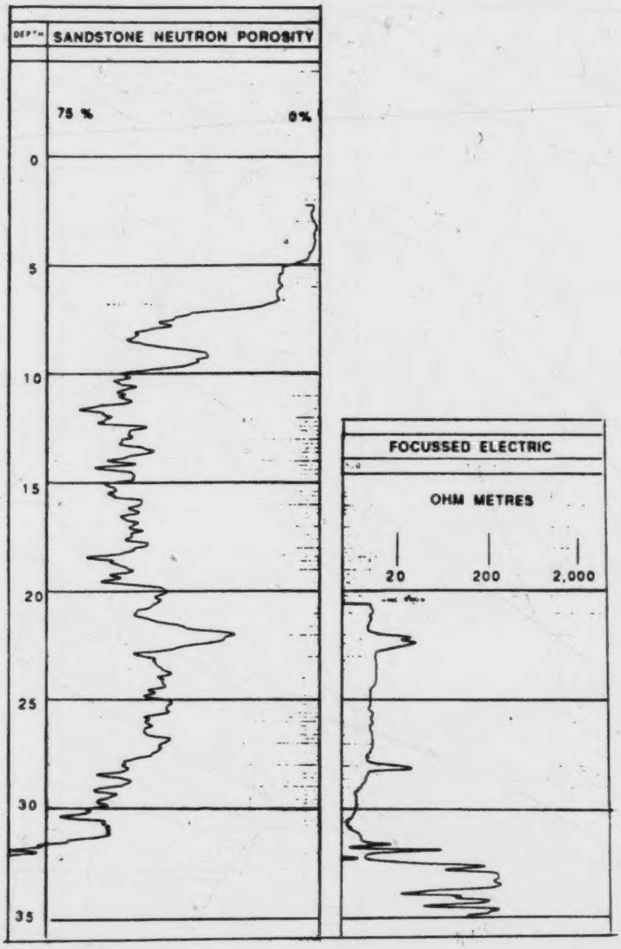

Figure B.6 (cont'd) Multichannel Sonic Geophysical Logs for hole S6

APPENDIX C - RESULTS OF DEFORMATION MONITORING

Six inclinometers, S1 to S6, were installed on 50 metres centres to measure subsurface movements. Their locations are shown in Table A.1. Surveys were conducted from two control points, BM1 and BM2, to the inclinometers to track their total movement. Table C.1 below describes the locations of the control points. Tables C.2 and C.3 at the end of the Appendix provide details on the locations of the highwall and important dates related to the deformation monitoring program.

Table C.1
Location of Control Points

Control Point	NORTHING (metres)	EASTING (metres)
BM 1	926.5	-3786.6
BM 2	934.8	-4107.1

C.1 Inclinometers

Figures C.1 to C.12 present the Northward (into the pit) and Eastward (parallel to the crest) movements measured at the six inclinometers. These movements were relative to the base of the inclinometers and do not take into account basal displacements.

Distinct shear planes were observed in the bentonite and along the sandstone/mudstone contact.

Inclinometer S2 showed an odd deformation pattern. Because movements into the highwall were unreasonable, this pattern was attributed to the casing buckling within the borehole. Although the hole was grouted, the grout may have been washed away by groundwater before it had a chance to harden.

C.2 Surveys

Figures C.13 and C.14 illustrate the contribution made by the surveys. In these figures, the movement of the top of inclinometer S6 was tracked by the inclinometer itself and the surveys. In Figure C.13, the lower plot shows the northward movements of the top referenced to the inclinometer base while the upper one shows the absolute movement of the top referenced to the Transalta Utilities survey network. The difference between these two plots is attributed to movements of the inclinometer base. Figure C.13 indicates that the base moved a significant distance into the pit.

Figures C.14 shows that the basal movements had a minor component parallel to the highwall.

This exercise demonstrates how the surveys and inclinometers were combined to obtain the deformation patterns in the overburden.

C.3 Combined Inclinometer and Survey Results

Figures C.15 to C.26 show the Northward and Eastward global movements of the base of inclinometers S1 to S6 as obtained by the previous exercise. The Eastward component of the basal movements was found to be minor, and was therefore neglected in further discussion.

Upon reviewing Figures C.15 to C.26, it was expected that substantial movements had developed in the overburden before the inclinometers and survey control points were installed. To account for this, the magnitude of previous movement was estimated at each inclinometer location. This was established by making a key assumption: that the trends of movement tended to be similar at each location after each highwall was cut. Then, by trial and error, the initial movements were estimated and the trends compared to the other inclinometers. The estimated magnitudes were found to be reasonable.

Figures C.27 to C.32 show the revised movement over time plots that include the estimates of initial movements.

TABLE C.2
EAST END OF PIT 03, HIGHVALE MINE
HIGHWALL POSITION FROM JUNE 1987 TO MAY 1988

CUT	CREST OF HIGHWALL		TOE OF HIGHWALL	
NUMBER	ELEV. (metres)	NORTHING (metres)	ELEV. (metres)	NORTHING (metres)
18	742	1228	721	1247
19	741.5	1182	720	1202
20	743	1131	719	1155
21	745	1090	719	1116
22	745 +/-	1040 +/-	719 +/-	1076 +/-
23	745 +/-	990 +/-	719 +/-	1030 +/-

EASTINGS ARE IRRELEVANT SINCE HIGHWALL WAS ORIENTED EAST-WEST FOR EACH CUT.

DATA FOR CUTS 21 AND 22 CAN BE OBTAINED FROM MANALTA COAL AT THE HIGHVALE MINE.

TABLE C.3

IMPORTANT DATES RELATED TO DEFORMATION MONITORING

DATE	DAY NUMBER	COMMENT
June 23, 1987	0	Install S1 and S2.
June 25, 1987	2	Install S3, S4, S5, and S6.
June 26, 1987	3	Cut 17 passed in front of site.
Sept. 22, 1987	91	Cut 18 passed in front of S2.
Sept. 24, 1987	93	Cut 18 passed in front of S1.
Sept. 28, 1987 bench	97	S1 and S2 lowered to new level. S1 and S2 now 50 metres from highwall crest.
Nov. 30, 1987	160	Blast bench in front of S1 and S2.
Dec. 8, 1987	168	Cut 19 passed in front of S2.
Dec. 9, 1987	169	Cut 19 passed in front of S1. S1 and S2 now at highwall crest.
Dec. 11, 1987	171	S3 and S4 lowered to new bench level. S3 and S4 now 50 metres from highwall crest.
March 1 to 3, 1988	251	Blast bench in front of S3 and S4. Destroy S1 and S2.

TABLE C.3(cont'd)

DATE	DAY NUMBER	COMMENT
March 8 to 11, 1988	258	Cut 20 passed in front of S3 and S4. S3 and S4 now 10 metres from highwall crest. S5 and S6 were not yet lowered to the new bench. They are now 60 m from the highwall crest.
April 27, 1988	308	Blast bench east of S4.
April 29, 1988	310	Blast bench east of S3 and west of S4. Destroy S4.
May 2, 1988	312	Blast bench west of S3. Destroy S3.
May 13, 1988	323	Cut 21 passed in front of S5 and S6. S5 and S6 were lowered to the new bench, but S6 was accidentally destroyed. S5 now 10 m from highwall crest.
August 29, 1988	431	Take last readings of S5.
Sept., 1988		Blasting destroyed S5 and S6.
Fall, 1988		S5 and S6 removed by dragline as it made cut 22.

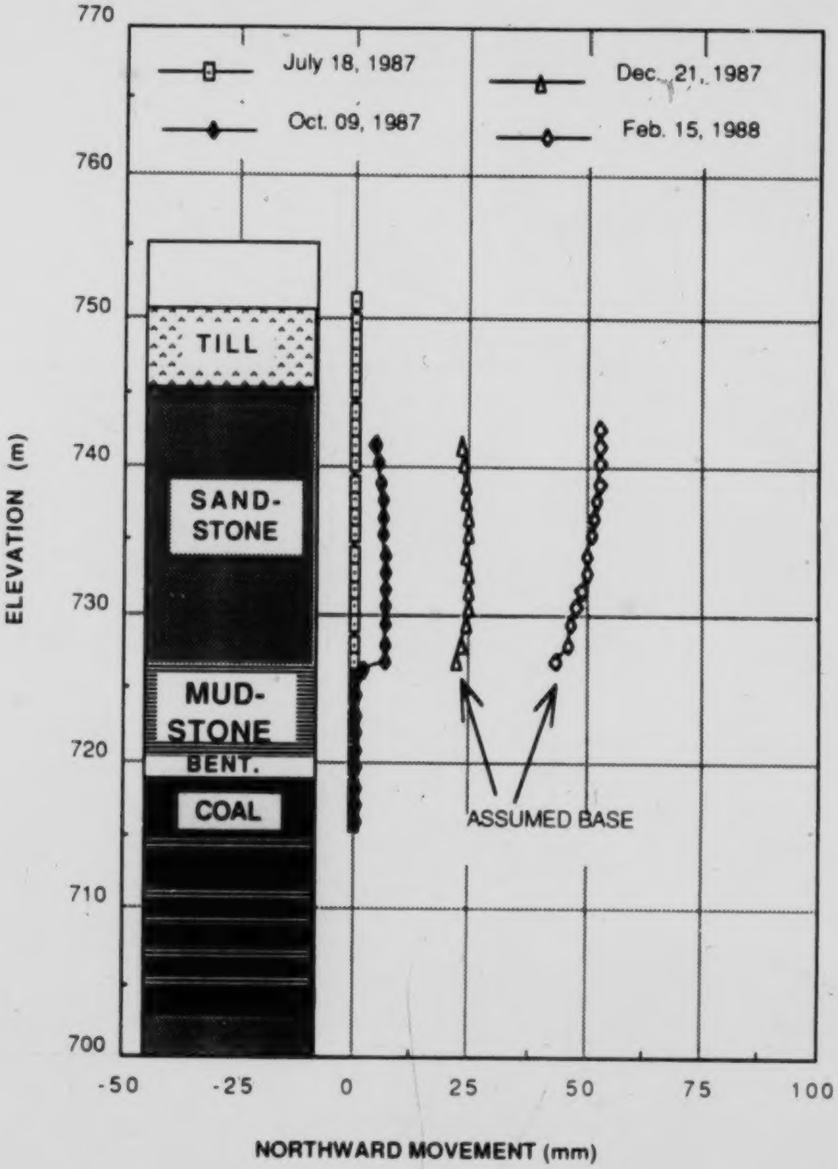

Figure C.1 Northward movement of inclinometer S1 relative to its base

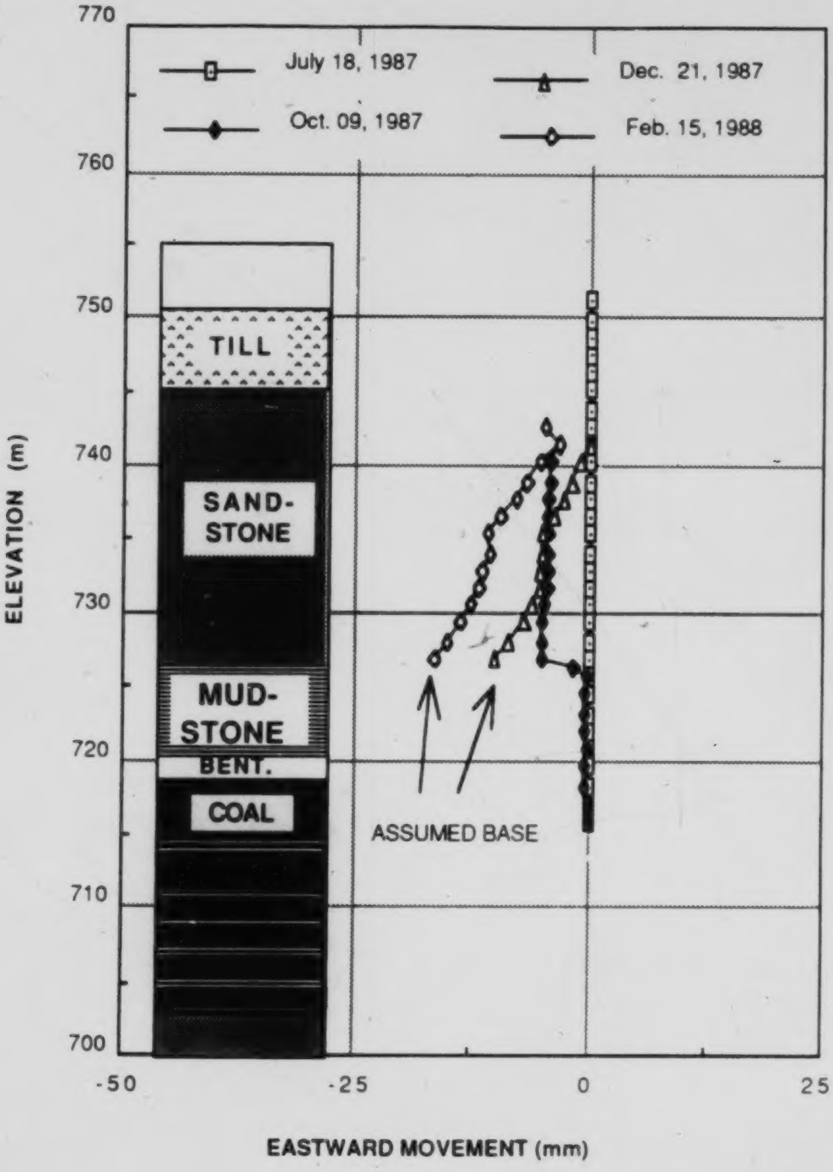

Figure C.2 Eastward movement of inclinometer S1 relative to its base

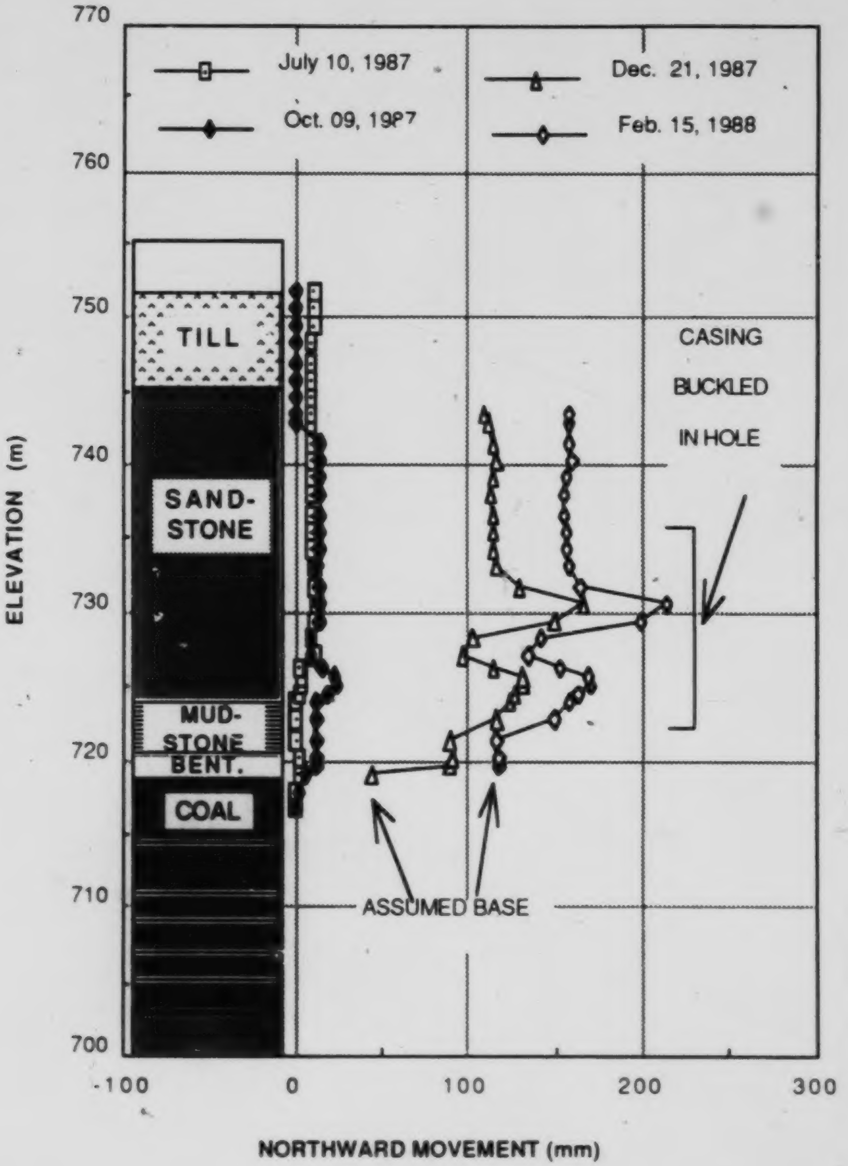

Figure C.3 Northward movement of inclinometer S2 relative to its base

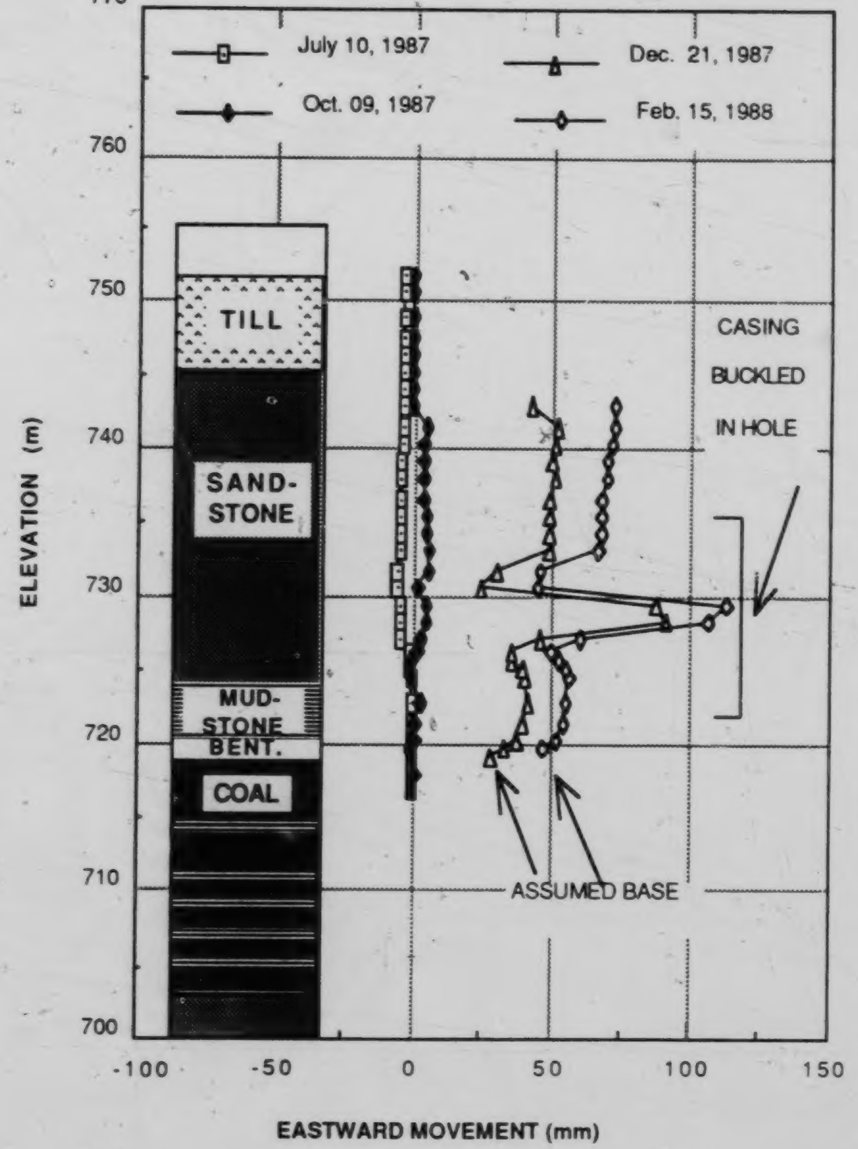

Figure C.4 Eastward movement of inclinometer S2 relative to its base

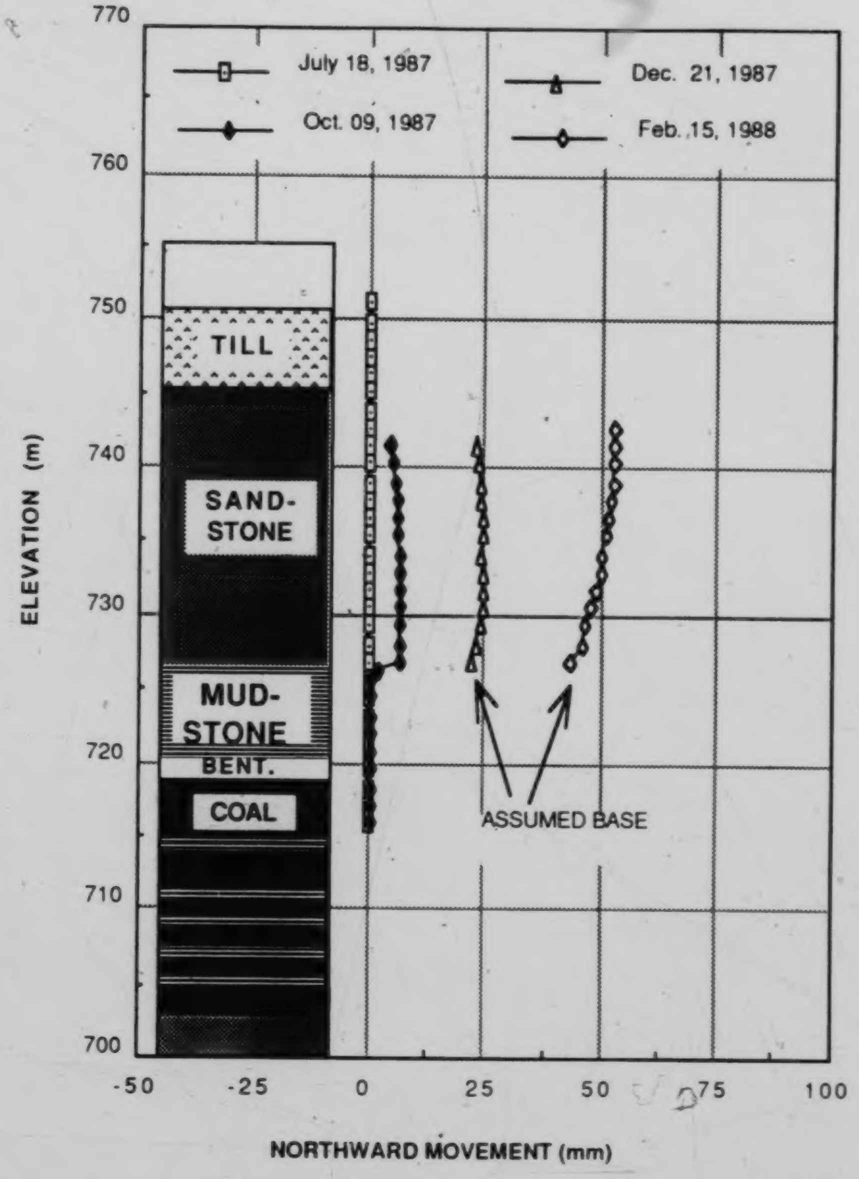

Figure C.5 Northward movement of inclinometer S3 relative to its base

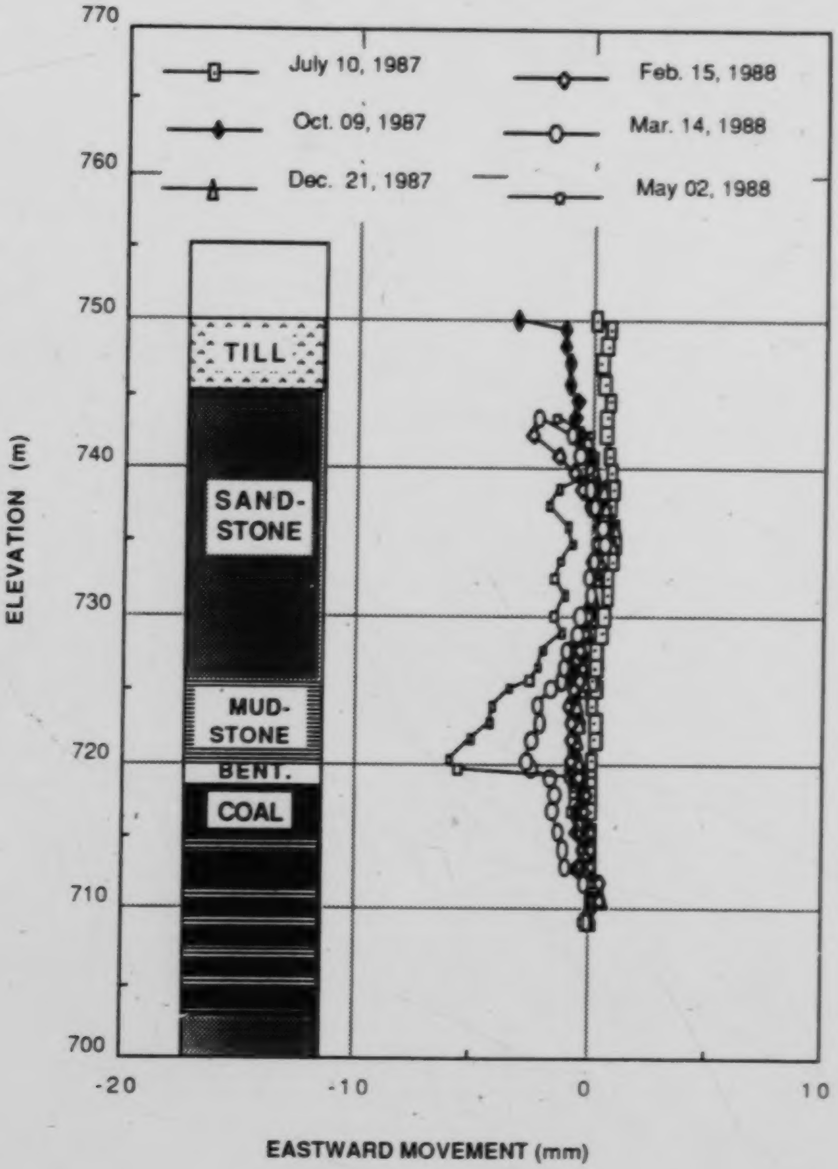

Figure C.6 Eastward movement of inclinometer S3 relative to its base

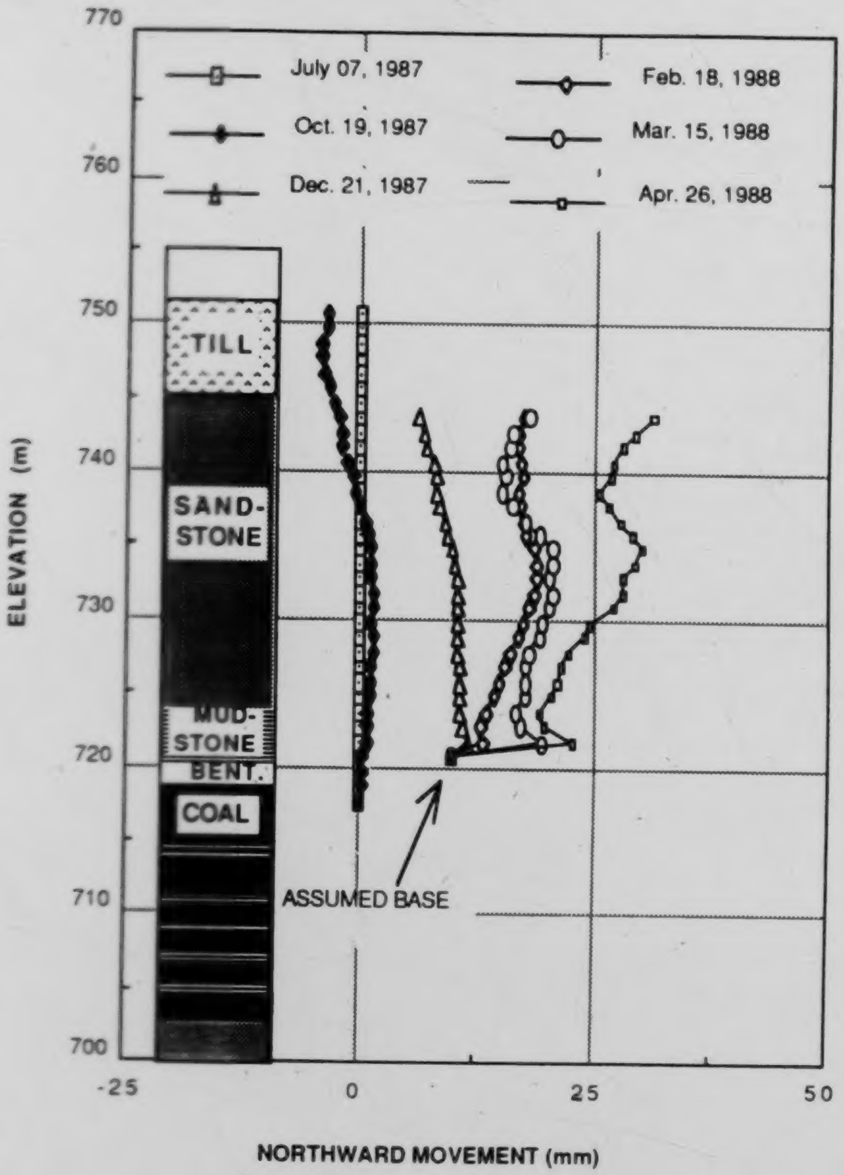

Figure C.7 Northward movement of inclinometer S4 relative to its base

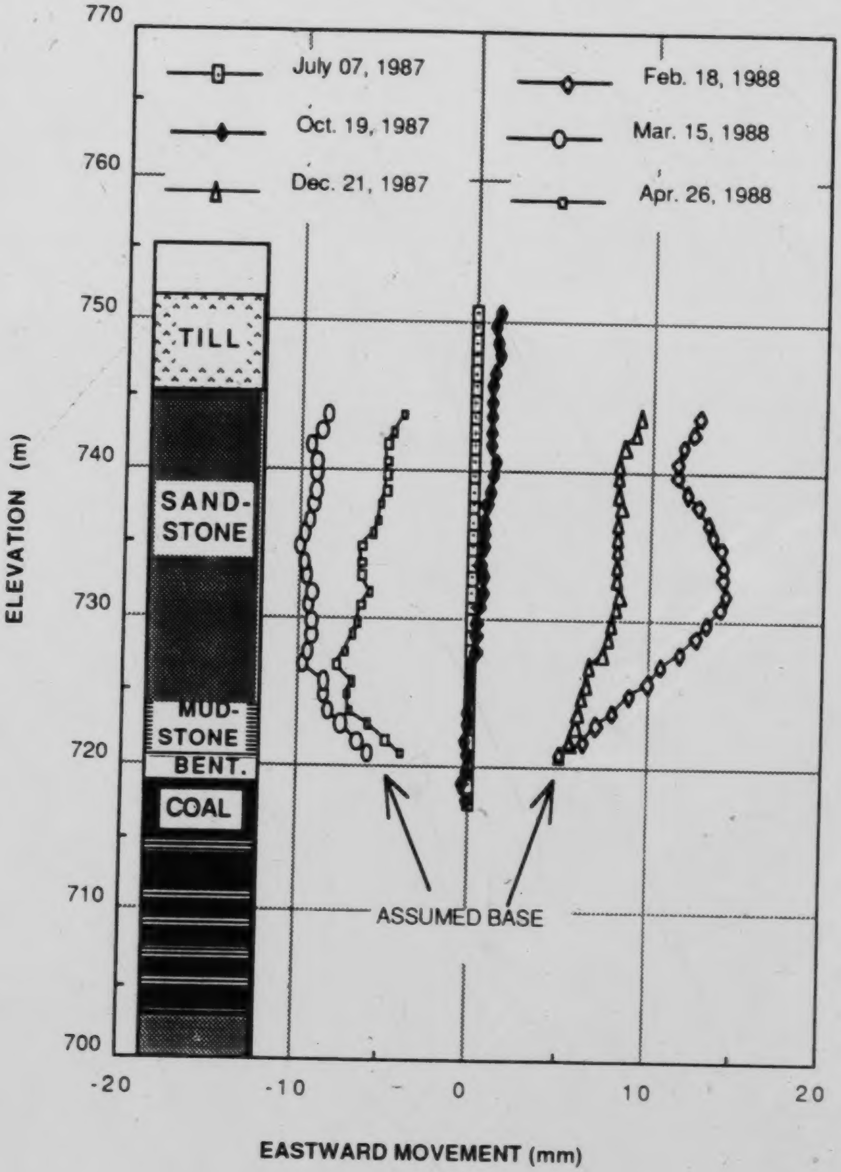

Figure C.8 Eastward movement of inclinometer S4 relative to its base

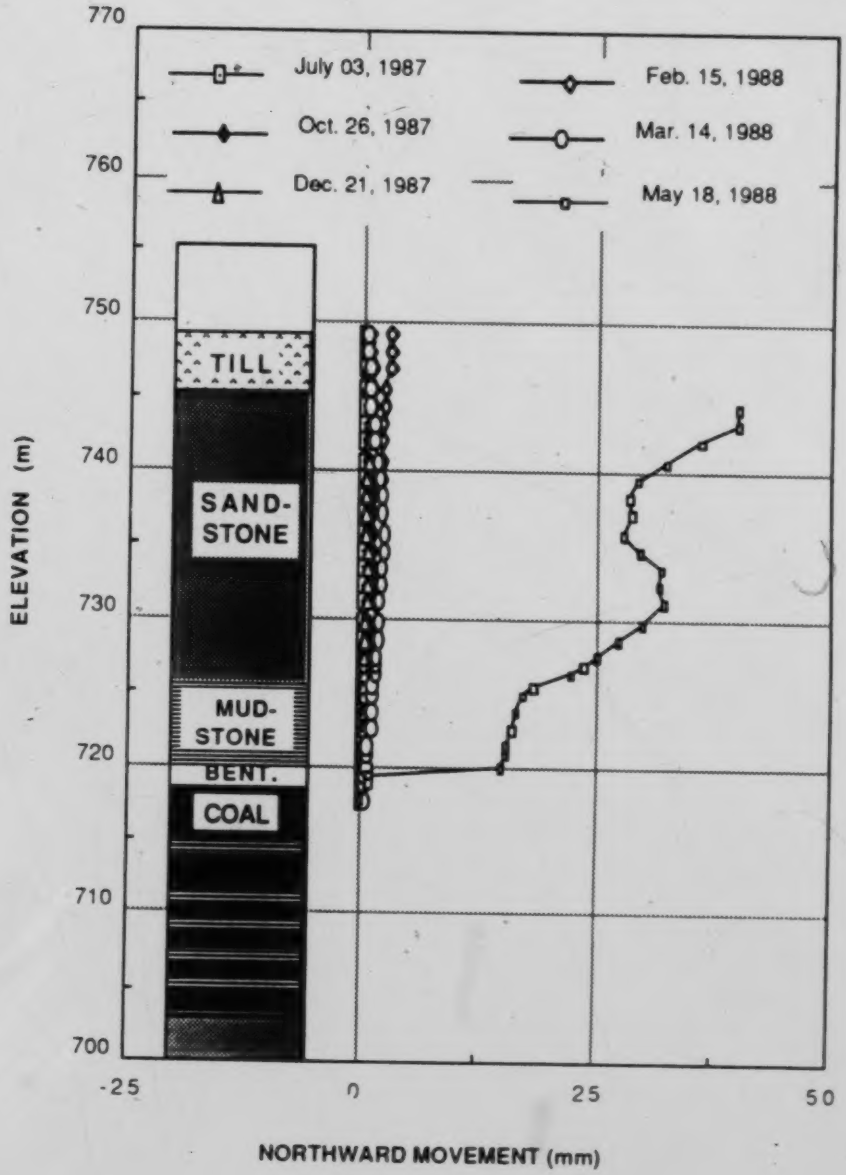

Figure C.9 Northward movement of inclinometer S5 relative to its base

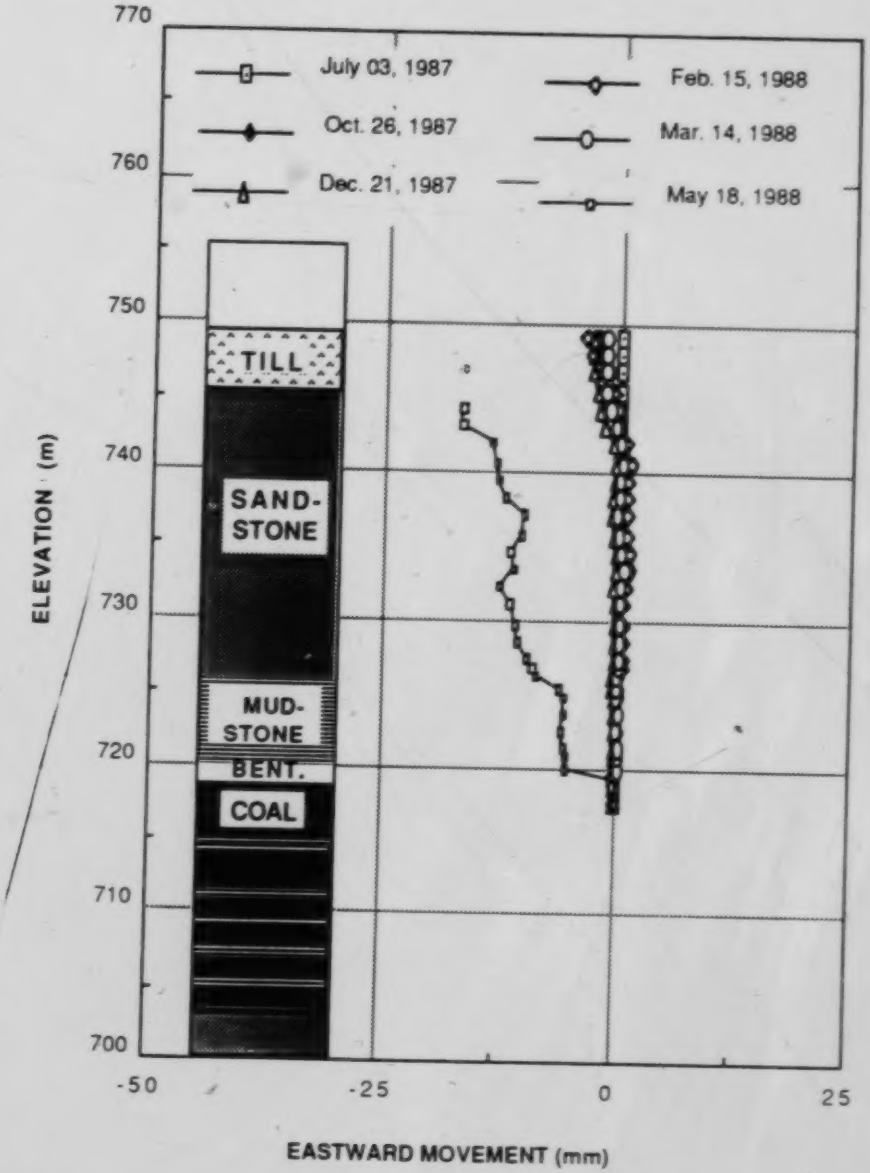

Figure C.10 Eastward movement of inclinometer S5 relative to its base

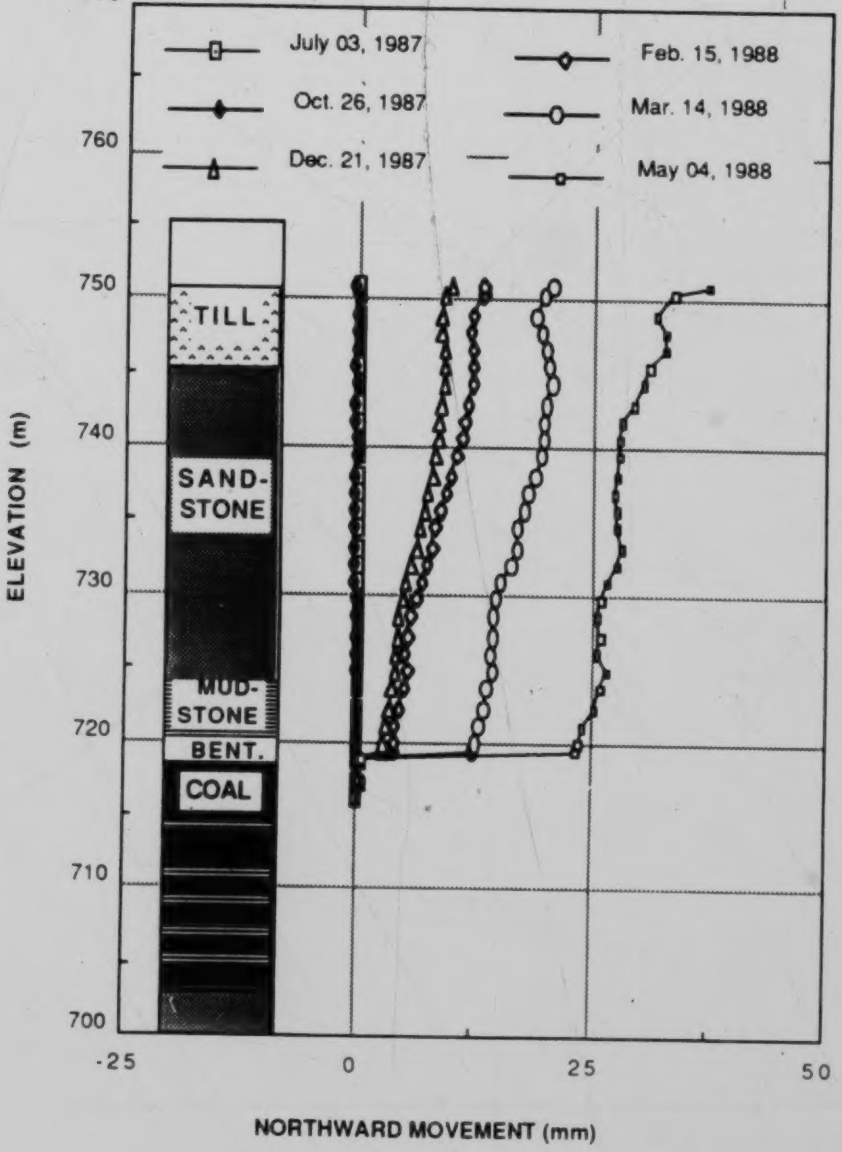

Figure C.11 Northward movement of inclinometer S6 relative to its base

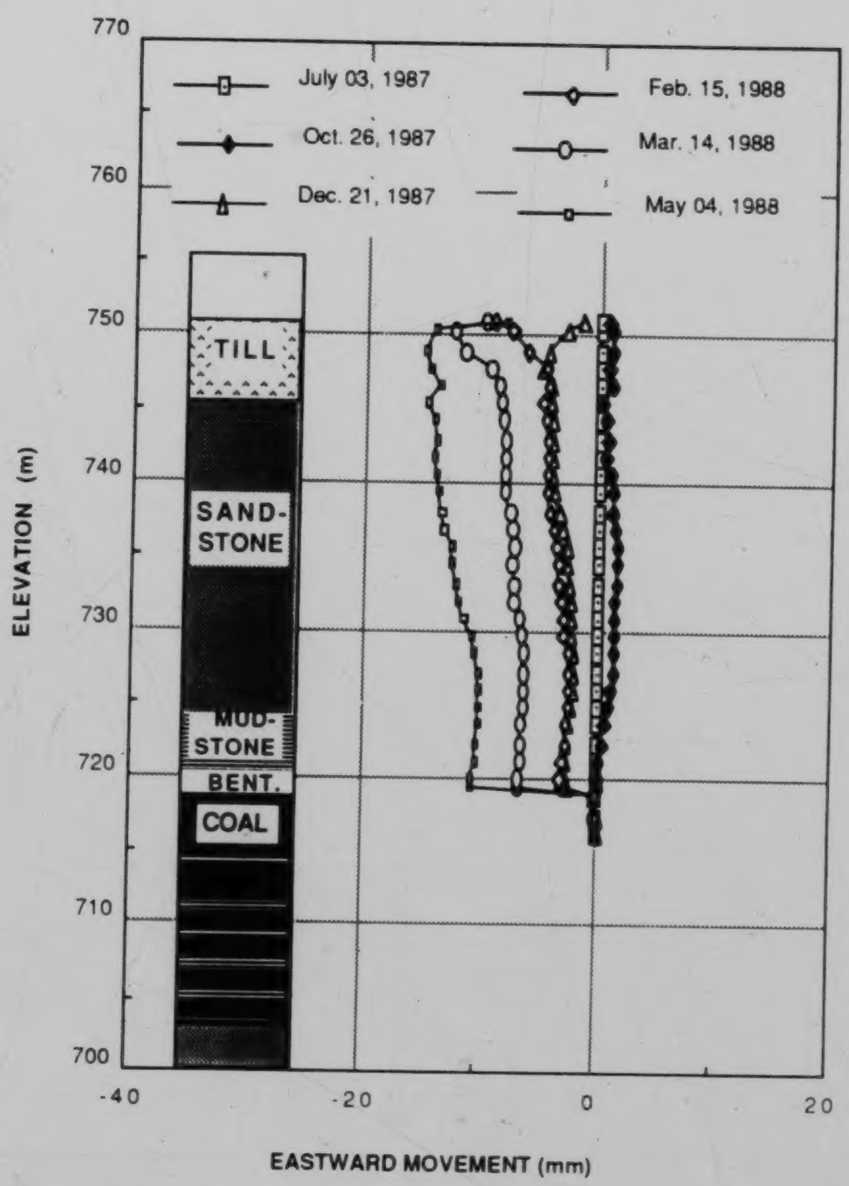

Figure C.12 Eastward movement of inclinometer S6 relative to its base

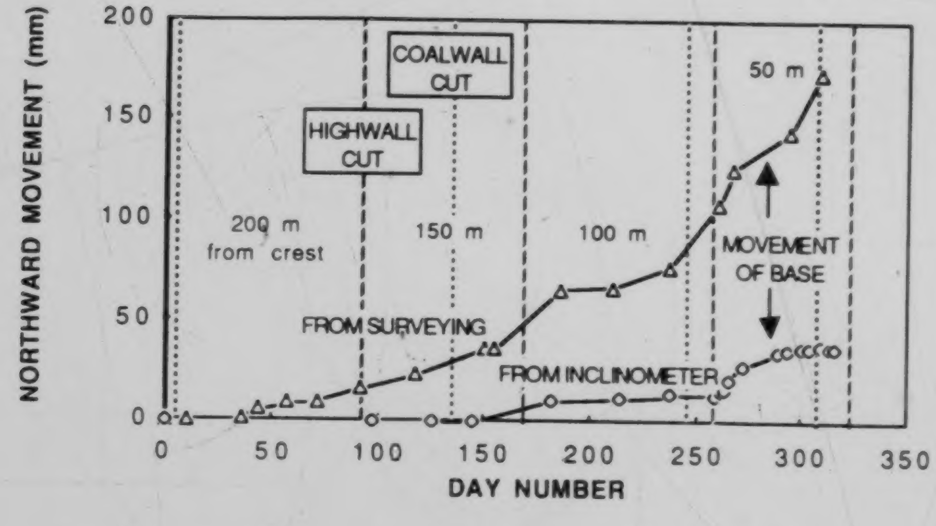

Figure C.13 Northward movement over time of the top of inclinometer S6

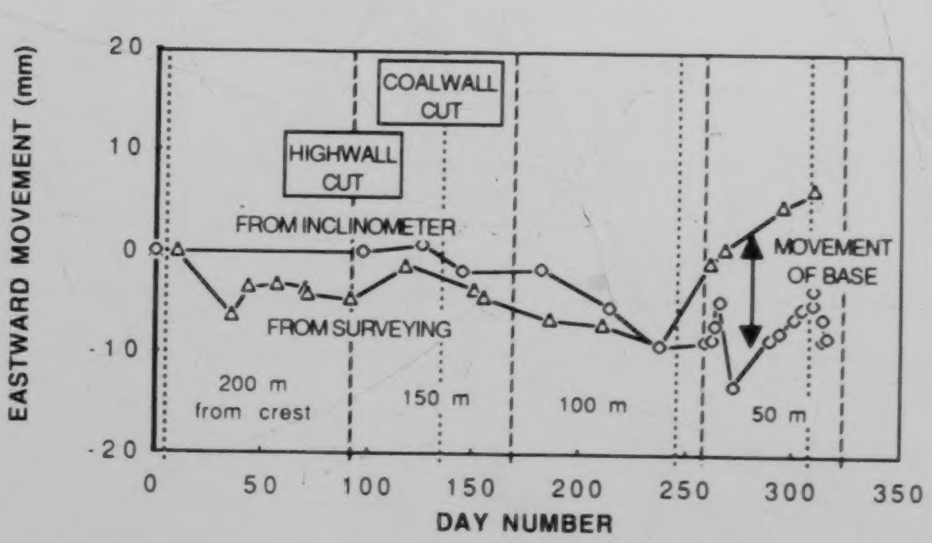

Figure C.14 Eastward movement over time of the top of inclinometer S6

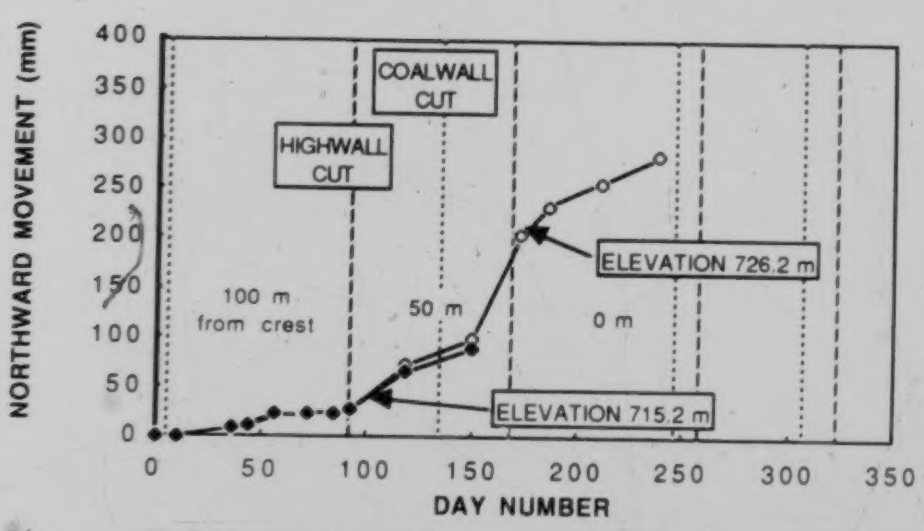

Figure C.15 Northward movement over time of base of inclinometer S1

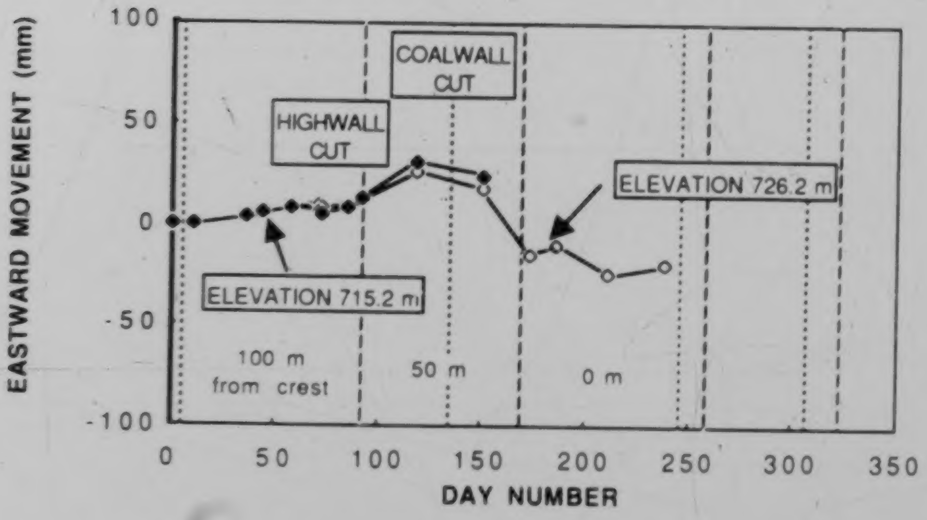

Figure C.16 Eastward movement over time of base of inclinometer S1

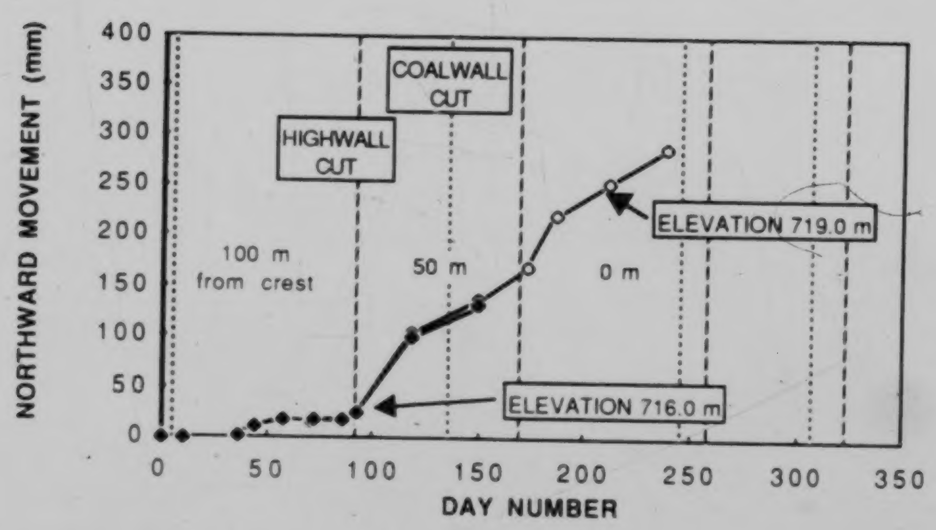

Figure C.17 Northward movement over time of base of inclinometer S2

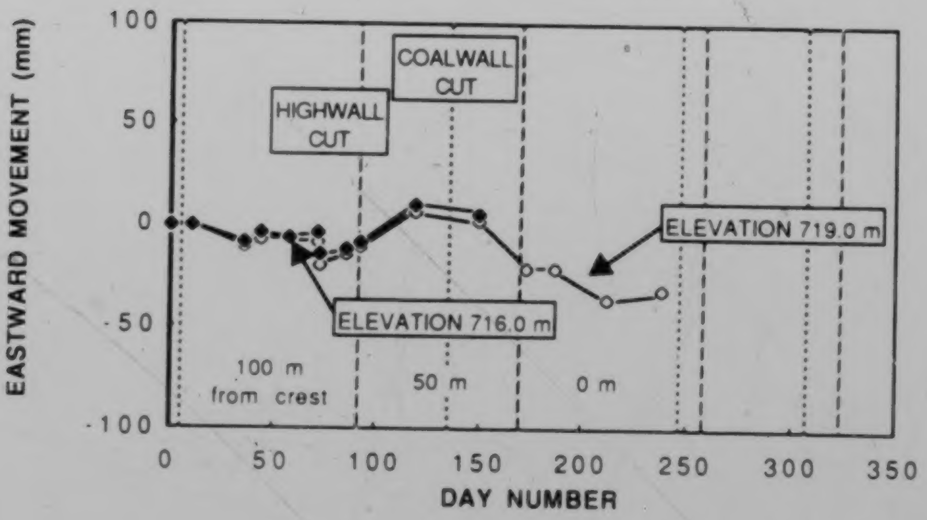

Figure C.18 Eastward movement over time of base of inclinometer S2

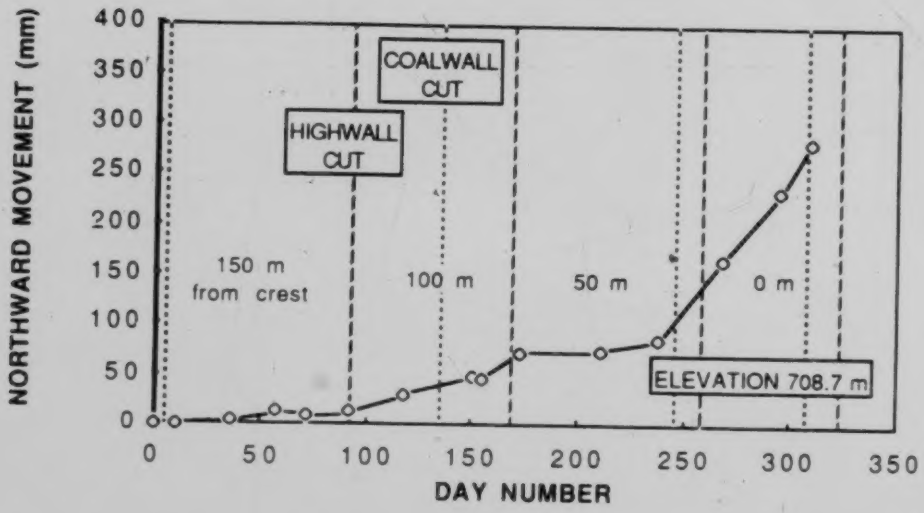

Figure C.19 Northward movement over time of base of inclinometer S3

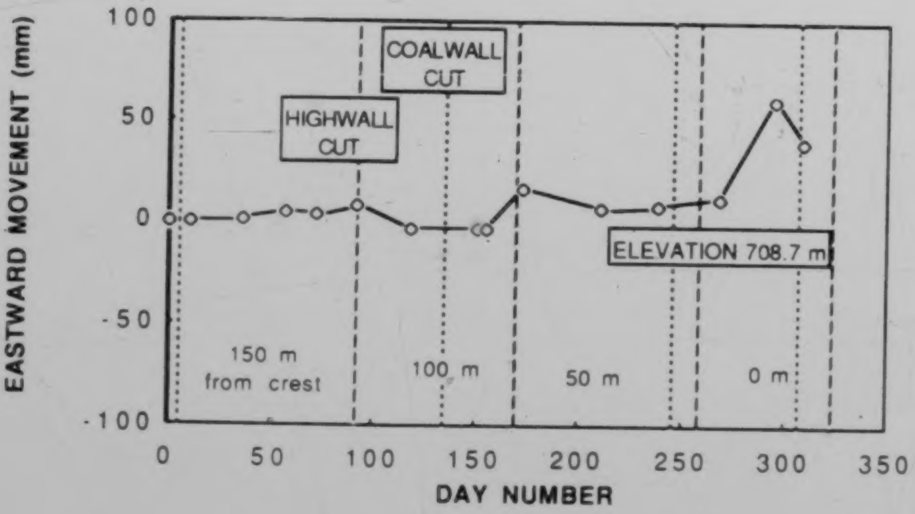

Figure C.20 Eastward movement over time of base of inclinometer S3

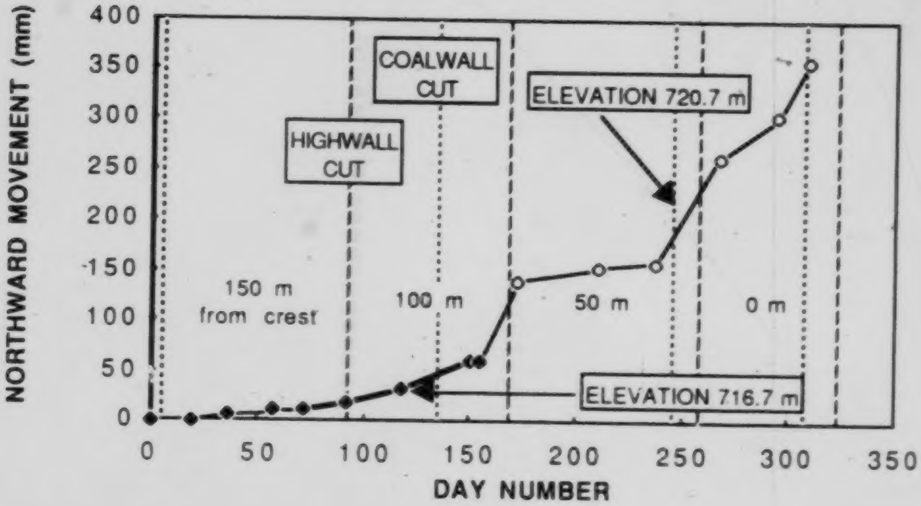

Figure C.21 Northward movement over time of base of inclinometer S4

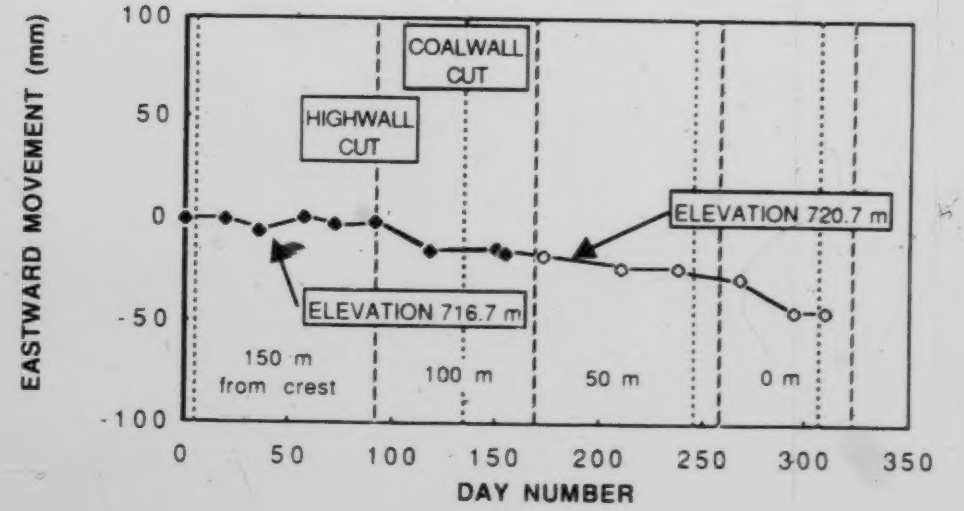

Figure C.22 Eastward movement over time of base of inclinometer S4

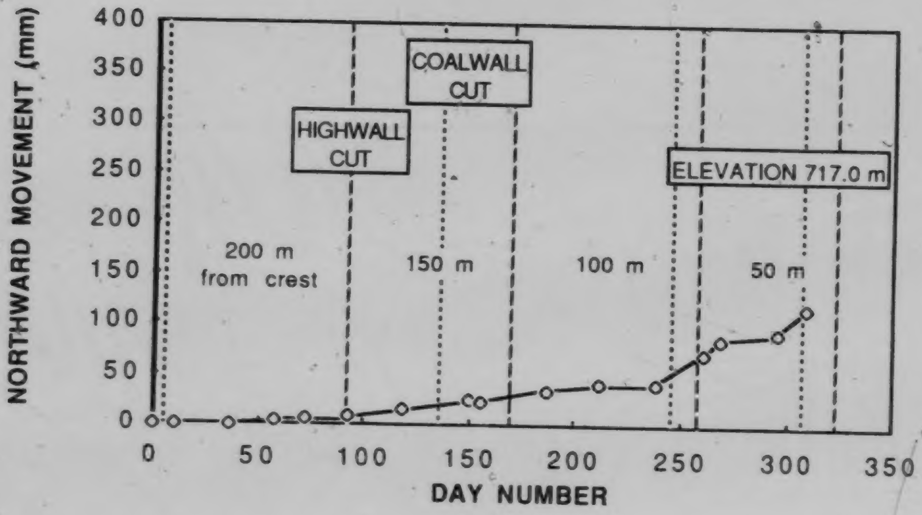

Figure C.23 Northward movement over time of base of inclinometer S5

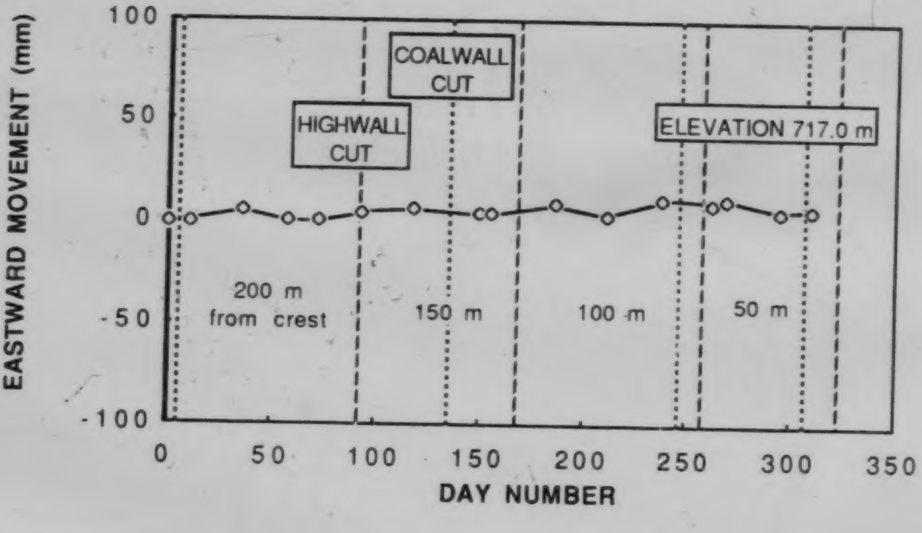

Figure C.24 Eastward movement over time of base of inclinometer S5

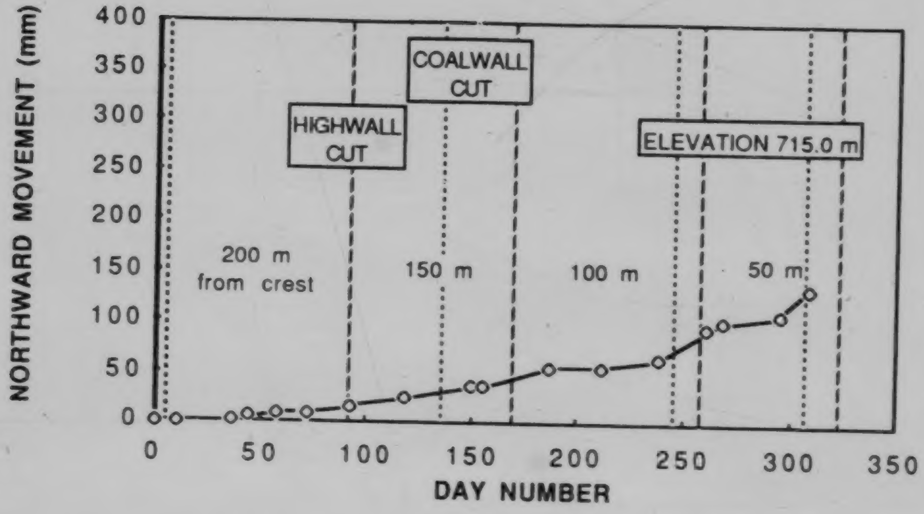

Figure C.25 Northward movement over time of base of inclinometer S6

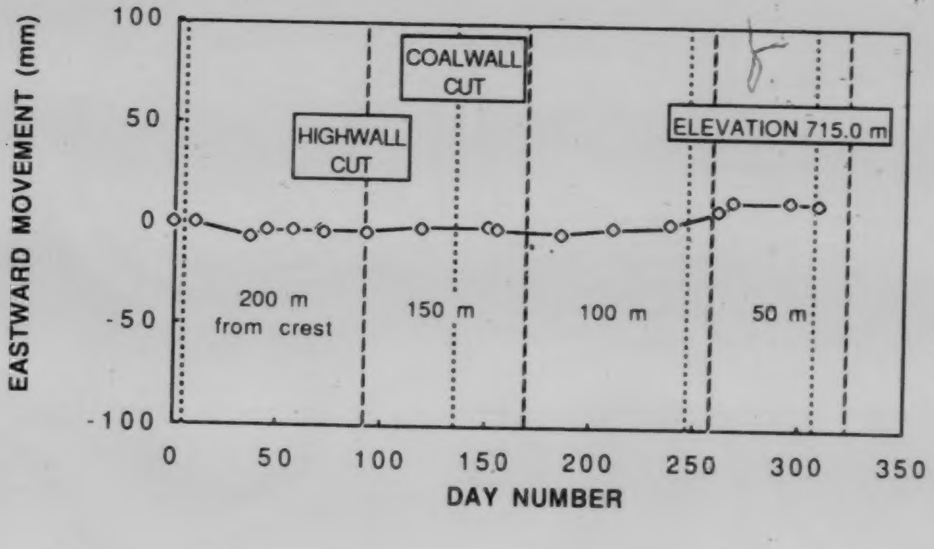

Figure C.26 Eastward movement over time of base of inclinometer S6

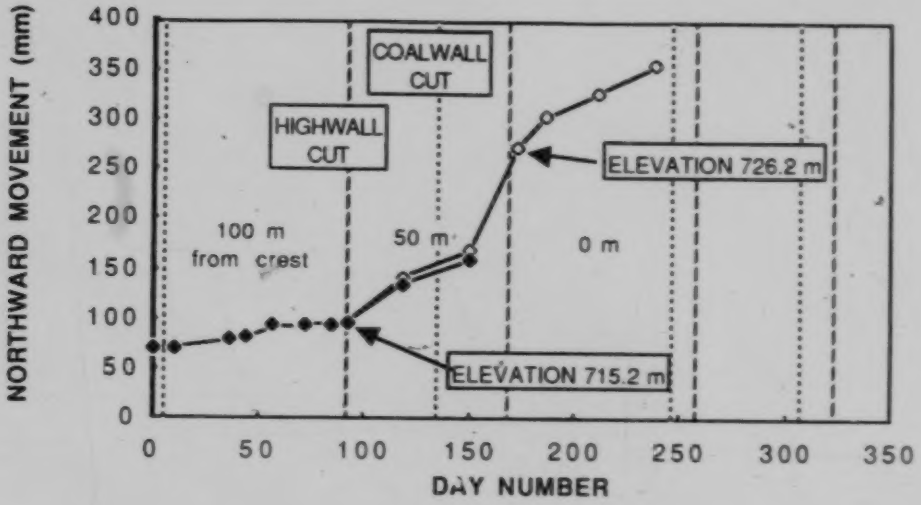

Figure C.27 Northward movement over time of base of inclinometer S1. Adjusted for movements that occurred prior to instrument installation

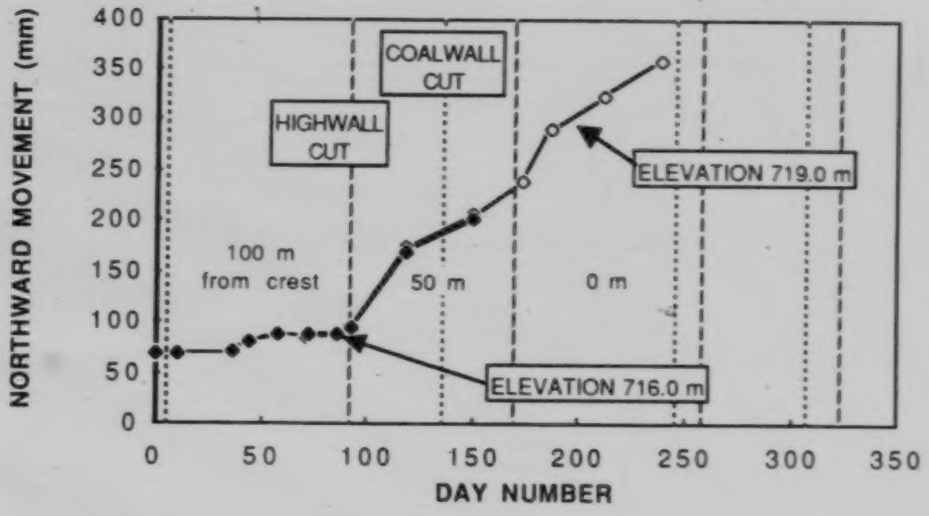

Figure C.28 Northward movement over time of base of inclinometer S2. Adjusted for movements that occurred prior to instrument installation

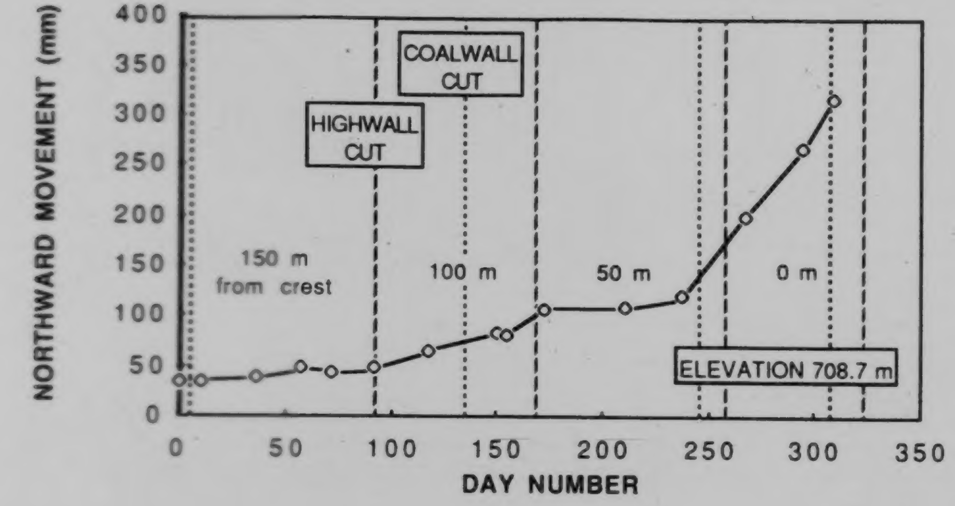

Figure C.29 Northward movement over time of base of inclinometer S3. Adjusted for movements that occurred prior to instrument installation

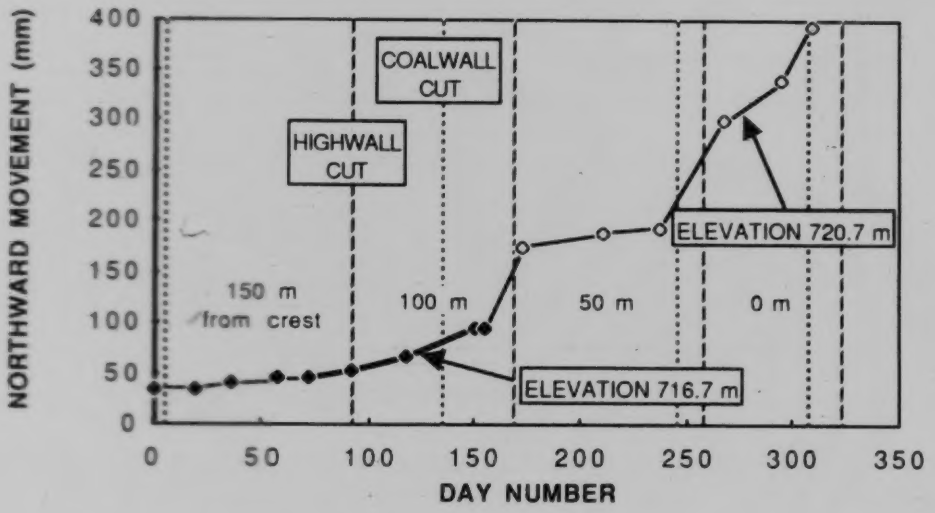

Figure C.30 Northward movement over time of base of inclinometer S4. Adjusted for movements that occurred prior to instrument installation

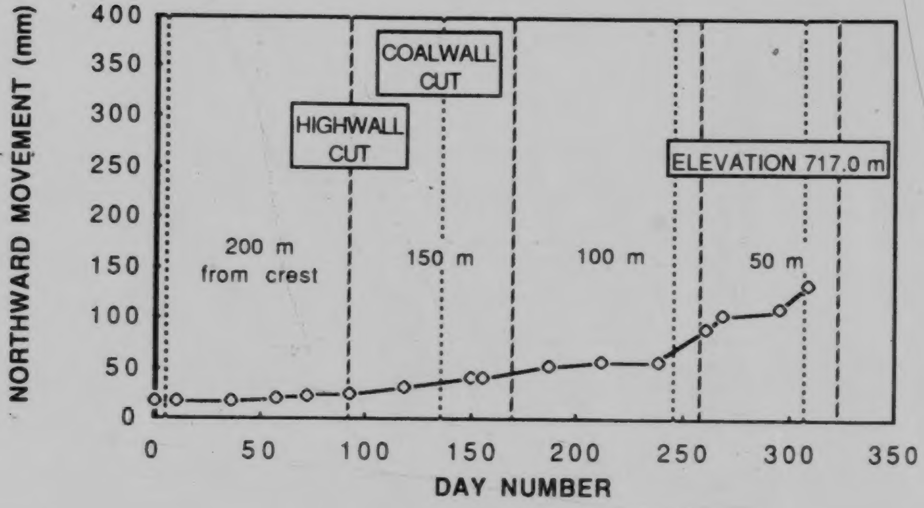

Figure C.31 Northward movement over time of base of inclinometer S5. Adjusted for movements that occurred prior to instrument installation

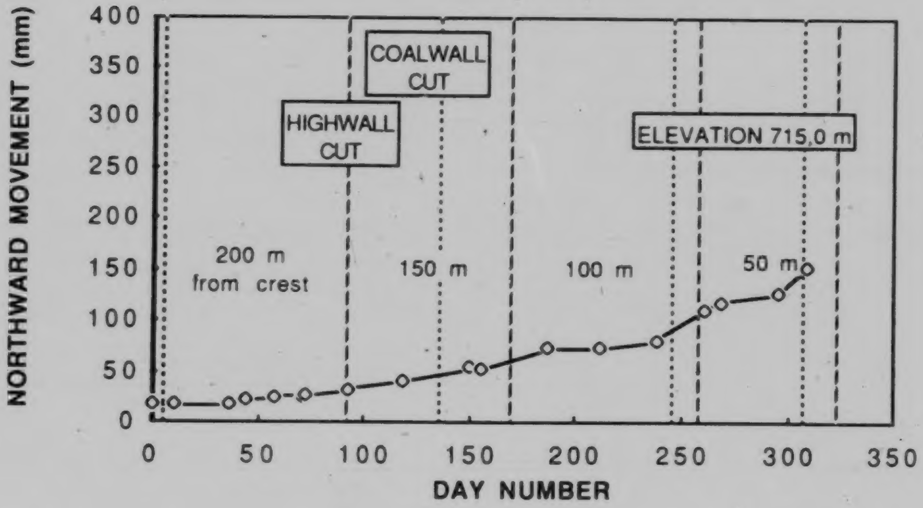

Figure C.32 Northward movement over time of base of inclinometer S6. Adjusted for movements that occurred prior to instrument installation

APPENDIX D - DISPLACEMENT FIELD

Section 4.2.2 describes how the deformation field was obtained. Figures D.1 to D.15 present the deformation field at elevation 730 metres for each day that a survey was made.

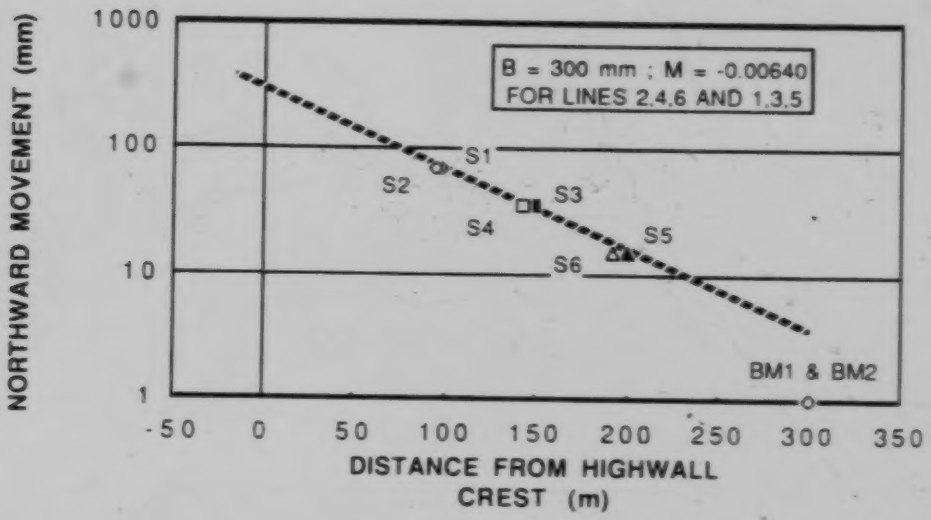

Figure D.1 Displacement field at elevation 730 metres on July 3, 1987 (Day 10)

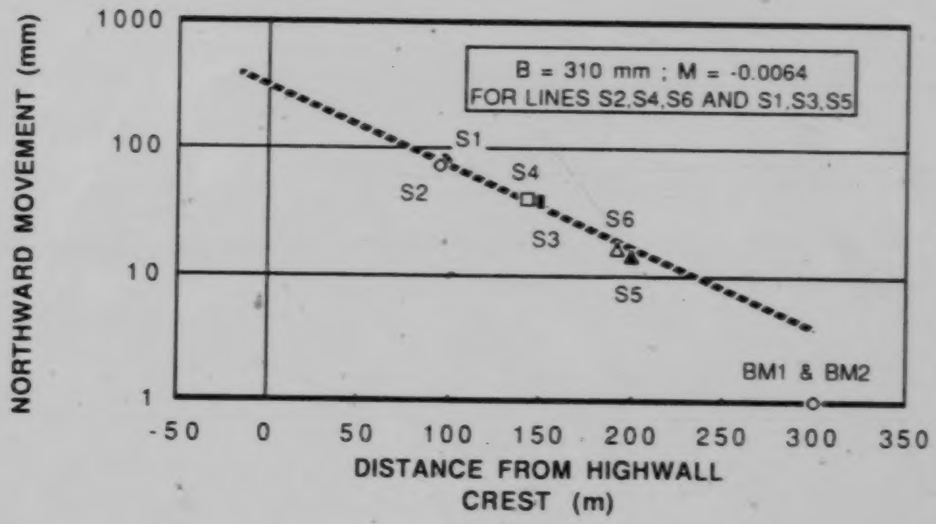

Figure D.2 Displacement field at elevation 730 metres on July 29, 1987 Day 36)

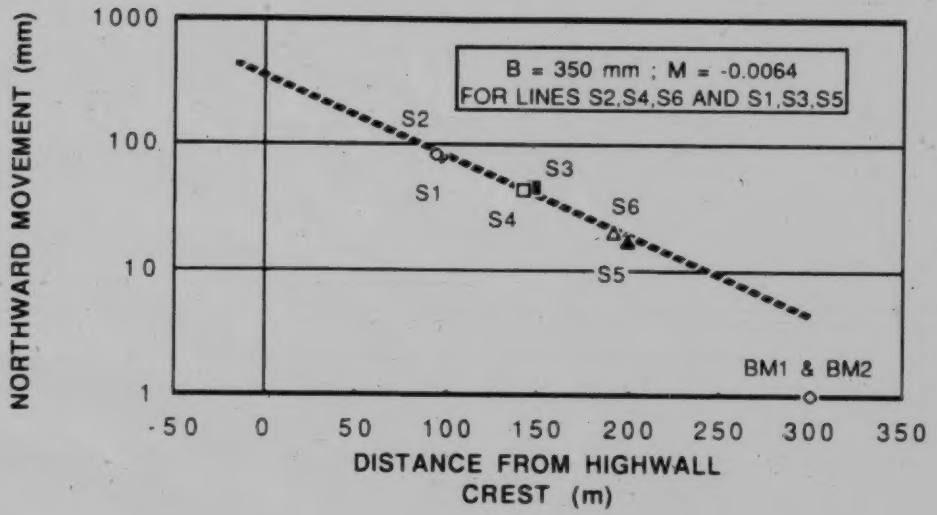

Figure D.3 Displacement field at elevation 730 metres on August 6, 1987 (Day 44)

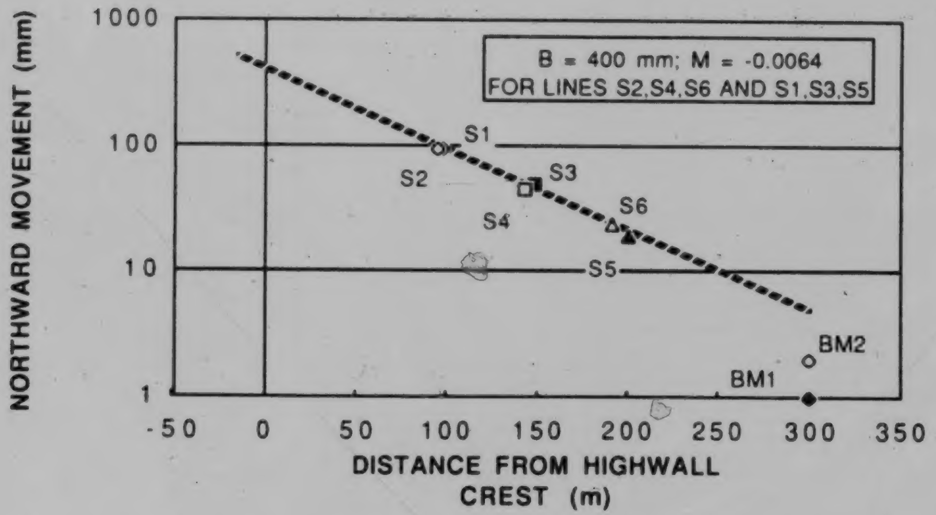

Figure D.4 Displacement field at elevation 730 metres on August 19, 1987 (Day 57)

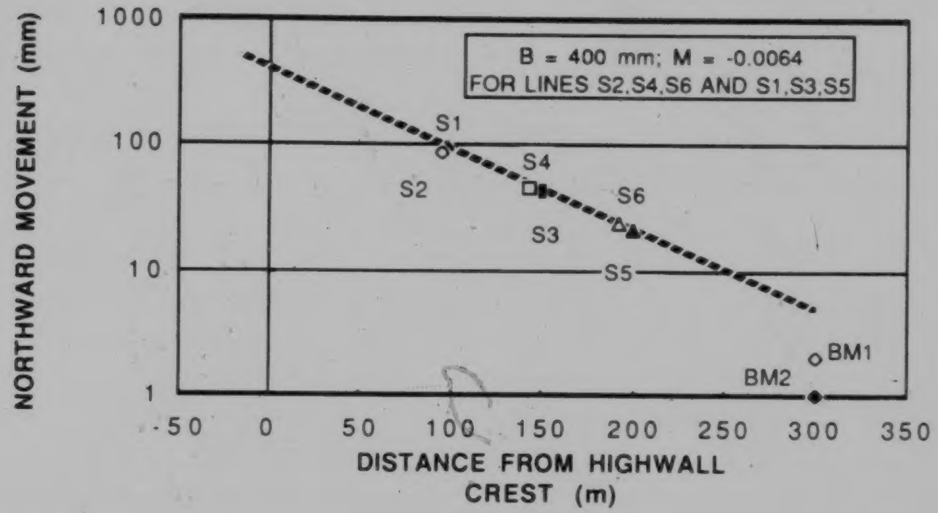

Figure D.5 Displacement field at elevation 730 metres on September 2, 1987 (Day 71)

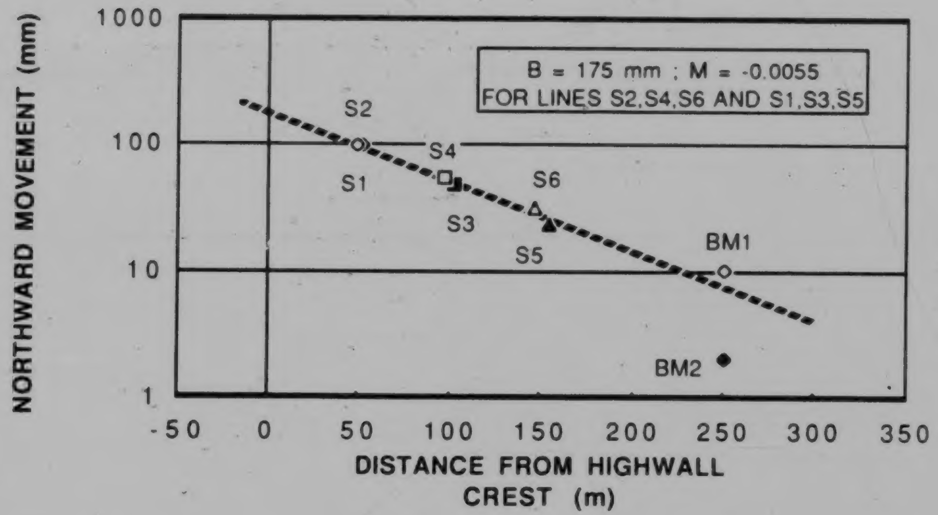

Figure D.6 Displacement field at elevation 730 metres on September 23, 1987 (Day 92)

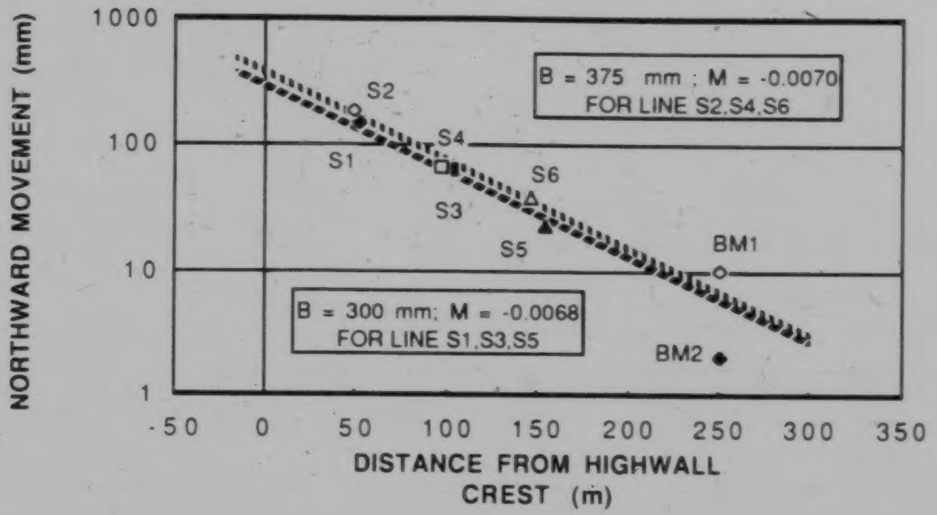

Figure D.7 Displacement field at elevation 730 metres on October 19, 1987 (Day 118)

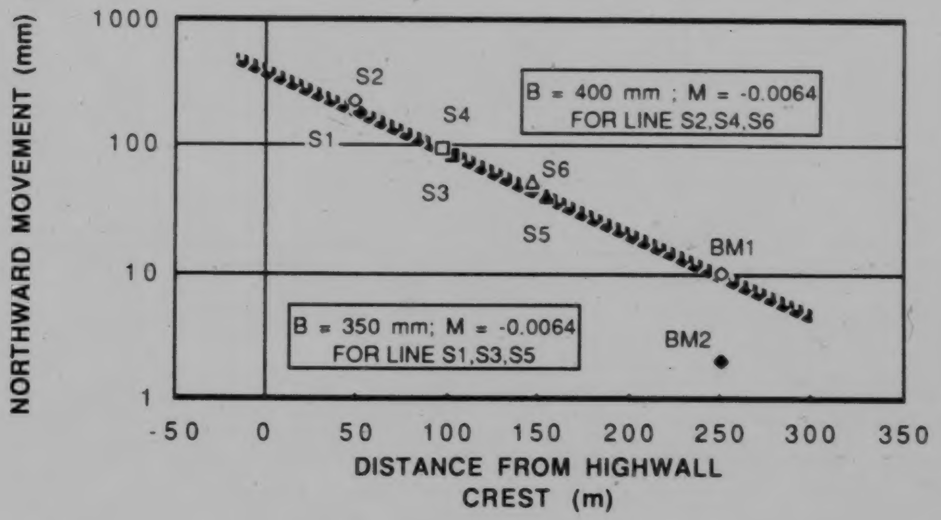

Figure D.8 Displacement field at elevation 730 metres on November 20, 1987 (Day 150)

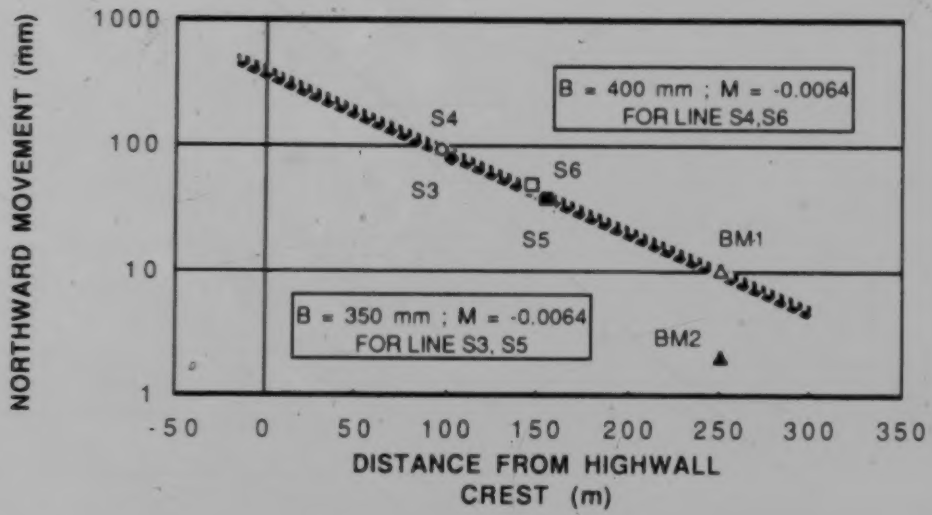

Figure D.9 Displacement field at elevation 730 metres on November 25, 1987 (Day 155)

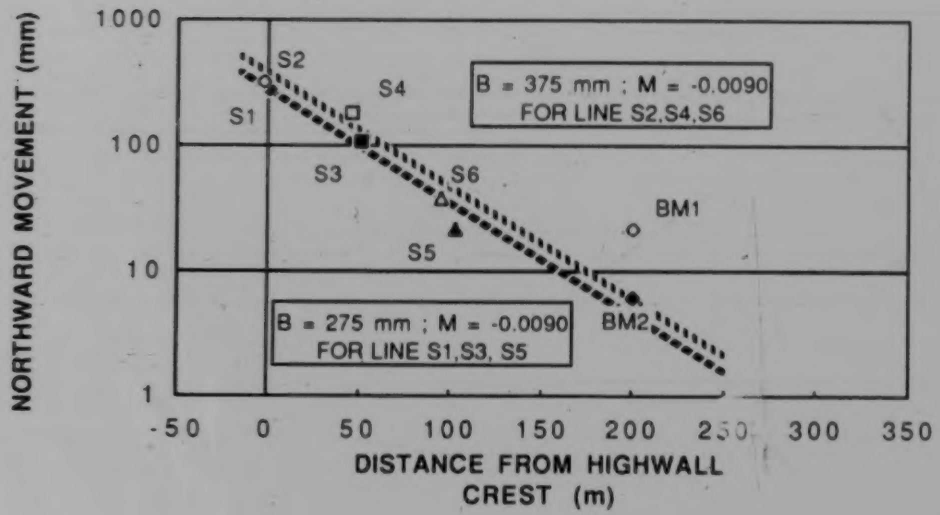

Figure D.10 Displacement field at elevation 730 metres on December 13, 1987 (Day 173)

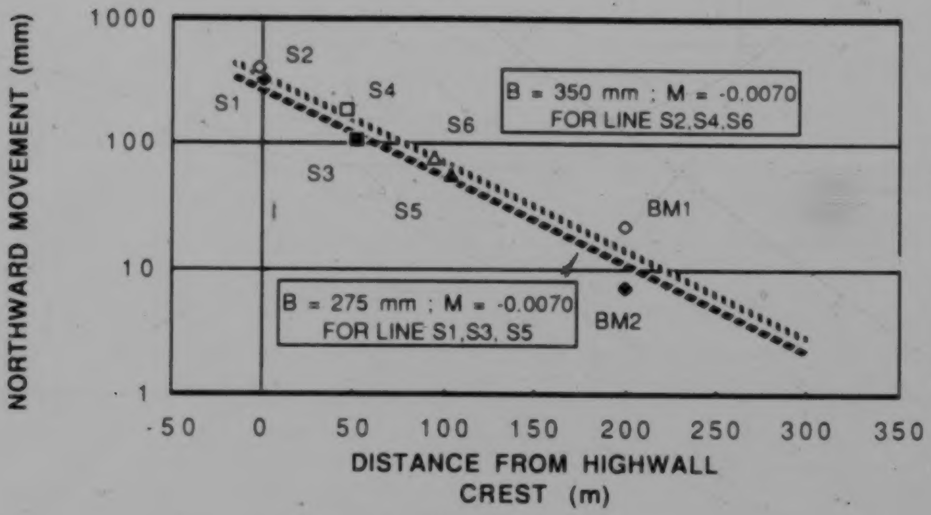

Figure D.11 Displacement field at elevation 730 metres on January 20, 1988 (Day 211)

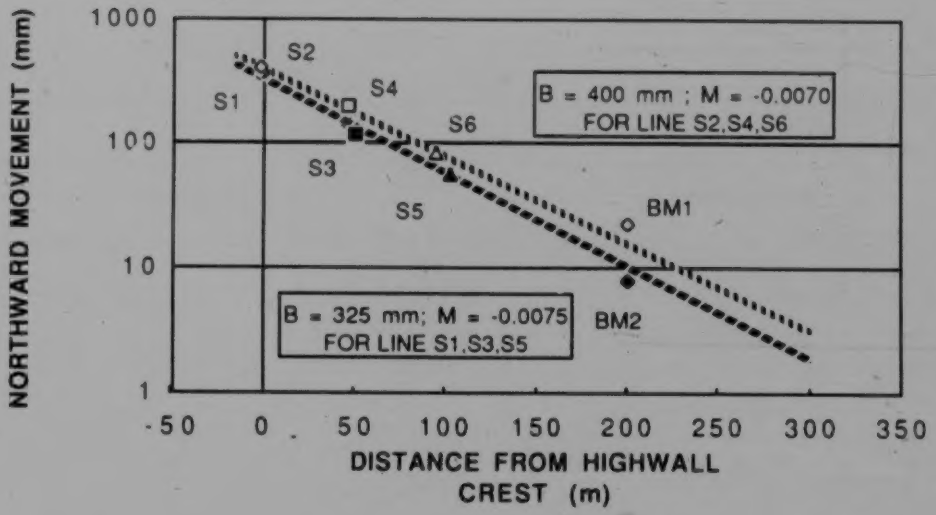

Figure D.12 Displacement field at elevation 730 metres on February 15, 1988 (Day 238)

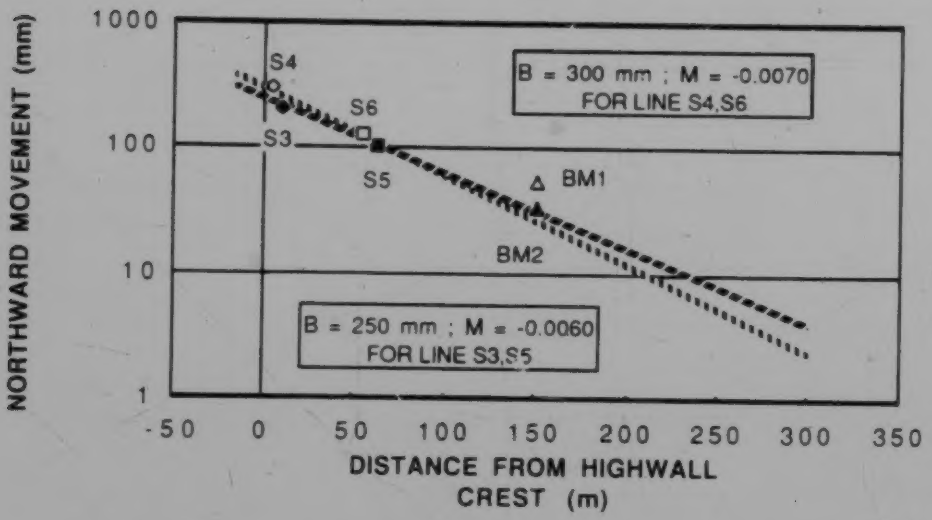

Figure D.13 Displacement field at elevation 730 metres on March 17, 1988 (Day 268)

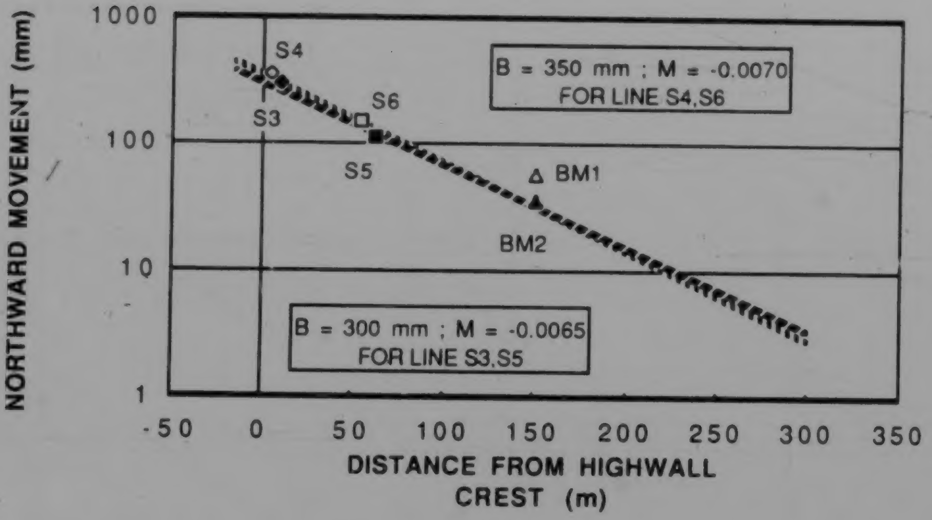

Figure D.14 Displacement field at elevation 730 metres on April 13, 1988 (Day 295)

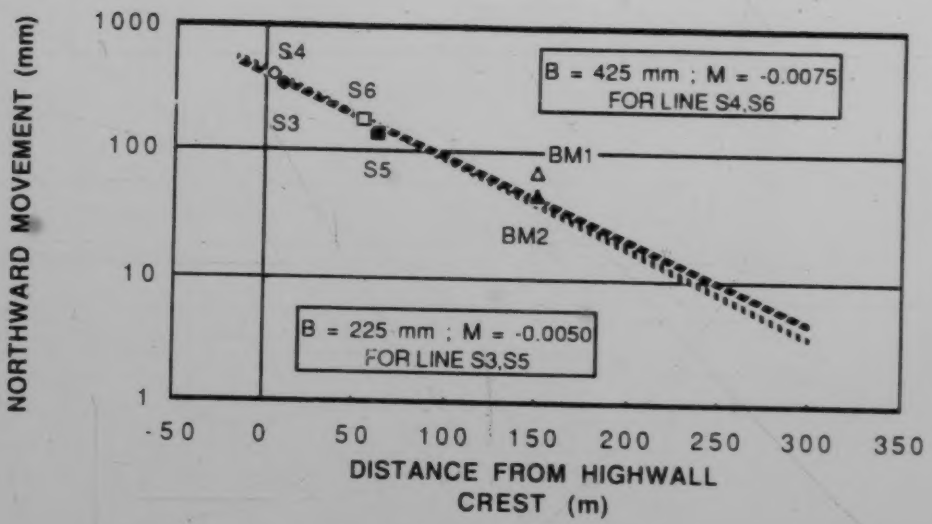

Figure D.15 Displacement field at elevation 730 metres on April 27, 1988 (Day 309)

APPENDIX E - STRAIN FIELD

Section 4.2.3 details how the strain field was determined. Figures E.1 to E.15 present the lateral strain field at elevation 730 metres at each survey date.

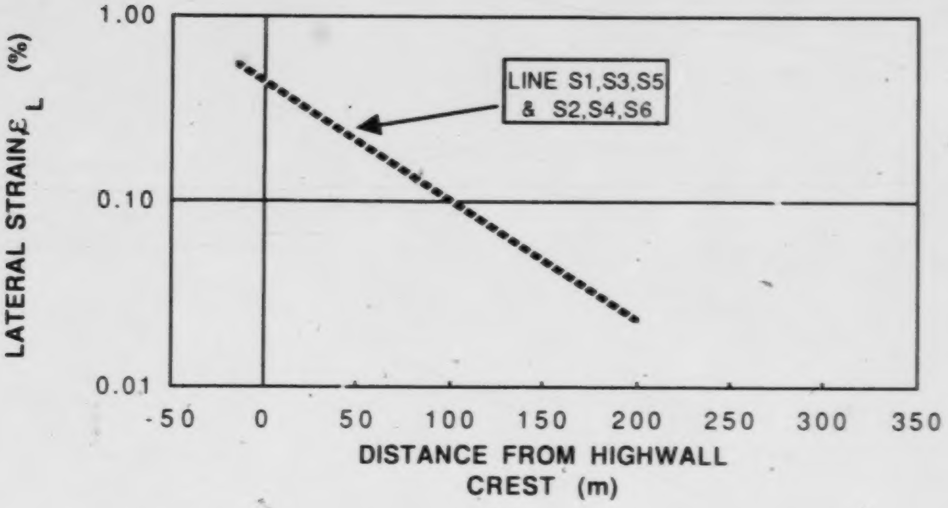

Figure E.1 Strain field at elevation 730 metres on July 3, 1987 (Day 10)

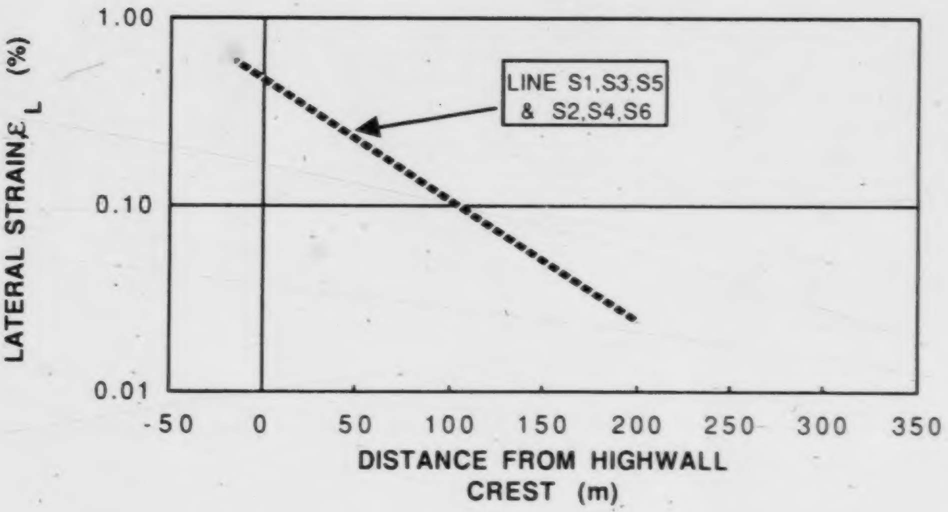

Figure E.2 Strain field at elevation 730 metres on July 29, 1987 (Day 36)

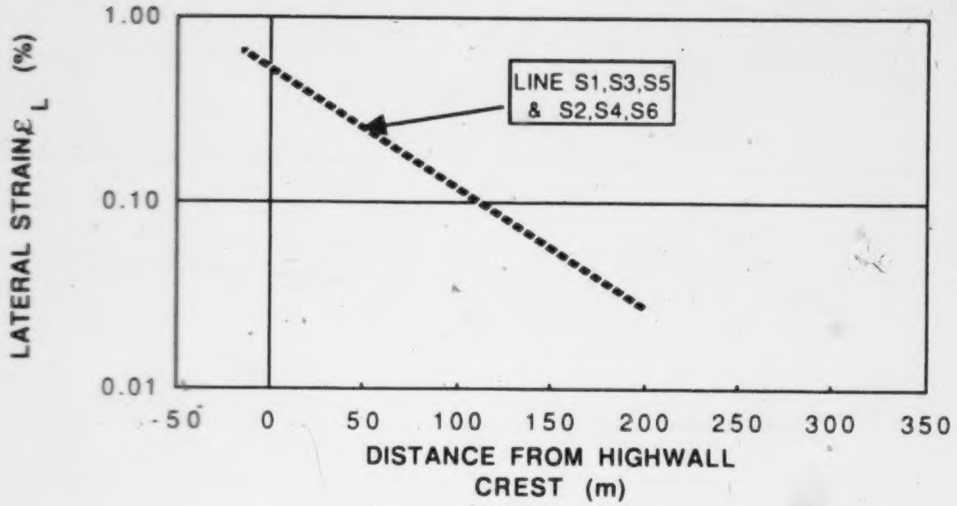

Figure E.3 Strain field at elevation 730 metres on August 6, 1987 (Day 44)

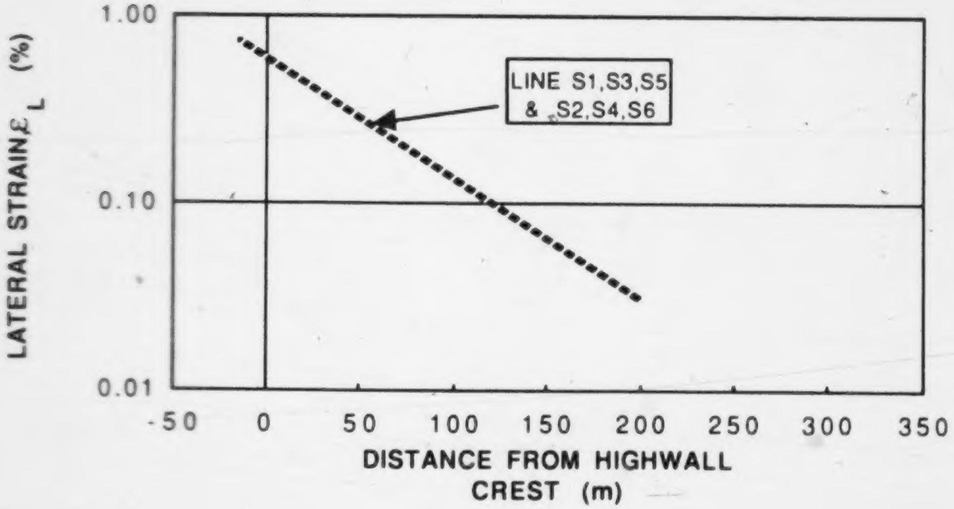

Figure E.4 Strain field at elevation 730 metres on August 19, 1987 (Day 57)

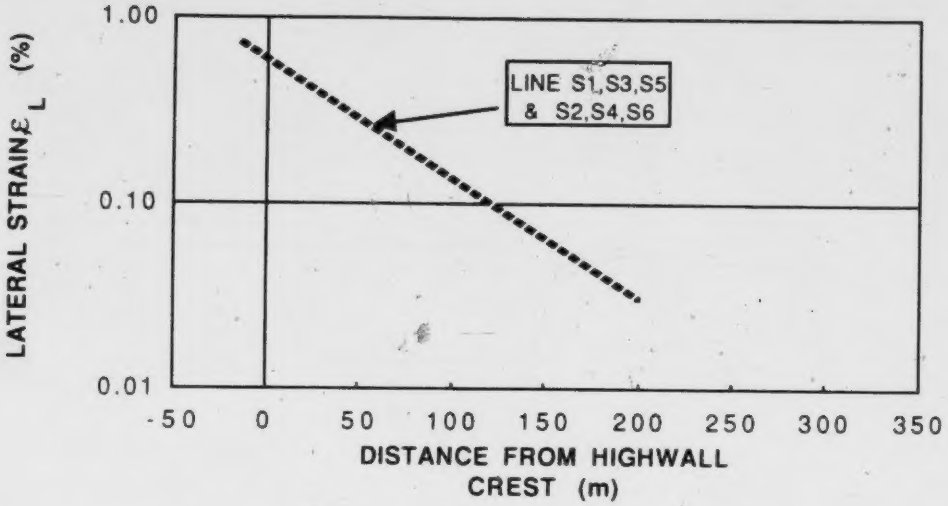

Figure E.5 Strain field at elevation 730 metres on September 2, 1987 (Day 71)

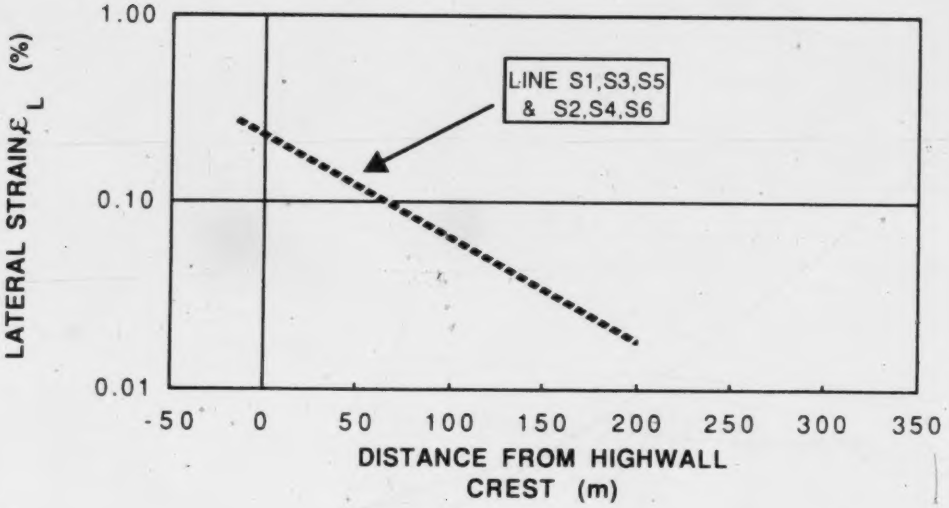

Figure E.6 Strain field at elevation 730 metres on September 23, 1987 (Day 92)

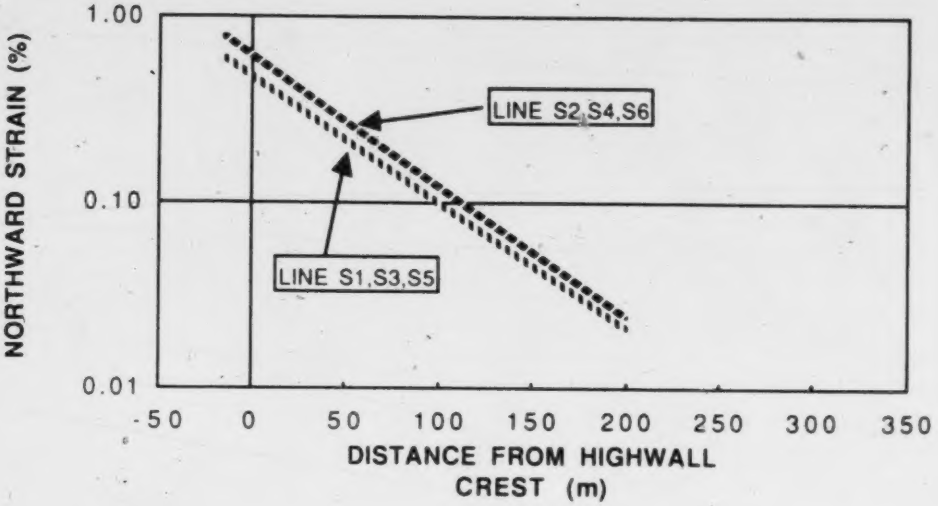

Figure E.7 Strain field at elevation 730 metres on October 19, 1987 (Day 118)

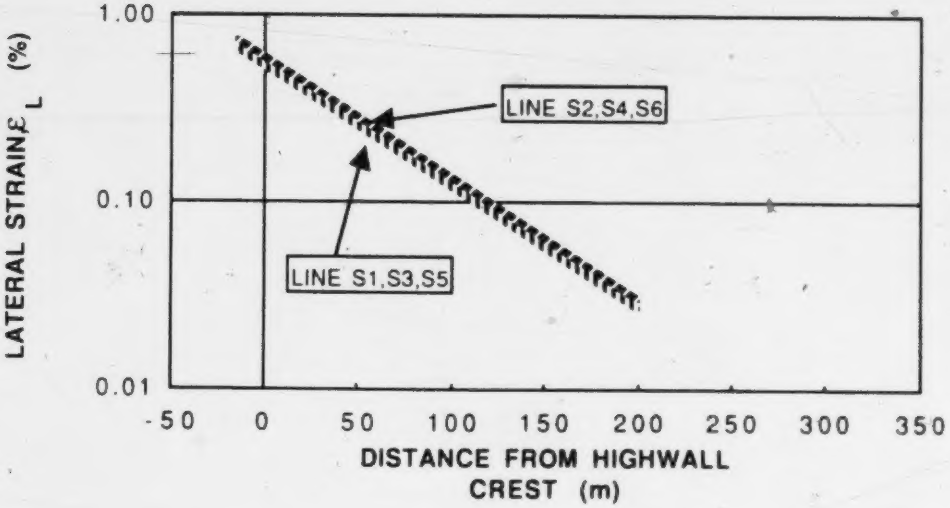

Figure E.8 Strain field at elevation 730 metres on November 20, 1987 (Day 150)

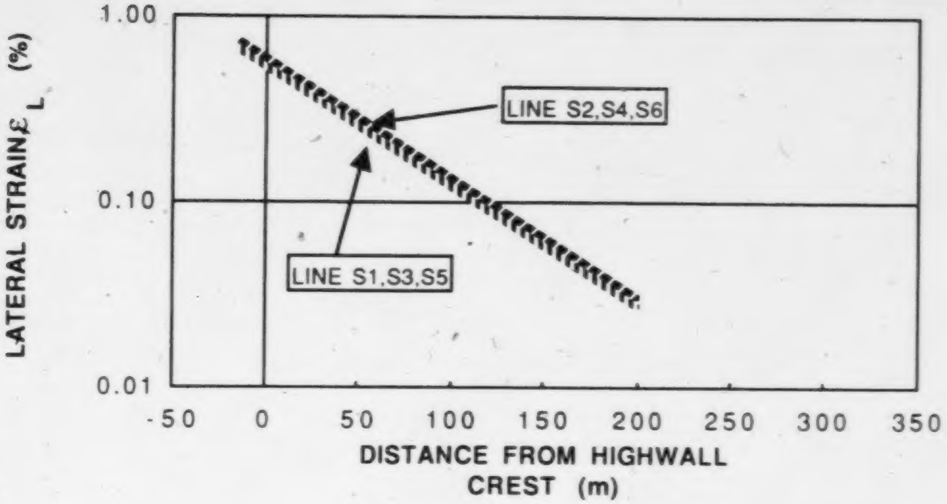

Figure E.9 Strain field at elevation 730 metres on November 25, 1987 (Day 155)

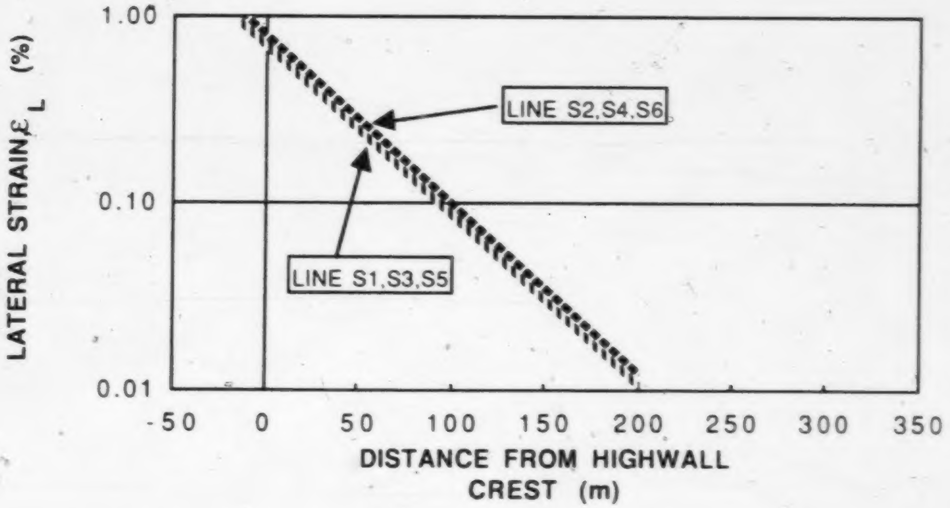

Figure E.10 Strain field at elevation 730 metres on December 13, 1987 (Day 173)

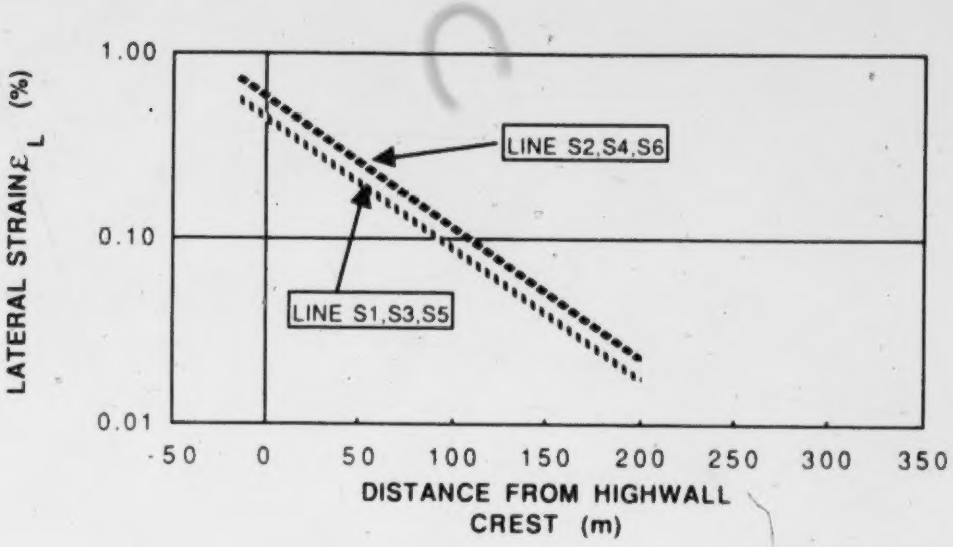

Figure E.11 Strain field at elevation 730 metres on January 20, 1988 (Day 211)

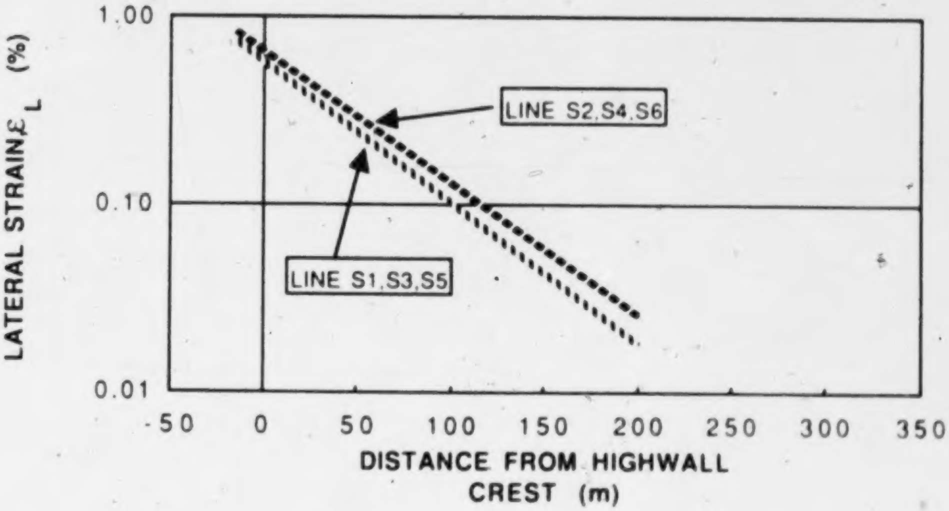

Figure E.12 Strain field at elevation 730 metres on February 15, 1988 (Day 238)

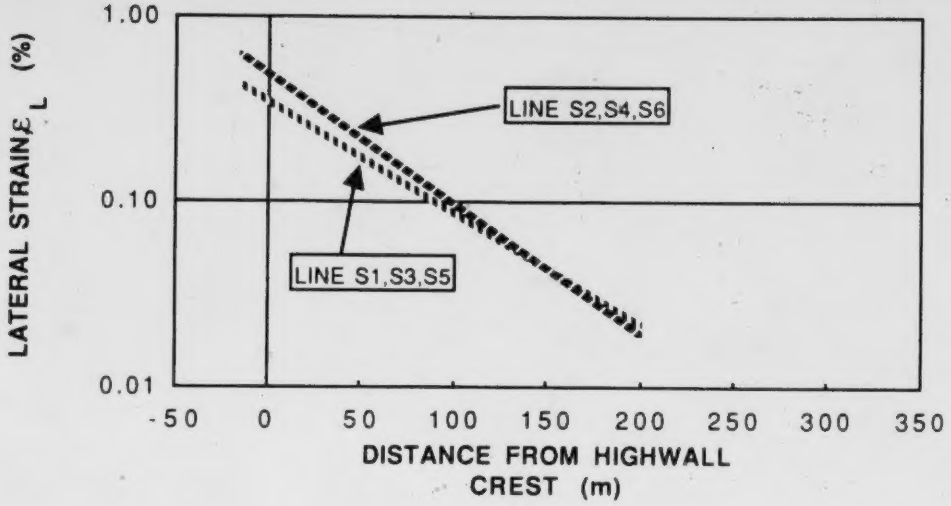

Figure E.13 Strain field at elevation 730 metres on March 17, 1988 (Day 268)

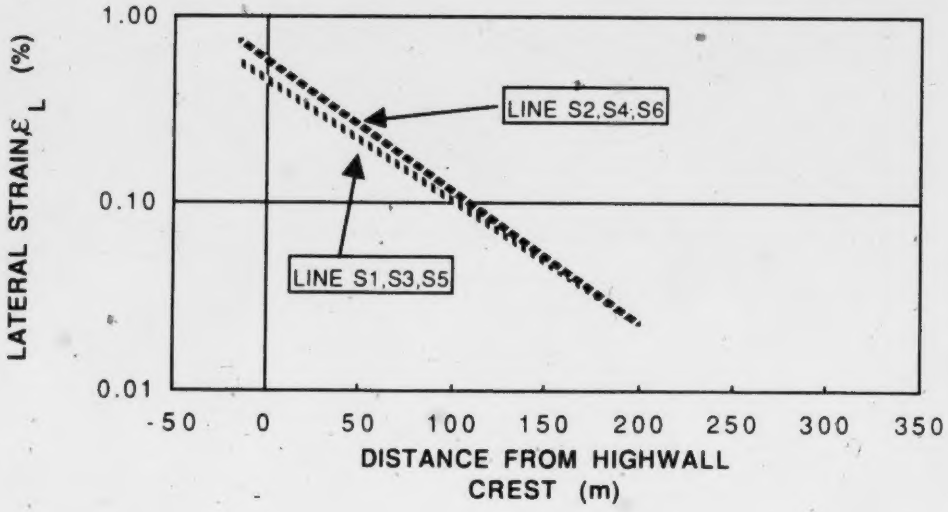

Figure E.14 Strain field at elevation 730 metres on April 13, 1988 (Day 295)

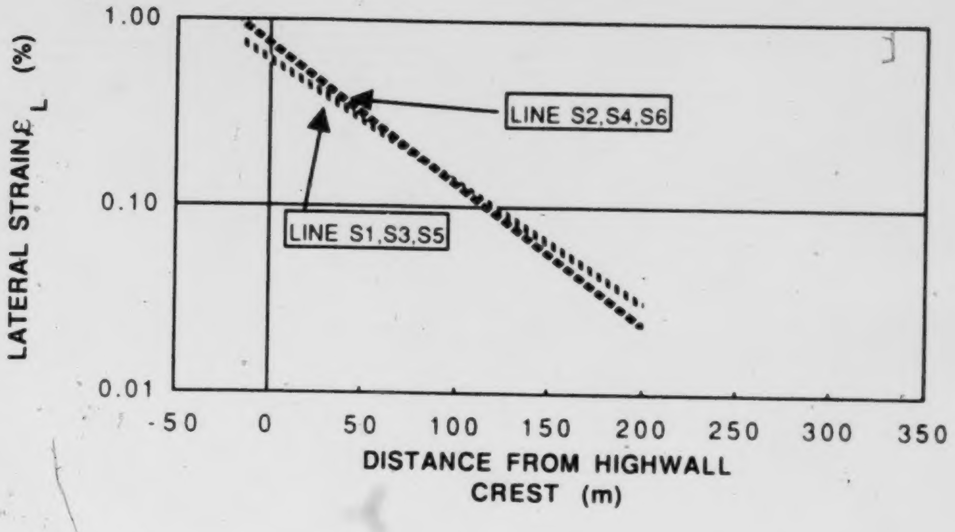

Figure E.15 Strain field at elevation 730 metres on April 27, 1988 (Day 309)

APPENDIX F - PIEZOMETER RESULTS

Section 3.6 describes the instrumentation used to measure pore water pressures. Their results are presented in Figures F.1 to F.13 and show the variation of Total Head over time. The times of the highwall and coalwall excavations are also included.

Table F.1
Location of Piezometers

U of A HOLE NUMBER	T.A.U. HOLE NUMBER	NORTHING (metres)	EASTING (metres)	TIP ELEVATION (metres)
P7	HV87-417	1132.4	-3836.4	T = 721.62 B = 718.11
P8	HV87-418	1079.4	-3889.4	T = 726.20
P9	HV87-419	1086.7	-3838.6	T = 732.90 B = 724.60
P10	HV87-420	1085.1	-3839.0	T = 721.28 B = 716.70
P11	HV87-421	1031.4	-3882.1	T = 721.85 B = 719.10
P12	HV87-422	1039.2	-3831.5	T = 725.80 B = 720.98
P13	HV87-423	1040.2	-3832.2	T = 734.90 B = 726.01

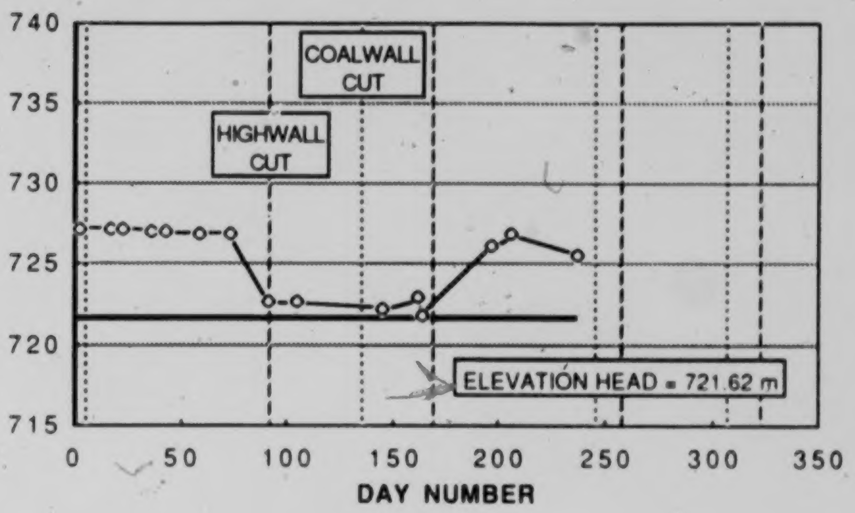

Figure F.1 Piezometric head over time for pneumatic piezometer P7-T

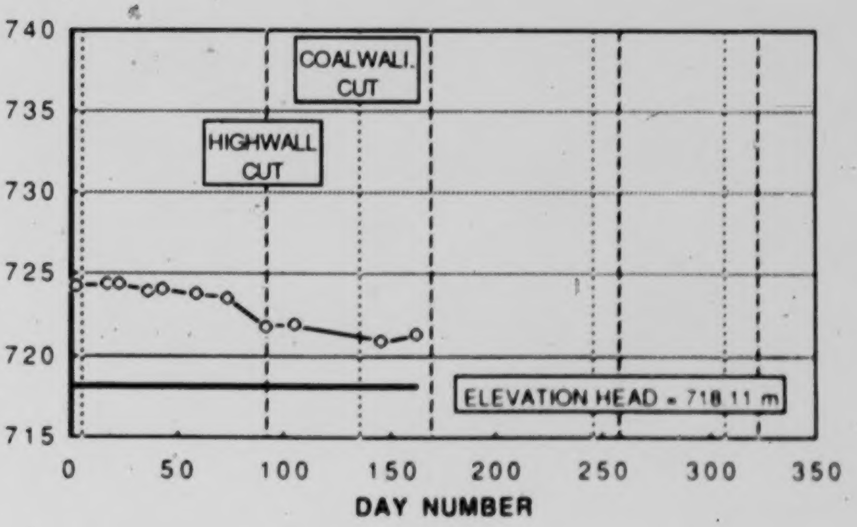

Figure F.2 Piezometric head over time for pneumatic piezometer P7-B

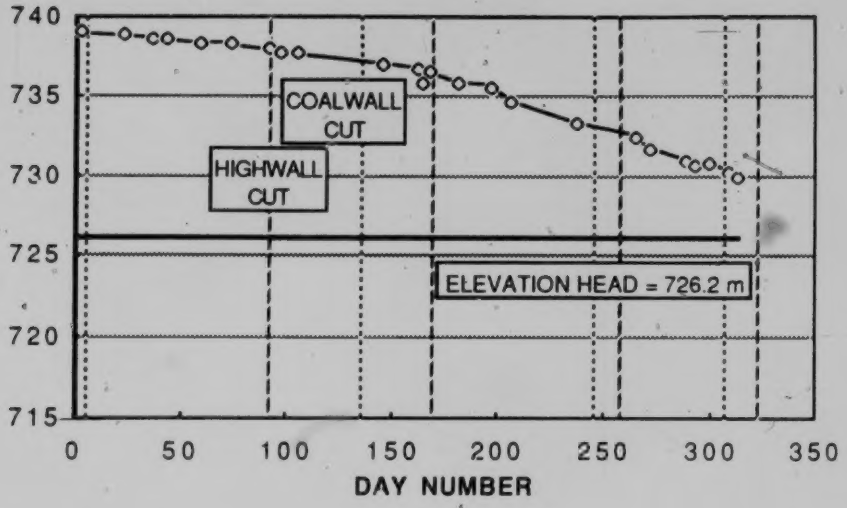

Figure F.3 Piezometric head over time for sealed tip standpipe piezometer P8-T

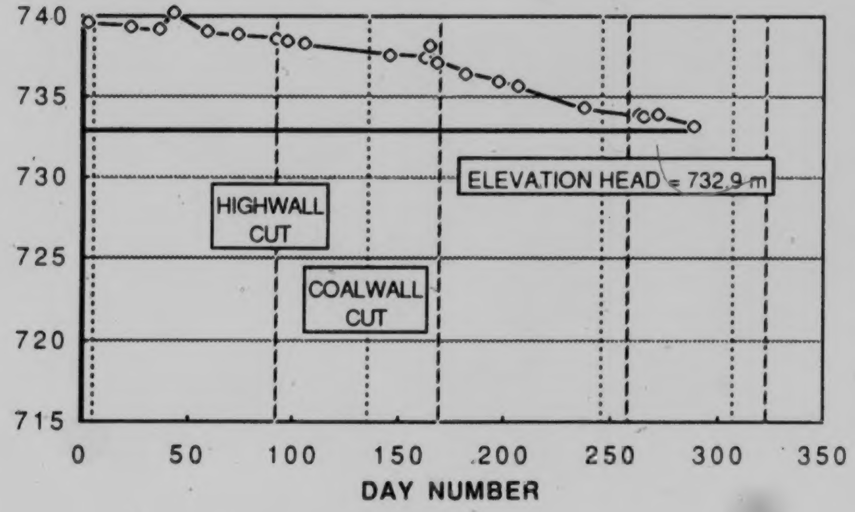

Figure F.4 Piezometric head over time for sealed tip standpipe piezometer P9-T

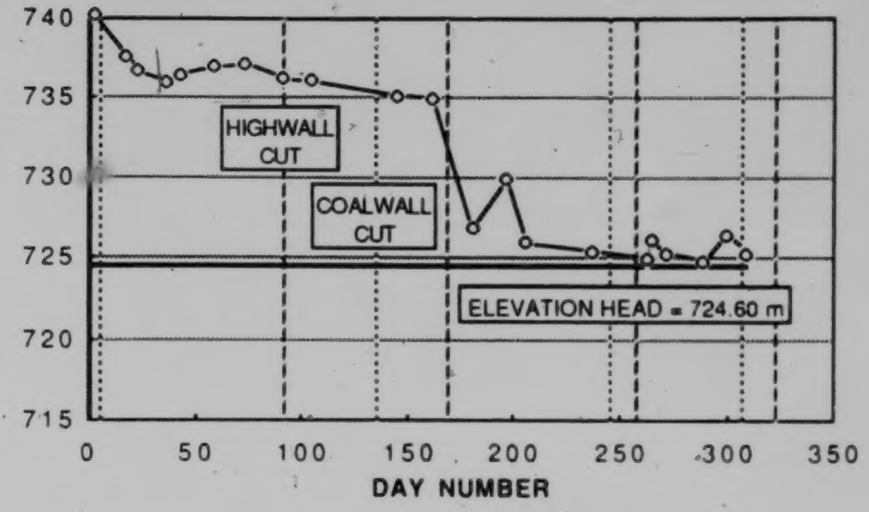

Figure F.5 Piezometric head over time for pneumatic piezometer P9-B

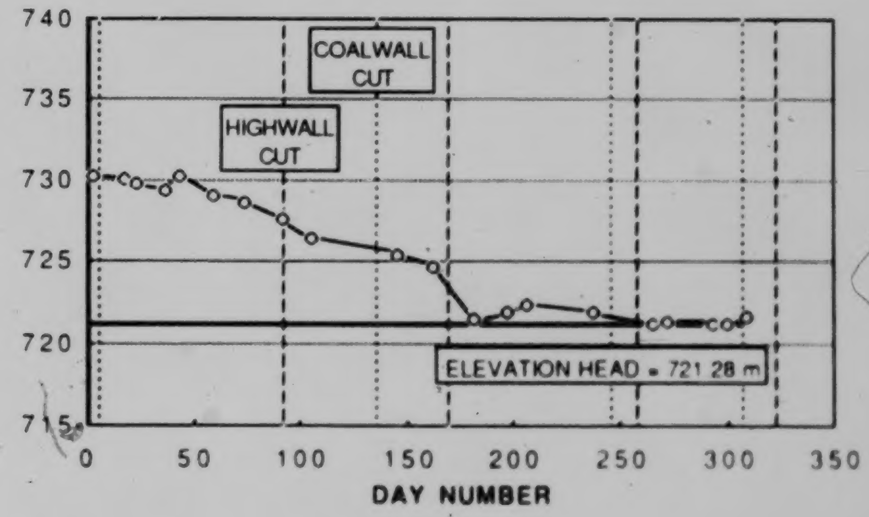

Figure F.6 Piezometric head over time for pneumatic piezometer P10-T

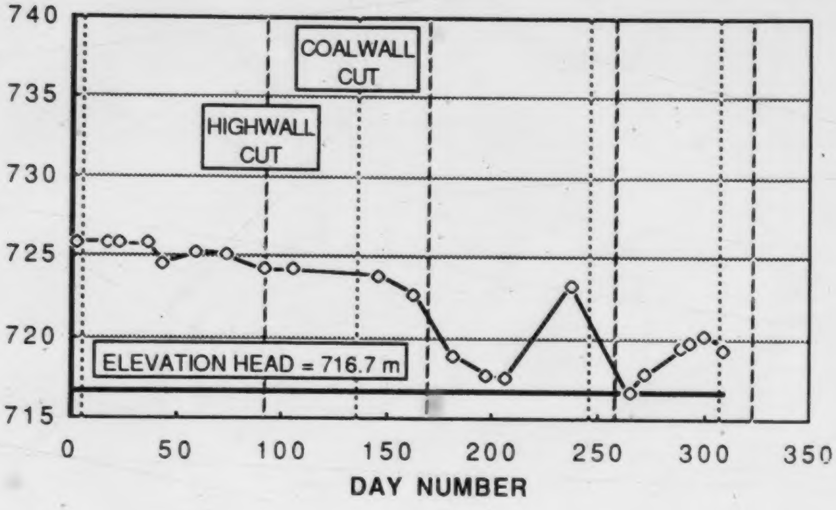

Figure F.7 Piezometric head over time for pneumatic piezometer P710-B

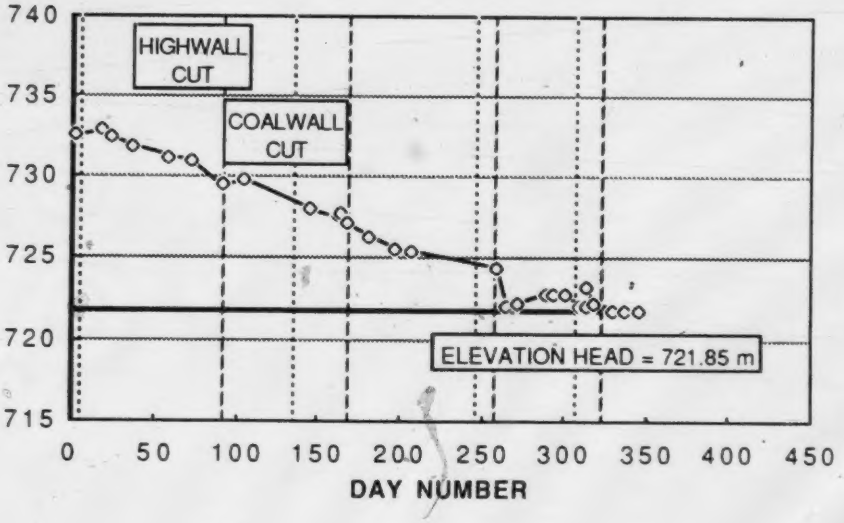

Figure F.8 Piezometric head over time for pneumatic piezometer P11-T

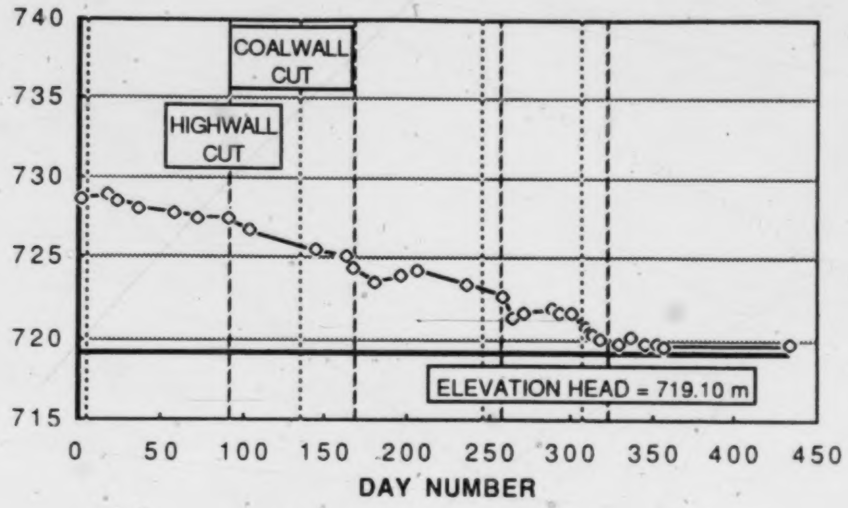

Figure F.9 Piezometric head over time for pneumatic piezometer P11-B

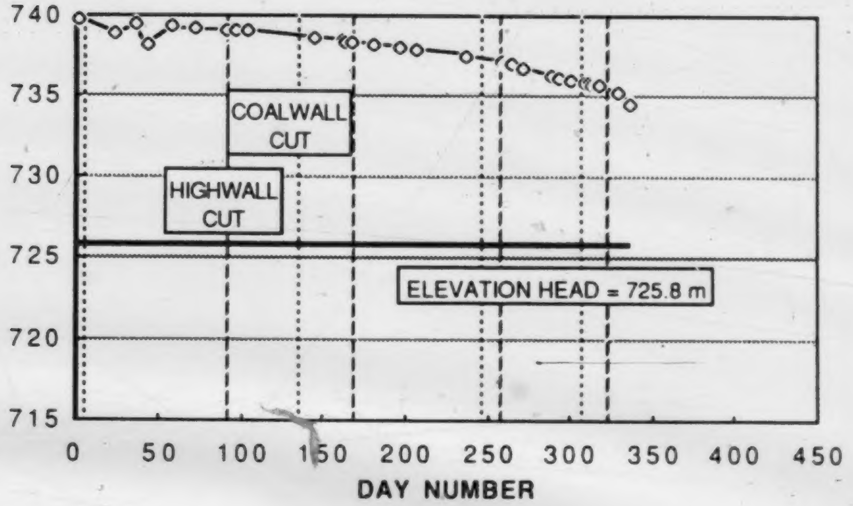

Figure F.10 Piezometric head over time for sealed tip standpipe piezometer P12-T

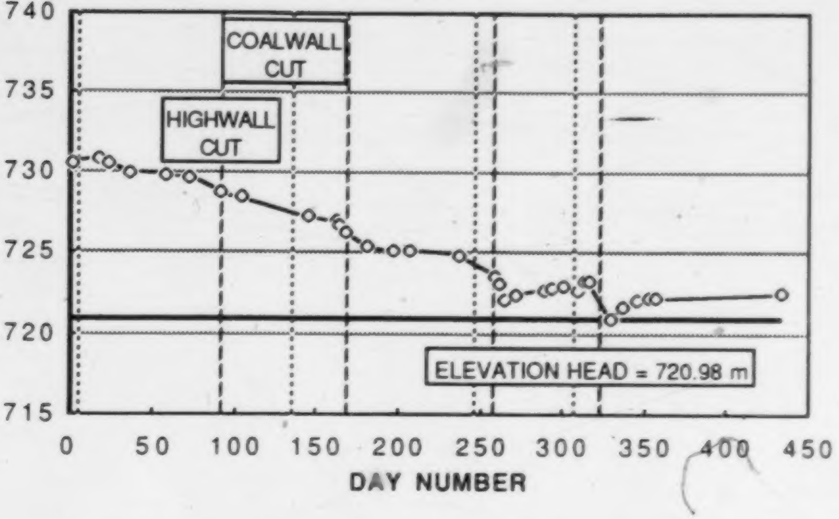

Figure F.11 Piezometric head over time for pneumatic piezometer P12-B

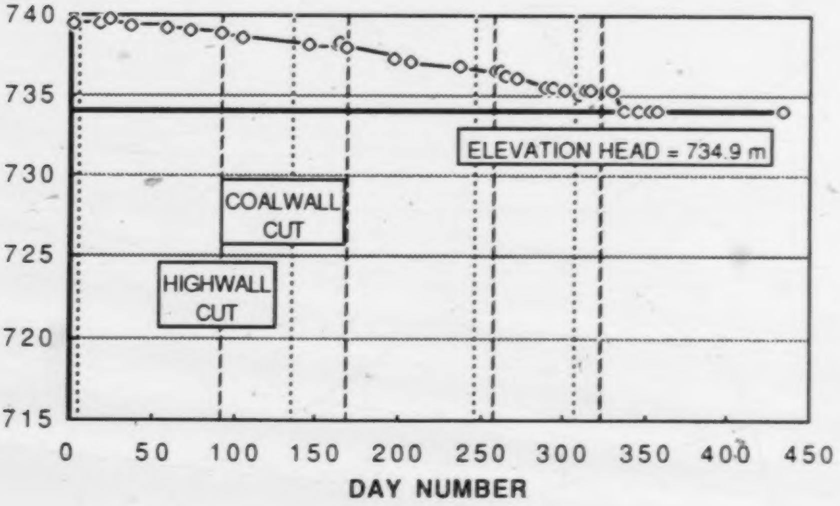

Figure F.12 Piezometric head over time for pneumatic piezometer P13-T

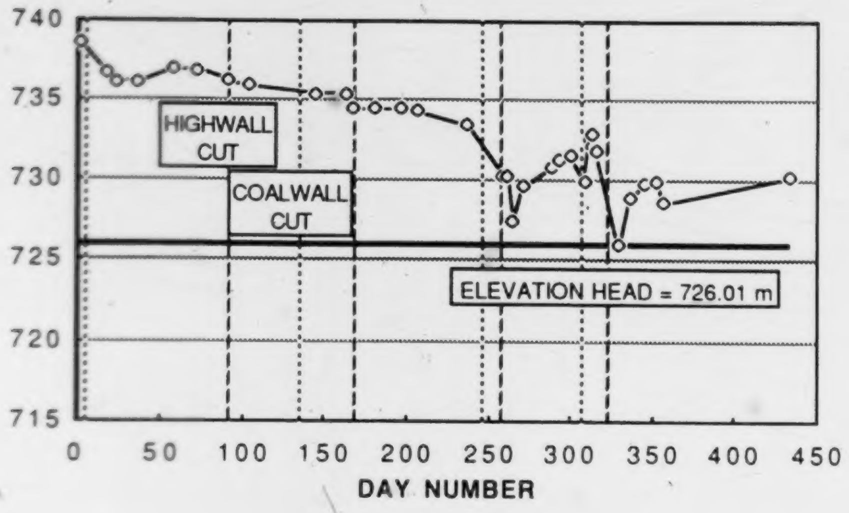

Figure F.13 Piezometric head over time for pneumatic piezometer P13-B

APPENDIX G - INDEX TESTING RESULTS

Chapter 5 describes and summarizes the index testing program. Tables G.1 to G.5 provide complete results of all of the index tests that were performed.

Table G.1

Results of Moisture Content Testing

Lithology	Hole	Depth (metres)	Elev. (metres)	m.c. (%)	γ_T (kn/m^3)	γ_d (kn/m^3)
Till	S6	1.0	749.5	20.9	-	-
	S4	2.8	748.5	21.8	19.2	15.7
	S4	2.8	748.5	24.6	18.0	14.4
	S4	2.8	748.5	27.9	-	-
	S4	3.2	748.0	24.2	-	-
AVERAGE				23.9	18.6	15.0
Weathered Sandstone	S4	5	746	9.0	-	-
	S6	8.0	742.6	9.8	-	-
	S4	9	742	12.4	18.9	16.8
	S4	9	742	13.2	-	-
AVERAGE				11.1	18.9	16.8
Unweathered Sandstone (Cont'd)	S6	14.0	736.4	15.3	-	-
	S4	19.0	732.4	15.3	19.9	17.3
	S4	20.0	731.3	15.1	20.3	17.6
	S4	20.3	731.1	17.6	18.7	15.9
	S4	20	731	25.5	-	-
	S3	19.1	730.8	15.7	20.4	17.6
	S3	19.2	730.7	16.0	20.3	17.5
	S6	20.7	729.8	13.5	21.6	19.0
	S3	20.5	729.4	15.0	20.0	17.4
	S3	21.4	728.5	14.8	20.9	18.2

Table G.1 (continued)
Results of Moisture Content Testing

Lithology	Hole	Depth (metres)	Elev. (metres)	m.c. (%)	γ_T (kn/m^3)	γ_d (kn/m^3)
Unweathered Sandstone	S6	23.4	727.1	13.3	21.7	19.2
	S3	22.9	727.0	15.5	20.0	17.3
	S3	23.2	726.7	16.2	20.3	17.5
	S3	23.5	726.4	16.4	21.0	18.0
	S4	27.5	724	13.5	-	-
	S4	27	724	12.7	20.3	18.0
	S4	28.5	723	12.8	20.1	17.8
AVERAGE				15.5	20.4	17.7
Mudstone	S3	24.9	725.0	16.2	18.7	16.1
	S4	29.0	722.4	16.9	20.6	17.8
	S4	29.5	722	17.2	19.7	16.8
	S4	29.5	722	18.5	-	-
	S4	30.0	721.4	19.8	19.6	16.4
	S4	30	721	23.0	-	-
	S4	30.5	720.9	17.6	-	-
	S6	30.3	720.2	22.6	19.9	16.2
AVERAGE				19.6	19.8	16.6
Siltstone	S6	29.9	720.6	14.6	22.0	19.1
	S4	30.9	720.5	14.6	21.3	18.6
AVERAGE				14.6	21.7	18.8
Bentonite	S4	31.8	719.6	50.9	16.8	11.1

m.c. = moisture content

γ_T = total wet density, γ_d = dry density

Table G.2

Results of Grain Size Analyses

Lithology	Hole	Depth (metres)	Elev. (metres)	Percent Passing (Sieve Opening, mm)		
				#4. (4.76)	#200 (0.074)	(0.002)
Till	S6	1.0	749.5	99	90	-
Weathered Sandstone	S6	8.0	742.6	100	38	-
Unweathered Sandstone	S6	14.0	736.4	100	34	-
	S4	19	732.4	100	28	-
	S4	19	732.4	100	20	-
	S3	20	729.9	100	10	-
	S6	23.5	727.0	100	40	-
	S3	23.5	726.4	100	10	-
	FROM FAILURE AREA			99	19	-
	FROM FAILURE AREA			100	12	-
Mudstone	S3	24.9	725.0	100	100	60
	S4	29	722.4	100	100	55
	S4	30	721.4	100	100	50
	S6	30.3	720.2	100	92	65
	AVERAGE			100	98	57
Siltstone	S6	29.8	720.7	100	100	47
	S4	30.9	720.5	100	68	31
	AVERAGE			100	84	39
Bentonite	S4	31.9	719.5	100	100	78

Table G.3
Results of Atterberg Limits

Lithology	Hole	Depth (metres)	Elev. (metres)	P_L (%)	L_L (%)	I_P (%)
Mudstone	S3	24.9	725.0	31	66	35
	S4	29.0	722.4	24	58	34
	S4	30.0	721.4	21	56	35
	S6	30.3	720.2	31	74	43
			AVERAGE	27	63	37
Siltstone	S6	29.8	720.7	25	54	29
	S4	30.9	720.5	17	47	30
			AVERAGE	21	50	29
Bentonite	S4	31.9	719.5	51	146	95

Table G.4
Liquidity Indices

Lithology	Hole	Depth (metres)	Elev. (metres)	m.c. (%)	P_L (%)	I_P (%)	I_P (%)
Mudstone	S3	24.9?	725.0?	16.2	31	35	-0.42
	S4	29.0	722.4	16.9	24	34	-0.21
	S4	30.0	721.4	19.8	21	35	-0.03
	S6	30.3	720.2	22.6	31	43	-0.20
					AVERAGE		-0.22
Siltstone	S6	29.8	720.7	14.6	25	29	-0.36
	S4	30.9	720.5	14.6	17	30	-0.08
					AVERAGE		-0.22
Bentonite	S4	31.9	719.5	51	51	95	0.00

Table G.5
Activity

Lithology	Hole	Depth (metres)	Elev. (metres)	I_p (%)	C.F. (%)	A (%)
Mudstone	S3	24.9	725.0	35	60	0.58
	S4	29.0	722.4	34	55	0.62
	S4	30.0	721.4	35	50	0.70
	S6	30.3	720.2	43	65	0.66
			AVERAGE	37	57	0.64
Siltstone	S6	29.8	720.7	29	47	0.62
	S4	30.9	720.5	30	31	0.97
			AVERAGE	29	39	0.80
Bentonite	S4	31.9	719.5	95	78	1.22

C.F. = Clay Fraction (less than 2 microns)

A = Activity